Role of Caspase 3/Caspase Activated DNase induced DNA Strand Breaks during Skeletal Muscle Differentiation.

Brian Daniel Larsen

Thesis submitted to the
Faculty of Graduate and Postdoctoral Studies
In partial fulfillment of the requirements
For a Ph.D. degree in
Cellular and Molecular Medicine

Department of Cellular and Molecular Medicine
Faculty of Medicine
University of Ottawa

Abstract

Cell fate decisions incorporate distinct and overlapping mechanisms. The activity of caspase 3 was initially understood to be a cell death restricted event, however numerous studies have implicated this enzyme in the regulation of both differentiation and proliferation. How the activity of caspase 3 promotes a non-death cell fate remains unclear. Here we examine the role caspase 3 activity plays during skeletal muscle differentiation; in particular we explore the hypothesis that the mechanism of inducing DNA strand breaks during cell death is also a key feature of differentiation, albeit with a distinctly different outcome. We delineate the transient formation of Caspase 3/Caspase activated DNase (CAD) dependent DNA strand breaks during differentiation. The formation of these breaks is essential for differentiation and the regulation of specific genes. In particular expression of the cell cycle inhibitor p21 is related to the formation of a DNA strand break within the gene's promoter element. Further, we explored the genome wide association of CAD using Chromatin Immunoprecipitation coupled to high through put sequencing (ChIP-seq). This approach identified a potential role for Caspase3/CAD in regulating the expression of Pax7. Here, a CAD directed DNA strand break in the Pax7 gene is correlated with decreased Pax7 expression, an outcome that has been shown to be critical for progress of the myogenic differentiation program. The regulation of Pax7 expression through a CAD induced DNA strand break raises an intriguing connection between this regulation and oncogenic transformation observed in alveolar rhabdomyosarcoma. The putative site of CAD induced DNA strand breaks that promote decreased Pax7 expression during differentiation corresponds to site of

chromosomal translocations responsible for Pax7 fusion events in alveolar rhabdomyosarcoma.

Acknowledgements

In the course of my PhD I have had the opportunity to interact with numerous individuals that have provided assistance not only on the bench but through insightful conversation. First a clear acknowledgement of Dr. Lynn Megeney, for initially providing me the opportunity to pursue my PhD and then for your support for the duration. I have benefited not only from the independent research environment you sustain but also from your pragmatic and all too often frustrating requests. I also thankfully acknowledge the members of my graduate studies committee Drs. Valerie Wallace, Ruth Slack, and Steffany Bennett as well as Dr. Jeffery Dilworth for their guidance throughout this project. I thank the former and present members of the Megeney lab for not only assistance at the bench but also the friendship. In particular I thank Leanne Burns for entertaining my mentorship and critical contributions to the body of work presented in this thesis. I thank my parents and family for their love and support as I pursue my career. Finally I thank my canine companions, Shylo, Fitch and Hudson, you have provided a silent sounding board for my ideas and have patiently missed more than one walk as I have worked. Thank you.

"Every sentence I utter must be understood not as an affirmation, but as a question."

Niels Bohr

Authorization

Contents

List of Figures

Chapter 1: General Introduction

Chapter 2: Caspase 3/Caspase Activated DNase Promote Cell Differentiation by Inducing DNA Strand Breaks

List of Tables

Appendix II.

List of Abbreviations

AID	Activation-induced cytidine deaminase
Apaf1	Apoptosis activating factor-1
ATM	Ataxia-telagastia mutated
ATR	Ataxia-telagastia and Rad3 related
bHLH	Basic Helix Loop Helix
Bid	Interacting domain death agonist
BSA	Bovine Serum Albumin
CAD	Caspase Activated Nuclease
Caspase	Cysteinyl-aspartate specific protease
cDNA	Complementary Deoxyribonucleic acid
cFLIP	Cellular caspase 8-like inhibitory protein
ChIP	Chromatin Immunoprecipitation
ChIP-Seq	ChIP couple to high throughput sequencing
CSR	Class Switch Recombination
DAPI	4,6-Diamidino-2-phenylindole
DEPC	Diethylpyrocarbonate
DFF	DNA Fragmentation Factor
DMEM	Dulbecco's Modified Eagle Medium
DMSO	Dimethyl Sulfoxide
DNA-PK	DNA Protein Kinase
DSB	DNA double strand break
EDTA	Eythylenediaminetetraacetic acid
ES	Embryonic stem cell
FADD	Fas Activated Death Domain
FBS	Fetal Bovine Serum
FMK	Fluoromethylketone
GAPDH	Glyceraldehyde-3-phosphate dehydrogenase
HMG	High mobility group protein
HMGB	High mobility group B protein
HRR	Homologous Recombination Repair
HsTSN	Human tudor staphylococcal nuclease
IAP	Inhibitor of Apoptosis Protein
ICAD	Inhibitor of CAD
ISNT	In situ nick translation
KD	Knock down
KO	Knock out
LINE	Long interspersed nuclear element
LM-PCR	Ligation Mediated Polymerase Chain Reaction
MACs	Model Based Analysis of ChIP-seq
MAPK	Mitogen Activated Protein Kinase

MCF-7	Michigan Cancer Foundation -7
MEF2	Myocyte Enhancer Factor 2
MeOH	Methanol
MHC	Myosin Heavy Chain
miR	microRNA
MLL	Mixed lineage leukemia
MRFs	Master Regulatory Factors
MSC	Melanocyte stem cell
MST	Mammalian Sterile Twenty-like kinase
NHEJ	Non-homologous End Joining
NSC	Neuronal stem cell
ORF	Open Reading Frame
PARP	Poly (ADP-ribose) polymerase
PBS	Phosphate Buffered Saline
PCR	Polymerase Chain Reaction
qPCR	Quantitative Polymerase Chain Reaction
RAG(1-2)	Recombination-activating-gene protein 1-2
RNA	Ribonucleic Acid
ROS	Reactive Oxygen Species
RSS	Recombination Specific Sequence
RT-PCR	Reverse-transcriptase Polymerase Chain Reaction
SC	Satellite Cell
SEM	Standard error
SHM	Somatic Hypermutation
shRNA	Short hairpin Ribonucleic Acid
SINE	Short interspersed nuclear element
SOP	Sensory Organ Progenitors
ssDNA	DNA single strand break
t-AML	Secondary acute myeloid leukemia
tBid	Truncated Bid
TBS	Tris Buffered Saline
TopoIIB	Topoisomerase II Beta
UV	Ultraviolet
V(D)J	Variable(diversity)joining
z-DEVD-fmk	N-benzyloxycarbonyl-Asp-Glu-Val-Asp-fluomethylketone

Chapter 1: General Introduction

1.0 Introduction

The development and maintenance of multi-cellular organisms is dependent on a number of key decision points that are encountered at the level of an individual cell. These cell fate choices can be generally categorized as proliferation, differentiation, or death. Transition between each distinct cell fate is dependent on complex alterations in gene expression that in turn are moderated by multi-step signalling events. Each cell fate has been assumed to originate with a unique molecular signature, yet numerous studies suggest that all cell fate decisions may share an overlapping signal pathway. For example, a prominent member of the family of cysteine proteases, caspase 3, has been demonstrated to have decisive roles in cell differentiation and proliferation (Lamkanfi et al, 2007). This thesis aims to further explore how caspase 3 promotes myoblast differentiation, and whether this enzyme directs non-death outcomes by inducing cellular changes that are traditionally associated with apoptosis/cell death. Specifically, we are exploring the hypothesis that caspase 3 mediates the cell fate decision of differentiation by inducing DNA strand breaks, an event that will in turn alter gene expression to propel changes in the cell.

1.1 Caspase enzymes a primary conduit of apoptotic signal transduction

A clear morphological definition of apoptosis was outlined by Kerr et al. (1972) through the compilation of observations published from 1951 through 1972. The process can be considered in two elements, the first a cell autonomous disassembly marked by "cytoplasmic and nuclear condensation and breaking up of the cell into a number of membrane-bound, ultrastructurally well preserved fragments" (Kerr et al, 1972). The second element considers the removal of the cellular debris primarily through phagocytic uptake. Following these early descriptive studies, the first biochemical hallmark, DNA

fragmentation, was described for apoptotic cell death (Wyllie, 1980). Despite these early advances a further 18 years would pass before a molecular mechanism would be fully characterized for this standard feature of apoptotic cell death (see below).

Caspase enzymes were initially linked to apoptotic induction through elegant genetic studies in *Caenorhabditis elegans* (Ellis & Horvitz, 1986; Yuan & Horvitz, 1990). Here, mutations linked to Ced-3 were shown to prevent the developmentally timed loss of cells, a well characterized feature of the *C. elegans* model system. Ced-3 was noted to share homology with the human interleukin converting enzyme, caspase 1, suggesting Ced-3 acted as a cysteine protease (Miura et al, 1993; Yuan et al, 1993). Using homology to Ced-3, mammalian caspases linked to cell death were identified, with caspase 3 showing the closest homology. Simple over expression of this caspase enzyme in mammalian cells results in cataclysmic loss of cell viability by apoptosis (Fernandes-Alnemri et al, 1994). These initial studies led to expanded efforts that ultimately characterized an evolutionarily conserved cell death signalling network (Ameisen, 2002; Crawford & Wells, 2011).

Caspase enzymes, use a cysteine nucleophile to cleave proteins at an aspartic acid residue in recognized amino acid motifs (Stennicke & Salvesen, 1997). Translated as inactive zymogens, caspases require two specific cleavage events to be processed into an active state. Proteolytic cleavage first separates the prodomain from the catalytic subunits, the second cleavage then separates the large and small catalytic domains. The catalytic domains subsequently associate as a heterodimer forming the catalytic site. Caspases do not act as stochastic proteases but utilize motif recognition to designate the site of cleavage which specifically modifies the activity of the substrate (Earnshaw et al,

1999). The topology of the catalytic site determines the amino acid motif preferentially processed by the caspase family member (Crawford & Wells, 2011).

The transduction of a cell death signal via caspase enzymes utilizes a hierarchy of initiator and effector caspases. Initiator caspases include family members 8, 9, and 10 while effector caspases include caspase 3, 6, and 7. Initiator caspases can further be classified on the basis of their activation through an external (extrinsic) signal or an internal (intrinsic) signal (Figure 1). An induced proximity model is purposed for the autocatalyic activation of initiator caspases that will then proteolytically process and activate the effector caspases (Boatright et al, 2003). Internal perturbations, such as oxidative stress or excessive DNA damage, signal the activation of intrinsic caspase dependent apoptosis. These stress events are transduced to the mitochondria where the signal is translated by altering the inhibitory effects that the pro-survival Bcl-2 family members (Bcl-2, Bcl-xl, Mcl-1) exert on the pro-apoptotic members of this protein family (Bax, Bad) (Chipuk et al, 2010). Unhinging the balance towards increased activity of the apoptotic members promotes the loss of mitochondrial membrane permeability, releasing cytochrome c into the cytoplasm (Kluck et al, 1997; Yang et al, 1997). Outside the mitochondria, cytochrome c triggers the formation of the multiprotein complex termed the apoptosome, apoptosis activating factor-1 (Apaf-1) complexes with cytochrome c and serves to recruit procaspase 9 (Zou et al, 1999). This recruitment concentrates caspase 9 zymogens together facilitating autoprocessing through induced proximity to form active caspase 9. Upon activation, caspase 9 will then target and process caspase 3 into an enzymatic active state. Extrinsic signals can be interpreted through the activation of caspase 8, the ligand binding of cell surface receptors such as Fas or death receptors signal the internal formation of the death inducing signalling complex (DISC). This

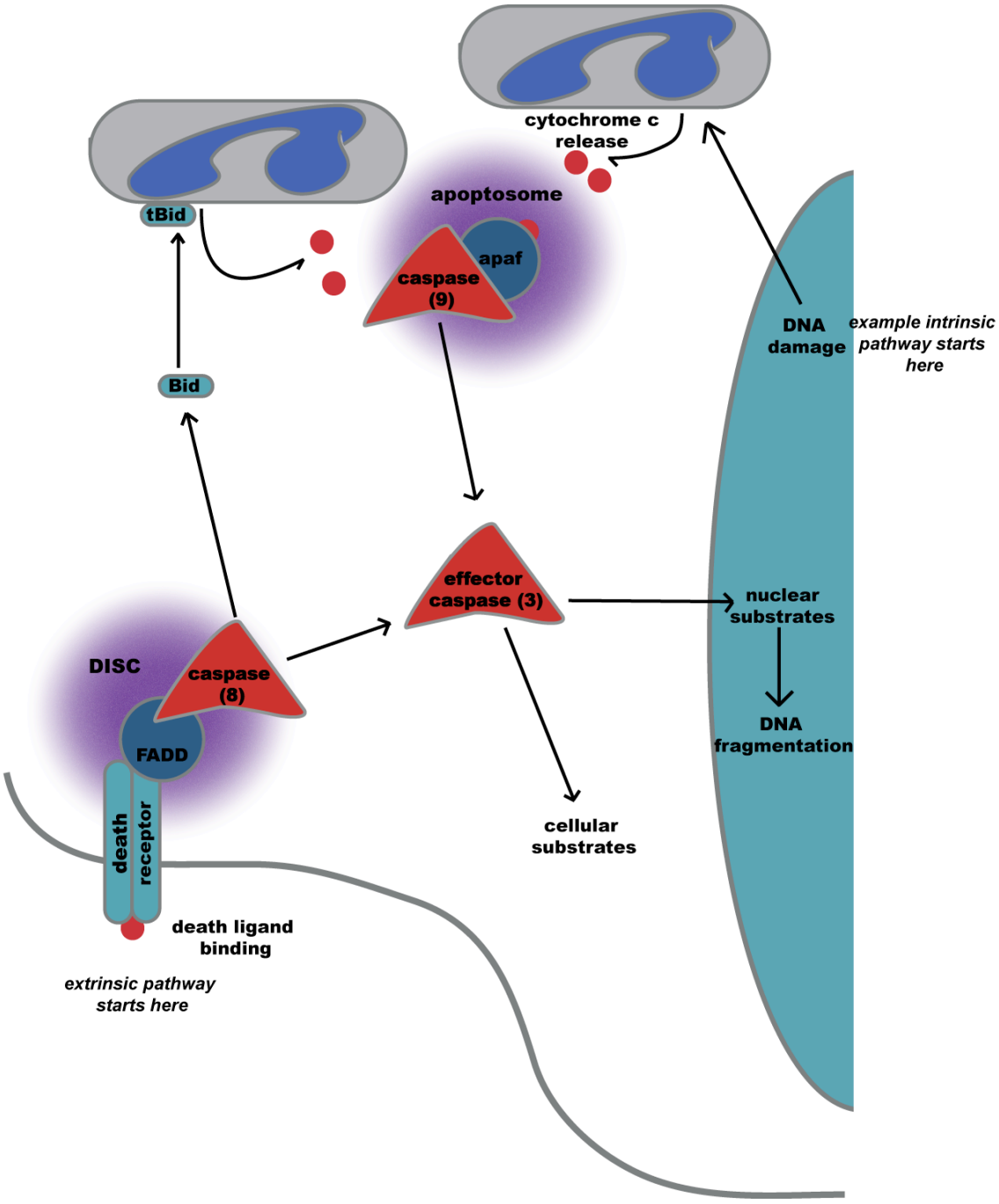

Figure 1. Apoptotic caspase cascade. Extensive DNA damage can initiate the intrinsic pathway by signalling the release of cytochrome c from the mitochondria activating caspase 9. Binding of a death ligand can initiate the extrinsic pathway resulting in the activation of caspase 8. Subsequent to their activation the initiator caspases can cleave and activate caspase 3 that directs the disassembly of the cell including DNA fragmentation.

activation platform forms by binding Fas activated death domain protein (FADD) to the cytoplasmic side of the ligated death receptor. FADD then serves to recruit and concentrate caspase 8 zymogens allowing induced proximity autoprocessing (Medema et al, 1997). Once activated, caspase 8 can directly process caspase 3 to its active state. Caspase 8 is also able to do this indirectly and simultaneously through the cleavage of the BH3-only family member Bid to tBid, which signals to the mitochondria for the activation of the intrinsic pathway of caspase activation (Li et al, 1998).

The cascade of caspase activation as described above is subject to extensive control points, acting to prevent premature or inappropriate enzyme stimulation. Stoichiometric balance between caspase 8 and cellular caspase 8-like inhibitory protein (cFLIP) short and long isoforms at the DISC will physically interfere with induced proximity autocatalytic activation (Irmler et al, 1997; Medema et al, 1997). Activation of intrinsic caspase signalling is tightly linked to the loss of mitochondrial membrane potential. Failure of an apoptotic perturbation to sufficiently terminate the pro-survival Bcl-2 members inhibition of the pro-apoptotic members prevents the loss of membrane potential and the activation of the intrinsic pathway (Chipuk et al, 2010). Members of the inhibitor of apoptosis (IAP) family can directly block the activity of activated caspases (including 3, 8 and 9) by direct binding to the caspase activity site and ubiquitnation. This ubquitnation can both promote the degradation of caspase enzymes and alter the catalytic activity (Srinivasula & Ashwell, 2008). The IAPs are key safeguards that protect the cell from spurious caspase activity. Interestingly, the IAP proteins are subject to regulation and can be directly neutralized during cell death events through the release of Smac/DIABLO and other IAP antagonists from the mitochondria (Du et al, 2000).

Caspase enzymes have an extensive number of protein substrates that can be cleaved to promote cell death. To date, caspase 3 has been demonstrated to target over 300 protein substrates (Crawford & Wells, 2011; Luthi & Martin, 2007). Substrate cleavage by a caspase can result in a loss of protein function, activation of function, or change in subcellular localization. Structural proteins, kinases, and transcription factors represent well documented examples of this proteolytic modification. However, a large number of the caspase substrates have no documented functional contribution to apoptosis and may very well be bystanders in the extensive activation of caspase enzymes used for cell death (Crawford & Wells, 2011). Caspase activation promotes ordered disassembly of a cell by stimulating cleavage of cytoskeletal proteins, inactivating key survival proteins, inhibiting the DNA damage repair process, all of which predate and lead to the fragmentation and condensation of the genome.

1.1.1 Caspase induction of cell autonomous DNA fragmentation

The enzymatic activity of caspases, particular caspase 3 has demonstrated a direct connection to initiating the genomic fragmentation associated with apoptotic cell death (Fernandes-Alnemri et al, 1994). DNA fragmentation during apoptosis progresses in two stages. First, early DNA damage events manifest as high molecular weight (HMW) fragments that result in 50 kbp DNA stretches. Late stage fragmentation appears as low molecular weight (LMW) fragments, resulting in periodic oligonucleosomal laddering. The stages of chromatin condensation temporally correlate with the extent of DNA fragmentation, early stages correspond to HMW cleavage, where later stages correspond to LMW cleavage (Figure 2A) (Samejima & Earnshaw, 2005). The primary mechanism by which caspase 3 activity mediates DNA fragmentation was reported in 1997 with the

discovery of the caspase-activated DNase (CAD, DFF40, DFFB) and the inhibitor of caspase-activated DNase (ICAD, DFF45, DFFA) (Liu et al, 1997).

The development of an in vitro assay to examine effectors of DNA fragmentation allowed the purification of CAD and ICAD. For example, incubating healthy purified nuclei with cellular fractions that had been treated with recombinant active caspase 3, demonstrated that the DNA laddering could be induced (Liu et al, 1997). CAD was identified as the activatable nuclease and ICAD an inhibitory chaperone protein that could be cleaved and inactivated by caspase 3 (Figure 2B) (Enari et al, 1998; Sakahira et al, 1998). CAD and ICAD associate through interactions between their N-terminal CIDE-N domains (Inohara et al, 1998). ICAD association with CAD is required as early as CAD translation, to ensure the nuclease is held in check but also to act as a critical folding chaperone for CAD (McCarty et al, 1999). Following translation, the complex translocates to the nucleus in conjunction with importin α/β protein complex (Lechardeur et al, 2000; Neimanis et al, 2007). Through alternative splicing two isoforms of ICAD are expressed, the full length 45 kDa ICAD-L that is required for as the CAD chaperone, and a 35 kDa ICAD-S which lacks the N-terminal NLS and is thought to act only as an inhibitor to activated CAD (Sakahira et al, 1999; Widlak et al, 2003). The caspase 3 zymogen is cytoplasmic, however once activated the enzyme can localize to the nucleus and inactivate ICAD via proteolytic cleavage at aspartic acids 117 and 224 (Figure 2C). This cleavage event releases CAD, allowing it to form an active homodimer (Lechardeur et al, 2000). The active CAD homodimer has a scissor-like structure with the catalytic site buried within a deep cleft formed by the two dimers (Woo et al, 2004). This structure is unique among nucleases, as is CAD's targeted activity towards both chromatin and naked

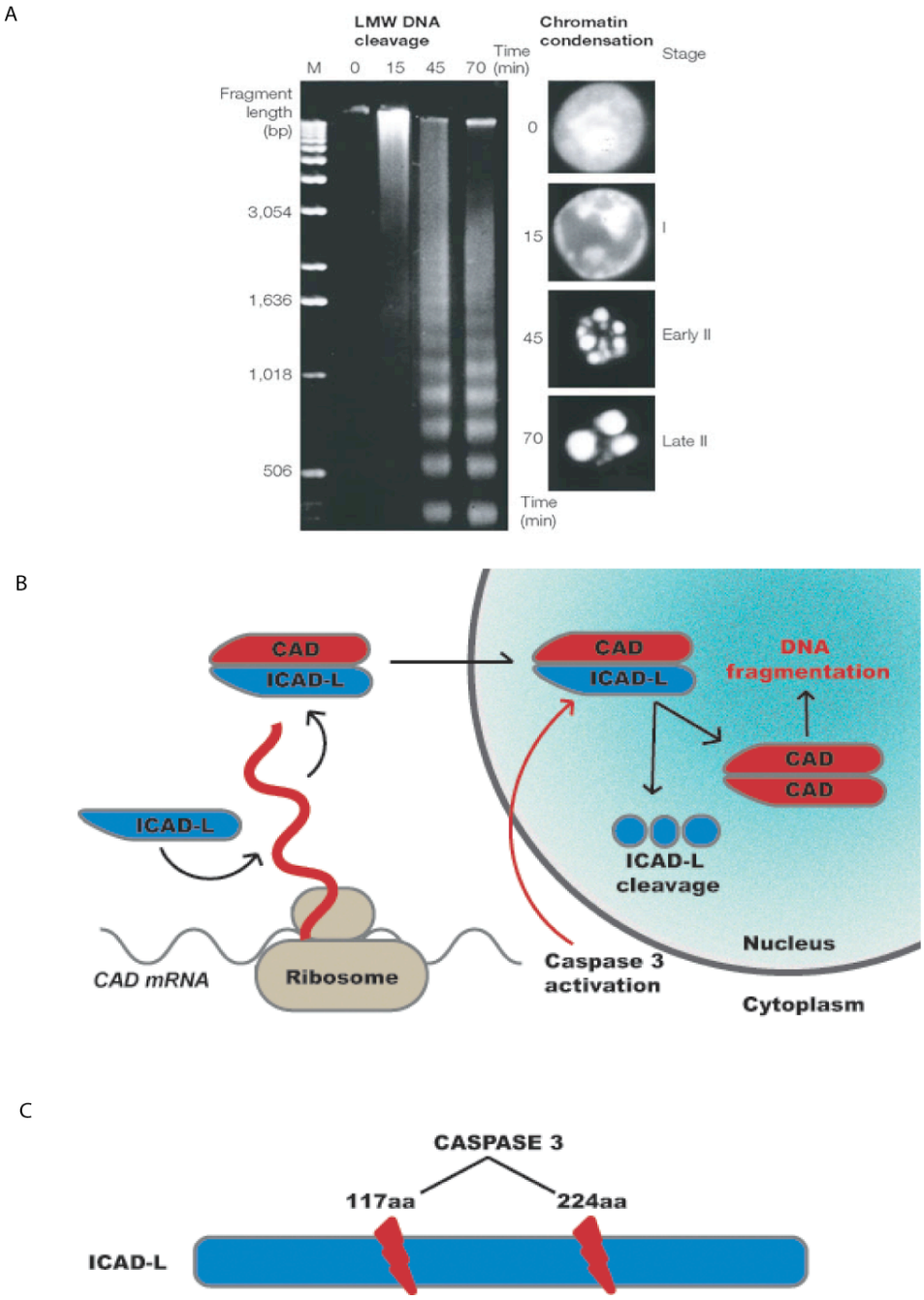

Figure 2. Caspase 3 induces DNA fragmentation during apoptosis by activating CAD. A.) LMW DNA fragmentation as viewed by agarose gel separation is presented during late stages of apoptosis and corresponds to late stages of chromatin condensation.(reprinted by permission from Macmillan Publishers Ltd: Nat Rev Mol Cell Biol 6(9): 677-88 © 2005) B.) ICAD-L acts as a chaperone ensuring proper folding of CAD as it is translated off the ribosome. The complex translocates to the nucleus where ICAD-L can be cleaved by caspase 3 during apoptosis promoting its disassociation from CAD. This disassociation allows CAD to form a nuclease active dimer. C) Caspase 3 cleaves ICAD-L at aspartic acid 117 and 224.

DNA (Widlak et al, 2000). During apoptosis CAD is directed by chromatin topology to cleave double stranded DNA between internucleosomal sequences. Additional factors can influence CAD activity including specific histone H1 variants, high mobility group proteins (HMGB1/2), heat shock protein 70 (HSP70), poly(ADP-ribose) polymerase -1(PARP-1) and topoisomerase II (Durrieu et al, 2000; Kalinowska-Herok & Widlak, 2008; Liu et al, 2003a; Ninios et al, 2010; West et al, 2005). These factors not only participate in localizing CAD, as CAD lacks a defined sequence specificity, but additionally stimulate its nuclease activity. LMW fragmentation is primarily attributed to CAD nuclease activity, as ablation of CAD expression or introduction of caspase-resistant ICAD constructs in cells lead to a loss of DNA fragmentation. In a number of cell types CAD has also been implicated in HMW fragmentation along with topoisomerase II (Samejima & Earnshaw, 2005). Following the description of CAD a number of additional nucleases have been implicated in cell autonomous DNA fragmentation. Endonuclease G (Endo G) has garnered particular interest as a mitochondrial localized nuclease that can be released in a caspase independent manner during the induction of apoptosis (Li et al, 2001). DNase Y has been hypothesized to act strictly in terminally differentiated cells, further its expression is dramatically enhanced during differentiation of skeletal muscle and neuronal cells. DNA fragmentation during apoptosis in these fully differentiated cell types is dependent on DNase Y and not CAD (Shiokawa et al, 2002; Shiokawa & Tanuma, 2004).

Albeit a biochemical hallmark of apoptosis, DNA fragmentation is surprisingly dispensable in the execution of cell death (Zhang et al, 1998). For example, it has been hypothesized that DNA fragmentation improves the efficiency of cell death rather than being an absolute requirement. Here, the contention is that DNA fragmentation leads to

the presentation of nucleosomes at the cell surface and release of nucleotides that in turn promote phagocytosis of apoptotic cells (Elliott et al, 2009; Radic et al, 2004). Indeed, targeted gene ablation of CAD or ICAD in the mouse has demonstrated no gross developmental deficit, and developmental cell death remains unaffected in the absence of LMW fragmentation (Kawane et al, 2003; Zhang et al, 1998).

1.2 Caspase activity directs non-death cell functions

Caspase proteases are integral components of the cell death machinery, yet numerous non-death functions have been attributed to this class of proteins. The first caspase, caspase 1, was described for its non-apoptotic role in monocyte activation during inflammation (Thornberry et al, 1992). Microbial pathogens signal the formation of the inflammasome which contains both caspase 1 and caspase 5. Once activated, these caspases process the proforms of interleukin-1β and interleukin-18 into active conformations (Yazdi et al, 2010). Although both caspase 1 and caspase 5 have been implicated in cell death, the non-death role appears to be the primary function. This was the first biochemical function described for a caspase enzyme, yet subsequent studies largely relegated this class of proteins as pro-death/pro-apoptotic. Despite the wealth of data linking caspase activity to cell death, numerous studies suggested that caspases (in particular caspase 3) could direct a cell fate that did not result in death or cell destruction.

1.2.1 Caspases promote cell differentiation. The attenuated cell death phenotype.

A number of differentiation processes retain remarkable similarity to cell death. Loss of organelles and cellular structures typify the specialization of a number of cells including lens fiber cells, epithelia cornification, erythroblasts, thrombocytes, and sperm. Indeed, the differentiation of these various cell types are absolutely dependent on the proteolytic activity of a range of caspases.

Caspase 14 is uniquely expressed during keratinocyte differentiation or cornification (Eckhart et al, 2000). This process involves the detachment of the proliferating keratinocytes from the basement membrane and exit from the cell cycle. Cell cycle exit triggers the expression of caspase 14, the cells progressively flatten and lose organelles, including the nucleus, via caspase mediated substrate targeting. Specifically, caspase 14 functions in the proper formation of the epithelial barrier through the cleavage degradation of (pro)fliggrin (Denecker et al, 2007). Interestingly caspase 14 does not appear to perform any apoptotic role in keratinocytes (Denecker et al, 2007). In addition to caspase 14, caspase 3 activity modifies skin development, yet the effect is restricted to the embryonic development of skin. Specifically in the absence of caspase 3 the proliferation of keratinocytes increase while differentiation decreases, suggesting a role in regulating the terminal exit from the cell cycle. However, while loss of caspase 3 retards skin maturation, the phenotype is corrected by birth (Okuyama et al, 2004).

Lens fiber differentiation and erythroblast differentiation both exhibit transient caspase activity during the loss of organelles and enucleation (Carlile et al, 2004; Ishizaki et al, 1998; Zandy et al, 2005; Zermati et al, 2001). Chemical inhibition of caspase-like activity in both instances can impair the differentiation and enucleation process. These studies demonstrate that the caspase activity is not involved in cell death per se but rather a specific remodelling event that leads to a change in cell fate. Of interest, the caspase activation during erythroblast enucleation has been linked to the cleavage of the nuclear proteins lamin B and acinus (Zermati et al, 2001). These caspase nuclear targets participate in the loss of nuclear integrity and chromatin condensation during apoptosis. DNA fragmentation also accompanies enucleation of these differentiating cells, although the participation of CAD has not been explored (Launay et al, 2005).

Clearly, processes where caspase activity has been linked to the removal or deconstruction of cellular organelles indicates that caspase proteins must be tightly regulated so as not to progress to a cell death event. A picture of one mechanism that may participate in protecting the overall cellular integrity whilst selective structures are removed has been noted during erythroblast differentiation where association of the chaperone Hsp70 to the erythroid transcription factor GATA-1 protects the transcription factor from caspase cleavage during differentiation (Ribeil et al, 2007).

1.2.2 Caspases promote cellular differentiation. The non-cell death phenotype.

Caspase gene ablation in the mouse manifest developmental defects that do not share a clear resemblance to cell death. Caspase 3 null mice are born below Mendalian ratios and display perinatal lethality (Kuida et al, 1996). Caspase 3 ablation presents overt developmental defects including neuronal dysphasia, reduced skeletal muscle mass and bone ossification (Fernando et al, 2002; Kuida et al, 1996; Miura et al, 2004). Caspase 7 shares extensive homology and substrate specificity with caspase 3 and it is suggested that caspase 7 may compensate for the loss of caspase 3 activity (Lakhani et al, 2006). Of interest, caspase 7 null mice develop normally, however mice that are deficient for both caspase 3 and 7 die at birth owing to defective cardiac development (Lakhani et al, 2006). Additionally, caspase 8 null mice die in utero at E11 also resulting from impaired cardiac and vascular development (Varfolomeev et al, 1998). Caspase 9 null mice, similar to caspase 3 null mice, are also perinatal lethal and have marked neuronal dysphasia (Kuida et al, 1998).

The observed developmental deficits present in the caspase null models are suggestive of but not conclusive that caspase activity moderates or impacts cell function beyond cell death. These studies were uniformly interpreted as confirming a crucial role

for caspase activity in the removal of cells and sculpting of the developing embryo rather than a non-death role per se. However, many of the prototypical morphology associated with apoptosis is also a feature of cell differentiation including remodelling of microtubules, membrane deformations and changes to nuclear morphology (see above). Subsequently, the enzymatic activity of caspase 3 has been shown to be critical for the differentiation of macrophages, neuronal stem cells, cardiomyoctes, osteoblasts, embryonic and hematopoietic stem cells and skeletal muscle (Abdul-Ghani et al, 2011; Fernando et al, 2005; Fernando et al, 2002; Fujita et al, 2008; Janzen et al, 2008; Miura et al, 2004). The cardinal difference in the activation of caspase 3 in these various cell lineages with caspase activation during cell death appears to be in the duration and intensity of protease activity, i.e. differentiating cells have a transient induction of caspase activity followed by a return to basal levels, whereas apoptotic cells engage sustained high level caspase activation (Fernando & Megeney, 2007).

Pronounced neuronal dysplasia observed in both caspase 3 and 9 null mice indicates a critical role for caspases in regulating neuronal cell number during embryogenesis. Loss of caspases clearly impacts the apoptotic removal of excessive neuronal cells during development (Kuida et al, 1998; Kuida et al, 1996). Compounding this pathology the perturbed differentiation of neuronal progenitor cells may also contribute to the increase in cell number. Modelling neuronal differentiation in isolated neuronal stem cells (NSC) revealed that transient activation of caspase 3 influenced the activity of pro-neurogenic kinases (Fernando et al, 2005). In turn, blockade of caspase activity led to a significant reduction in the differentiation of numerous neuronal cell types including astrocytes, oligodendrocytes and neurons proper, however there was limited impact on the cell death process that is known to occur during differentiation

(Fernando et al, 2005). In addition, caspase activity has been suggested to contribute to correct cytoskeletal rearrangements and cell dispersal during neuronal differentiation (Rohn et al, 2004). In vivo non-apoptotic caspase 3 activity has been localized to the developing cerebellar cortex present in both proliferating and differentiated neuronal cells of the ventricular zone and the external granular layer (Oomman et al, 2004; Oomman et al, 2006). The development of postnatal Bergman glia cells in the cerebellum are also associated with a transient activation of caspase 3 during differentiation, with activity peaking in rats by day 15 following birth in the absence of appreciable evidence of apoptosis (Finckbone et al, 2009; Oomman et al, 2006).

Cardiac deformities are presented in both caspase 8 and caspase 3/7 null mice suggesting a potential role for this conduit in the development of this organ (Lakhani et al, 2006; Varfolomeev et al, 1998). Abdul-Ghani et al have demonstrated the participation of non-canonical Wnt11 in signalling the activation of caspase 8 and caspase 3 in differentiating cardiomyoctes (Abdul-Ghani et al, 2011). This activity promotes the repression of canonical Wnt signalling by cleavage inactivation of β-catenin.

1.3 Skeletal muscle differentiation

Cellular differentiation of skeletal muscle, myogenesis, is initiated when muscle progenitor cells, myoblasts, exit the cell cycle and revamp gene expression to manufacture genes dedicated to muscle function. Ultimately these events lead to muscle cell fusion to form multinucleated myotubes that are the precursor to the fully differentiated myofiber of the organism (Figure 3). Molecular characterization of this event has benefited from the ability to model this process in vitro with isolated myoblasts and the unambiguous outcome of the process. A hierarchy of master regulatory transcription factors (MRFs/myogenic regulatory factors) operates in a feed forward

mechanism to induce changes in gene expression during myoblast differentiation (Tapscott, 2005). These transcription factors are a related group of 4 basic helix-loop-helix (bHLH) proteins, MyoD, Myf5, myogenin, and Mrf4, that display temporal activation during myoblast differentiation (Berkes & Tapscott, 2005; Olson & Klein, 1994). Furthermore, the bHLH proteins activate/recruit additional transcription factors and mediate changes in the core promoter recognition complexes (Deato et al, 2008; Puri & Sartorelli, 2000).

In vertebrate development, muscle progenitor cells originate from the somites along the neural tube that eventually give rise to the myotome. The cells that locate to the dorsal myotome, the dermomyotome, will give rise to the skeletal muscle of the trunk and limbs (Buckingham, 2006). Lineage tracing studies have identified that the muscle precursor cells initially do not express MRFs but rather are specified by the expression of the homeodomain transcription factors Pax3 and Pax7 (Hutcheson et al, 2009; Relaix et al, 2005; Schienda et al, 2006). This population is proliferative and members will delaminate from the dermomyotome and begin the migration into the limb bud. External signals such as sonic hedgehog (shh) and wingless (Wnt) are believed to impart the determination of the migrating cells to muscle by activating the MRFs, Myf5 and MyoD (Buckingham & Vincent, 2009). The presence of Myf5 or MyoD is required for this specification as ablation of both genes results in the absence of skeletal muscle in the limbs (Rudnicki et al, 1993). This interference imparts an inability of the precursor cells to localize to sites of myogenesis resulting in the adoption of different cell fates (Tajbakhsh et al, 1996). Following determination the cells are directed to exit the cell cycle and differentiate, here MyoD is further required for transcriptional events during differentiation, such as the induction and activity of myogenin (Tapscott, 2005).

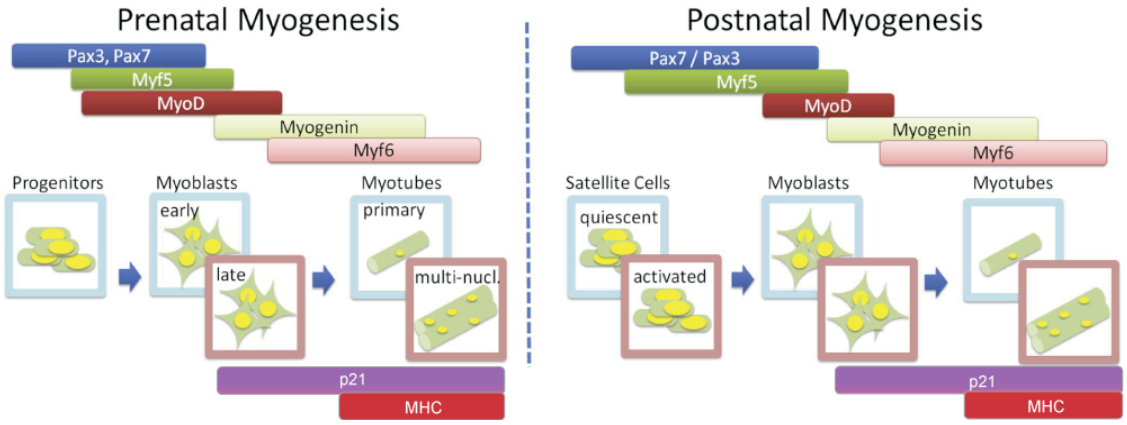

Figure 3. Skeletal muscle differentiation. The progression of myogenic cells through differentiation to terminally differentiated myotubes requires progressive transcriptional regulation by the Paired homeodomain proteins and the myogenic regulatory factors. Parallel to the upregulation of myogenin during differentiation is the upregulation of the cell cycle inhibitor p21. Upon reaching late differentiation the production of muscle structural proteins such as myosin heavy chain (MHC) is observed. (Modified from Rubin et al, 2010; reprinted by permission from Elsevier Ltd: Cancer Cell 19(2):177-91©2011)

Adult vertebrates have retained the capacity for skeletal muscle differentiation, which gives the organism the capability of growth and for the repair of damaged muscle tissue. A muscle stem cell or satellite cell (SC) population resides in the basal lamina along the muscle tissue and are marked by the expression of Pax7 (Seale et al, 2000). These cells exist in a primarily quiescent state until muscle injury activates the satellite cell population. The activated SC will then exit the basal lamina and increase the expression of Pax7 and MyoD allowing the cell to undergo multiple rounds of replication and migrate into the site of injury. At the end of this bout of replication the cells will begin to upregulate myogenin and down regulate Pax7, exit the cell cycle, and begin to differentiate. To ensure self renewal of the SC population, a small number of the activated cells will retain their expression of Pax7, lose the expression of myogenic genes, and return to a quiescent state under the basal lamina (Le Grand & Rudnicki, 2007).

Additional transcription factors coordinate and cooperate with the MRFs during skeletal muscle differentiation including the myocyte enhancer factor-2 (MEF2). MEF2 members belong to the MADS domain proteins that can synergistically act with MRFs at muscle specific gene promoters to enhance expression (Olson et al, 1995). Additional post-translation modification of the MRFs and MEF2s such as kinase phosphorylation by the p38 family of mitogen activated kinases (MAPK) contributes to the feed forward transcriptional program (Tapscott, 2005).

1.3.1 Caspase activity during skeletal muscle differentiation.

The marked reduction in the skeletal muscle mass of caspase 3 null mice was an observation difficult to reconcile with aberrant apoptotic signalling, prompting the examination of a cell autonomous role for caspase 3 during skeletal muscle differentiation

(Fernando et al, 2002). Myoblasts isolated from caspase 3 null animals showed a clear deficiency to differentiate into multinucleated myotubes compared to heterozygous or wildtype littermates (Figure 4A). Enzymatic activity of caspase 3 transiently increased during skeletal muscle differentiation peaking by 24 hours of differentiation (Figure 4B). Further inhibition of caspase 3 activity by chemical inhibition elicited a differentiation deficit similar to the caspase 3 null myoblasts (Figure 4C). Additionally both caspase 8 and caspase 9 are also activated during differentiation (Fernando et al, 2002; Murray et al, 2008). Although the mechanism of the initiator caspase activation remains unclear, over expression of the pro-survival Bcl-2 family member Bcl-xl can block the activation of caspase 9 and subsequently caspase 3 impairing differentiation (Murray et al, 2008). This effect appears to be unrelated to extensive loss of mitochondrial membrane integrity, although this observation would benefit from further scrutiny. Finally, over expression of ARC, an inhibitor of caspase 8, can also effect the myogenic differentiation program in rat H9C2 cells (Hunter et al, 2007). The activity of caspase 3 is clearly required for skeletal muscle differentiation, yet little has been elucidated in terms of defining the substrates that promote this outcome.

1.4 Physiologic non-death functions of DNA strand breaks.

The morphological and biochemical parallels between cell differentiation and apoptotic cell death strongly suggest a conservation of mechanisms that promote these disparate outcomes. An additional and less expected similarity in these cell fate outcomes may involve the induction of DNA strand breaks. The extensive DNA fragmentation observed during apoptosis has been traditionally considered a detrimental event, leading to the irreparable destruction of the cell (Samejima & Earnshaw, 2005). However, DNA damage is well documented to incite oncogenic mutations that

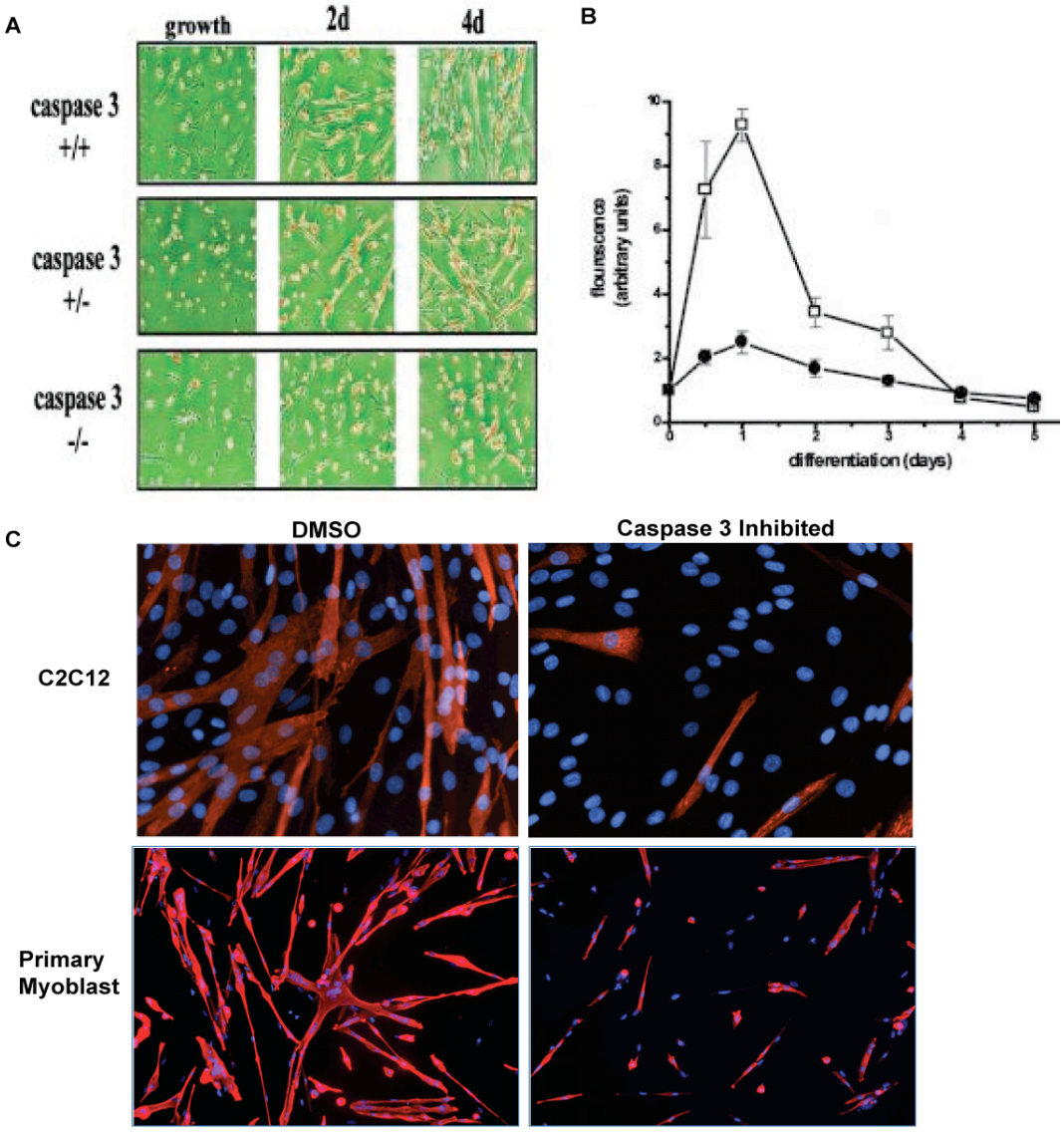

Figure 4. Caspase 3 activity promotes the differentiation of skeletal muscle. A) Caspase 3 null myoblasts show a cell autonomous defect in differentiation compared to there wildtype and heterozygous litter mates. As demonstrated by the impaired formation of multinucleated myotubes by null myoblasts following induction to differentiate. B.) Caspase 3 (□) and 8 (●) activity is transiently increased during C2C12 myoblast differentiation. (Panels A and B reprinted from Fernando et al. 2002 with permission from the National Academy of Science: PNAS. 99(17):11025-30©2002) C.) Chemical inhibition of caspase 3 activity impairs differentiation of both C2C12 myoblasts and Primary myoblasts. As demonstrated by the reduced formation of myosin heavy chain positive multinucleated myotubes in treated cells compared to the vehicle only control following induction to differentiate.

dramatically enhance the growth capacity and mortality of the affected cell (Hanahan & Weinberg, 2011). Moreover, there is a growing body of evidence to suggest that focal DNA damage can be utilized to promote a number of normal cellular functions. Specifically, controlled DNA strand breaks have been demonstrated to propagate alterations in gene expression. These break induced alterations in gene expression are generally subdivided in two classes, with DNA damage events associated with a requirement (or not) for follow on recombination. DNA strand breaks that give rise to the plethora of antibody production and responses such as those required for adaptive immunity or those that propagate meiotic crossover, generally involve a follow on recombination event (Jung & Alt, 2004; Li & Ma, 2006). More recent studies have demonstrated the utilization of breaks without follow on recombination can promote gene expression independent of cell death (Haffner et al, 2010; Ju et al, 2006).

1.4.1 Controlled DNA strand breaks are the molecular basis for adaptive immunity

Adaptive immunity is the mechanism whereby vertebrate organisms respond to microbial infections. The key cellular responders of this process, lymphocytes, generate unique antigen receptors by regulated DNA strand breaks that act to directly edit the genome within the antigen receptor genes (Jung & Alt, 2004). DNA strand breaks are first utilized for V(D)J recombination then for class switch recombination (CSR) and somatic hypermutation (SHM). V(D)J recombination is initiated by the RAG recombinases, RAG1 and RAG2, that bind to and cleave DNA at recombination signal sequences (RSS) that flank the variable (V), diverse (D) and joining (J) elements. When cleaved, a coding and RSS DNA ends are generated, where the RSS end is then precisely ligated, and the coding end is processed in such a way that may involve nucleotide loss or

gain preceding the ligation step. This addition or removal of nucleotides then provides the genetic variation required for variable antigen receptor generation (Jung & Alt, 2004).

Additional antigen receptor diversity is imparted by CSR and SHM that again utilize DNA strand breaks to further modulate the coding region. Both of these modifications require the activation-induced cytidine deaminase (AID) that can instigate the induction of a single stranded DNA break during the repair of an enzymatic deamination of deoxycytidine to deoxyuracil (Xu et al, 2005). During CSR, AID induces ssDNA breaks on both sides of the DNA within the switch regions that are positioned between respective immunoglobin chain constant region genes (Xu et al, 2005). The ssDNA breaks progress to double stranded DNA breaks (DSB) that are required for the switch recombination. SHM also involves these ssDNA breaks within the rearranged V region to improve efficacy of the receptor (Zan et al, 2003). SHM has also been shown to benefit from the activity of DNase Y, an endonuclease that can induce DSBs specifically in the V region however not in the S regions (Okamoto et al, 2005; Okamoto et al, 2009). Additionally, Endonuclease G has been suggested to participate in CSR through the induction of AID independent double stranded breaks within the switch region (Zan et al, 2011).

1.4.2 Topoisomerase II induced DNA strand breaks regulate transcription.

DNA structure can present several topological constraints that may limit or act as a natural barrier for regulated/physiologic strand break induction. During transcription and replication the processive unwinding of the double helix will result in over- and under-winding of adjacent regions. This topological strain is resolved by DNA topoisomerases, enzymes that pass one segment of DNA through a break in another. This activity has been suggested to regulate transcription at the elongation step by relieving

RNA polymerase II induced supercoils (Mondal & Parvin, 2001). Additionally a more direct role in regulating gene expression has emerged for topoisomerase II beta (Topo IIB), specifically through the induction of DNA strand breaks within the promoter elements of glucocorticoid responsive genes (Haffner et al, 2010; Ju et al, 2006).

TopoIIB has been observed to be recruited to the promoter elements of a number of glucocorticoid responsive genes in Michigan Cancer Foundation (MCF) -7 cells (Ju et al, 2006). This recruitment stimulated the activity of TopoIIB to induce a site specific break, which signalled the localized induction of PARP-1 activity to poly(ADP-ribosyl)ate histone H1. This modification to histone H1 facilitated the exchange for HMGB1/2 at specific nucleosomes, which was stimulatory for the expression of a glucocorticoid responsive gene, following repair of the break. Inhibitors to either Topo IIB or PARP-1 prevent the nucleosome specific exchange of H1 for HMGB1/2 that impedes the expression of the stimulated gene (Ju et al, 2006). The participation of TopoIIB induced breaks in glucocorticoid stimulated gene expression may be a conserved event as a similar response has been noted for androgen mediated signalling in prostate cell lines (Haffner et al, 2010). These observations indicate that through a site specific DNA strand break the local chromatin topology can be changed to alter the expression of a specific gene. Given that the targeted strand breaks are occurring simultaneously at numerous loci, the observations above suggest a novel mechanism for radical genome wide reprogramming of gene expression.

1.4.3 Repair of DNA strand breaks

Clearly, undirected DNA damage can pose as an existential threat to the life of a cell. As such, utilization of DNA strand breaks to coordinate gene expression would require an equally robust DNA repair mechanism to limit the negative repercussions of

unrepaired or excessive DNA damage. Indeed the cell is able to respond to a diverse array of genotoxic insults through a number DNA damage repair pathways (Figure 5) (Ciccia & Elledge, 2010). Many aspects of how a cell copes and repairs stochastic DNA damage have been implicated in the repair of directed breaks.

Homologous recombination-mediated repair (HRR) is a high fidelity method of DNA repair, provided the cells have access sister chromatids. DNA strand breaks encountered during S and G2 phases of the cell cycle activate this mechanism of repair. The undamaged sister chromatid is used as a template to repair damage presented on the other chromatid. This repair pathway also responds to the SPO11 induced breaks that promote recombination during meiosis (Li & Ma, 2006). In the absence of a sister chromatid, double stranded DNA breaks are directly resected through non-homologous end joining (NHEJ). This process involves the rapid association of Ku to the ends of the break followed by the recruitment and activity of DNA-PK that directs the end processing and subsequent ligation. DNA strand breaks associated with V(D)J recombination are resected in this manner (Lieber et al, 2004). In the absence of functional DNA-PK, an alternative NHEJ (alt-NHEJ) mechanism has been proposed, here PARP-1 can rapidly accumulate to the end of the DNA strand breaks promoting the resectioning through the MRN complex, the scaffold protein XRCC1, and DNA Ligase III (Ciccia & Elledge, 2010; Wang et al, 2006). Interestingly the repair of the TopoIIB induced breaks in glucocorticoid stimulated cells involves both recruitment and activity of PARP-1 and KU/DNA-PK to the ends of the breaks, however the ligase ability of TopoIIB is employed to seal the break (Ju et al, 2006).

1.4.4 DNA strand breaks and cellular differentiation.

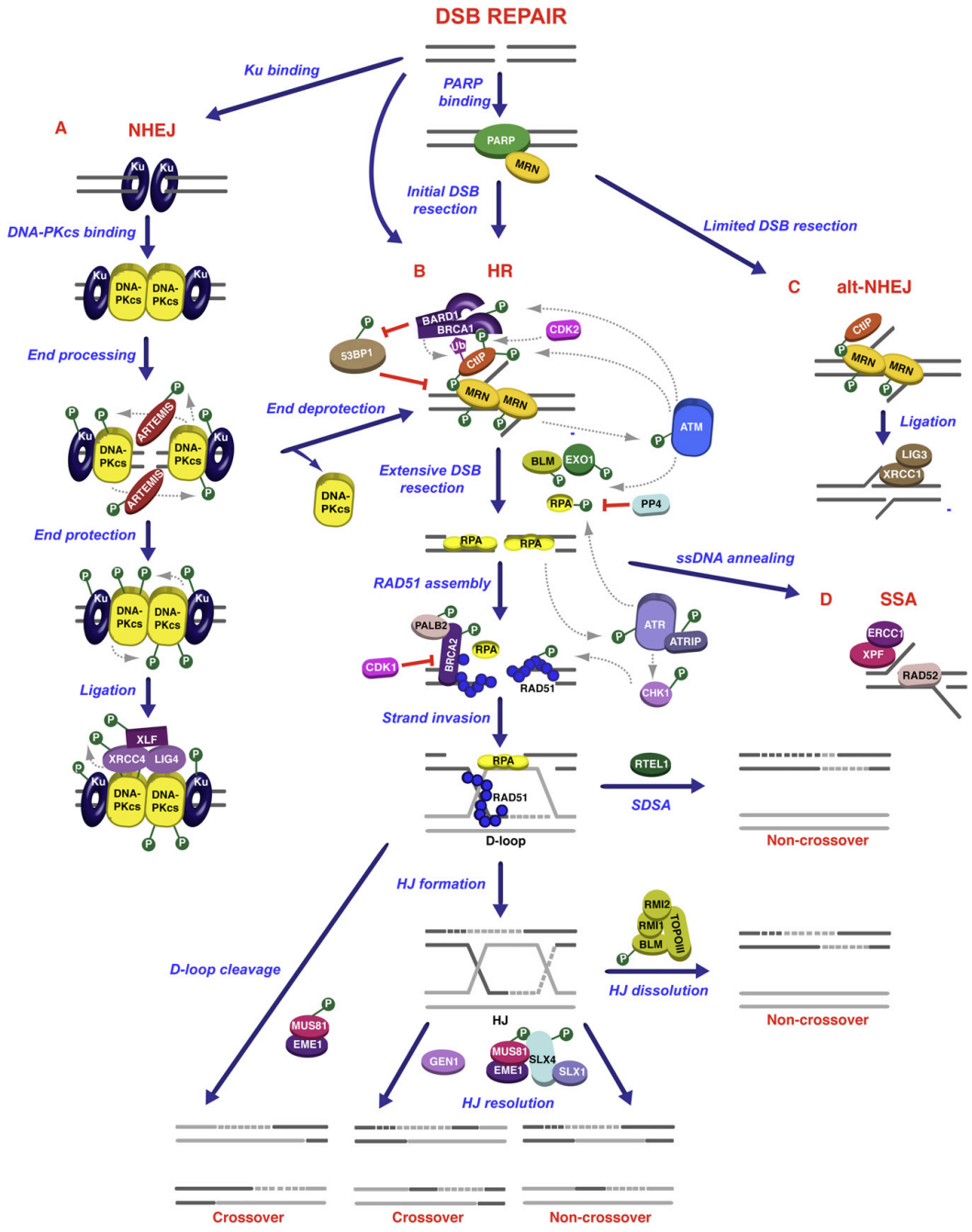

Figure 5. Mechanisms of DNA damage repair. A) The rapid recruitment of Ku to the DNA ends of a DSB facilitates DNA-PK binding that subsequently promotes the resectioning of the strand break by NHEJ. B) PARP binding to the break can promote HRR in the presence of a sister chromatid, or C) the activation of the alt-NHEJ. D) The repair of single strand DNA breaks can also be promoted by PARP involving the recruitment of Rad52. (reprinted by permission from Elsevier Ltd: Mol Cell 40(2):179-204©2010)

Stochastic DNA damage in some cells types have yielded a surprising observation the induction of terminal differentiation. For example, extensive DNA damage in melanocyte stem cells conspicuously prompts cell cycle exit and differentiation to mature melanocytes in the absence of apoptosis (Inomata et al, 2009). Similarly DNA damage by the photomimetic drug Neocarzinostatin can promote the myogenic differentiation of cultured Drosophila Schneider cells (Hossain et al, 2003). The mechanism by which DNA damage elicits the induction of differentiation in these circumstances remains unknown. Nevertheless, a distinct possibility is that the DNA damage and subsequent repair response of the cell orchestrates a genome wide reorganization of chromatin to alter the gene expression landscape, akin to the role of topoisomerase in glucocorticoid mediated signalling.

A number of studies have suggested that DNA strand breaks accompany the early stages of skeletal muscle differentiation (Dawson & Lough, 1988; Farzaneh et al, 1985). The breaks appear to be transient and additionally correspond to increased activity of PARP-1 (Farzaneh et al, 1985). Despite these observations the significance of this occurrence to the skeletal muscle differentiation process has remained undetermined. Interestingly, this transient event parallels the observed caspase 3 activity profile during differentiation, presenting an intriguing possibility of a mechanistic relationship between the two events that will be explored in this thesis. Indeed, the obligate caspase signal, caspase 3 directed activation of CAD (caspase activated DNase) may function in a manner analogous to the glucocorticoid directed activation of TopoIIB, inducing DNA strand breaks to direct changes in gene expression and cell fate independent of cell death.

1.5 Hypothesis

DNA strand breaks induced by caspase 3 activity are required for skeletal muscle differentiation.

1.6 Aims

1. Characterize the occurrence and significance of DNA strand breaks during differentiation of skeletal muscle.
2. Determine the mechanism inflicting DNA strand breaks during differentiation of skeletal muscle and effect inhibition of this mechanism has on differentiation.
3. Determine the involvement of DNA damage repair in responding to the formation of DNA strand breaks during differentiation.

Chapter 2: Caspase 3/Caspase Activated DNase Promote Cell Differentiation by Inducing DNA Strand Breaks

Caspase 3/caspase-activated DNase promote cell differentiation by inducing DNA strand breaks.

Brian D. Larsen [a,b], Shravanti Rampalli [a,b], Leanne E. Burns[a,b], Steve Brunette[a], F. Jeffrey Dilworth[a,b], and Lynn A. Megeney [a,b, 1]

Published: March 2, 2010, Proceedings of the National Academy of Science, volume 107, number 9, pages 4230-4235.

Contribution of Co-Authors

Dr. Shravanti Rampalli of Dr. F. Jeffrey Dilworth's laboratory provided the CAD and Mock ChIP samples used in Figure 4C. Leanne E. Burns took a lead role in the collaboration to examine DNA strand breaks in differentiating myoblasts by the single cell electrophoresis assay (Supplemental Figure 1) and assisted in the characterization of the C2C12 CAD knockdown cells (Figure 3B and Figure 4A). Steve Brunette contributed in the generation of the mutant ICAD constructs used in Figure 2E. Dr. Lynn A. Megeney contributed in experimental design and writing of the manuscript.

Abstract

Caspase 3 is required for the differentiation of a wide variety of cell types, yet it remains unclear how this apoptotic protein could promote such a cell fate decision. Caspase signals often result in the activation of the specific nuclease caspase activated DNase (CAD), suggesting that cell differentiation may be dependent on a CAD mediated modification in chromatin structure. In this study we have investigated whether caspase 3/CAD plays a role in initiating the DNA strand breaks that are known to occur during the terminal differentiation of skeletal muscle cells. Here we demonstrate that inhibition of caspase 3 or reduction of CAD expression leads to a dramatic loss of strand break formation and a block in the myogenic program. Caspase dependent induction of differentiation results in CAD targeting of the p21 promoter, and loss of caspase 3 or CAD leads to a significant down regulation in p21 expression. These results demonstrate that caspase 3/CAD promotes cell differentiation by directly modifying the DNA/nuclear micro-environment, which enhances the expression of critical regulatory genes.

Introduction

Differentiation is a deterministic process that ensures cell specialization in complex organisms. In general terms, the cellular diversity that originates from differentiation has been attributed to the activation of lineage specific transcription factors (1, 2). Despite the propensity to consider differentiation as a tissue specific event, emerging evidence suggests that this cell fate choice may also be dependent on the activity of a common signal pathway or protein. One factor that appears to be highly conserved in the induction of differentiation is the caspase 3 protease (3). Caspase 3 was originally identified as the penultimate step in apoptotic/programmed cell death pathways, acting to cleave vital protein substrates through aspartic acid directed targeting (4). Subsequently, transient caspase activation has been reported to be indispensible for maturation of numerous cell lineages, across a broad range of species (3, 4).

The mechanism by which caspase 3 promotes non-death outcomes remains poorly defined. A number of studies have demonstrated that differentiation is dependent on caspase cleavage of select kinase substrates (5-7). For example, caspase 3 induction of skeletal myoblast differentiation is associated with the cleavage activation of the ste-20 like kinase MST1. However, restoration of active MST1 in caspase null myoblasts provides only a partial rescue of the differentiation defect, indicating that caspase activity must engage additional substrates to promote or sustain non-death cell fate outcomes (6). Other reports have demonstrated that caspase 3 regulates differentiation indirectly, by targeting and inactivating proteins that maintain stem cell self-renewal/pluripotency (8, 9). Although these later interactions contribute to the caspase effect, the targeting of

these proteins does not explain the widespread alterations in gene expression and genomic reprogramming that typify differentiation.

One hallmark of caspase mediated apoptosis that may also propel cell differentiation is chromatin alteration and DNA damage/fragmentation. A select handful of nucleases have been implicated in apoptotic DNA fragmentation, caspase activated DNase (CAD) being the most characterized (10). CAD is held in check through association with its inhibitor, ICAD, which is cleaved by caspase 3 to release CAD (10, 11). Following activation, unobstructed CAD configures into a scissor like dimer, cleaving DNA with minimal sequence specificity (10, 12). CAD is also ubiquitously expressed, suggesting a highly conserved function for this nuclease.

Although DNA damage is considered to be detrimental to cell integrity, DNA strand breaks have been demonstrated to coordinate physiologic changes in gene expression independent of cell death. For example, V(D)J recombination is a mechanism in which DNA strand breaks precede a recombination event to generate variable expression of antigen receptor genes (13). In addition, a recent study has suggested that glucocorticoid mediated gene expression is dependent on the formation of a strand break in target promoter elements, whereby the DNA damage acts to facilitate nucleosome reorganization toward an active conformation, allowing gene expression to proceed (14). Interestingly the appearance of transient DNA strand breaks during in vitro skeletal muscle differentiation and in vivo regeneration have been documented (15-17).Although the role of DNA damage was not investigated, these studies suggested an intriguing hypothesis that the differentiation process maybe dependent on controlled DNA damage events.

Here, we investigated the role of caspase 3/CAD mediated DNA strand breaks as a prerequisite for inducing cell differentiation. We demonstrate that the caspase activation of CAD participates in the formation of transient genome wide DNA damage/strand breaks during early stages of the skeletal muscle differentiation. Reduction in CAD leads to absence of strand break formation with a near complete blockade of differentiation. In turn we demonstrate that caspase 3/CAD activity induces strand breaks in the promoter of a critical cell cycle regulatory factor p21, strand breaks that are associated with the induction of p21 gene expression.

Results and Discussion

Transient DNA Strand Breaks are Detectable During Myoblast Differentiation

We initially monitored DNA strand break formation in individual myoblasts using single cell gel electrophoresis (COMET assay). Myoblasts displayed evidence of DNA strand breaks between 12 and 48 h post low serum induction of differentiation that were qualitatively different from the DNA fragmentation associated with apoptosis (Fig. S1). This biochemical assay demonstrated accumulation of DNA damage during myoblast differentiation, however this assay was limited in the ability to discriminate DNA damage associated with healthy or early apoptotic cell types.

Therefore, to confirm the cellular status associated with the DNA strand break formation, we used in situ nick translation (ISNT) coupled with fluorescence microscopy. This technique uses the enzymatic ability of DNA Polymerase I to recognize and repair single stranded (ss) DNA breaks in cells and to incorporate labeled nucleotides (15, 18, 19). Applying this technique to proliferating C2C12 myoblasts demonstrated no incorporation of the labeled nucleotide, yet induction of apoptosis with Actinomycin D, or post fixation treatment with DNase I demonstrated robust nuclear incorporation (Fig. S2). Subsequently, ISNT was utilized to monitor the appearance of strand breaks during the progression of C2C12 and primary myoblast differentiation program, this protocol was coupled with DAPI nuclear counter stain to assess nuclear integrity. Within 12 h post low serum induction of differentiation, a significant portion of the healthy non-apoptotic myoblast population, both in C2C12s and primary cells displayed robust label incorporation (~70%; Fig.1A and C). Strand break formation was transient, C2C12 cells

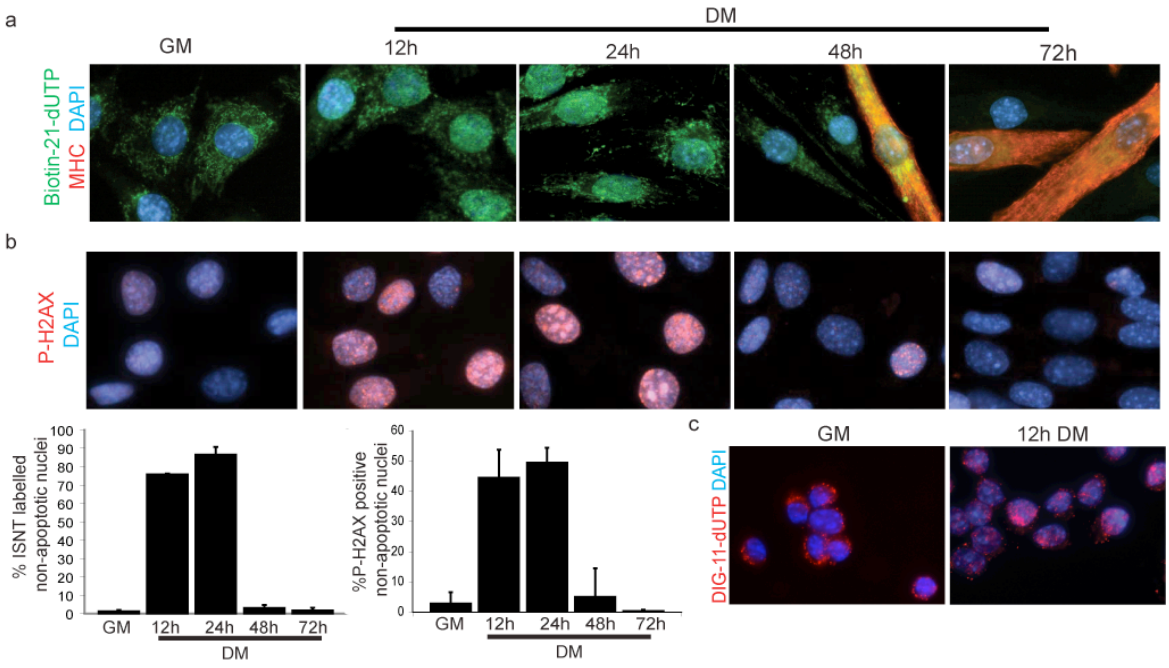

Fig. 1. Transient DNA strand breaks are detected early during C2C12 myoblast differentiation. (A) ISNT labels methanol-fixed C2C12 nuclei at 12 and 24 h after being switched from growth media (GM) to low serum differentiation media (DM). Cells were stained for incorporated biotin-21-dUTP (green), myosin heavy chain (MHC) (red), and DAPI (blue). (Error bars are SD). (B) Phosphorylated H2AX foci are detected in differentiating C2C12 myoblasts at 12 and 24 h after low serum induced differentiation. Cells were fixed with 95% ethanol and 5% acetic acid and stained for P-H2AX (red) and DAPI (blue). (Error bars are SD). (C) ISNT labels fixed primary myoblast nuclei at 12 h when switched to DM. Cells were stained for incorporated DIG-11-dUTP (red) and DAPI (blue).

reached an apex early in the differentiation program (85% of muscle cells at 24 h), followed by an equally rapid disappearance of strand break formation by 48 h (Fig. 1A and C). Primary muscle cells displayed a more rapid disappearance of strand breaks by 24 h. Collectively, these results demonstrate that the viable muscle cells population is subject to extensive DNA damage/strand break formation during differentiation.

The transient nature of the DNA nick/strand breaks suggested that an active DNA repair process was engaged. ATM (ataxia-telangiectasia mutated) is a member of a serine/threonine kinase family that consists of ATR and DNA-protein kinase (PK), all of which respond to DNA strand breaks (20). ATM/ATR/DNA-PK phosphorylates and activates DNA repair proteins such as Histone 2A family member X (H2AX), which act to stabilize the multi-protein complexes which facilitate the repair of DNA strand breaks (21). To examine the activation of the DNA repair process, the phosphorylation of the histone H2A variant H2AX was examined. Phospho-H2AX foci were observed in the vast majority of the differentiating muscle cells, suggesting an active and coordinated repair of strand breaks during myoblast differentiation (Fig. 1B). Importantly, we noted an absence of ISNT detectable DNA strand breaks and phospho-H2AX foci in HeLa cells when transferred to low serum conditions (Fig. S3), suggesting that the low serum conditions used to differentiate myoblasts did not induce the observed DNA strand breaks and subsequent repair.

Caspase 3 Induces DNA Strand Breaks Through the Activation of CAD

Caspase 3 activity has been shown to be a cell autonomous requirement for skeletal myoblast differentiation, with an activation profile that parallels the formation of the observed DNA strand breaks (6). When differentiating C2C12 myoblasts were treated

with caspase 3 peptide inhibitors, the ensuing blockade in myoblast differentiation was accompanied by an almost complete absence of DNA strand break formation as detected by ISNT (Fig. 2A, Fig. S4). In addition, there was a notable reduction in the DNA damage repair response following caspase 3 inhibition, as measured by the reduction in number of phosphorylated H2AX positive nuclei accompanied with a visual decrease in the intensity of the staining in the remaining positive nuclei (Fig. 2B). We speculate that the ability of the cell to monitor and detect internal DNA strand breaks and elements of the repair process, as measured by phosphorylation of H2AX, appears more qualitative that the ISNT technique in fixed cells. As such, labelling of H2AX is able to detect DNA strand breaks at a lower threshold. These results establish that caspase 3 activity initiated the formation and eventual repair of DNA strand breaks during myoblast differentiation.

We next examined whether the caspase 3 mediated DNA damage response was associated with activation of CAD. CAD exists in complex with its inhibitor protein referred to as ICAD (inhibitor of caspase activated DNase). Activated caspase 3 cleaves ICAD at two aspartic acid residues (D117 and D224), releasing CAD from inhibition and allowing the DNase to target and fragment DNA (10). Partial ICAD cleavage at D117 was observed during early stages of myoblast differentiation corresponding to the period of DNA strand break formation (Fig. 2C). The cleavage of ICAD at D117 has been demonstrated to be necessary and sufficient for the release of CAD activity during apoptosis (11). We observed that inhibition of caspase 3 activity attenuated the cleavage of ICAD during myoblast differentiation, confirming that the ICAD partial cleavage stemmed from caspase 3 activity (Fig. 2D). No change in CAD expression was observed through the time course examined (Fig. 2C). In addition to ICAD cleavage, we also

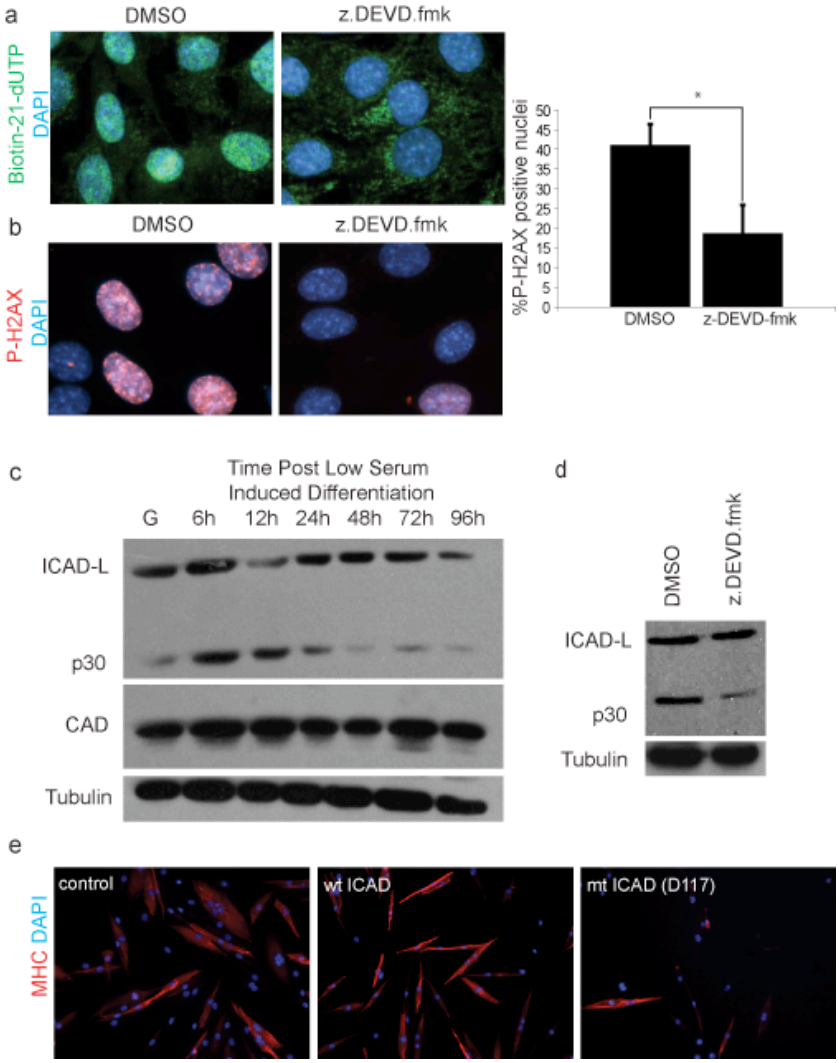

Fig. 2. DNA strand breaks are dependent on Caspase 3 activity. (A) The caspase 3 inhibitor, z.DEVD.fmk, blocks the formation of DNA strand breaks detectable by ISNT. C2C12 myoblasts were induced to differentiate under low serum conditions treated with either 10μM z.DEVD.fmk or DMSO, cells were fixed and stained as in Fig. 1A. (B) Formation of P-H2AX foci at 24h of low serum differentiation are diminished when myoblasts are treated with z.DEVD.fmk. Cells were treated as in A and fixed and stained as in Fig. 1B. (Error bars are SD; $P<0.001$). (C) Partial cleavage of ICAD corresponds to the transient formation of DNA strand breaks in differentiating C2C12 myoblasts. The ratio of p30 cleavage fragment to full length ICAD increase by 4.6-fold at 12h compared to growth. Protein lysates were collected from differentiating C2C12 myoblasts and western blot analysis for ICAD and CAD was performed. Tubulin was used as a loading control. (D) Caspase 3 inhibition impairs the partial cleavage of ICAD observed during differentiation. C2C12 myoblasts were differentiated for 12 h with 10 μM z.DEVD.fmk or DMSO. Protein lysates were collected, and Western blot analysis for ICAD was performed. (E) Expression of ICAD mutated at D117 impairs myoblast differentiation. Myoblasts were transfected with empty pMEV-2HA (control), wildtype-hICAD, or mutant D117E –hICAD. Stable expression was selected with G418, and then, myoblasts were induced to differentiate under low serum conditions. Differentiation was assessed by the upregulation of myosin heavy chain (red).

measured global nuclease activity during myoblast differentiation. Interestingly, lysates derived from differentiating myoblasts displayed temporally sensitive nuclease activity that was consistent with the formation of the caspase-sensitive DNA nicks/breaks (Fig. S5). The partial cleavage of ICAD at D117 lead us to assess the functional significance this event played during myoblast differentiation, by generating pooled stable myoblasts expressing the wild type or mutant D117E human ICAD. Over expression of the mutant ICAD adversely impacted differentiation as demonstrated by impaired myosin heavy chain expression and myotube formation (Fig. 2E).

To directly assess the role of CAD in the caspase mediated differentiation signal, we generated stable myoblast cell lines expressing a short hairpin RNA directed to CAD. The stable myoblast cell lines displayed between 50-60% reduction in CAD expression compared to the negative control shRNA cell line (Fig. 3A). These cells were affected by a profound inhibition in the differentiation program as measured by the failure to generate myosin heavy chain positive myotubes (Fig. 3B). Interestingly, up-regulation of the transcription factor myogenin was unaffected in the CAD shRNA clones, suggesting that CAD regulation of muscle gene expression appears to be specific for a subset of differentiation specific loci (Fig 3C). This observation is consistent with previous reports which demonstrate that inhibition of caspase 3 activity limited myoblast differentiation without negatively impacting myogenin expression (6). The impaired differentiation program in the CAD knockdown cell lines was also preceded by a substantial reduction in the formation of strand breaks (Fig. S6), with a corresponding absence of detectable DNA repair events as measured by phosphorylated H2AX foci (Fig. 3D). Collectively, these

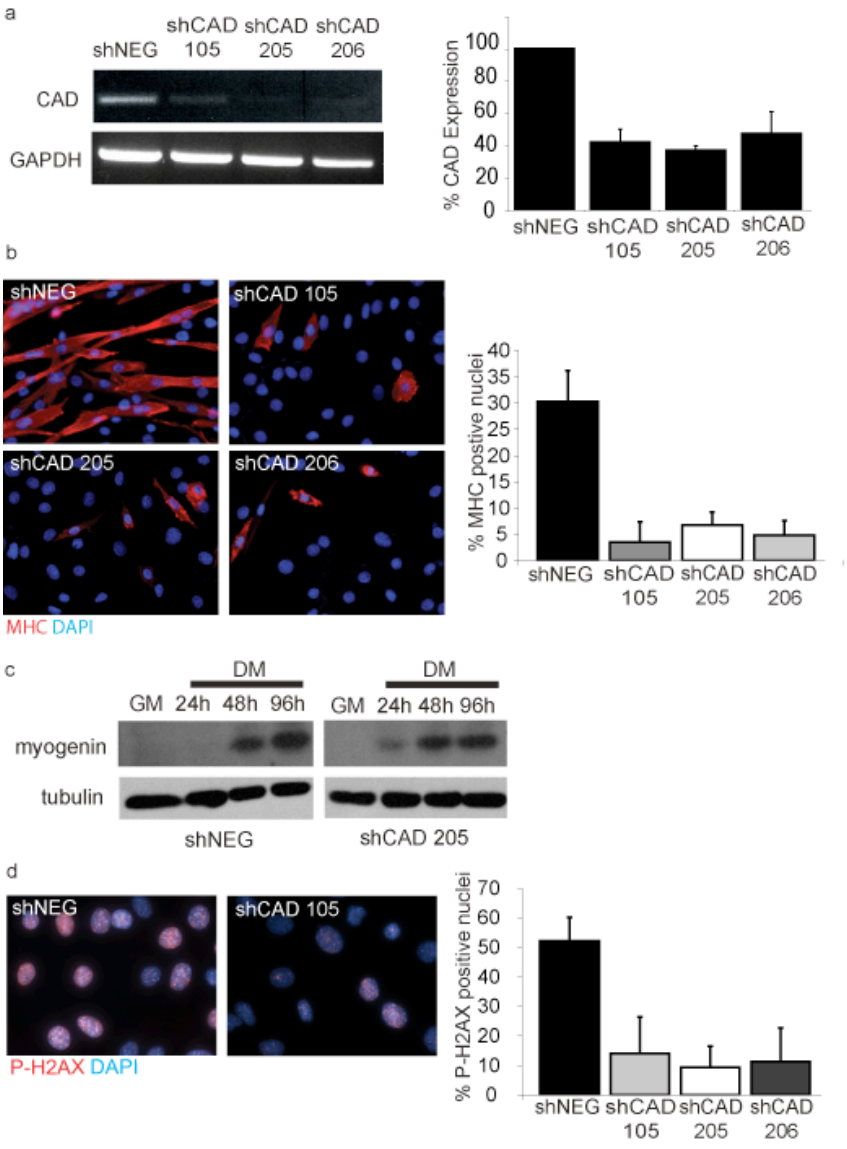

Fig. 3. Stable knockdown of CAD in C2C12 myoblasts affects differentiation. (A) RT-PCR for CAD showing knockdown in stable C2C12 clones with shCAD compared to a C2C12 clone with a negative control shRNA vector. RT-PCR for GAPDH was used as a loading control. (Error bars are SEM) (B) Up regulation of myosin heavy chain is impaired in the stable cell lines compared to negative control. Cells were induced to differentiate for 72 h, fixed, and stained for MHC (red). MHC positive nuclei were counted from three independent experiments. (Error bars are SD). (C) Myogenin expression during differentiation is not affected in the stable cell lines. Protein lysates were collected from differentiating stable cell lines and Western blot analysis for myogenin expression was performed. Tubulin was used as a loading control. (D) Formation of phosphorylated H2AX foci at 24 h differentiation is diminished in shCAD stables compared to negative control. Cells were induced to differentiate for 24 h, fixed, and stained for P-H2AX.

results strongly implicate CAD nuclease activity in promoting skeletal myogenesis through direct DNA damage/strand break formation.

Up-regulation of the Cell Cycle Inhibitor p21 Requires CAD

The profound blockade in differentiation coupled with the failure to reduce myogenin expression in the CAD knock down myoblasts strongly suggests that CAD directs differentiation by activating a general mechanism, rather than engaging a tissue specific or lineage restricted gene expression program. One family of proteins that act as critical regulators of cell differentiation in this regard are the cyclin/CDK inhibitors. For example, the increased expression of the CDK inhibitor p21 (p21CIP/WAF1) is indispensable for differentiation in numerous cell types including skeletal myoblasts, yet is not directly dependent on muscle transcription factor activity (22, 23). Compounds that induce apoptosis or cell cycle arrest (UV, 5-azacytidine) have been demonstrated to induce the expression of p21 while inflicting DNA damage within the p21 promoter (24-26). We noted that the normal up-regulation of p21 gene expression was impaired in the CAD shRNA clones prompting the examination of a direct role for CAD in regulating p21 expression (Fig. 4A and B).

Activated CAD as well as the CAD-ICAD complex has been demonstrated to form stable complexes with substrate DNA, suggesting that ICAD may be cleaved by caspase-3 in this DNA associated complex to activate CAD in a specific manner (12). This stable association allowed for Chromatin immuno-precipitation (ChIP) with an antibody specific for CAD to precipitate associated genomic regions at 12 and 24 h post induction of differentiation in C2C12 myoblasts. CAD showed strong enrichment

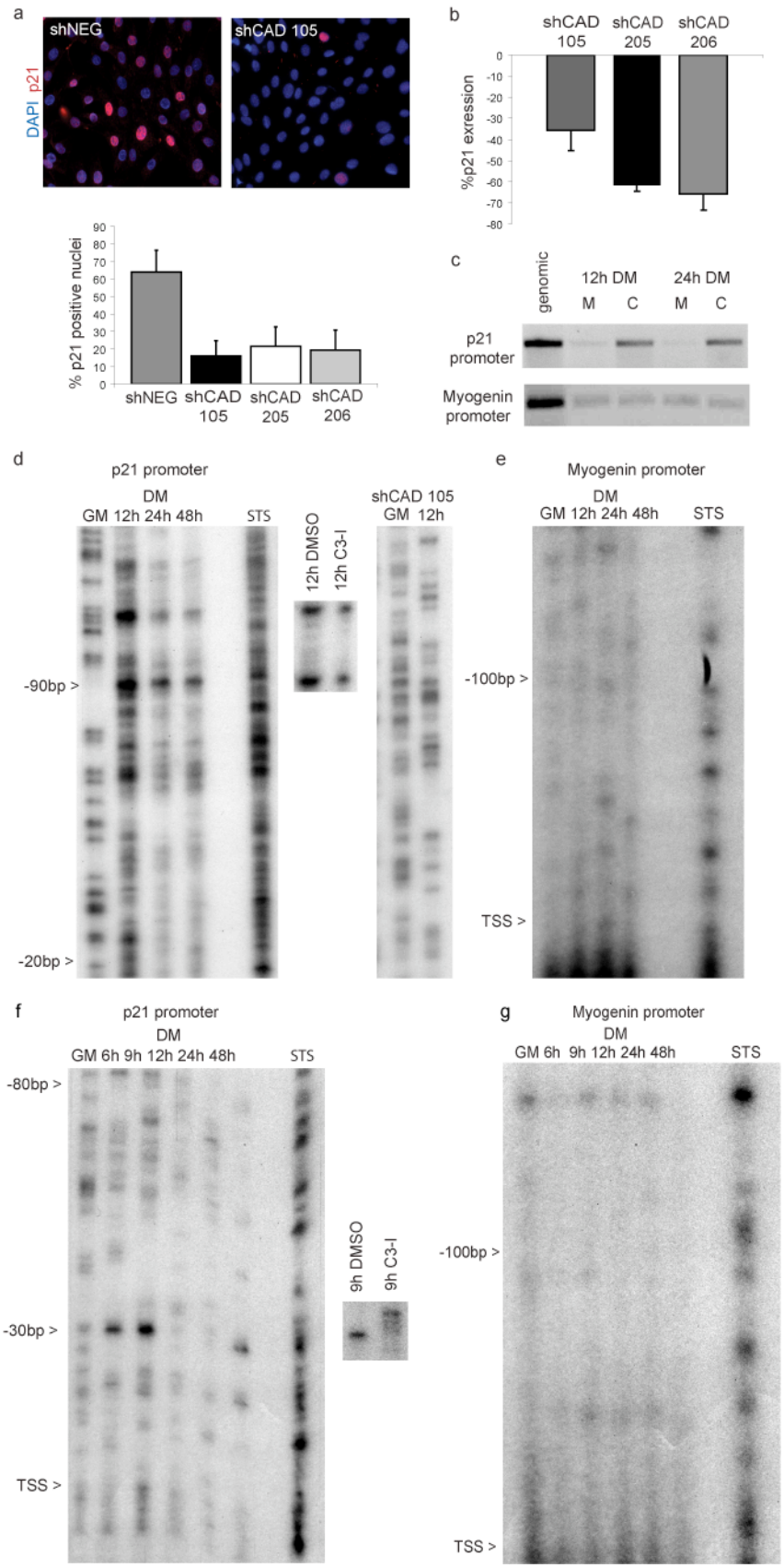
a
shNEG
shCAD 105
DAPI p21
% p21 positive nuclei
shNEG
shCAD 105
shCAD 205
shCAD 206
b
shCAD 105
shCAD 205
shCAD 206
%p21 expression
c
genomic
12h DM
24h DM
M
C
M
C
p21 promoter
Myogenin promoter
d
p21 promoter
DM
GM 12h 24h 48h
STS
12h DMSO
12h C3-I
shCAD 105
GM 12h
-90bp >
-20bp >
e
Myogenin promoter
DM
GM 12h 24h 48h
STS
-100bp >
TSS >
f
p21 promoter
DM
GM 6h 9h 12h 24h 48h
STS
-80bp >
-30bp >
TSS >
9h DMSO
9h C3-I
g
Myogenin promoter
DM
GM 6h 9h 12h 24h 48h
STS
-100bp >
TSS >

Fig. 4. Caspase 3/CAD inflict DNA strand breaks within the promoter of the cell cycle inhibitor p21. (A) Up regulation of the cell cycle inhibitor p21 is reduced in the stable shCAD cell lines compared to negative control. Cells were induced to differentiate for 24 h, fixed, and stained for p21 (red). Nuclei were counter stained with DAPI (blue). p21 positive nuclei were counted from 3 independent experiments. (Error bars are SD.) (B) p21 transcripts levels are reduced in the shCAD cell lines compared to negative control. RNA was isolated 24 hours after the induction of differentiation and subject to semiquantitative RT-PCR. Multiplex PCR to p21 and GAPDH cDNA was run in triplicate for an n=3 experiment. Percent reduction in p21 transcript in the CAD knock down (KD) myoblasts is compared to the negative control line. (C) CAD associates with the p21 promoter during C2C12 myoblast differentiation. ChIP using rabbit IgG (M) or an antibody against CAD (C), shows enrichment at the p21 promoter at 12 (2.5 fold) and 24 h (2.6 fold) after the induction of differentiation; no enrichment was observed of the myogenin promoter. (D and F) LM-PCR delineates the formation of DNA strand breaks within the p21 promoter of differentiating C2C12 and primary muscle cells. Genomic DNA was isolated from proliferating, differentiating, and apoptotic (staurosporine (STS)) muscle cells and subjected to LM-PCR. Primers specific to the p21 promoter allowed analysis of ~200bp prior to the transcriptional start site (TSS; n=3). Inset (D Inset and F Inset) Chemical inhibition of caspase 3 reduces the formation of strand breaks within the p21 promoter. Differentiating C2C12 and primary cells were treated with either 10μM z.DEVD.fmk or DMSO; genomic DNA was extracted and subjected to LM-PCR (n=3). Reduction in CAD expression impairs the formation of strand breaks within the p21 promoter in genomic DNA isolated from shCAD105 cells under low serum conditions (D Inset; n=2). (E and G) LM-PCR shows the absence of robust DNA strand breaks in the myogenin promoter during differentiation of C2C12 and primary muscle cells. Primers specific to the myogenin promoter allowed analysis of ~200bp prior to the TSS. (n=3)

(~2.5 fold) at the p21 proximal promoter at 12 and 24 h differentiation (Fig. 4C). Examination of the myogenin promoter showed no enrichment for CAD at these time points. To localize the formation of strand breaks in the p21 promoter we utilized a modified ligation mediated PCR (LM-PCR) protocol, LM-PCR has been used to map DNA strand breaks that occur during apoptosis as well as site specific strand breaks that result from glucocoticoid stimulation of Michigan Cancer Foundation (MCF)-7 cells (14, 27). Briefly, the DNA linker is ligated to a DNA strand break. Then, directed PCR, with primers that overlap the genomic region of interest, and the DNA linker amplify the target region of interest. Subsequently, the PCR product is radiolabeled and electrophoresised on a sequencing gel to visualize the location of DNA strand breaks. Within 12 h low-serum induction of differentiation, LM-PCR revealed a number of strand breaks in the p21 promoter, occurring within -200bp of the transcriptional start site (Fig. 4D and F). The extent of the strand breaks observed during differentiation were markedly reduced in comparison to those observed under apoptotic conditions further suggesting that strand break formation during differentiation is a well controlled event. Interestingly, reduction in CAD or inhibition of caspase 3 activity during myoblast differentiation led to attenuated formation of strand breaks suggesting that caspase/CAD activity was the primary determinant in strand break formation (Fig. 4D and F). Although we observed consistent formation of DNA strand breaks within the proximal region of the p21 promoter, we noted the positioning of the prominent break differs by ~50 bps between the primary versus C2C12 differentiating myoblasts. This variable positioning in the strand break is likely derived from an epigenetic influence related to the different genetic origin of the primary versus C2C12 myoblasts. Indeed, during apoptosis CAD itself is known to retain only limited (if any) DNA sequence specificity, rather the nuclease appears to rely

on nuclear architecture to position strand breaks. We further examined the myogenin promoter and found no evidence of strand breaks within -200 bp of the transcriptional start site during the induction of differentiation (Fig 4E and G).

Collectively, our observations suggest that CAD drives myoblast differentiation by targeting DNA strand breaks to specific genomic loci. However, studies have reported that genotoxic stress, which triggers random DNA damage, can induce premature differentiation (28, 29). To test this supposition, we treated myoblasts with neocarzinostatin, a compound that induces indiscriminate DNA double strand breaks. Interestingly, we noted that neocarzinostatin treatment leads to only sporadic myoblast differentiation, confirming that random DNA damage per se is not a developmental trigger for inducing the differentiation program (Fig S7).

These observations suggest that modification of the p21 promoter by transient strand break formation acts as an inductive event to establish p21 gene expression. This supposition is supported by the observation that transient formation of caspase 3/CAD dependent breaks within the p21 promoter element are concurrent to the upregulation of p21 in muscle differentiation and our observation of impaired expression of p21 in CAD shRNA myoblasts. Although the mechanism by which the strand break leads to gene activation has yet to be elucidated, the caspase/CAD strand break may act to initiate histone modifications and/or changes in histone composition that ensure a more permissive gene expression environment. Alternatively, the strand breaks and the subsequent repair process may act to remove DNA marks that are repressive. In this regard, we observed that, in normal proliferating C2C12 myoblasts, MspI restriction enzyme digest of the p21 promoter displayed an identical corresponding strand break

between -89bp and -90bp from the transcription start site as that observed in early differentiating C2C12 myoblasts (Fig. S8A). However, we have not observed any alterations in the methylation status of the p21 promoter during myoblast differentiation (Fig. S8B). As such, we anticipate that the strand breaks in the p21 gene may act as points of assembly for the transcriptional machinery in a manner similar to the topoisomerase-II induced strand break transcription that has been reported for glucocorticoid sensitive gene expression (14).

The results presented here establish induction of caspase 3/CAD dependent DNA strand breaks as a primary end point in the caspase signal that propels differentiation. This signaling end point coupled with caspase directed activation of select kinase substrates such as MST1, may act in concert to precipitate the alterations in gene expression that promotes myoblast differentiation. However, these caspase dependent activities do not preclude a role for additional caspase signalling events in regulating cell fate alterations. For example, the human tudor staphylococcal nuclease, HsTSN (p100) has been identified as a phylogenetically conserved substrate of caspase 3 (30). Cleavage of HsTSN by caspase 3 impairs mRNA splicing during apoptosis, an event that may also be a prerequisite for cell differentiation (30). Alternatively, HsTSN may function in a manner analogous to CAD as a caspase responsive nuclease.

Despite the evidence that CAD appears to target discrete loci, the molecular mechanism that dictates CAD genome specificity remains unknown. CAD targeting preference may originate with simultaneous chromatin/epigenetic modifications that either promote and/or limit CAD accessibility to DNA. Alternatively, CAD may interact with a protein or proteins that direct the nuclease to a discrete genomic location. Our

observations implicate caspase/CAD induction of p21 gene expression, yet the pattern of strand break formation and repair (ISNT-labeled foci and phospho-H2AX) during myoblast differentiation is consistent with a genome wide modification rather than targeting of a single loci. Previous studies have linked CAD targeting to regions of DNA that have equitable distribution, such as accessible intra-nucleosomal linker regions and/or matrix attachment regions (MARs) (10, 27). Depending on the context of these targeted regions one would predict that the CAD directed cleavage events may be repressive for some genes/genomic loci while inductive for others. In this manner caspase/CAD activity would provide an epigenetic mechanism to rapidly modify global gene expression patterns, an event entirely consistent with the genome reorganization that occurs during differentiation (31). As such, our results conclude that caspase/CAD regulated DNA strand breaks may be a broadly conserved mechanism for managing the genome alterations that promote cell differentiation.

Methods and Materials

Cell Culture

C2C12 myoblasts were cultured and induced to differentiate as described in Fernando et al. (6) For caspase 3 inhibition, myoblasts were pretreated with 10μM N-benzyloxycaronyl-Asp-Glu-Val-Asp-fluoromethylketone (z-DEVD-fmk) for 2-3 h before the induction of low serum induced differentiation when fresh inhibitor was added; inhibitor was refreshed every 24 h. Primary myoblasts were isolated from 4 week old B6C3F1 mice, cultured and induced to differentiate as described in Fernando et al. (6)

ISNT

C2C12 myoblasts were cultured on glass coverslips and fixed with 90% Methanol and 10% PBS after indicated treatment. C2C12 myoblast apoptosis was induced by treatment with 1mM Actinomycin D for 12h at 37°C or 1 μg/ml anti-Fas monoclonal antibody for 4h prior to fixation For DNase I (NEB) treatment, fixed cells were incubated with 2U DNase I for 10 minutes at 37°C for 10 minutes. Nick translation reaction (50mM Tris HCl pH7.9, 50 μg/ml BSA, 5mM MgCl2, 10mM β-mercaptoethanol, 10μM dCTP, dATP, dGTP, 1μM dTTP, and 1μM dUTP-21-Biotin (Clontech) or 1μM dUTP-11-DIG (Roche)) was run with 10U/ml DNA Polymerase I (NEB) for 1 hour at 37°C. Subsequent detection of incorporated labeled dUTP was performed using appropriate primary antibody; where indicated myosin heavy chain was stained to mark differentiation, and nuclei were counterstained with DAPI (Sigma).

ChIP

ChIP assays were run as described Rampalli et al.(32) Primers to the p21 promoter were 5'-CCCGAAACCCAGGATTTTAT-3' and 5'-TCCCCTCTGGGAATCTAAGC-3'. PCR for the myogenin promoter were run using the following primer pairs 5'-AGAGGGAAGGGGAATCACAT-3' and 5'-ATAGAAGTGGGGCTCCTGGT-3'. PCR product amplification was quantified using AlphaEaseFC software (Alpha Innotech).

LM-PCR

LM-PCR was run as described by Carey and Smale (33) with some modifications. Briefly genomic DNA was isolated using Sigma Genlute Mammalian Genomic DNA Miniprep Kit. Primer extension using primer 1 was run with 500ng of purified DNA using pfu polymerase (Biovision). Linker DNA was ligated over night at 16°C with T4 Ligase (Invitrogen). Amplification was run using primer 2 and Phusion DNA polymerase (NEB). ^{32}P labeled primer 3 was used to label PCR products using Phusion DNA polymerase. PCR products were resolved on a 6% denaturing acrylamide sequencing gel. Primers to the p21 promoter were primer 1 (5'- ACTCCAATTCCCCTAGACTCTGA – 3'), primer 2 (5'- CCAATTCCCCTAGACTCTGACAC-3'), and primer 3 (5'- GACTCT GACACCGCGGCGGCTCACACCTCT- 3'). Primers to the myogenin promoter were primer 1 (5'-CTGAAGGTGGACAGGAAGGTAGTT - 3'), primer 2 (5'-TGTCTCATACAGCTCCATCAGGTCGG-3'), and primer 3 (5'-CAGCTCCATCAGGTCGGCAAAGGCTTGTTC -3'). Linker DNA 1 (5'-GCGGTGACCCGGGAGATCTGAATTC-3') and Linker DNA 2 (5'-GAATTCAGATC-3') were annealed by heating to 98°C for 5 min then cooled gradually to room temperature.

Acknowledgements

The authors thank Michael Rudnicki, Peter Lansdorp, Pasan Fernando, Matt Lorinzc, and Shayesta Seenundun for helpful discussions. B.D.L. is supported by a Computational Regulomics Training Program Graduate Student Fellowship from the Ontario Ministry of Research and Innovation Ontario Research Fund. L.A.M. is the Mach Gaensslen Chair in Cardiac Research. This work was supported by grants from the Canadian Institutes of Health Research and the Muscular Dystrophy Association (L.A.M.).

Supporting Information

SI Methods and Materials

Reagents and Antibodies

Antibodies used anti-biotin (Sigma), anti-myogenin, anti-CAD, normal rabbit IgG (Santa Cruz), anti-p21, anti-ICAD (BD Bioscience), anti-phosphoH2AX, (Cell Signalling, Upstate), anti-DIG (Roche), anti-ATM(P-S1981) (Chemicon), anti-myosin heavy chain and anti-tubulin (Developmental Hybridoma). Secondary antibodies used anti-rabbit HRP and anti-mouse HRP (BioRad); anti-goat Alexa Fluor 488, anti-rabbit Alexa Fluor 488, and anti-mouse Alexa Fluor 594 (Molecular Probes). Actinomycin D and caspase 3 inhibitor, z-DEVD-fmk, were obtained from Biovision. Staurosporine and neocarzinostatin were obtained from Sigma.

CAD shRNA stable cell lines

shRNA constructs, non-silencing pGIPZ (shNEG) and CAD pSM2c (shCAD) were obtained from Open Biosystems. C2C12 cells were transfected using Lipofectamine 2000 (Invitrogen) and stable clones were selected using puromycin. RNA was extracted using Trizol (Invitrogen) and RT was run using Superscript II (Invitrogen). 32 cycles of PCR for CAD was run using the following primer pair 5'-CCATCCAGATGTCTCCTGGT-3' and 5'- GAACTCCAGTCCAGCCAGAG-3'. PCR for GAPDH was run using the following primer pair 5'-TGACTCCACTCACGGCAAATTCAA–3' and 5'-TGCCTGCTTCACCACCTTCTTGAT – 3'. PCR for p21 was run using the following primer pair 5'-TGTCCAATCCTGGTGATGTCC-3' and 5'-TCAGACACCAGAGTG

CAAGAC - 3'. PCR product amplification was quantified using AlphaEaseFC software (Alpha Innotech). Western blots were run as described in Fernando et al.(6)

In vitro Plasmid Digest

Nuclear lysates from differentiating C2C12 cells were incubated with the pUC19 plasmid for 2 hours at 37°C in reaction buffer composed of 2mM Hepes pH7.5, 7.5mM NaCl, 0.5mM MgCl2, 0.2mM DTT, 0.1mM EGTA, 0.1mM EDTA.. Proteinase K was added to clean up DNA–protein interactions and reaction was run on a 1% agarose gel.

Single cell gel electrophoresis (COMET assay)

The alkaline comet assay was performed using the COMET assay kit (Trevigen). Gel Bond Film agarose gel support medium (Lonza) was used as support matrix for the LM agarose embedded cells. Cells were electrophoresed at 30V at 4°C for 30 minutes then stained with Sybr Green.

Plasmid Construction

The human ICAD cDNA encoding the long isoform of ICAD was obtain from Open Biosystems. Wild type human ICAD was cloned into the reading frame A, between the BamHI and NotI restriction site, of pMEV-2HA (Biomyx) mammalian expression vector, PCR primers used included the BamHI (forward) and NotI (reverse) restriction sites (bold) , forward 5'-AT**GGATCC**GAGGTGACCGGGGACGCC-3' and reverse 5'-TA**GCGGCCGC**CTATGTGGGATCCTGTCTG-3'. Two step mega primer approach was used to introduce the D117E mutation. PCR using the forward primer from above and reverse primer 5'- CTGCCCCG**CTC**TCTGTTTCATC-3' (change position in bold)

generated the megaprimer that was purified and used with the reverse primer to generate the full length ICAD sequence containing the mutation by PCR. The PCR product was inserted between the BamHI and NotI restriction site of pMEV-2HA as above. Constructs were verified by sequencing.

Generation of pooled primary myoblasts expressing ICAD constructs

Primary myoblasts were transfected with empty pMEV-2HA, pMEV-2HA-wtICAD, or pMEV-2HA-mtICAD (D117E) by Lipofectamine 2000, 48 hours after transfection growth media contain G418 (400 ug/ml) was added to select for transfected cells. Once discrete colonies were observed cells were trypsinized and replated to generated pooled clones. Expression of the constructs was confirmed by western blot. Cells were induced to differentiate as described previously.

Methylated Chromatin Precipitation

Methylated DNA was captured from sonicated C2C12 DNA during growth and low serum induced differentiation using the Methyl Collector Kit (Active Motif) as per manufacturer's instructions. PCR analysis for the p21 proximal promoter was performed using the primers described for the CAD ChIP. Included positive and negative controls were used to validate the protocol used to isolate methylated DNA as per the manufacturer's instructions.

Statistical analysis

Statistical significance in Fig. 2 was determined using Student’s t-test.

Supporting Figures

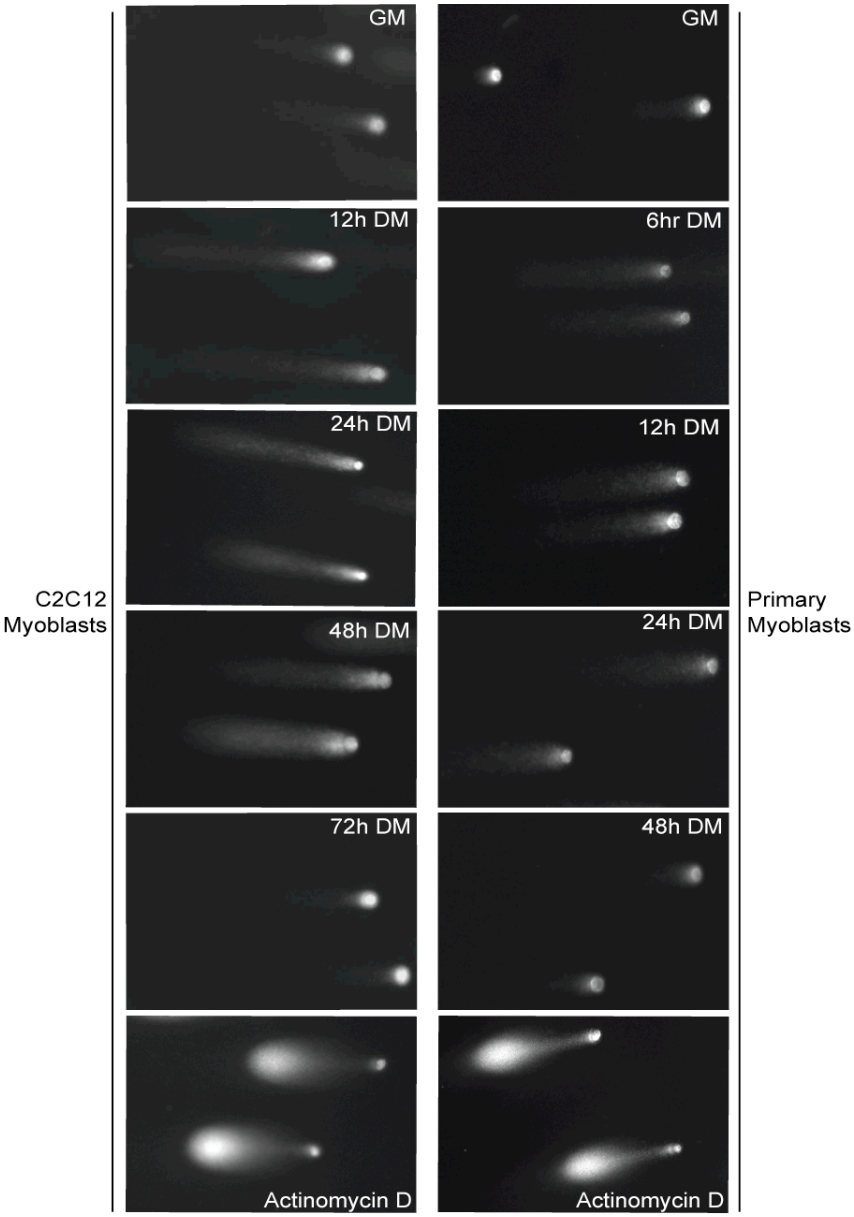

Fig. S1. Single cell gel electrophoresis (COMET) of differentiating and apoptotic myoblasts demonstrate qualitatively different morphology. Cells were collected at the indicated differentiation time points or after 18 hours of Actinomycin D treatment (1 μM). Agarose embedded cells were electrophoresed under alkaline conditions (pH≥13) and stained with Sybr Green. Representative images of each condition are presented.

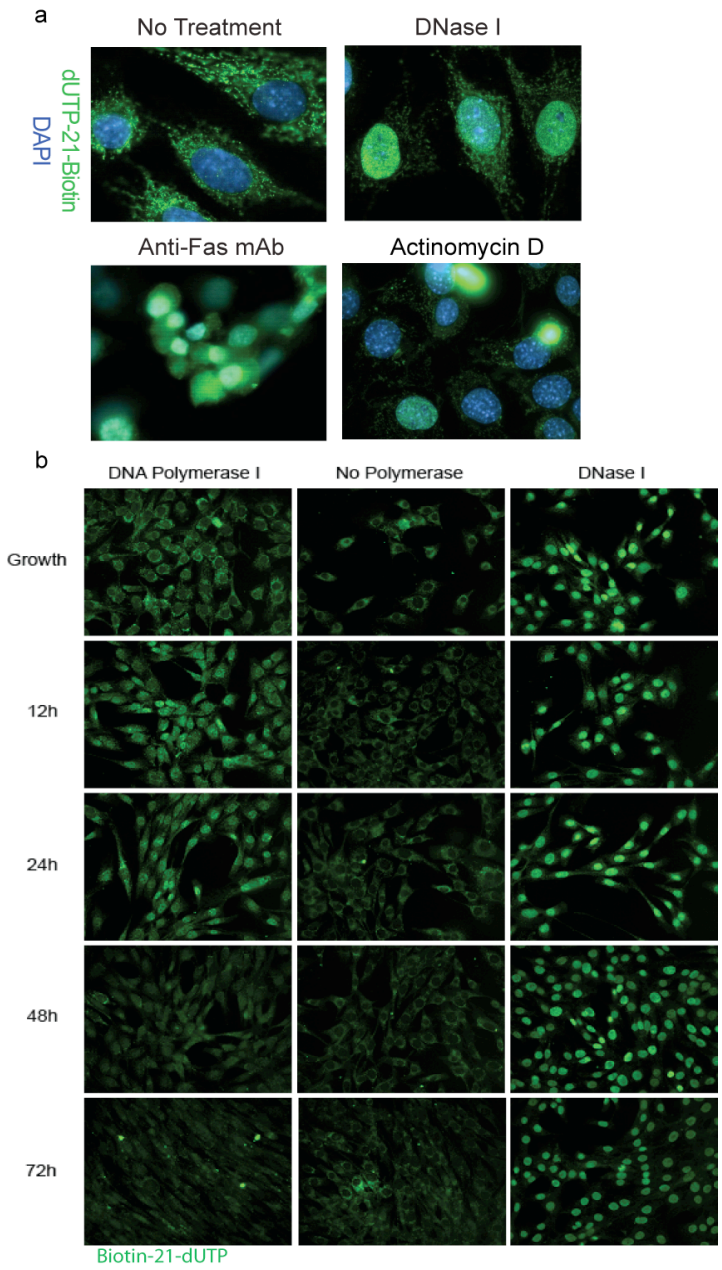

Fig S2. ***In situ*** **nick translation (ISNT) labels C2C12 myoblasts when DNA strand breaks are induced**. a) Myoblasts cultured on glass coverslips were methanol fixed and the nick translation reaction was run with 10U/ml DNA Polymerase I to incorporate dUTP-21-Biotin for 1 hour at 37°C, subsequent detection of incorporated biotin was performed using a goat anti-biotin followed by a donkey anti-goat Alexa Fluor 488, nuclei were counterstained with DAPI. DNase I, Anti-Fas mAB, Actinomycin D pre-treatment led to the induction of DNA nicks/strand breaks that could be detected by ISNT. b) Incorporation of biotin labeled nucleotide during myoblast differentiation is dependent on the addition of DNA Polymerase I and the presence of DNA strand breaks. ISNT was applied to fixed C2C12 myoblasts over a differentiation time course with or without DNA polymerase I, no incorporation of biotin label was observed in cells without DNA polymerase. Treatment of fixed cells prior to ISNT with DNase I to inflict strand breaks, shows robust incorporation of label at all time points. (n=3)

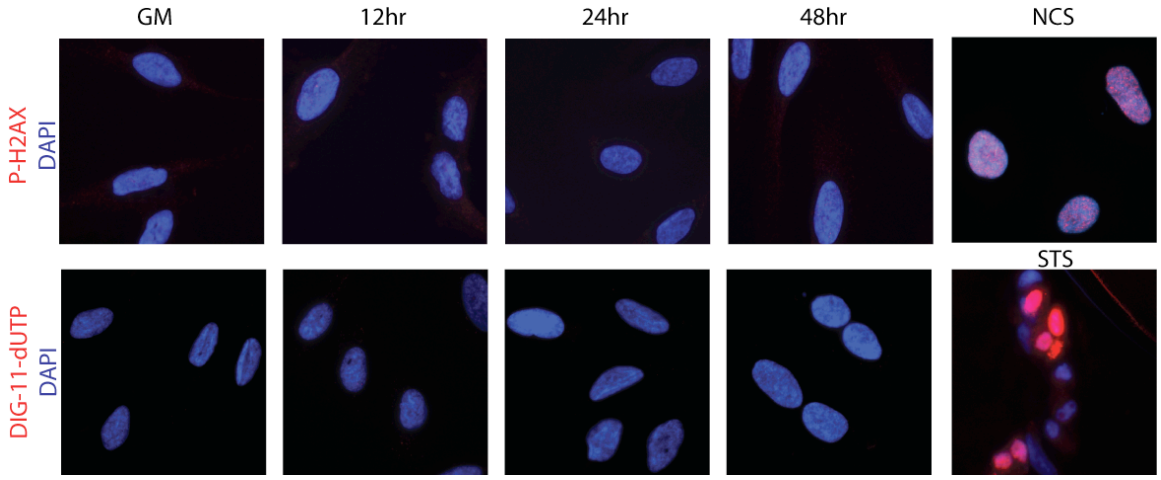

Fig S3. Induction of DNA strand breaks under low serum conditions is specific to differentiating myoblasts. Low serum treatment of HeLa cells does not induce the phosphorylation of H2AX or the induction of DNA strand breaks detected by ISNT. HeLa cells were switched from growth media (GM) to low serum media used to induce differentiation in C2C12 myoblasts. Cells were fixed at the indicated time points, ISNT was performed as previously described or stained for P-H2AX as previously described. Induction of apoptosis using staurosporine (STS) was used as a positive control for ISNT. Treatment with neocarzinostatin (NCS) was used as a positive control for the phosphorylation of H2AX.

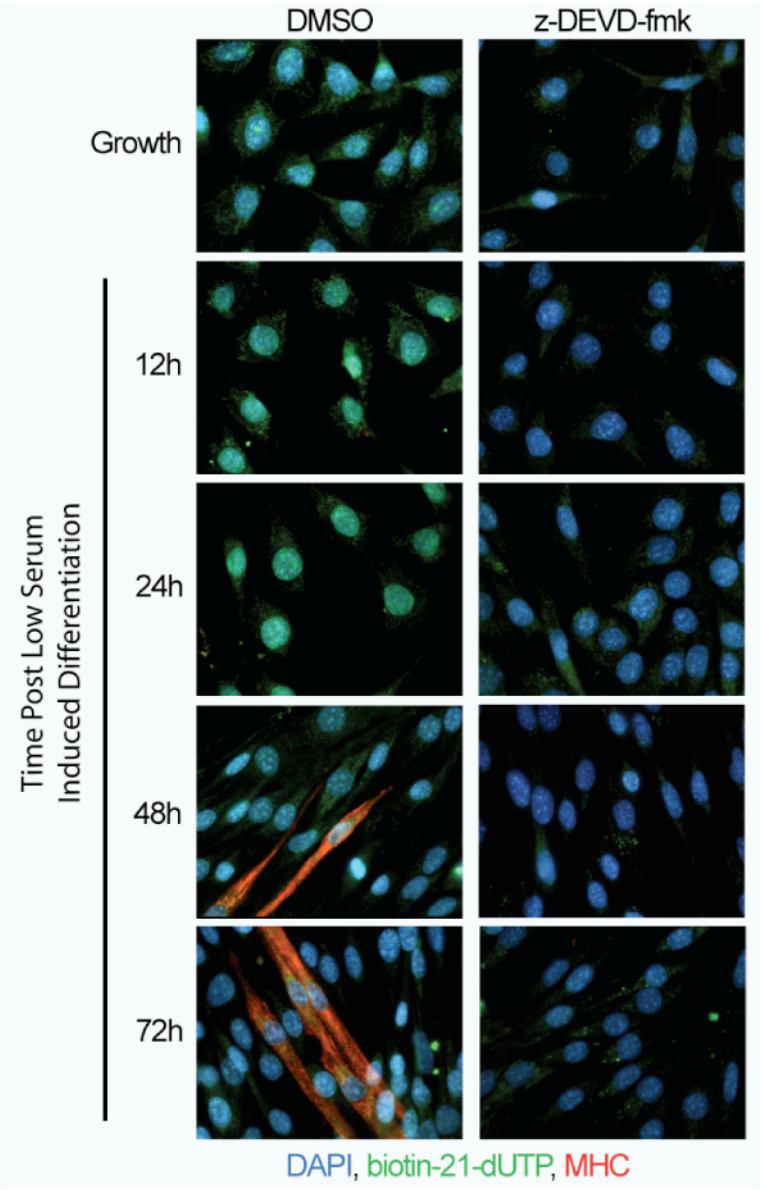

Fig S4. Chemical inhibition of caspase 3 activity prevents the detection of DNA strand breaks during differentiation of C2C12 myoblasts. C2C12 myoblasts were induced to differentiate and treated with the caspase 3 inhibitor, z-DEVD-fmk (10μM) or DMSO. Cells were fixed at the indicated time points and treated as previously described. Nick translation (ISNT) failed to label the nuclei of caspase 3 inhibited cells at 12hrs and 24 hrs post differentiation but not DMSO treated cells. (n=3)

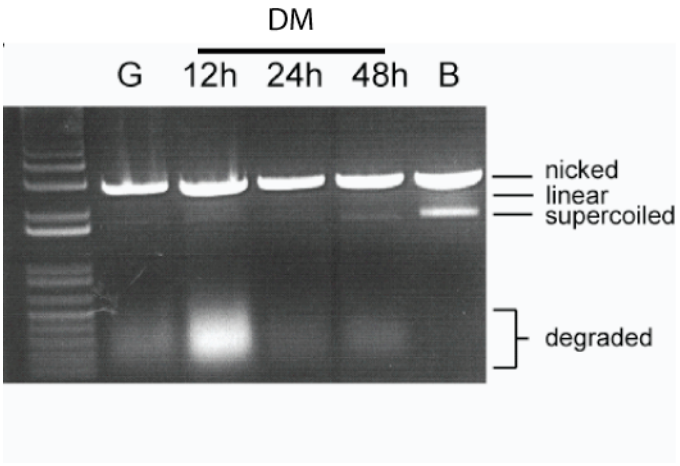

Fig S5. Nuclease activity present during the C2C12 myoblast differentiation. *In vitro* plasmid digest assay shows an increase in nuclease activity in nuclear lysates from C2C12 cells 12 hours after differentiation is induced, as indicated by an increase in degraded plasmid DNA. pUC19 plasmid was incubated with nuclear lysates for 2 hours at 37°C, followed by proteinase K clean up to remove DNA-protein interactions. Samples were resolved on a 1% agarose gel with ethidium bromide and visualized under UV light. B: blank, untreated control.

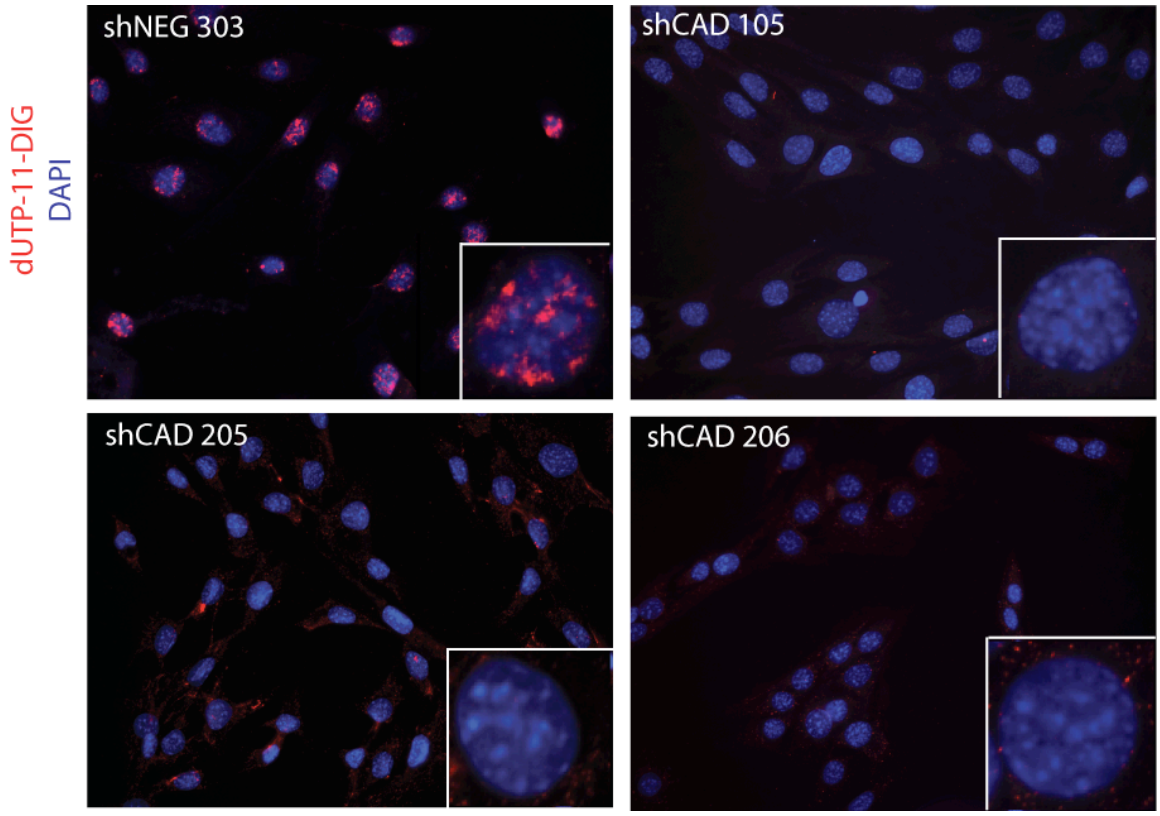

Fig S6. Low serum treated C2C12 shCAD stables display reduced *in situ* nick translation incorporation of labeled nucleotide. shCAD myoblasts were induced to differentiate under low serum conditions, fixed at 24hrs and ISNT protocol was applied. ISNT failed to incorporate the DIG labeled nucleotide (red) into shCAD myoblasts at 24hrs. Nuclei were counterstained with DAPI. (n=3)

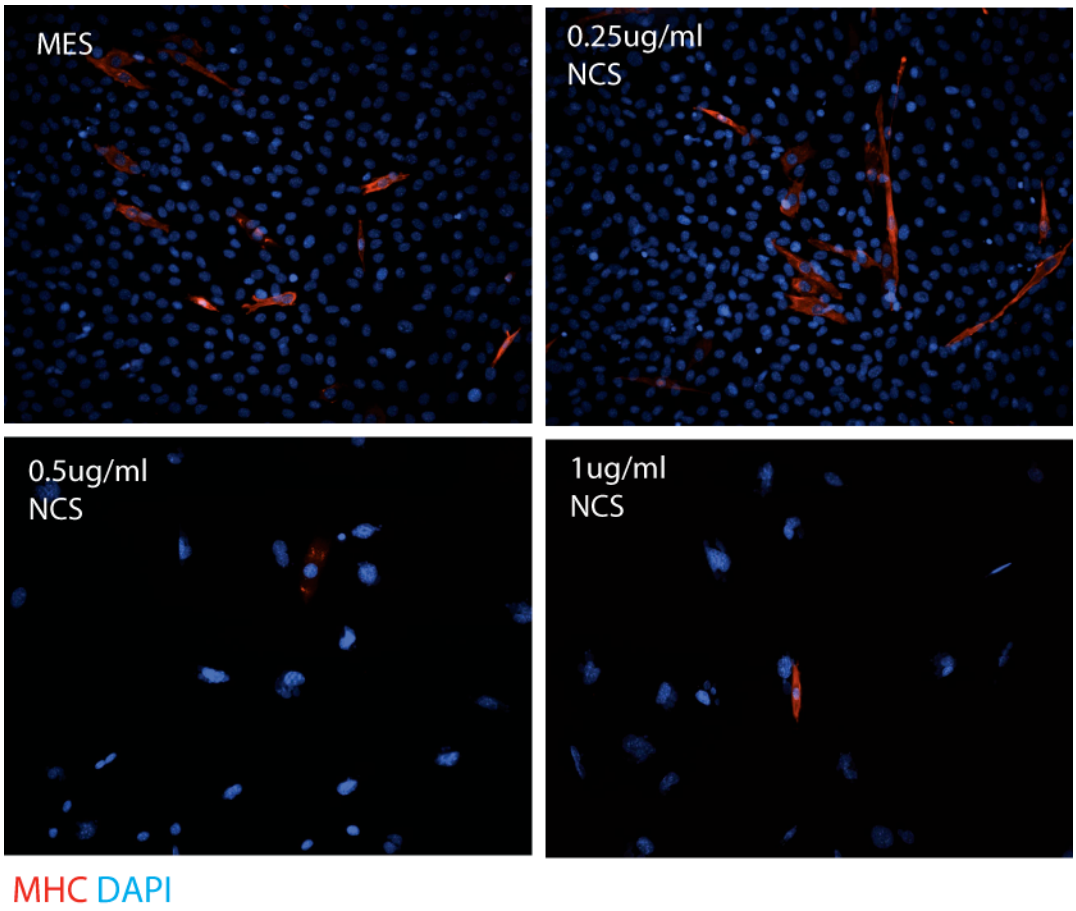

Fig S7. Neocarzinostatin (NCS) treatment does not induce spontaneous differentiation in C2C12 myoblasts. Cells at 60% confluency were treated with indicated concentrations of NCS for 1 hour in growth media, differentiation was assessed 72 hours after treatment by myosin heavy chain staining.

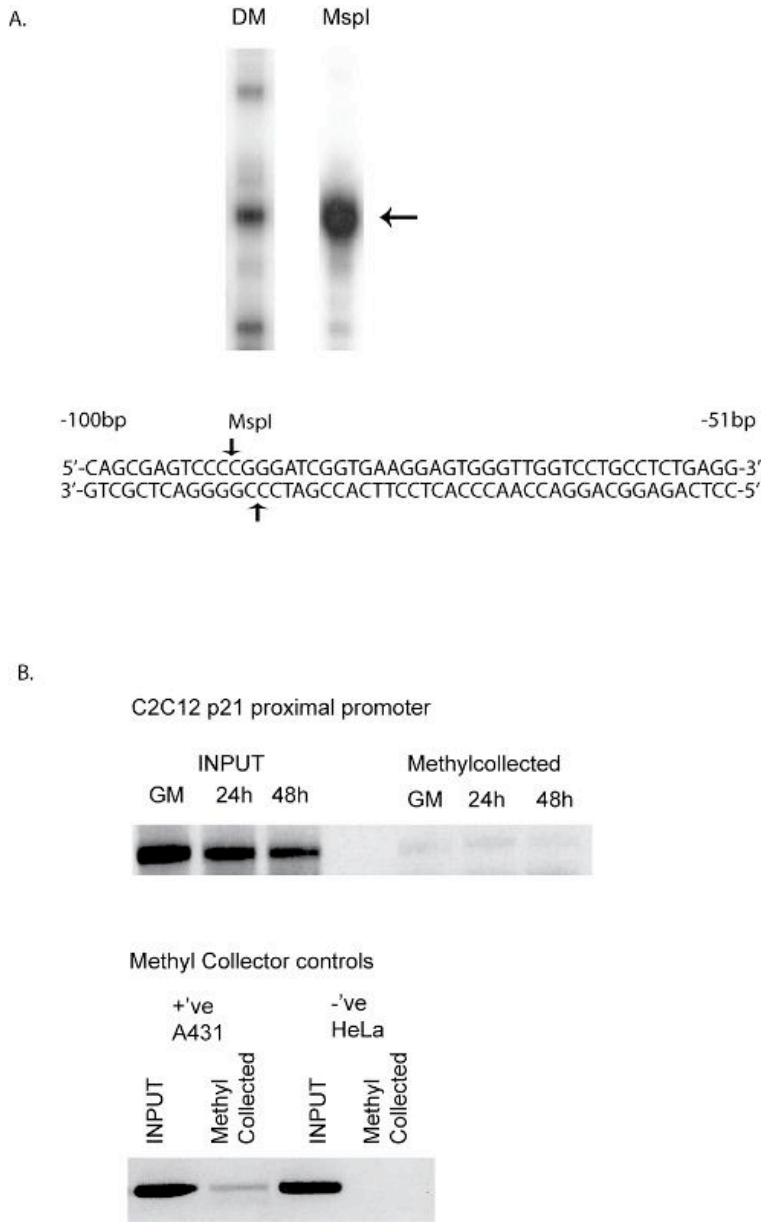

Fig S8. A) DNA strand break detected by LM-PCR of the p21 promoter correspond with the MspI sensitive restriction site in C2C12 myoblasts. Genomic DNA from C2C12 myoblasts was isolated 24 hours after the induction of differentiation. DNA from proliferating C2C12 myoblasts was treated with the MspI restriction enzyme. LM-PCR and subsequent analysis was run as previously described. Arrow indicates corresponding MspI induced strand break occurs between -89 and -90 bp from the p21 transcription start site. B) Methylation analysis of the p21 promoter demonstrates no change in methylation status during low serum differentiation of C2C12 myoblasts. Sonicated C2C12 genomic DNA from the indicated time points was collected (input) and methylated DNA was captured using His-tagged MDB2b/MBD3L1 with magnetic isolation. PCR for the p21 proximal promoter from the collected DNA showed limited enrichment and no change in methylation during differentiation in C2C12 myoblasts. Methyl Collector positive (A431) and negative (HeLa) controls for the MCJ locus authenticate the protocol used to isolate methylated DNA.

Chapter 3: Pax7 Gene Expression is Regulated by Caspase 3/CAD during Differentiation: Implications in the Origin of Alveolar Rhabdomyosarcoma

Contribution of Collaborators

The experimental work and preparation of this thesis chapter were carried out by the thesis author with the following exception. Steve Brunette assisted in the generation of the ICAD constructs used in Figure 4. Dr. Sharavanti Rampalli in the laboratory of Dr. Jeffrey Dilworth provided the CAD and mock ChIP samples for Solexa/Illumina sequencing. Chris Porter carried out the MACS analysis of the ChIP-seq data.

3.1 Genome Wide examination of CAD association

In the previous chapter we identified the promoter element of the CDKN1A gene (p21) as a bona fide CAD target during skeletal muscle differentiation. The extent of DNA breaks observed during differentiation however suggests that CAD can simultaneously target a number of genomic loci. To obtain a genome wide assessment of potential CAD DNA targets we used ChIP coupled to high throughput sequencing (ChIP-seq). As noted previously, the application of ChIP technology to define CAD targets is a viable approach, i.e. CAD retains the ability to form stable associations with its substrate DNA, a feature that is unique for a nuclease. This association can occur both as an active dimer and when in complex with ICAD (Korn et al, 2005). This suggests that CAD could be activated directly on DNA via the caspase 3 cleavage of ICAD. Accordingly, we chose to employ ChIP-seq analysis for CAD at a time that was consistent with the formation of DNA strand breaks during C2C12 cell differentiation. CAD and mock IgG ChIP isolated samples were collected from 12 hour post low serum induced myoblasts and analyzed via the Solexa/Illumina sequencing service within the BC Cancer Agency's Genomics Core facility. Libraries for both the mock and CAD ChIP samples were prepared and run on independent flow lanes. The Illumina Eland Analysis Pipeline was used to measure cluster intensities, conduct base-calling, and align the returned sequences to the genome (Bentley et al, 2008).

To identify the genomic sites that were enriched for CAD association, the Model-based analysis of ChIP-seq (MACS) was used to parse enriched regions over the mock control background (Zhang et al, 2008). The analysis was run against uniquely-mapped

A

Location	Repetitive Element	Overlaping genes	Nearby genes
Chr1:12629975-12630067	Simple repeat		
Chr14:103222648-103222698	Simple repeat		
Chr11:25000153-25000211	Simple repeat		
Chr5:114434107-114434180	SINE	Acacb	
Chr9:62406581-62406689	Simple repeat		
Chr3:148180604-148180656	LINE		
Chr6:69445927-69445967	srpRNA		
Chr13:41000747-41000790	SINE		
Chr9:122496766-122496825	SINE		
Chr5:24812777-24813009		Mll3	Mll3
Chr10:21278083-21278136	Simple repeat		
Chr1:33935554-33935593			
Chr9:102630445-102630485	SINE		
Chr13:39431345-39431386	SINE		
Chr3:145628402-145628476	Simple repeat		

B

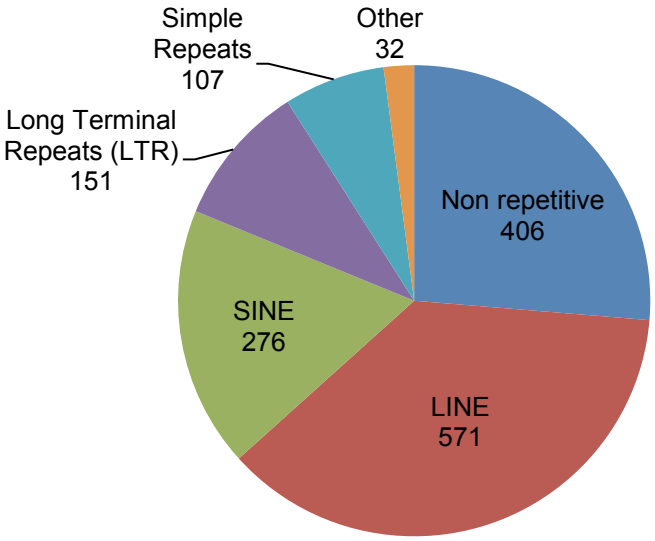

Figure 1. Identification of CAD enriched genomic elements by MACS during skeletal muscle differentiation. A.) Tabulation of the top 15 enriched regions identified by MACS. B.) Characterization of CAD enriched genomic elements identified by MACS.

sequencing reads, allowing for one or two mismatches. MACS identified 1543 CAD binding sites with tiling of sequence tags at 30 – 238 bp ($p < 10^{-5}$). Four hundred and sixty-one of these hits overlapped genes from the RefSeq database and 234 were located within 100 kb of RefSeq genes. The top 15 CAD enriched regions are tabulated in Figure 1A and the complete list presented in Appendix 2. We noted from the MACS identified sites that CAD localized largely to repetitive elements, particularly long interspersed nuclear elements (LINES) and short interspersed nuclear elements (SINES) (Figure 1B). A functional role for these elements in skeletal muscle differentiation has not been addressed. However, recent observations suggest that these elements play a critical role in initiation of transcription and spatial organization of chromatin in the nucleus (Faulkner et al, 2009; O'Sullivan et al, 2009).

Although significant enrichment for CAD at the p21 gene was not observed, some enrichment was represented compared to the myogenin gene (Figure 2). Library construction in the Solexa/Illumina method can introduce several sources of bias into the results. Particularly regions with high GC content can be underrepresented owing to difficulties with PCR amplification during the cluster generation. In addition, extended repeats present in the genome can result in sequenced reads that are unable to be uniquely mapped (Barski & Zhao, 2009). The p21 promoter is a well characterized CpG island with a high GC content, as such this factor may have contributed to the limited amplification in this region. Moreover, the formation of an endogenous DNA strand break could in some regions not be sufficiently repaired during library construction and potentially could interfere with the Solexa/Illumina sequencing (Barski & Zhao, 2009).

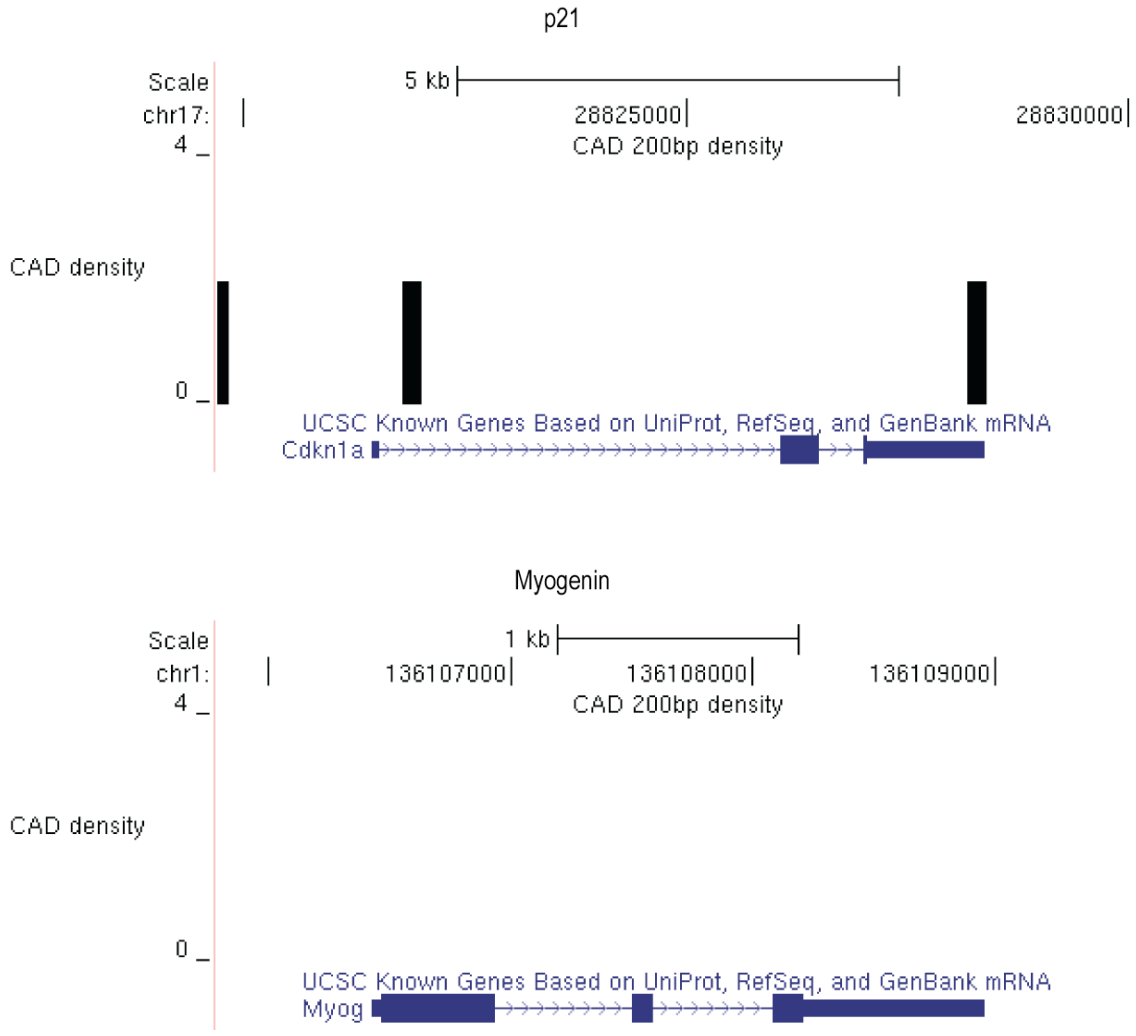

Figure 2. MACS analysis of CAD association to the p21 and myogenin genes in differentiating C2C12 cells. CAD enriched regions from the MACS analysis were mapped with the UCLA genome browser. Shown is the CAD enrichment density to the p21 gene and the myogenin gene. Limited enrichment is observed at the p21 gene compared to the myogenin gene.

Given that the p21 gene is subject to multiple strand breaks, it is not unexpected that ChIP-seq detection of p21 was limited.

3.2 Caspase 3/CAD activity regulates the expression of Pax7 during skeletal muscle differentiation.

Examination of the CAD ChIP-seq data revealed a potential association to the Pax7 gene (Figure 3A). Although this association was below the significance cut off of $p<10^{-5}$, it represented a biologically relevant observation. Pax7 expression promotes the survival and proliferation of satellite cells, it also acts to prevent premature entry into differentiation (Relaix et al, 2006; Seale et al, 2004; Seale et al, 2000). As such the expression of Pax7 is rapidly down regulated at the onset of differentiation. One component of this downregulation is the induction of microRNAs by MyoD. Specifically, induction of miR-1, miR-206, and miR-486 decrease transcript levels of Pax7 corresponding to diminished protein levels (Chen et al., 2010; Dey et al., 2011). This post transcriptional regulation likely coordinates with multiple mechanisms to silence Pax7 expression.

To determine if caspase3/CAD could affect the repression of Pax7 transcription, we examined whether chemical inhibition of caspase 3 during myoblast differentiation led to any significant change in Pax7 expression. Examining Pax7 transcript levels 24 hours after the induction of differentiation by qPCR, we noted a significant albeit modest difference between the caspase 3 inhibited and DMSO treated cultures (Figure 3B, P=0.0076), i.e. the caspase 3 inhibited cultures retained a higher level of Pax7 transcript than the control DMSO treated cells. To determine if the decrease in Pax7 transcript

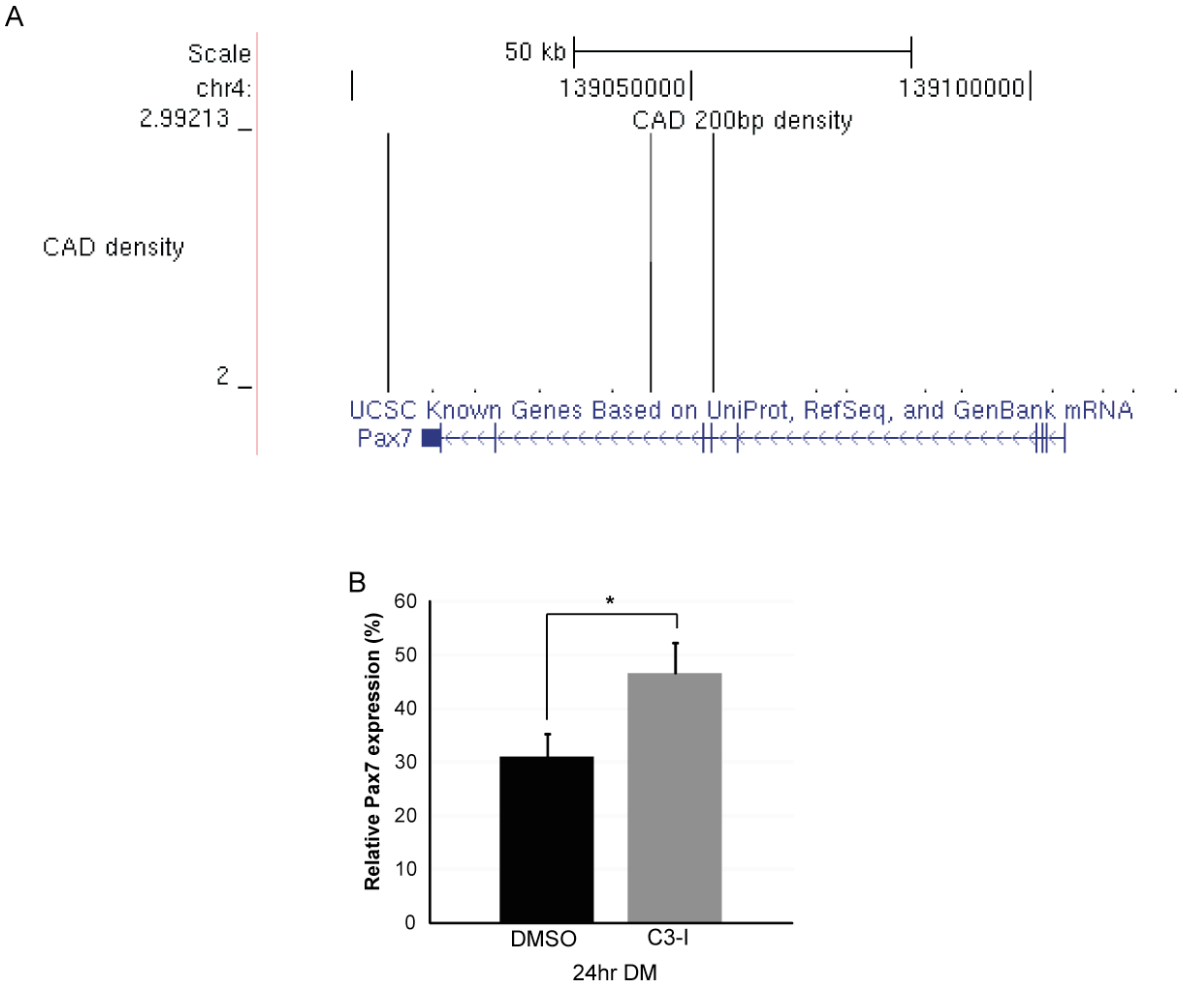

Figure 3. Pax7 gene repression can be regulated by caspase 3/CAD. A) UCLA genome browser output of CAD association to the Pax7 gene in differentiating C2C12 cells identified by MACS. B) Caspase 3 inhibition impairs Pax7 repression during differentiation. Primary myoblasts were induced to differentiate with either 15 μM of the caspase 3 inhibitor, z-DEVD-fmk, or the vehicle only control DMSO. RNA was collected 24 hours after the induction of differentiation and representative cDNA libraries were generated. Relative Pax7 expression at 24 hours was determined by qPCR and normalized to growth conditions. N=4 in triplicate. (Error bars are s.e.m.; P=0.0076)

levels was related to activation of CAD specifically, we examined Pax7 expression in primary myoblast cultures stably expressing mtICAD constructs. The rationale for this experiment is based on the premise that expression of ICAD constructs that have mutations in the caspase 3 cleavage sites will render ICAD protein resistant to cleavage, thereby maintaining a physical interaction with CAD and limiting CAD function (Yuste et al., 2005). Recall that caspase 3 cleavage of ICAD occurs at 2 conserved aspartic acid residues, D117 and D224, however only the cleavage event at D117 leads to a loss of the ICAD inhibition of CAD nuclease activity (Yuste et al., 2005). Following exposure to low serum conditions, myoblasts expressing either the empty vector, wtICAD, or the D224E mtICAD displayed a normal differentiation pattern (as assessed by the formation of multi-nucleated myotubes and expression of myosin heavy chain) (Figure 4A). Interestingly, expression of D117E mtICAD or the double D117/224E mtICAD impaired differentiation (Figure 4A). Empty vector control cultures demonstrated a clear reduction in Pax7 transcript levels by 24hrs, while the overexpression of the wtICAD and the D224E constructs had a minimal effect on the depression of expression (Figure 4B). Overexpression of mtICAD constructs containing the D117E mutation had a more pronounced effect on Pax7 expression (Figure 4B, $P=0.043$). Although it appears that the overexpression of the single D117E mutation exerted a stronger inhibitory influence on the expression of Pax7 compared to the double mtICAD mutant, this latter construct exhibited lower expression levels than the single ICAD mutation (Figure 4C). As such, assigning a less prominent role to the double ICAD caspase cleavage mutant should be approached with caution.

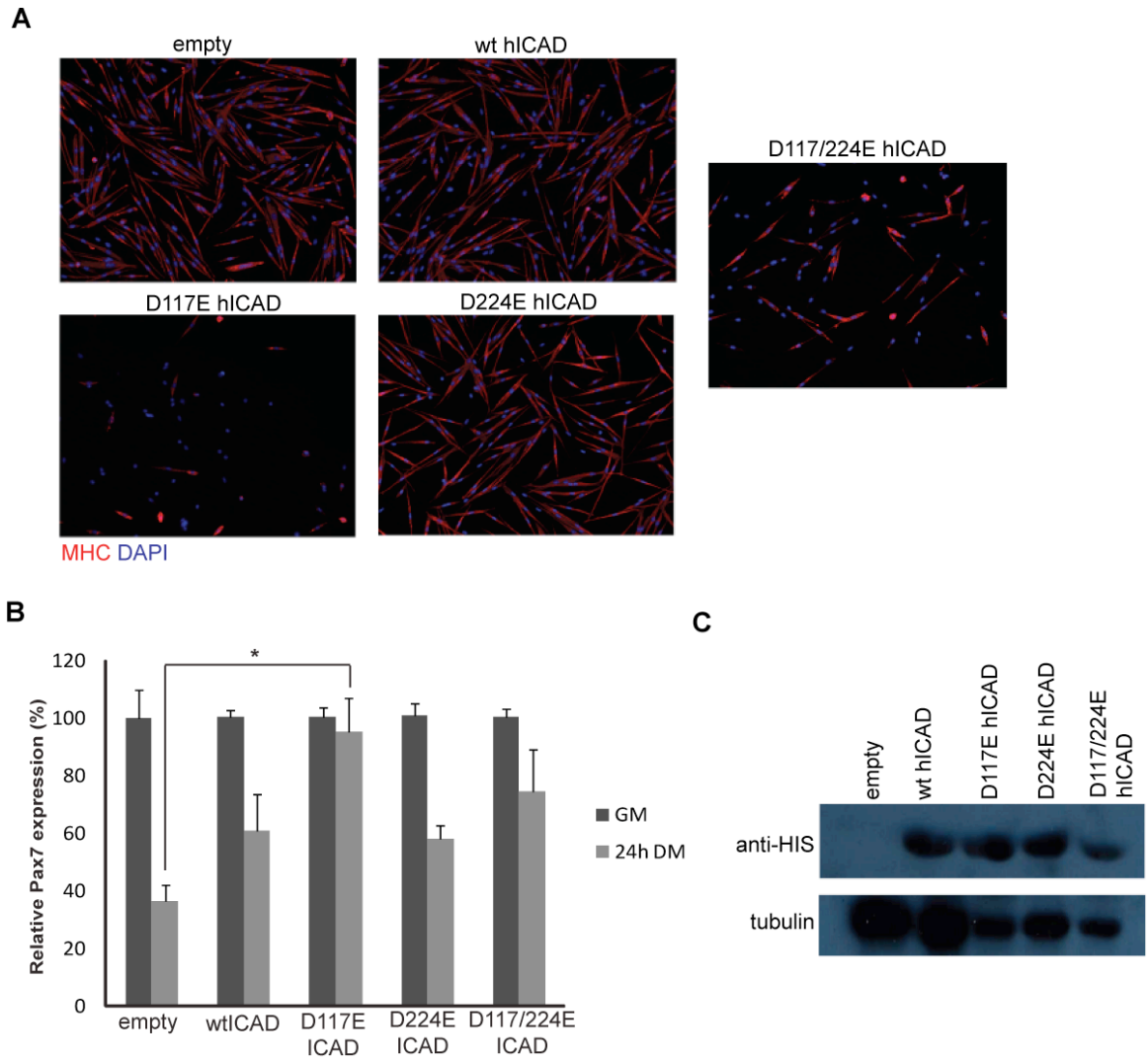

Figure 4. Expression of ICAD mutated at aspartic acid 117 impairs differentiation of primary myoblasts. A.) Primary myoblasts expressing the D117E hICAD or D117/224E hICAD demonstrated impaired differentiation. Cells were induced to differentiate under low serum conditions for 72 hours, fixed with 90% MeOH/10% PBS, and myosin heavy chain (MHC, red) was stained with mouse anti-MHC (MF20, 1:200, Developmental Hybridoma) followed by goat anti-mouse AlexaFluor 598 (1:2500, Molecular Probes), nuclei were counterstained with DAPI (blue). B) Stable expression of ICAD constructs in primary myoblast influences Pax7 depression following the induction of differentiation. Relative expression of Pax7 at 24 hours following the induction of differentiation was determined and normalized to the Pax7 expression in each individual cell line at growth. N=4 in triplicate. (Error bars are s.e.m.; P=0.043) C) His-tagged ICAD constructs are expressed in G418 selected primary myoblasts. Protein lysates were collected from selected myoblast and subject to western blot analysis. His-tagged ICAD constructs were detected with a mouse anti-His (1:1000, Cell Signal) primary antibody and subsequently a goat anti-mouse HRP secondary anti body. Tubulin was used to control for loading.

3.3 Regulation of Pax7 gene expression by Caspase3/CAD may contribute to chromosome translocations.

The potential association of CAD to intron 7 of Pax7 gene was not only a biologically significant observation (for the potential role in regulating Pax7 expression) but this region is also a well characterized site of genomic rearrangements. Chromosomal translocation between Pax7 intron 7 and intron 1 of Foxo1a is a well characterized oncogenic event in development of alveolar rhabdomyosarcoma (ARMS) (Figure 5A) (Xia et al., 2002). Here, breakpoint translocations between these loci lead to the formation of a potent transformative factor whereby the N terminal portion of Pax7 is fused to the C terminal region of Foxo1a, producing a hyperactive transcription factor (Xia et al, 2002). Of considerable interest, we also noted a potential enrichment of CAD to intron 1 of Foxo1 in the CAD ChIP-seq data set (Figure 5B). CAD association to these sites suggests that the prospective origin of chromosomal translocation in ARMS may be derived from a CAD directed event in muscle progenitor cells, specifically cells that have initiated the differentiation program.

Given that CAD is associated with the regions in the murine genome that are syntenic with the breakpoint translocations in humans ARMS we reasoned that a similar translocation event may also occur between the Pax7 and Foxo1 loci in murine muscle cells. To address this hypothesis we investigated whether such a fusion transcript could be detected between the Pax7 and Foxo1 gene in a population of differentiating primary myoblasts. Here, primers specific to the 5' end of the Pax7 transcript and the 3' end of the Foxo1 transcript were used to probe cDNA libraries generated from RNA isolated from differentiating primary myoblasts. A putative Pax7-Foxo1 fusion transcript was

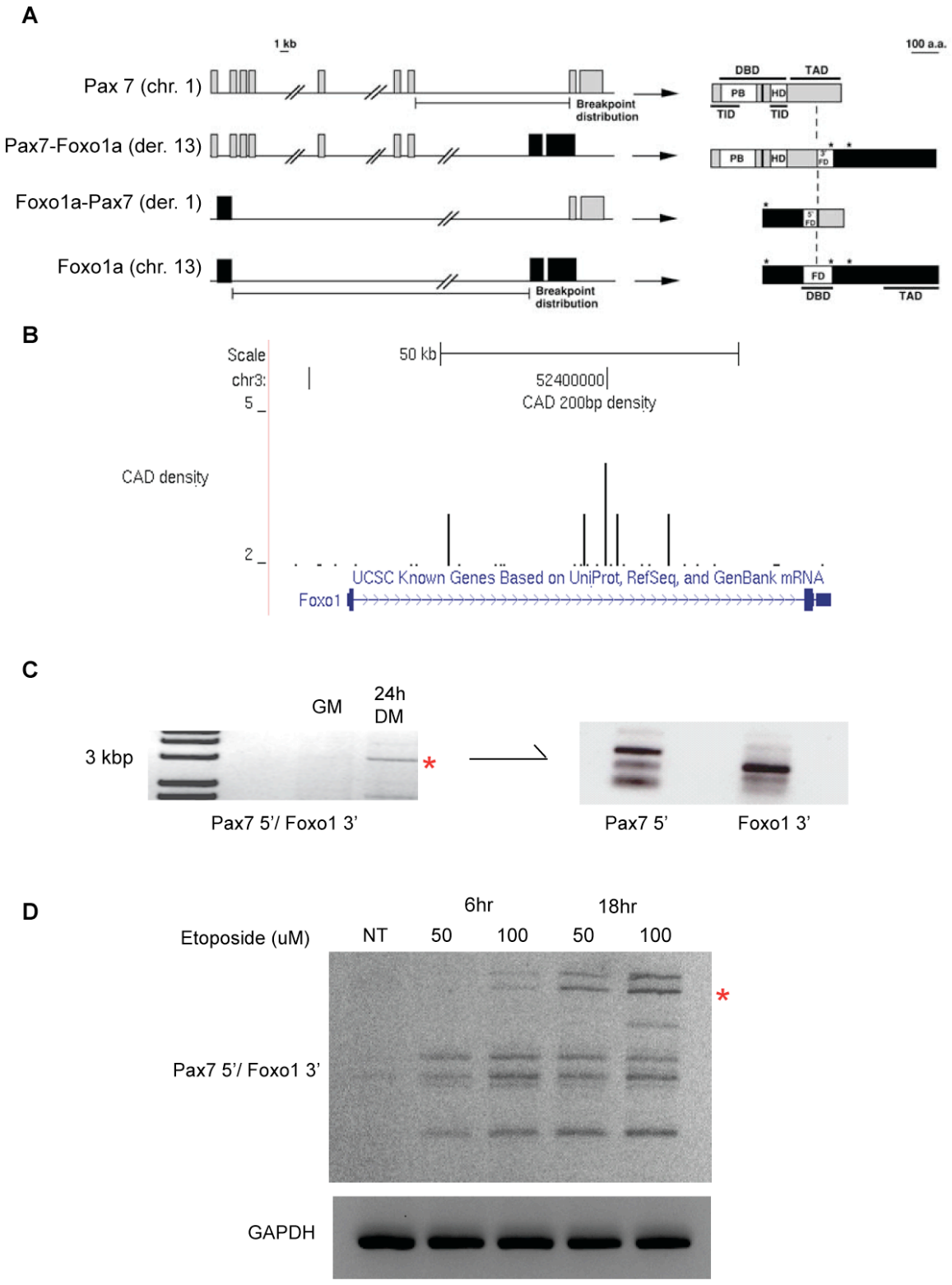
A
1 kb
100 a.a.
Pax 7 (chr. 1)
Breakpoint distribution
DBD
TAD
PB
HD
TID
TID
Pax7-Foxo1a (der. 13)
Foxo1a-Pax7 (der. 1)
Foxo1a (chr. 13)
Breakpoint distribution
FD
DBD
TAD
B
Scale
50 kb
chr3:
52400000
5
CAD 200bp density
CAD density
2
UCSC Known Genes Based on UniProt, RefSeq, and GenBank mRNA
Foxo1
C
GM
24h DM
3 kbp
Pax7 5'/ Foxo1 3'
Pax7 5'
Foxo1 3'
D
6hr
18hr
Etoposide (uM)
NT
50
100
50
100
Pax7 5'/ Foxo1 3'
GAPDH

Figure 5. Detection of a putative Pax7-Foxo1 fusion transcript. A.) Schematic outline of chromosomal translocations and resulting chimeric proteins involving the Pax7 and Foxo1a genes. (Modified from Xia et al, 2002. Reprinted by permission from Landes Biosciences: Cancer Biol Ther. 1(2):97-104©2002) B.) CAD enrichment at the intron 1 of Foxo1 during C2C12 differentiation. MACS output of CAD enriched regions was mapped using the UCLA genome browser, the enrichment of CAD at the Foxo1 genomic loci at 12 hours of differentiation is presented. C.) Detection of a putative Pax7-Foxo1 fusion transcript in differentiating primary myoblasts. Primers specific to the 5' region of the Pax7 transcript and the 3' region of the Foxo1 transcript were used to probe cDNA libraries of differentiating primary myoblasts for the appearance of a fusion transcript. A PCR product was observed at ~3000 bp that corresponded to the expected size of a Pax7-Foxo1 transcript. Secondary PCR from the isolated 3000bp band was preformed for the 5' region of the Pax7 transcript and 3' region of the Foxo1 transcript. (N=2) D.) Etoposide induction of the putative Pax7-Foxo1 fusion transcript in C2C12 cells. C2C12 cells were treated under growth conditions with the indicated concentrations of etoposide. RNA was isolated at the indicated time and used to generate cDNA libraries. PCR for the fusion transcript was run as described above, the induction of a putative fusion transcript corresponding to the transcript in differentiating primary myoblasts is indicated. (N=1)

detected from myoblasts at 24 hours post low serum induction of differentiation (Figure 5C). Interestingly, this fusion transcript was not observed during myoblast growth (Figure 5C). To confirm this observation, we performed a follow on PCR reaction using the gel purified band that corresponded to the appropriate sized transcript. Here, we noted that the transcript indeed contained the 5' coding region of Pax7 and 3' coding region of Foxo1 (Figure 5C). These results suggest that a bona fide fusion event occurs between the Pax7 and Foxo1 genes during myoblast differentiation and that this fusion event may be evolutionarily conserved between murine and human genomes.

The origin of such gene fusion events have been the subject of intense investigation. Given the number of mechanisms whereby DNA damage can be inflicted on a cell in a controlled and precise manner, the hypothesis that such damage arises primarily from random events may be in need of reassessment (Bartek et al, 2010; Mathas & Misteli, 2009). For example, secondary acute myeloid leukemia (t-AML) can originate in patients following treatment with topoisomerase inhibitors and is often associated with translocations within the MLL gene. However, numerous studies have reported that the inhibition of topoisomerase by etoposide does not cause direct damage to MLL gene. Rather at low dosages, etoposide may activate caspase 3, that in turn will activate CAD leading to the formation of specific breaks in the MLL gene (Betti et al, 2001; Betti et al, 2003; Betti et al, 2005; Hars et al, 2006). The similarity between this mechanism and our observations prompted us to examine if a similar stress signal could trigger the formation of a fusion transcript between Pax7 and Foxo1 in myogenic cells. C2C12 cells were treated with 50 and 100 μM of etoposide and RNA was collected 6 and 18 hours after treatment. Samples were assessed for the putative Pax7-Foxo1 fusion transcript by PCR

from cDNA libraries. We noted the induction of the putative fusion transcript following treatment with etoposide indicating that a chromosomal translocation between the Pax7 and Foxo1 genes had been promoted (Figure 5D). This observation suggests that etoposide may be able to illicit chromosomal translocations through the activation of CAD in myogenic cells as it does in t-AML(Hars et al, 2006). Moreover, these results suggest that DNA damage may induce the activation of CAD at genomic elements that are prone to breakage and that these regions may be conserved across species.

Chapter 4: General Discussion

4.1 Control of gene expression through directed DNA damage. Potential regulatory mechanisms.

We observed the concurrent induction of DNA strand breaks by caspase 3 mediated activation of CAD during skeletal muscle differentiation. Moreover, CAD associates with genomic loci that correlate to altered levels of gene expression during skeletal muscle differentiation. A role for DNA strand breaks regulating changes in gene expression and genomic reprogramming has been characterized in a number of processes that do not involve CAD. What remains unknown is an appreciation for the mechanism whereby induction of a strand break by CAD can moderate or lead to a change in gene expression regulation. Indeed, it is not unreasonable to suggest that localized CAD activation may coordinate with other DNA damage inducing proteins to promote break induced alterations in gene regulation beyond the scenarios we have investigated.

For example, glucocorticoid stimulated gene expression involves topoisomerase II dependent DNA strand breaks. Topoisomerase IIB (TopoIIB) is co-recruited to regulatory elements of both estrogen receptor and androgen receptor responsive genes (Haffner et al, 2010; Ju et al, 2006). In estrogen-responsive MCF-7 cells, topoisomerase activity has been linked to the exchange of histone H1 for HMGB1/2 promoting induction of expression (Ju et al., 2006). Although the analysis of estrogen-responsive genes that utilize a DNA strand break has been limited to a small subset, the complex formation of TopoIIB with the estrogen receptor appears to be a conserved process in this subset (Ju et al, 2006). Interestingly p21 is an estrogen responsive gene, and the estrogen receptor associates to the same promoter element that we have observed during the formation of a CAD dependent DNA strand break (Mandal & Davie, 2010).

Although type II topoisomerases have been well described to induce double strands breaks, these enzymes are also known to act as DNA unwinding enzymes, leading to the suggestion that other nucleases may assist or direct the DNA damage event that is targeted by a TopoII enzyme (Durrieu et al, 2000). Interestingly, glucocorticoid stimulated TopoIIB breaks can be stabilized by inhibiting the ligase activity of topoisomerase, although the direct catalytic cleavage by topoisomerase has not been demonstrated (Haffner et al, 2010; Ju et al, 2006). A cooperation between CAD and topoisomerase II in stimulating the formation of glucocorticoid stimulated breaks was not examined in these studies, yet such a coordination could direct and stimulate the induction of DNA strand breaks. Indeed, interplay between CAD and topoisomerase II has been reported in the initial induction of DNA strand breaks that occur during apoptosis, and the proteins co-localize in both healthy and apoptotic cells (Durrieu et al, 2000). It is well documented that MCF-7 cells lack caspase 3, nevertheless cleavage of ICAD and subsequent activation of CAD can be achieved in these cells by related effector caspases (Tang & Kidd, 1998). Indeed, these observations combined with the weak inherent nuclease activity of topoisomerase II in comparison to other endonucleases suggest that CAD may provide the operative strand break capacity in such forms of gene expression (Capranico et al, 1990; Muller & Mehta, 1988).

4.2 DNA strand breaks as an inductive mechanism for DNA demethylation.

DNA demethylation has been postulated to involve the formation of DNA strand breaks as a means to excise the methylated base followed by a DNA repair step (Kress et al, 2006; Wossidlo et al, 2010). In this regard several proteins have been implicated that can also contribute to the formation of regulated DNA strand breaks. The cytidine

deaminase AID has been reported to act as a demethylation agent in primordial germ cells and in nuclear reprogramming of somatic cells via induced pluripotency (iPS) (Bhutani et al, 2010; Popp et al, 2010). As discussed in the introduction, AID has been well studied for its role in antibody diversification where it is thought to stimulate a directed DNA strand break through deamination, leading to activation of the base excision repair pathway (Petersen-Mahrt et al, 2002). This diversification in the case of somatic hypermutation (SHM) can be enhanced by DNase Y, suggesting that additional nucleases are coordinated with AID (Zan et al, 2011). AID has been shown to associate with methylated promoters of pluripotency genes in fibroblasts but not unmethylated promoters in undifferentiatied ES cells, and knockdown of AID gene expression impeded the demethylation of these promoters in heterokaryon fusions (Bhutani et al, 2010). Interestingly global DNA demethylation is observed in skeletal muscle differentiation concurrent to the period of CAD induced DNA strand breaks (Jost et al, 2001). Although we observed unaltered DNA methylation at the p21 promoter, these breaks may signal at other loci for the removal of the repressive mark, a step that may be dependent on a CAD like scission event.

4.3 Mechanism of gene repression by the induction of DNA strand breaks.

The mechanisms outlined above appear to promote the expression of genes through the induction of DNA strand breaks, and such mechanisms are consistent with our observations of directed damage and the elevated expression of the p21 gene. However, we have also observed that the breaks may contribute to repression of genes as demonstrated with Pax7. Indeed repair of DNA strand breaks within a gene have been demonstrated to prevent expression of the gene in question until the damage is repaired.

Several studies have demonstrated that the localization of a DNA strand break influences the kinetics of DNA damage repair. These studies have largely focused on ATM kinase activity in response to DNA strand breaks and whether the damage occurred in heterochromatic or euchromatic chromatin. ATM has been suggested to facilitate DNA repair in tightly condensed heterochromatin through directing localized decondensation (Noon et al, 2010). However, in euchromatic regions ATM directs the placement of repressive chromatin marks that silence transcription kilobases from the DNA strand break (Shanbhag et al, 2010). In part this repression comes from the induced activity of the E3 ubiquitin ligases, RNF8 and RNF168, that ubiquinate histone H2A in these regions of DNA (Shanbhag et al, 2010). Additionally, PARP-1 can promote the recruitment of repressive polycomb and histone deacetylase complexes to the sites of DNA damage terminating transcription within the damaged region of the genome (Chou et al, 2010). Moreover, these mechanisms of transcriptional repression are transiently maintained until the DNA damage is repaired.

Although Pax7 is required for commitment to the skeletal muscle lineage, progression of myoblast differentiation requires the rapid depletion of Pax7. This a critical requirement for muscle precursors to terminally exit the cell cycle while engaging a MRF directed transcription program (Perez-Ruiz et al, 2008; Relaix et al, 2006). Recent reports have shown that Pax7 expression is inhibited at the onset of differentiation by elevated expression of miRNAs directed to the Pax7 gene (Chen et al, 2010; Dey et al, 2011). However, given the critical need to limit Pax7 expression during differentiation, it is not unreasonable to suggest that multiple regulatory mechanisms exist to ensure that timely repression of Pax7. Clearly, CAD may participate in Pax7 repression through the

spread of a repressive chromatin signature as noted above. Alternatively, the placement of the break within the PAX7 gene at an exon-intron boundary may lead to a simple structural impediment, whereby transcription of the Pax7 gene cannot proceed through the region of damage. Future studies of the chromatin alterations at the Pax7 loci should clarify the molecular basis of this strand break mediated repression.

4.4 Regulation of Caspase 3/CAD signalling in skeletal muscle differentiation.

Paramount among the unresolved questions that have been raised by our study is how the CAD nuclease is directed to induce strand breaks yet not destroy the genome? Two independent mechanisms may be considered that contribute to a restrained activation of CAD. First, is the putative existence of two pools of ICAD/CAD a DNA bound and unbound pool. We speculate that the DNA associated pool of CAD maybe selectively targeted for activation during non-apoptotic conditions such as cell differentiation. CAD has been shown to be complexed with ICAD in a nuclear position, a localization that would permit ready activation following a directed interaction from caspase 3 (Korn et al, 2005; Reh et al, 2005). In contrast, excessive caspase 3 activation during apoptosis would allow for targeting of both the DNA bound and unbound CAD/ICAD complexes, the latter being free to indiscriminately inflict breaks through the genome. Consistent with this hypothesis we have noted that the p21 promoter is subject to specific localized strand breaks during differentiation, while apoptotic muscle cells display wide spread formation of strand breaks that are variable from experiment to experiment. Nevertheless, a confirmation of this hypothesis will require a definitive visualization of distinct ICAD/CAD pools that are specific to each cell fate outcome.

Second, we hypothesize that caspase targeting of ICAD during differentiation is directed at the D117 cleavage site, where as the greatly elevated caspase activity associated with apoptosis would result in cleavage at both D117 and D224. In this model of CAD activation, caspase cleavage at D117 site would lead to partial release of CAD while caspase targeting of both sites would remove any ICAD mediated inhibition with a higher resulting level of CAD activity. The ICAD cleavage observed during differentiation is consistent with this supposition, and mutation at D117 but not D224 leads to a reduction in myoblast differentiation (Chapter 3 Figure 4A). Indeed, this discrete activation pattern of CAD highlights the fact that the level of caspase 3 activity likely acts as the overriding determinant in CAD activity and function. Here the prediction is that unrestrained caspase activity associated with apoptosis leads to unrestrained CAD activation through one or both mechanisms described above, whereas restrained caspase 3 activation leads to limited CAD engagement, with discrete targeting of the genome.

The observations presented in this thesis demonstrate that caspase 3 activation of CAD is the primary step in promoting DNA strand breaks during myoblast differentiation. Nevertheless, caspase 3 is known to target a wide variety of substrates suggesting that this protease may utilize additional protein modifications to ensure efficient activity of the CAD nuclease. Apoptotic signalling pathways modify chromatin ultra-structure prior to DNA damage and nuclear dissolution. In this regard, caspases induce post-translational modifications of histones by altering the activity of chromatin modifying enzymes (Fullgrabe et al, 2010). As such it is reasonable to conjecture that similar events pre-empt or assist CAD to promote DNA strand breaks during cell

differentiation. Caspase 3 cleavage activation of the ste20-like kinase MST1 could be such an event. Here, one could anticipate that caspase 3 cleavage activated MST1 modifies the activity of chromatin regulatory proteins through direct phosphorylation. We assert this supposition based on the following observations. First, MST1 was initially characterized as a pro-apoptotic, caspase 3 sensitive kinase that was demonstrated to directly phosphorylate histone H2B (at serine 14) leading to chromatin compaction and apoptosis (Ahn et al, 2005b; Cheung et al, 2003; Graves et al, 1998). Secondly, MST1 has been characterized to exert a non-apoptotic function, specifically in promoting myoblast differentiation (Fernando et al, 2002). Here, expression of activated MST1 kinase (the caspase 3 cleavage activated kinase domain) provided partial rescue of differentiation in caspase 3 null myoblasts, yet prolonged activation of MST1 led to formation of picnotic nuclei and apoptosis. Following this observation of Fernando et al., MST1 was also been reported to limit cell cycle progression in both mammalian and Drosophila systems (Zeng & Hong, 2008). Together these observations suggest that MST1 may stimulate differentiation by modulating chromatin remodeling proteins to enhance CAD access to DNA.

Caspase 3 can also target DNA binding proteins to modulate gene expression and several of these targets have the potential to modify CAD access to sensitive genomic elements. The matrix attachment protein, Special AT-rich binding protein 1 (SATB1), is a global organizer of chromatin that facilitates the interaction of DNA elements termed matrix attachment regions (MARs) to the nuclear matrix. SATB1 is a demonstrated cleavage target of caspase 3/6 under both apoptotic and non-apoptotic conditions (Gotzmann et al, 2000; Sun et al, 2006; Tan et al, 2008). Cleavage of SATB1 releases

MARs from the nuclear matrix leading to chromatin disruption (Liu et al, 2003b). A specific role for caspase cleavage of SATB1 during differentiation has not been demonstrated, yet it is reasonable to suggest that removal of SATB1 (or SATB1 related proteins such as SATB2) may in some instances expose genomic elements that are targeted by CAD, allowing CAD to then induce strand breaks to coordinate gene expression.

CAD activity during cell differentiation may also be moderated by additional modifications independent of caspase function. CAD/ICAD association to DNA can be potentiated by interaction with the C-terminal of histone H1, this association can further stimulate the nuclease activity of CAD (Liu et al, 1999). Specifically, CAD has been shown to dynamically associate with the histone H1 variants, namely H1.5 and H1.0 in both healthy and apoptotic cells (Ninios et al, 2010). Moreover, H1 variants can affect specific gene expression by cooperating with additional regulatory factors (Izzo et al, 2008). This preferential association to histone variants could partly influence where in the genome CAD inflicts DNA strand breaks. Of interest, coordination between the H1.5 variant and the transcription factor Msx1 has been demonstrated to occur at the promoters of repressed genes in proliferating myoblasts (Lee et al, 2004). For example, expression of p21, which appears to be a bona fide CAD target, is impeded by Msx1 prior to myoblast differentiation (Odelberg et al, 2000). Based on these observations it is a reasonable conjecture that CAD may be directed to relieve this repressed state and engage p21 expression by interacting with H1.5 and thereby displacing Msx1. Alternatively, CAD may interact with H1.5 for the induction of the strand break that facilitates the exchange of H1.5 for an undetermined nucleosome factor such as HMGB1/2. Such an

event would relieve Msx1 repression by removing a preferred interacting partner at the p21 gene.

The transient activity of caspase 3 and CAD in differentiating cells suggests the deployment of a mechanism(s) to moderate or terminate this signal prior to inducing extensive DNA damage. Several studies have examined the signal cascades that activate and modulate caspase 3 during non-death responses, yet a definitive control mechanism has not been elucidated (Hunter et al, 2007; Koto et al, 2009; Murray et al, 2008). Such inactivation could indirectly end CAD activity by discontinued proteolysis of ICAD. Intact ICAD (both long and short isoforms) can disassemble the CAD dimer. We observe that ICAD-L is only partially cleaved and a large pool of intact ICAD-L remains during differentiation, suggesting that this mechanism maybe operative to prevent extensive DNA fragmentation (Woo et al, 2004).

Intriguingly, alternate mechanisms that block the nuclease activity of CAD have been noted. Admittedly, these cellular responses have been implicated primarily in response to caspase activity in apoptotic settings or to restrain CAD activity when this nuclease is activated as a by stander of another molecular mechanism. Nevertheless, it is reasonable to suggest that these same factors may moderate CAD activity during cellular differentiation. Polyribosylation of CAD by PARP-1 can further restrict CAD nuclease activity, as a transient increase in PARP-1 activity is concurrent with the observed DNA strand breaks during skeletal muscle differentiation this could be an avenue regulating the duration of nuclease activity (Farzaneh et al, 1985; West et al, 2005). Growth factors or cytokines may also provide a signal conduit to moderate CAD activity in both apoptotic and cell differentiation scenarios. For example, nerve growth factor (NGF) protects

neuronal cells from apoptosis through a number of mechanisms, two of these mechanisms involve inhibition of CAD. NGF stimulates nucleophosmin and Ebp1 to directly interact with CAD, diminishing its nuclease activity while not preventing caspase cleavage of ICAD itself (Ahn et al, 2005a; Ahn et al, 2006). Such a signal conduit has not been shown to be operative during myoblast differentation, yet it is reasonable to assume that a related molecule/protein restrains CAD activity in many non-apoptotic scenarios.

4.5 Role of differentiation induced DNA strand breaks by CAD in aberrant chromosomal translocations.

Aberrant chromosomes typify most cancer cells. Chromosomal translocations, where separate chromosomes suffer DNA damage but are erroneously repaired and fused together, are a significant oncogenic event. Fusion events can occur between two genes that result in a chimeric product with accelerated or expanded transforming properties (Mitelman et al, 2007; Rabbitts, 2009). The formation of such fusion genes has long been attributed to random DNA damage, however the consistent presentation of specific fusion events between precise regions of the genome suggest that a stochastic mechanism is unlikely to be the source of the initial break. Our observations and observations of other groups suggest that such break points may originate from a mechanism used to moderate transcription in an otherwise normal biologic event (Haffner et al, 2010; Lin et al, 2009).

The enzymatic activity of AID, for example in stimulating DNA breaks required for antibody diversification, can result in off target strand breaks within the c-MYC gene that precede MYC-IGH translocations characteristic of Burkitt's lymphoma (Robbiani et al, 2008). AID has also been implicated in prostate cancer translocations involving the TMPRSS2 gene through an association with the androgen receptor (AR) (Lin et al, 2009).

Interestingly, chromosomal translocations involving the TMPRSS2 gene have also been linked to TopoIIB induced DNA strand breaks involved in glucocorticoid stimulated gene expression (Haffner et al, 2010). These observations suggest not only that regulated DNA strand breaks may underlie specific translocations but also suggest that the cell lineage and its transcriptional signature can influence the site of translocation.

As a terminally differentiated tissue, skeletal muscle does not contribute largely to adult cancers, however muscle cancers termed rhabdomyosarcoma (RMS) do arise in infancy. Two forms of RMS are commonly reported, the embryonal RMS (ERMS) and alveolar RMS (ARMS), with ARMS having a very poor prognostic outcome (Xia et al, 2002). ARMS as discussed in Chapter 3 is characterized by a translocation event between Pax 3 or Pax7 with Foxo1 that results in a chimeric transcription factor. Although the origin of these translocation events is unresolved, we present the hypothesis that DNA strand breaks induced by CAD during muscle differentiation may instigate this event. In support of this hypothesis we observed the association of CAD to the known breakpoint regions of Pax7 and Foxo1a in differentiating myoblasts. Further we implicate the involvement of Caspase3/CAD in regulating the transcription of Pax7 during differentiation presumably through the induction of a DNA strand break. The induction of a strand break is supported by the observation that a putative Pax7-Foxo1a fusion transcript is observed during differentiation. This observation suggests that a DNA breakage event occurs within the Pax7 gene during differentiation and that in a rare instance may participate in a translocation. Such a role is further supported by the reports outlining a Caspase3/CAD nexus in promoting topoisomerase II poison induced chromosomal translocations (Betti et al, 2003; Betti et al, 2005; Hars et al, 2006).

Surprisingly we were capable of inducing the formation of the putative Pax7-Foxo1a fusion transcript in proliferating C2C12 cells with a low concentration of etoposide. This suggests that CAD is predetermined to target specific genomic loci following caspase induction. Importantly these observations suggest a possible origin for the Pax7-Foxo1 translocation seen in ARMS, as an aberrant outcome of the normal biological process of myoblast differentiation.

4.6 Translation of stochastic DNA damage by caspase 3/CAD to promote non-death cell fates.

The cellular response to DNA damage, particularly extensive damage, is entry into cell death or cell senescence. However examples of translating DNA damage to promote terminal differentiation have emerged. This response to DNA damage particularly in stem cell niches would be favorable to prevent the transmission of potentially oncogenic mutations provided the cell manages to evade cell death or senescence. Outstanding is an appreciation of how DNA damage can activate a cellular differentiation program. DNA damage presented to embryonic stem cells or neuronal stem cells has been shown to limit self renewal in a p53 dependent manner (Lin et al, 2005; Sherman et al, 2011). In ES cells, p53 will directly repress the expression of the pluripotency factor Nanog, this limitation in self renewal promotes the differentiation of the ES cells (Lin et al, 2005). It is speculated that damaged cells engaged in the differentiation process can then more efficiently undergo senescence or apoptosis. The response of p53 however does not appear to be a conserved mechanism in directing differentiation of DNA damaged stem cells. For example, melanocyte stem cells (MCS) differentiate to mature melanocytes in their niche in response to ionizing radiation in a

p53 independent manner (Inomata et al, 2009). Interestingly this differentiation program is characterized by notable levels of DNA damage. Although the cells survive the challenge, the premature differentiation depletes the MSC pool resulting in loss of hair pigmentation. The activity of caspase enzymes have not been explored in this phenomenon, nevertheless the exposure to low levels of DNA damage, such as those induced by topoisomerase poisons, has been noted to stimulate the tempered activation of caspase 3 and CAD in some cell types (Hars et al, 2006). These observations raise an interesting possibility that some forms of stochastic DNA damage may activate a subdued caspase cascade similar to what is observed during normal cell differentiation.

Although this thesis has primarily examined the direct role for CAD induced DNA strand breaks in regulating gene expression during myoblast differentiation a more general mechanism may also be considered in directing non-death cell fates. The BH3 mimetic ABT-737 can induce cell death by antagonizing the function of several Bcl-2 family members in a number of cancers, however many solid tumors do not share this sensitivity. Cell lines derived from solid tumors display resistance to cell death by ABT-737 and can enter cellular senescence following exposure to this compound (Song et al, 2011) In these instances, ABT-737 increases the cellular levels of reactive oxygen species that in turn stimulate caspase activation, cleavage of ICAD and activation of CAD. The activation of CAD induced a moderate level of DNA damage that led to the expression of p53 dependent senescence related genes including p21 (Song et al, 2011). It was undetermined if CAD directly induced DNA strand breaks under these conditions, yet our observations suggest that CAD could coordinate its DNA damaging activity with p53 to control the induction of senescence related genes. During skeletal muscle

differentiation transient induction of p53 expression has been reported, however this protein does not appear to participate in the induction of p21 directly (Parker et al, 1995).

4.7 Future Directions

The observations presented in this thesis suggest that caspase 3/CAD can simultaneously induce DNA strand breaks at multiple genomic loci during skeletal muscle differentiation. We present a survey of potential loci that CAD associates to during differentiation, yet this approach does not indicate the induction of a strand break per se. Direct mapping of the DNA strand breaks by ChIP of TUNEL end labelled products coupled to Solexa/Illumina high throughput sequencing has been suggested as a mapping approach for CAD induced breaks. However, the introduction of a repetitive terminal label during application of this method may introduce unexpected complications in the sequencing step (Leduc et al, 2011; Lin et al, 2009). We prefer the use of a ligation mediated end labelling approach, here the ligation of a biotin labelled adaptor to the end of a DNA strand break would facilitate direct isolation for high through-put sequencing. Subsequent analysis of the sequence would allow the direct mapping of the DNA strand break to a region of the genome by first discarding reads that do not contain the adaptor sequence and then positioning the sequence that directly follows the adaptor to the genome region. The use of this approach in parallel with mapping the CAD associated elements would provide a genome wide identification of the loci that are regulated through a caspase 3/CAD induced DNA strand break.

The requirement of caspase 3 activity in the differentiation of multiple cell lineages raises the possibility that the activation of CAD along with directed DNA damage maybe a broadly conserved reprogramming event in cell differentiation.

Notably, the induction of p21 is required for the terminal differentiation of a number of cell lineages and our observations suggest that this inductive event is associated with a CAD induced strand DNA break in the p21 promoter (Macleod et al, 1995) . As outlined in the introduction, several aspects of neuronal development require the non-apoptotic activity of caspase 3. The differentiation of isolated neuronal stem cells into key neuronal lineages requires the transient activation of caspase 3 that influences the activity of pro-neurogenic kinases (Fernando et al, 2005). In addition, kinase regulation by non-apoptotic caspase activity has been shown to promote the specification of Drosophila sensory organ precursor (SOP) cells (Kanuka et al, 2005; Kuranaga et al, 2006). Given the similar role of caspase activity during neural and skeletal muscle differentiation, it is reasonable to suggest that non-apoptotic activation of CAD may also participate in differentiation of neuronal cell types.

This supposition can find support in the observations that DNA repair events appear to impact neuronal development (Barzilai et al, 2008). For example, a number of DNA repair proteins have been suggested to participate in regulating neuronal differentiation (Fernandes et al, 2007; Lee et al, 2009). Targeted deletion of the base excision repair protein XRCC1 causes significant disruption in neural development and a significant impairment in the differentiation of the cerebellar interneuron population (Lee et al. 2009). The impaired neural development in this latter study was suggested to arise as a secondary consequence from a loss of DNA repair capacity. However, the obvious inhibition of interneuron differentiation suggests that a DNA repair process and perhaps an initial DNA damage event is a crucial factor in this process. In view of our observations, it is not unreasonable to suggest that the XRCC1 null phenotype originates

from an inability to repair DNA strand breaks that arise during normal developmental processes. The corollary to this hypothesis would be that CAD or a CAD like nuclease induces strand breaks in neurons to derive the differentiation program, similar to what we have documented in skeletal muscle myoblasts. Failure to repair these breaks may lead to impaired differentiation and stimulation of apoptosis. Exploring the origin and cause of DNA strand breaks in models of neuronal differentiation may begin to address how broadly conserved the caspase 3/CAD signalling nexus plays in cell differentiation.

4.7 Conclusions

In this thesis we present data supporting the hypothesis that induction of DNA strand breaks participate in and promote cellular differentiation via the activation of the prototypical cell death pathway. During skeletal muscle differentiation, activation of the caspase 3 protease targets and removes the ICAD inhibitor protein leading to activation of the CAD. Further these CAD induced DNA strand breaks appear to target specific loci and correlate with changes in gene expression. Collectively, these data describe a novel and as of yet unknown role for Caspase3/CAD in inducing DNA strand breaks to positively impact and enhance cellular differentiation rather than the induction of cell death. Additionally, we present data to suggest that chromosomal translocations within the Pax7 gene that give rise to alveolar rhabdomyosarcoma, originate from CAD specific activity during early stages of myoblast differentiation.

References

References: Chapter 1, Chapter 3, and Chapter 4

Abdul-Ghani M, Dufort D, Stiles R, De Repentigny Y, Kothary R, Megeney LA (2011) Wnt11 promotes cardiomyocyte development by caspase-mediated suppression of canonical Wnt signals. *Mol Cell Biol* **31**(1)**:** 163-178

Ahn JY, Liu X, Cheng D, Peng J, Chan PK, Wade PA, Ye K (2005a) Nucleophosmin/B23, a nuclear PI(3,4,5)P(3) receptor, mediates the antiapoptotic actions of NGF by inhibiting CAD. *Mol Cell* **18**(4)**:** 435-445

Ahn JY, Liu X, Liu Z, Pereira L, Cheng D, Peng J, Wade PA, Hamburger AW, Ye K (2006) Nuclear Akt associates with PKC-phosphorylated Ebp1, preventing DNA fragmentation by inhibition of caspase-activated DNase. *EMBO J* **25**(10)**:** 2083-2095

Ahn SH, Cheung WL, Hsu JY, Diaz RL, Smith MM, Allis CD (2005b) Sterile 20 kinase phosphorylates histone H2B at serine 10 during hydrogen peroxide-induced apoptosis in S. cerevisiae. *Cell* **120**(1)**:** 25-36

Ameisen JC (2002) On the origin, evolution, and nature of programmed cell death: a timeline of four billion years. *Cell Death Differ* **9**(4)**:** 367-393

Barski A, Zhao K (2009) Genomic location analysis by ChIP-Seq. *J Cell Biochem* **107**(1)**:** 11-18

Bartek J, Hamerlik P, Lukas J (2010) On the origin of prostate fusion oncogenes. *Nat Genet* **42**(8)**:** 647-648

Barzilai A, Biton S, Shiloh Y (2008) The role of the DNA damage response in neuronal development, organization and maintenance. *DNA Repair (Amst)* **7**(7)**:** 1010-1027

Bentley DR, Balasubramanian S, Swerdlow HP, Smith GP, Milton J, Brown CG, Hall KP, Evers DJ, Barnes CL, Bignell HR, Boutell JM, Bryant J, Carter RJ, Keira Cheetham R, Cox AJ, Ellis DJ, Flatbush MR, Gormley NA, Humphray SJ, Irving LJ, Karbelashvili MS, Kirk SM, Li H, Liu X, Maisinger KS, Murray LJ, Obradovic B, Ost T, Parkinson ML, Pratt MR, Rasolonjatovo IM, Reed MT, Rigatti R, Rodighiero C, Ross MT, Sabot A, Sankar SV, Scally A, Schroth GP, Smith ME, Smith VP, Spiridou A, Torrance PE, Tzonev SS, Vermaas EH, Walter K, Wu X, Zhang L, Alam MD, Anastasi C, Aniebo IC, Bailey DM, Bancarz IR, Banerjee S, Barbour SG, Baybayan PA, Benoit VA, Benson KF, Bevis C, Black PJ, Boodhun A, Brennan JS, Bridgham JA, Brown RC, Brown AA, Buermann DH, Bundu AA, Burrows JC, Carter NP, Castillo N, Chiara ECM, Chang S, Neil Cooley R, Crake NR, Dada OO, Diakoumakos KD, Dominguez-Fernandez B, Earnshaw DJ, Egbujor UC, Elmore DW, Etchin SS, Ewan MR, Fedurco M, Fraser LJ, Fuentes Fajardo KV, Scott Furey W, George D, Gietzen KJ, Goddard CP, Golda GS, Granieri PA, Green DE, Gustafson DL, Hansen NF, Harnish K, Haudenschild CD, Heyer

NI, Hims MM, Ho JT, Horgan AM, Hoschler K, Hurwitz S, Ivanov DV, Johnson MQ, James T, Huw Jones TA, Kang GD, Kerelska TH, Kersey AD, Khrebtukova I, Kindwall AP, Kingsbury Z, Kokko-Gonzales PI, Kumar A, Laurent MA, Lawley CT, Lee SE, Lee X, Liao AK, Loch JA, Lok M, Luo S, Mammen RM, Martin JW, McCauley PG, McNitt P, Mehta P, Moon KW, Mullens JW, Newington T, Ning Z, Ling Ng B, Novo SM, O'Neill MJ, Osborne MA, Osnowski A, Ostadan O, Paraschos LL, Pickering L, Pike AC, Chris Pinkard D, Pliskin DP, Podhasky J, Quijano VJ, Raczy C, Rae VH, Rawlings SR, Chiva Rodriguez A, Roe PM, Rogers J, Rogert Bacigalupo MC, Romanov N, Romieu A, Roth RK, Rourke NJ, Ruediger ST, Rusman E, Sanches-Kuiper RM, Schenker MR, Seoane JM, Shaw RJ, Shiver MK, Short SW, Sizto NL, Sluis JP, Smith MA, Ernest Sohna Sohna J, Spence EJ, Stevens K, Sutton N, Szajkowski L, Tregidgo CL, Turcatti G, Vandevondele S, Verhovsky Y, Virk SM, Wakelin S, Walcott GC, Wang J, Worsley GJ, Yan J, Yau L, Zuerlein M, Mullikin JC, Hurles ME, McCooke NJ, West JS, Oaks FL, Lundberg PL, Klenerman D, Durbin R, Smith AJ (2008) Accurate whole human genome sequencing using reversible terminator chemistry. *Nature* **456**(7218)**:** 53-59

Berkes CA, Tapscott SJ (2005) MyoD and the transcriptional control of myogenesis. *Semin Cell Dev Biol* **16**(4-5)**:** 585-595

Betti CJ, Villalobos MJ, Diaz MO, Vaughan AT (2001) Apoptotic triggers initiate translocations within the MLL gene involving the nonhomologous end joining repair system. *Cancer Res* **61**(11)**:** 4550-4555

Betti CJ, Villalobos MJ, Diaz MO, Vaughan AT (2003) Apoptotic stimuli initiate MLL-AF9 translocations that are transcribed in cells capable of division. *Cancer Res* **63**(6)**:** 1377-1381

Betti CJ, Villalobos MJ, Jiang Q, Cline E, Diaz MO, Loredo G, Vaughan AT (2005) Cleavage of the MLL gene by activators of apoptosis is independent of topoisomerase II activity. *Leukemia* **19**(12)**:** 2289-2295

Bhutani N, Brady JJ, Damian M, Sacco A, Corbel SY, Blau HM (2010) Reprogramming towards pluripotency requires AID-dependent DNA demethylation. *Nature* **463**(7284)**:** 1042-1047

Boatright KM, Renatus M, Scott FL, Sperandio S, Shin H, Pedersen IM, Ricci JE, Edris WA, Sutherlin DP, Green DR, Salvesen GS (2003) A unified model for apical caspase activation. *Mol Cell* **11**(2)**:** 529-541

Buckingham M (2006) Myogenic progenitor cells and skeletal myogenesis in vertebrates. *Curr Opin Genet Dev* **16**(5)**:** 525-532

Buckingham M, Vincent SD (2009) Distinct and dynamic myogenic populations in the vertebrate embryo. *Curr Opin Genet Dev* **19**(5)**:** 444-453

Capranico G, Jaxel C, Roberge M, Kohn KW, Pommier Y (1990) Nucleosome positioning as a critical determinant for the DNA cleavage sites of mammalian DNA

topoisomerase II in reconstituted simian virus 40 chromatin. *Nucleic Acids Res* **18**(15)**:** 4553-4559

Carlile GW, Smith DH, Wiedmann M (2004) Caspase-3 has a nonapoptotic function in erythroid maturation. *Blood* **103**(11)**:** 4310-4316

Chen JF, Tao Y, Li J, Deng Z, Yan Z, Xiao X, Wang DZ (2010) microRNA-1 and microRNA-206 regulate skeletal muscle satellite cell proliferation and differentiation by repressing Pax7. *J Cell Biol* **190**(5)**:** 867-879

Cheung WL, Ajiro K, Samejima K, Kloc M, Cheung P, Mizzen CA, Beeser A, Etkin LD, Chernoff J, Earnshaw WC, Allis CD (2003) Apoptotic phosphorylation of histone H2B is mediated by mammalian sterile twenty kinase. *Cell* **113**(4)**:** 507-517

Chipuk JE, Moldoveanu T, Llambi F, Parsons MJ, Green DR (2010) The BCL-2 family reunion. *Mol Cell* **37**(3)**:** 299-310

Chou DM, Adamson B, Dephoure NE, Tan X, Nottke AC, Hurov KE, Gygi SP, Colaiacovo MP, Elledge SJ (2010) A chromatin localization screen reveals poly (ADP ribose)-regulated recruitment of the repressive polycomb and NuRD complexes to sites of DNA damage. *Proc Natl Acad Sci U S A* **107**(43)**:** 18475-18480

Ciccia A, Elledge SJ (2010) The DNA damage response: making it safe to play with knives. *Mol Cell* **40**(2)**:** 179-204

Crawford ED, Wells JA (2011) Caspase substrates and cellular remodeling. *Annu Rev Biochem* **80:** 1055-1087

Dawson BA, Lough J (1988) Immunocytochemical localization of transient DNA strand breaks in differentiating myotubes using in situ nick-translation. *Dev Biol* **127**(2)**:** 362-367

Deato MD, Marr MT, Sottero T, Inouye C, Hu P, Tjian R (2008) MyoD targets TAF3/TRF3 to activate myogenin transcription. *Mol Cell* **32**(1)**:** 96-105

Denecker G, Hoste E, Gilbert B, Hochepied T, Ovaere P, Lippens S, Van den Broecke C, Van Damme P, D'Herde K, Hachem JP, Borgonie G, Presland RB, Schoonjans L, Libert C, Vandekerckhove J, Gevaert K, Vandenabeele P, Declercq W (2007) Caspase-14 protects against epidermal UVB photodamage and water loss. *Nat Cell Biol* **9**(6)**:** 666-674

Dey BK, Gagan J, Dutta A (2011) miR-206 and -486 induce myoblast differentiation by downregulating Pax7. *Mol Cell Biol* **31**(1)**:** 203-214

Du C, Fang M, Li Y, Li L, Wang X (2000) Smac, a mitochondrial protein that promotes cytochrome c-dependent caspase activation by eliminating IAP inhibition. *Cell* **102**(1)**:** 33-42

Durrieu F, Samejima K, Fortune JM, Kandels-Lewis S, Osheroff N, Earnshaw WC (2000) DNA topoisomerase IIalpha interacts with CAD nuclease and is involved in chromatin condensation during apoptotic execution. *Curr Biol* **10**(15)**:** 923-926

Earnshaw WC, Martins LM, Kaufmann SH (1999) Mammalian caspases: structure, activation, substrates, and functions during apoptosis. *Annu Rev Biochem* **68:** 383-424

Eckhart L, Declercq W, Ban J, Rendl M, Lengauer B, Mayer C, Lippens S, Vandenabeele P, Tschachler E (2000) Terminal differentiation of human keratinocytes and stratum corneum formation is associated with caspase-14 activation. *J Invest Dermatol* **115**(6)**:** 1148-1151

Elliott MR, Chekeni FB, Trampont PC, Lazarowski ER, Kadl A, Walk SF, Park D, Woodson RI, Ostankovich M, Sharma P, Lysiak JJ, Harden TK, Leitinger N, Ravichandran KS (2009) Nucleotides released by apoptotic cells act as a find-me signal to promote phagocytic clearance. *Nature* **461**(7261)**:** 282-286

Ellis HM, Horvitz HR (1986) Genetic control of programmed cell death in the nematode C. elegans. *Cell* **44**(6)**:** 817-829

Enari M, Sakahira H, Yokoyama H, Okawa K, Iwamatsu A, Nagata S (1998) A caspase-activated DNase that degrades DNA during apoptosis, and its inhibitor ICAD. *Nature* **391**(6662)**:** 43-50

Farzaneh F, Shall S, Johnstone AP (1985) The dynamic nature of DNA-strand breaks present in differentiating muscle cells and quiescent lymphocytes. *FEBS Lett* **189**(1)**:** 62-66

Faulkner GJ, Kimura Y, Daub CO, Wani S, Plessy C, Irvine KM, Schroder K, Cloonan N, Steptoe AL, Lassmann T, Waki K, Hornig N, Arakawa T, Takahashi H, Kawai J, Forrest AR, Suzuki H, Hayashizaki Y, Hume DA, Orlando V, Grimmond SM, Carninci P (2009) The regulated retrotransposon transcriptome of mammalian cells. *Nat Genet* **41**(5)**:** 563-571

Fernandes-Alnemri T, Litwack G, Alnemri ES (1994) CPP32, a novel human apoptotic protein with homology to Caenorhabditis elegans cell death protein Ced-3 and mammalian interleukin-1 beta-converting enzyme. *J Biol Chem* **269**(49)**:** 30761-30764

Fernandes ND, Sun Y, Price BD (2007) Activation of the kinase activity of ATM by retinoic acid is required for CREB-dependent differentiation of neuroblastoma cells. *J Biol Chem* **282**(22)**:** 16577-16584

Fernando P, Brunette S, Megeney LA (2005) Neural stem cell differentiation is dependent upon endogenous caspase 3 activity. *Faseb J* **19**(12)**:** 1671-1673

Fernando P, Kelly JF, Balazsi K, Slack RS, Megeney LA (2002) Caspase 3 activity is required for skeletal muscle differentiation. *Proc Natl Acad Sci U S A* **99**(17)**:** 11025-11030

Fernando P, Megeney LA (2007) Is caspase-dependent apoptosis only cell differentiation taken to the extreme? *Faseb J* **21**(1)**:** 8-17

Finckbone V, Oomman SK, Strahlendorf HK, Strahlendorf JC (2009) Regional differences in the temporal expression of non-apoptotic caspase-3-positive bergmann glial cells in the developing rat cerebellum. *Front Neuroanat* **3:** 3

Fujita J, Crane AM, Souza MK, Dejosez M, Kyba M, Flavell RA, Thomson JA, Zwaka TP (2008) Caspase activity mediates the differentiation of embryonic stem cells. *Cell Stem Cell* **2**(6)**:** 595-601

Fullgrabe J, Hajji N, Joseph B (2010) Cracking the death code: apoptosis-related histone modifications. *Cell Death Differ* **17**(8)**:** 1238-1243

Gotzmann J, Meissner M, Gerner C (2000) The fate of the nuclear matrix-associated-region-binding protein SATB1 during apoptosis. *Cell Death Differ* **7**(5)**:** 425-438

Graves JD, Gotoh Y, Draves KE, Ambrose D, Han DK, Wright M, Chernoff J, Clark EA, Krebs EG (1998) Caspase-mediated activation and induction of apoptosis by the mammalian Ste20-like kinase Mst1. *EMBO J* **17**(8)**:** 2224-2234

Haffner MC, Aryee MJ, Toubaji A, Esopi DM, Albadine R, Gurel B, Isaacs WB, Bova GS, Liu W, Xu J, Meeker AK, Netto G, De Marzo AM, Nelson WG, Yegnasubramanian S (2010) Androgen-induced TOP2B-mediated double-strand breaks and prostate cancer gene rearrangements. *Nat Genet* **42**(8)**:** 668-675

Hanahan D, Weinberg RA (2011) Hallmarks of cancer: the next generation. *Cell* **144**(5)**:** 646-674

Hars ES, Lyu YL, Lin CP, Liu LF (2006) Role of apoptotic nuclease caspase-activated DNase in etoposide-induced treatment-related acute myelogenous leukemia. *Cancer Res* **66**(18)**:** 8975-8979

Hossain MS, Akimitsu N, Kurokawa K, Sekimizu K (2003) Myogenic differentiation of Drosophila Schneider cells by DNA double-strand break-inducing drugs. *Differentiation* **71**(4-5)**:** 271-280

Hunter AL, Zhang J, Chen SC, Si X, Wong B, Ekhterae D, Luo H, Granville DJ (2007) Apoptosis repressor with caspase recruitment domain (ARC) inhibits myogenic differentiation. *FEBS Lett* **581**(5)**:** 879-884

Hutcheson DA, Zhao J, Merrell A, Haldar M, Kardon G (2009) Embryonic and fetal limb myogenic cells are derived from developmentally distinct progenitors and have different requirements for beta-catenin. *Genes Dev* **23**(8)**:** 997-1013

Inohara N, Koseki T, Chen S, Wu X, Nunez G (1998) CIDE, a novel family of cell death activators with homology to the 45 kDa subunit of the DNA fragmentation factor. *EMBO J* **17**(9)**:** 2526-2533

Inomata K, Aoto T, Binh NT, Okamoto N, Tanimura S, Wakayama T, Iseki S, Hara E, Masunaga T, Shimizu H, Nishimura EK (2009) Genotoxic stress abrogates renewal of melanocyte stem cells by triggering their differentiation. *Cell* **137**(6)**:** 1088-1099

Irmler M, Thome M, Hahne M, Schneider P, Hofmann K, Steiner V, Bodmer JL, Schroter M, Burns K, Mattmann C, Rimoldi D, French LE, Tschopp J (1997) Inhibition of death receptor signals by cellular FLIP. *Nature* **388**(6638)**:** 190-195

Ishizaki Y, Jacobson MD, Raff MC (1998) A role for caspases in lens fiber differentiation. *J Cell Biol* **140**(1)**:** 153-158

Izzo A, Kamieniarz K, Schneider R (2008) The histone H1 family: specific members, specific functions? *Biol Chem* **389**(4)**:** 333-343

Janzen V, Fleming HE, Riedt T, Karlsson G, Riese MJ, Lo Celso C, Reynolds G, Milne CD, Paige CJ, Karlsson S, Woo M, Scadden DT (2008) Hematopoietic stem cell responsiveness to exogenous signals is limited by caspase-3. *Cell Stem Cell* **2**(6)**:** 584-594

Jost JP, Oakeley EJ, Zhu B, Benjamin D, Thiry S, Siegmann M, Jost YC (2001) 5-Methylcytosine DNA glycosylase participates in the genome-wide loss of DNA methylation occurring during mouse myoblast differentiation. *Nucleic Acids Res* **29**(21)**:** 4452-4461

Ju BG, Lunyak VV, Perissi V, Garcia-Bassets I, Rose DW, Glass CK, Rosenfeld MG (2006) A topoisomerase IIbeta-mediated dsDNA break required for regulated transcription. *Science* **312**(5781)**:** 1798-1802

Jung D, Alt FW (2004) Unraveling V(D)J recombination; insights into gene regulation. *Cell* **116**(2)**:** 299-311

Kalinowska-Herok M, Widlak P (2008) High mobility group proteins stimulate DNA cleavage by apoptotic endonuclease DFF40/CAD due to HMG-box interactions with DNA. *Acta Biochim Pol* **55**(1)**:** 21-26

Kanuka H, Kuranaga E, Takemoto K, Hiratou T, Okano H, Miura M (2005) Drosophila caspase transduces Shaggy/GSK-3beta kinase activity in neural precursor development. *EMBO J* **24**(21)**:** 3793-3806

Kawane K, Fukuyama H, Yoshida H, Nagase H, Ohsawa Y, Uchiyama Y, Okada K, Iida T, Nagata S (2003) Impaired thymic development in mouse embryos deficient in apoptotic DNA degradation. *Nat Immunol* **4**(2)**:** 138-144

Kerr JF, Wyllie AH, Currie AR (1972) Apoptosis: a basic biological phenomenon with wide-ranging implications in tissue kinetics. *Br J Cancer* **26**(4)**:** 239-257

Kluck RM, Bossy-Wetzel E, Green DR, Newmeyer DD (1997) The release of cytochrome c from mitochondria: a primary site for Bcl-2 regulation of apoptosis. *Science* **275**(5303)**:** 1132-1136

Korn C, Scholz SR, Gimadutdinow O, Lurz R, Pingoud A, Meiss G (2005) Interaction of DNA fragmentation factor (DFF) with DNA reveals an unprecedented mechanism for nuclease inhibition and suggests that DFF can be activated in a DNA-bound state. *J Biol Chem* **280**(7)**:** 6005-6015

Koto A, Kuranaga E, Miura M (2009) Temporal regulation of Drosophila IAP1 determines caspase functions in sensory organ development. *J Cell Biol* **187**(2)**:** 219-231

Kress C, Thomassin H, Grange T (2006) Active cytosine demethylation triggered by a nuclear receptor involves DNA strand breaks. *Proc Natl Acad Sci U S A* **103**(30)**:** 11112-11117

Kuida K, Haydar TF, Kuan CY, Gu Y, Taya C, Karasuyama H, Su MS, Rakic P, Flavell RA (1998) Reduced apoptosis and cytochrome c-mediated caspase activation in mice lacking caspase 9. *Cell* **94**(3)**:** 325-337

Kuida K, Zheng TS, Na S, Kuan C, Yang D, Karasuyama H, Rakic P, Flavell RA (1996) Decreased apoptosis in the brain and premature lethality in CPP32-deficient mice. *Nature* **384**(6607)**:** 368-372

Kuranaga E, Kanuka H, Tonoki A, Takemoto K, Tomioka T, Kobayashi M, Hayashi S, Miura M (2006) Drosophila IKK-related kinase regulates nonapoptotic function of caspases via degradation of IAPs. *Cell* **126**(3)**:** 583-596

Lakhani SA, Masud A, Kuida K, Porter GA, Jr., Booth CJ, Mehal WZ, Inayat I, Flavell RA (2006) Caspases 3 and 7: key mediators of mitochondrial events of apoptosis. *Science* **311**(5762)**:** 847-851

Lamkanfi M, Festjens N, Declercq W, Vanden Berghe T, Vandenabeele P (2007) Caspases in cell survival, proliferation and differentiation. *Cell Death Differ* **14**(1)**:** 44-55

Launay S, Hermine O, Fontenay M, Kroemer G, Solary E, Garrido C (2005) Vital functions for lethal caspases. *Oncogene* **24**(33)**:** 5137-5148

Le Grand F, Rudnicki MA (2007) Skeletal muscle satellite cells and adult myogenesis. *Curr Opin Cell Biol* **19**(6)**:** 628-633

Lechardeur D, Drzymala L, Sharma M, Zylka D, Kinach R, Pacia J, Hicks C, Usmani N, Rommens JM, Lukacs GL (2000) Determinants of the nuclear localization of the heterodimeric DNA fragmentation factor (ICAD/CAD). *J Cell Biol* **150**(2)**:** 321-334

Leduc F, Faucher D, Bikond Nkoma G, Gregoire MC, Arguin M, Wellinger RJ, Boissonneault G (2011) Genome-wide mapping of DNA strand breaks. *PLoS One* **6**(2)**:** e17353

Lee H, Habas R, Abate-Shen C (2004) MSX1 cooperates with histone H1b for inhibition of transcription and myogenesis. *Science* **304**(5677)**:** 1675-1678

Lee Y, Katyal S, Li Y, El-Khamisy SF, Russell HR, Caldecott KW, McKinnon PJ (2009) The genesis of cerebellar interneurons and the prevention of neural DNA damage require XRCC1. *Nat Neurosci* **12**(8)**:** 973-980

Li H, Zhu H, Xu CJ, Yuan J (1998) Cleavage of BID by caspase 8 mediates the mitochondrial damage in the Fas pathway of apoptosis. *Cell* **94**(4)**:** 491-501

Li LY, Luo X, Wang X (2001) Endonuclease G is an apoptotic DNase when released from mitochondria. *Nature* **412**(6842)**:** 95-99

Li W, Ma H (2006) Double-stranded DNA breaks and gene functions in recombination and meiosis. *Cell Res* **16**(5)**:** 402-412

Lieber MR, Ma Y, Pannicke U, Schwarz K (2004) The mechanism of vertebrate nonhomologous DNA end joining and its role in V(D)J recombination. *DNA Repair (Amst)* **3**(8-9)**:** 817-826

Lin C, Yang L, Tanasa B, Hutt K, Ju BG, Ohgi K, Zhang J, Rose DW, Fu XD, Glass CK, Rosenfeld MG (2009) Nuclear receptor-induced chromosomal proximity and DNA breaks underlie specific translocations in cancer. *Cell* **139**(6)**:** 1069-1083

Lin T, Chao C, Saito S, Mazur SJ, Murphy ME, Appella E, Xu Y (2005) p53 induces differentiation of mouse embryonic stem cells by suppressing Nanog expression. *Nat Cell Biol* **7**(2)**:** 165-171

Liu QL, Kishi H, Ohtsuka K, Muraguchi A (2003a) Heat shock protein 70 binds caspase-activated DNase and enhances its activity in TCR-stimulated T cells. *Blood* **102**(5)**:** 1788-1796

Liu QY, Ribecco-Lutkiewicz M, Carson C, Testolin L, Bergeron D, Kohwi-Shigematsu T, Walker PR, Sikorska M (2003b) Mapping the initial DNA breaks in apoptotic Jurkat cells using ligation-mediated PCR. *Cell Death Differ* **10**(3)**:** 278-289

Liu X, Zou H, Slaughter C, Wang X (1997) DFF, a heterodimeric protein that functions downstream of caspase-3 to trigger DNA fragmentation during apoptosis. *Cell* **89**(2)**:** 175-184

Liu X, Zou H, Widlak P, Garrard W, Wang X (1999) Activation of the apoptotic endonuclease DFF40 (caspase-activated DNase or nuclease). Oligomerization and direct interaction with histone H1. *J Biol Chem* **274**(20)**:** 13836-13840

Luthi AU, Martin SJ (2007) The CASBAH: a searchable database of caspase substrates. *Cell Death Differ* **14**(4)**:** 641-650

Macleod KF, Sherry N, Hannon G, Beach D, Tokino T, Kinzler K, Vogelstein B, Jacks T (1995) p53-dependent and independent expression of p21 during cell growth, differentiation, and DNA damage. *Genes Dev* **9**(8)**:** 935-944

Mandal S, Davie JR (2010) Estrogen regulated expression of the p21 Waf1/Cip1 gene in estrogen receptor positive human breast cancer cells. *J Cell Physiol* **224**(1)**:** 28-32

Mathas S, Misteli T (2009) The dangers of transcription. *Cell* **139**(6)**:** 1047-1049

McCarty JS, Toh SY, Li P (1999) Study of DFF45 in its role of chaperone and inhibitor: two independent inhibitory domains of DFF40 nuclease activity. *Biochem Biophys Res Commun* **264**(1)**:** 176-180

Medema JP, Scaffidi C, Kischkel FC, Shevchenko A, Mann M, Krammer PH, Peter ME (1997) FLICE is activated by association with the CD95 death-inducing signaling complex (DISC). *EMBO J* **16**(10)**:** 2794-2804

Mitelman F, Johansson B, Mertens F (2007) The impact of translocations and gene fusions on cancer causation. *Nat Rev Cancer* **7**(4)**:** 233-245

Miura M, Chen XD, Allen MR, Bi Y, Gronthos S, Seo BM, Lakhani S, Flavell RA, Feng XH, Robey PG, Young M, Shi S (2004) A crucial role of caspase-3 in osteogenic differentiation of bone marrow stromal stem cells. *J Clin Invest* **114**(12)**:** 1704-1713

Miura M, Zhu H, Rotello R, Hartwieg EA, Yuan J (1993) Induction of apoptosis in fibroblasts by IL-1 beta-converting enzyme, a mammalian homolog of the C. elegans cell death gene ced-3. *Cell* **75**(4)**:** 653-660

Mondal N, Parvin JD (2001) DNA topoisomerase IIalpha is required for RNA polymerase II transcription on chromatin templates. *Nature* **413**(6854)**:** 435-438

Muller MT, Mehta VB (1988) DNase I hypersensitivity is independent of endogenous topoisomerase II activity during chicken erythrocyte differentiation. *Mol Cell Biol* **8**(9)**:** 3661-3669

Murray TV, McMahon JM, Howley BA, Stanley A, Ritter T, Mohr A, Zwacka R, Fearnhead HO (2008) A non-apoptotic role for caspase-9 in muscle differentiation. *J Cell Sci* **121**(Pt 22)**:** 3786-3793

Neimanis S, Albig W, Doenecke D, Kahle J (2007) Sequence elements in both subunits of the DNA fragmentation factor are essential for its nuclear transport. *J Biol Chem* **282**(49)**:** 35821-35830

Ninios YP, Sekeri-Pataryas KE, Sourlingas TG (2010) Histone H1 subtype preferences of DFF40 and possible nuclear localization of DFF40/45 in normal and trichostatin A-treated NB4 leukemic cells. *Apoptosis* **15**(2)**:** 128-138

Noon AT, Shibata A, Rief N, Lobrich M, Stewart GS, Jeggo PA, Goodarzi AA (2010) 53BP1-dependent robust localized KAP-1 phosphorylation is essential for heterochromatic DNA double-strand break repair. *Nat Cell Biol* **12**(2)**:** 177-184

O'Sullivan JM, Sontam DM, Grierson R, Jones B (2009) Repeated elements coordinate the spatial organization of the yeast genome. *Yeast* **26**(2)**:** 125-138

Odelberg SJ, Kollhoff A, Keating MT (2000) Dedifferentiation of mammalian myotubes induced by msx1. *Cell* **103**(7)**:** 1099-1109

Okamoto M, Okamoto N, Yashiro H, Shiokawa D, Sunaga S, Yoshimori A, Tanuma S, Kitamura D (2005) Involvement of DNase gamma in the resected double-strand DNA breaks in immunoglobulin genes. *Biochem Biophys Res Commun* **327**(1)**:** 76-83

Okamoto N, Okamoto M, Araki S, Arakawa H, Mizuta R, Kitamura D (2009) Possible contribution of DNase gamma to immunoglobulin V gene diversification. *Immunol Lett* **125**(1)**:** 22-30

Okuyama R, Nguyen BC, Talora C, Ogawa E, Tommasi di Vignano A, Lioumi M, Chiorino G, Tagami H, Woo M, Dotto GP (2004) High commitment of embryonic keratinocytes to terminal differentiation through a Notch1-caspase 3 regulatory mechanism. *Dev Cell* **6**(4)**:** 551-562

Olson EN, Klein WH (1994) bHLH factors in muscle development: dead lines and commitments, what to leave in and what to leave out. *Genes Dev* **8**(1)**:** 1-8

Olson EN, Perry M, Schulz RA (1995) Regulation of muscle differentiation by the MEF2 family of MADS box transcription factors. *Dev Biol* **172**(1)**:** 2-14

Oomman S, Finckbone V, Dertien J, Attridge J, Henne W, Medina M, Mansouri B, Singh H, Strahlendorf H, Strahlendorf J (2004) Active caspase-3 expression during postnatal development of rat cerebellum is not systematically or consistently associated with apoptosis. *J Comp Neurol* **476**(2)**:** 154-173

Oomman S, Strahlendorf H, Dertien J, Strahlendorf J (2006) Bergmann glia utilize active caspase-3 for differentiation. *Brain Res* **1078**(1)**:** 19-34

Parker SB, Eichele G, Zhang P, Rawls A, Sands AT, Bradley A, Olson EN, Harper JW, Elledge SJ (1995) p53-independent expression of p21Cip1 in muscle and other terminally differentiating cells. *Science* **267**(5200)**:** 1024-1027

Perez-Ruiz A, Ono Y, Gnocchi VF, Zammit PS (2008) beta-Catenin promotes self-renewal of skeletal-muscle satellite cells. *J Cell Sci* **121**(Pt 9)**:** 1373-1382

Petersen-Mahrt SK, Harris RS, Neuberger MS (2002) AID mutates E. coli suggesting a DNA deamination mechanism for antibody diversification. *Nature* **418**(6893)**:** 99-103

Popp C, Dean W, Feng S, Cokus SJ, Andrews S, Pellegrini M, Jacobsen SE, Reik W (2010) Genome-wide erasure of DNA methylation in mouse primordial germ cells is affected by AID deficiency. *Nature* **463**(7284)**:** 1101-1105

Puri PL, Sartorelli V (2000) Regulation of muscle regulatory factors by DNA-binding, interacting proteins, and post-transcriptional modifications. *J Cell Physiol* **185**(2)**:** 155-173

Rabbitts TH (2009) Commonality but diversity in cancer gene fusions. *Cell* **137**(3)**:** 391-395

Radic M, Marion T, Monestier M (2004) Nucleosomes are exposed at the cell surface in apoptosis. *J Immunol* **172**(11)**:** 6692-6700

Reh S, Korn C, Gimadutdinow O, Meiss G (2005) Structural basis for stable DNA complex formation by the caspase-activated DNase. *J Biol Chem* **280**(50)**:** 41707-41715

Relaix F, Montarras D, Zaffran S, Gayraud-Morel B, Rocancourt D, Tajbakhsh S, Mansouri A, Cumano A, Buckingham M (2006) Pax3 and Pax7 have distinct and overlapping functions in adult muscle progenitor cells. *J Cell Biol* **172**(1)**:** 91-102

Relaix F, Rocancourt D, Mansouri A, Buckingham M (2005) A Pax3/Pax7-dependent population of skeletal muscle progenitor cells. *Nature* **435**(7044)**:** 948-953

Ribeil JA, Zermati Y, Vandekerckhove J, Cathelin S, Kersual J, Dussiot M, Coulon S, Moura IC, Zeuner A, Kirkegaard-Sorensen T, Varet B, Solary E, Garrido C, Hermine O (2007) Hsp70 regulates erythropoiesis by preventing caspase-3-mediated cleavage of GATA-1. *Nature* **445**(7123)**:** 102-105

Robbiani DF, Bothmer A, Callen E, Reina-San-Martin B, Dorsett Y, Difilippantonio S, Bolland DJ, Chen HT, Corcoran AE, Nussenzweig A, Nussenzweig MC (2008) AID is required for the chromosomal breaks in c-myc that lead to c-myc/IgH translocations. *Cell* **135**(6)**:** 1028-1038

Rohn TT, Cusack SM, Kessinger SR, Oxford JT (2004) Caspase activation independent of cell death is required for proper cell dispersal and correct morphology in PC12 cells. *Exp Cell Res* **295**(1)**:** 215-225

Rubin BP, Nishijo K, Chen HI, Yi X, Schuetze DP, Pal R, Prajapati SI, Abraham J, Arenkiel BR, Chen QR, Davis S, McCleish AT, Capecchi MR, Michalek JE, Zarzabal LA, Khan J, Yu Z, Parham DM, Barr FG, Meltzer PS, Chen Y, Keller C (2010) Evidence for an unanticipated relationship between undifferentiated pleomorphic sarcoma and embryonal rhabdomyosarcoma. *Cancer Cell* **19**(2)**:** 177-191

Rudnicki MA, Schnegelsberg PN, Stead RH, Braun T, Arnold HH, Jaenisch R (1993) MyoD or Myf-5 is required for the formation of skeletal muscle. *Cell* **75**(7)**:** 1351-1359

Sakahira H, Enari M, Nagata S (1998) Cleavage of CAD inhibitor in CAD activation and DNA degradation during apoptosis. *Nature* **391**(6662)**:** 96-99

Sakahira H, Enari M, Nagata S (1999) Functional differences of two forms of the inhibitor of caspase-activated DNase, ICAD-L, and ICAD-S. *J Biol Chem* **274**(22)**:** 15740-15744

Samejima K, Earnshaw WC (2005) Trashing the genome: the role of nucleases during apoptosis. *Nat Rev Mol Cell Biol* **6**(9)**:** 677-688

Schienda J, Engleka KA, Jun S, Hansen MS, Epstein JA, Tabin CJ, Kunkel LM, Kardon G (2006) Somitic origin of limb muscle satellite and side population cells. *Proc Natl Acad Sci U S A* **103**(4)**:** 945-950

Seale P, Ishibashi J, Scime A, Rudnicki MA (2004) Pax7 is necessary and sufficient for the myogenic specification of CD45+:Sca1+ stem cells from injured muscle. *PLoS Biol* **2**(5)**:** E130

Seale P, Sabourin LA, Girgis-Gabardo A, Mansouri A, Gruss P, Rudnicki MA (2000) Pax7 is required for the specification of myogenic satellite cells. *Cell* **102**(6)**:** 777-786

Shanbhag NM, Rafalska-Metcalf IU, Balane-Bolivar C, Janicki SM, Greenberg RA (2010) ATM-dependent chromatin changes silence transcription in cis to DNA double-strand breaks. *Cell* **141**(6)**:** 970-981

Sherman MH, Bassing CH, Teitell MA (2011) Regulation of cell differentiation by the DNA damage response. *Trends Cell Biol* **21**(5)**:** 312-319

Shiokawa D, Kobayashi T, Tanuma S (2002) Involvement of DNase gamma in apoptosis associated with myogenic differentiation of C2C12 cells. *J Biol Chem* **277**(34)**:** 31031-31037

Shiokawa D, Tanuma S (2004) Differential DNases are selectively used in neuronal apoptosis depending on the differentiation state. *Cell Death Differ* **11**(10)**:** 1112-1120

Song JH, Kandasamy K, Zemskova M, Lin YW, Kraft AS (2011) The BH3 mimetic ABT-737 induces cancer cell senescence. *Cancer Res* **71**(2)**:** 506-515

Srinivasula SM, Ashwell JD (2008) IAPs: what's in a name? *Mol Cell* **30**(2)**:** 123-135

Stennicke HR, Salvesen GS (1997) Biochemical characteristics of caspases-3, -6, -7, and -8. *J Biol Chem* **272**(41)**:** 25719-25723

Sun Y, Wang T, Su Y, Yin Y, Xu S, Ma C, Han X (2006) The behavior of SATB1, a MAR-binding protein, in response to apoptosis stimulation. *Cell Biol Int* **30**(3)**:** 244-247

Tajbakhsh S, Rocancourt D, Buckingham M (1996) Muscle progenitor cells failing to respond to positional cues adopt non-myogenic fates in myf-5 null mice. *Nature* **384**(6606)**:** 266-270

Tan JA, Sun Y, Song J, Chen Y, Krontiris TG, Durrin LK (2008) SUMO conjugation to the matrix attachment region-binding protein, special AT-rich sequence-binding protein-1 (SATB1), targets SATB1 to promyelocytic nuclear bodies where it undergoes caspase cleavage. *J Biol Chem* **283**(26)**:** 18124-18134

Tang D, Kidd VJ (1998) Cleavage of DFF-45/ICAD by multiple caspases is essential for its function during apoptosis. *J Biol Chem* **273**(44)**:** 28549-28552

Tapscott SJ (2005) The circuitry of a master switch: Myod and the regulation of skeletal muscle gene transcription. *Development* **132**(12)**:** 2685-2695

Thornberry NA, Bull HG, Calaycay JR, Chapman KT, Howard AD, Kostura MJ, Miller DK, Molineaux SM, Weidner JR, Aunins J, et al. (1992) A novel heterodimeric cysteine protease is required for interleukin-1 beta processing in monocytes. *Nature* **356**(6372)**:** 768-774

Varfolomeev EE, Schuchmann M, Luria V, Chiannilkulchai N, Beckmann JS, Mett IL, Rebrikov D, Brodianski VM, Kemper OC, Kollet O, Lapidot T, Soffer D, Sobe T, Avraham KB, Goncharov T, Holtmann H, Lonai P, Wallach D (1998) Targeted disruption of the mouse Caspase 8 gene ablates cell death induction by the TNF receptors, Fas/Apo1, and DR3 and is lethal prenatally. *Immunity* **9**(2)**:** 267-276

Wang M, Wu W, Rosidi B, Zhang L, Wang H, Iliakis G (2006) PARP-1 and Ku compete for repair of DNA double strand breaks by distinct NHEJ pathways. *Nucleic Acids Res* **34**(21)**:** 6170-6182

West JD, Ji C, Marnett LJ (2005) Modulation of DNA fragmentation factor 40 nuclease activity by poly(ADP-ribose) polymerase-1. *J Biol Chem* **280**(15)**:** 15141-15147

Widlak P, Lanuszewska J, Cary RB, Garrard WT (2003) Subunit structures and stoichiometries of human DNA fragmentation factor proteins before and after induction of apoptosis. *J Biol Chem* **278**(29)**:** 26915-26922

Widlak P, Li P, Wang X, Garrard WT (2000) Cleavage preferences of the apoptotic endonuclease DFF40 (caspase-activated DNase or nuclease) on naked DNA and chromatin substrates. *J Biol Chem* **275**(11)**:** 8226-8232

Woo EJ, Kim YG, Kim MS, Han WD, Shin S, Robinson H, Park SY, Oh BH (2004) Structural mechanism for inactivation and activation of CAD/DFF40 in the apoptotic pathway. *Mol Cell* **14**(4)**:** 531-539

Wossidlo M, Arand J, Sebastiano V, Lepikhov K, Boiani M, Reinhardt R, Scholer H, Walter J (2010) Dynamic link of DNA demethylation, DNA strand breaks and repair in mouse zygotes. *EMBO J* **29**(11)**:** 1877-1888

Wyllie AH (1980) Glucocorticoid-induced thymocyte apoptosis is associated with endogenous endonuclease activation. *Nature* **284**(5756)**:** 555-556

Xia SJ, Pressey JG, Barr FG (2002) Molecular pathogenesis of rhabdomyosarcoma. *Cancer Biol Ther* **1**(2)**:** 97-104

Xu Z, Fulop Z, Zhong Y, Evinger AJ, 3rd, Zan H, Casali P (2005) DNA lesions and repair in immunoglobulin class switch recombination and somatic hypermutation. *Ann N Y Acad Sci* **1050:** 146-162

Yang J, Liu X, Bhalla K, Kim CN, Ibrado AM, Cai J, Peng TI, Jones DP, Wang X (1997) Prevention of apoptosis by Bcl-2: release of cytochrome c from mitochondria blocked. *Science* **275**(5303)**:** 1129-1132

Yazdi AS, Guarda G, D'Ombrain MC, Drexler SK (2010) Inflammatory caspases in innate immunity and inflammation. *J Innate Immun* **2**(3)**:** 228-237

Yuan J, Shaham S, Ledoux S, Ellis HM, Horvitz HR (1993) The C. elegans cell death gene ced-3 encodes a protein similar to mammalian interleukin-1 beta-converting enzyme. *Cell* **75**(4)**:** 641-652

Yuan JY, Horvitz HR (1990) The Caenorhabditis elegans genes ced-3 and ced-4 act cell autonomously to cause programmed cell death. *Dev Biol* **138**(1)**:** 33-41

Zan H, Wu X, Komori A, Holloman WK, Casali P (2003) AID-dependent generation of resected double-strand DNA breaks and recruitment of Rad52/Rad51 in somatic hypermutation. *Immunity* **18**(6)**:** 727-738

Zan H, Zhang J, Al-Qahtani A, Pone EJ, White CA, Lee D, Yel L, Mai T, Casali P (2011) Endonuclease G plays a role in immunoglobulin class switch DNA recombination by introducing double-strand breaks in switch regions. *Mol Immunol* **48**(4)**:** 610-622

Zandy AJ, Lakhani S, Zheng T, Flavell RA, Bassnett S (2005) Role of the executioner caspases during lens development. *J Biol Chem* **280**(34)**:** 30263-30272

Zeng Q, Hong W (2008) The emerging role of the hippo pathway in cell contact inhibition, organ size control, and cancer development in mammals. *Cancer Cell* **13**(3)**:** 188-192

Zermati Y, Garrido C, Amsellem S, Fishelson S, Bouscary D, Valensi F, Varet B, Solary E, Hermine O (2001) Caspase activation is required for terminal erythroid differentiation. *J Exp Med* **193**(2)**:** 247-254

Zhang J, Liu X, Scherer DC, van Kaer L, Wang X, Xu M (1998) Resistance to DNA fragmentation and chromatin condensation in mice lacking the DNA fragmentation factor 45. *Proc Natl Acad Sci U S A* **95**(21)**:** 12480-12485

Zhang Y, Liu T, Meyer CA, Eeckhoute J, Johnson DS, Bernstein BE, Nusbaum C, Myers RM, Brown M, Li W, Liu XS (2008) Model-based analysis of ChIP-Seq (MACS). *Genome Biol* **9**(9)**:** R137

Zou H, Li Y, Liu X, Wang X (1999) An APAF-1.cytochrome c multimeric complex is a functional apoptosome that activates procaspase-9. *J Biol Chem* **274**(17)**:** 11549-11556

References: Chapter 2

1. Tapscott SJ (2005) The circuitry of a master switch: Myod and the regulation of skeletal muscle gene transcription. *Development* 132:2685-2695.
2. McKinsey TA, Zhang CL, & Olson EN (2002) Signaling chromatin to make muscle. *Curr Opin Cell Biol* 14:763-772.
3. Fernando P & Megeney LA (2007) Is caspase-dependent apoptosis only cell differentiation taken to the extreme? *Faseb J* 21:8-17.
4. Li J & Yuan J (2008) Caspases in apoptosis and beyond. *Oncogene* 27:6194-6206.
5. Fernando P, Brunette S, & Megeney LA (2005) Neural stem cell differentiation is dependent upon endogenous caspase 3 activity. *Faseb J* 19:1671-1673.
6. Fernando P, Kelly JF, Balazsi K, Slack RS, & Megeney LA (2002) Caspase 3 activity is required for skeletal muscle differentiation. *Proc Natl Acad Sci U S A* 99:11025-11030.
7. Kanuka H*, et al.* (2005) Drosophila caspase transduces Shaggy/GSK-3beta kinase activity in neural precursor development. *Embo J* 24:3793-3806.
8. Fujita J*, et al.* (2008) Caspase activity mediates the differentiation of embryonic stem cells. *Cell Stem Cell* 2:595-601.
9. Janzen V*, et al.* (2008) Hematopoietic stem cell responsiveness to exogenous signals is limited by caspase-3. *Cell Stem Cell* 2:584-594.
10. Nagata S, Nagase H, Kawane K, Mukae N, & Fukuyama H (2003) Degradation of chromosomal DNA during apoptosis. *Cell Death Differ* 10:108-116.
11. Yuste VJ*, et al.* (2005) The contribution of apoptosis-inducing factor, caspase-activated DNase, and inhibitor of caspase-activated DNase to the nuclear phenotype and DNA degradation during apoptosis. *J Biol Chem* 280:35670-35683.
12. Reh S, Korn C, Gimadutdinow O, & Meiss G (2005) Structural basis for stable DNA complex formation by the caspase-activated DNase. *J Biol Chem* 280:41707-41715.
13. Bredemeyer AL*, et al.* (2008) DNA double-strand breaks activate a multi-functional genetic program in developing lymphocytes. *Nature* 456:819-823.
14. Ju BG*, et al.* (2006) A topoisomerase IIbeta-mediated dsDNA break required for regulated transcription. *Science* 312:1798-1802.
15. Dawson BA & Lough J (1988) Immunocytochemical localization of transient DNA strand breaks in differentiating myotubes using in situ nick-translation. *Dev Biol* 127:362-367.
16. Coulton GR, Rogers B, Strutt P, Skynner MJ, & Watt DJ (1992) In situ localisation of single-stranded DNA breaks in nuclei of a subpopulation of cells within regenerating skeletal muscle of the dystrophic mdx mouse. *J Cell Sci* 102:653-662.
17. Farzaneh F, Zalin R, Brill D, & Shall S (1982) DNA strand breaks and ADP-ribosyl transferase activation during cell differentiation. *Nature* 300:362-366.

18. Fan Z, Beresford PJ, Oh DY, Zhang D, & Lieberman J (2003) Tumor suppressor NM23-H1 is a granzyme A-activated DNase during CTL-mediated apoptosis, and the nucleosome assembly protein SET is its inhibitor. *Cell* 112:659-672.
19. Iseki S (1986) DNA strand breaks in rat tissues as detected by in situ nick translation. *Exp Cell Res* 167:311-326.
20. Phillips ER & McKinnon PJ (2007) DNA double-strand break repair and development. *Oncogene* 26:7799-7808.
21. Paull TT*, et al.* (2000) A critical role for histone H2AX in recruitment of repair factors to nuclear foci after DNA damage. *Curr Biol* 10:886-895.
22. Parker SB*, et al.* (1995) p53-independent expression of p21Cip1 in muscle and other terminally differentiating cells. *Science* 267:1024-1027.
23. Zhang P*, et al.* (1999) p21(CIP1) and p57(KIP2) control muscle differentiation at the myogenin step. *Genes Dev* 13:213-224.
24. Gevry N, Chan HM, Laflamme L, Livingston DM, & Gaudreau L (2007) p21 transcription is regulated by differential localization of histone H2A.Z. *Genes Dev* 21:1869-1881.
25. Jiemjit A*, et al.* (2008) p21(WAF1/CIP1) induction by 5-azacytosine nucleosides requires DNA damage. *Oncogene* 27:3615-3623.
26. Palii SS, Van Emburgh BO, Sankpal UT, Brown KD, & Robertson KD (2008) DNA methylation inhibitor 5-Aza-2'-deoxycytidine induces reversible genome-wide DNA damage that is distinctly influenced by DNA methyltransferases 1 and 3B. *Mol Cell Biol* 28:752-771.
27. Liu QY*, et al.* (2003) Mapping the initial DNA breaks in apoptotic Jurkat cells using ligation-mediated PCR. *Cell Death Differ* 10:278-289.
28. Hossain MS, Akimitsu N, Kurokawa K, & Sekimizu K (2003) Myogenic differentiation of Drosophila Schneider cells by DNA double-strand break-inducing drugs. *Differentiation* 71:271-280.
29. Inomata K*, et al.* (2009) Genotoxic stress abrogates renewal of melanocyte stem cells by triggering their differentiation. *Cell* 137:1088-1099.
30. Sundstrom JF*, et al.* (2009) Tudor staphylococcal nuclease is an evolutionarily conserved component of the programmed cell death degradome. *Nat Cell Biol* 11:1347-1354.
31. Meshorer E & Misteli T (2006) Chromatin in pluripotent embryonic stem cells and differentiation. *Nat Rev Mol Cell Biol* 7:540-546.
32. Rampalli S*, et al.* (2007) p38 MAPK signaling regulates recruitment of Ash2L-containing methyltransferase complexes to specific genes during differentiation. *Nat Struct Mol Biol* 14:1150-1156.
33. Carey MS, S.T. (2000) *Transcriptional regulation in eukaryotes* (Cold Spring Harbor Laboratory Press, Cold Spring Harbour, N.Y.).

Appendix I: Supporting Methods and Materials for Chapter 3

Methods and Materials

1.1 Cell Culture

1.1.1 C2C12 cells.

C2C12 cells were obtained from American Type Culture Collection (ATCC) as frozen stocks in Dulbecco's Modified Eagle Medium (DMEM) supplemented with 10% Fetal Bovine Serum (FBS) and 10% DMSO. Cells were thawed in a 37ºC water bath, and then washed to remove the DMSO by adding 5 mL of growth media: DMEM (Invitrogen) supplemented with 10% FBS (Invitrogen) and 2% Penicillin/Streptomycin (Pen/Strep) (Invitrogen). Cells were subsequently pelleted by centrifugation at 750xg for 5min. The wash media was removed by aspiration and the pellet resuspended in more growth media. $1x10^6$ resuspended cells were plated onto a 10cm tissue culture plate to a total volume of 10mL of growth media per plate. Cells were incubated at 37ºC with 5% CO_2. Cells were passaged when they reached 80% confluency. Cell passaging was performed as follows, diminished growth media was removed, cells were washed with 5mL of 1X phosphate buffered saline (PBS), and this was replaced with 1mL of 0.25% Trypsin stock (Invitrogen). After gentle rocking to ensure even trypsin coverage over the cells, they were incubated for 3 minutes at 37ºC. Cells were examined at this time to ensure they had detached from the plate. 5mL growth media containing FBS was then pipetted onto cells to inactivate the trypsin and resuspend the cells. The cells were then transferred to a 15mL conical tube and centrifuged at 750xg for 5 minutes, the pelleted cells were then resuspended in fresh growth media. Cells were then replated onto new culture dishes, the density of cells plated was determined based on experimental requirements and culture dish size.

C2C12 cells were induced to differentiate under low serum conditions, cells were allowed to reach confluency, growth media was removed, cells were washed with 5mL of 1X PBS, then 10 mL of differentiation media (DMEM, 2% Horse Serum (Invitrogen), and 2% Pen/Strep) was applied. Cells were differentiated to the indicated times and then processed as required. Diminished differentiation media was replaced every 48 hours.

1.1.2 Primary Myoblast Isolation and Culture

Primary myoblasts were isolated from 4 week old B6C3F1 mice. Pups were decapitated then rinsed with 70% ethanol. An incision through the skin was made around the mid section of the mouse, then the skin was carefully pulled back over the hind limbs to the feet, the skin was then completely removed by removal of the feet. Care was taken in these steps to prevent hair from coming into contact with the exposed muscle, a troublesome source of microbial contamination. The exposed hind limbs were then detached from the trunk and rinsed in 1X PBS. The muscle from both hind limbs was then dissected from the bone into a petriplate containing 1mL of 1X PBS. The muscle tissue was then masticated with sterile razors for 5 minutes to a homogenous slurry. 5 mL of collagenase/dispase II (Roche) was pipette on to the muscle slurry and incubated for 45 minutes at 37ºC. To assist the enzymatic breakdown of the tissue, it was mechanically tutrated by pipetting up and down every 10 minutes using progressively smaller bore pipettes. With the addition of 5 mL of 1X PBS the digested muscle was filtered through a 50 μm Celltrics filter into a 50 mL conical tube. The petriplate was then rinsed with an additional 5 mL of 1X PBS to collect any remaining cells, and this was then again filtered through the Celltrics. The collected filtrated was then centrifuged at 750xg for 5 minutes, the supernatant was removed and the isolated pellet resuspended in 10 mL of Hams

Enrichment Media (HAMs F-10, 20% FBS, 2% Pen/Strep, and 2.5ng/µl HGF (Invitrogen)) and plated on to an uncoated 10 cm petriplate for overnight incubation at 37ºC. The next day the supernatant was transferred to a collagen coated 5 cm dish, allowing the myoblasts to adhere with overnight incubation. The enrichment media was replaced with Hams Growth media (HAMs F-10, 20% FBS, 2% Pen/Strep, and 2.5ng/µl bFGF (Invitrogen)) and the myoblasts were subsequently cultured in this complete media. At this point the culture contains a very large population of contaminating fibroblasts, to remove this contamination cultures underwent a series of preplating over a period of several weeks. Preplating onto non-collagen coated petriplates allows the fibroblasts to adhere to the plate while myoblasts remain in the supernatant, after 20 minutes of incubation the supernatant is gently removed and then applied to a fresh collagen coated petriplate. Once a pure culture of myoblasts was established care was taken to passage the myoblast before reaching 70% confluency. To differentiate primary myoblasts, the cells were allowed to reach 80% confluency, the growth media was removed, the cells were wash with 1X PBS, and then low serum differentiation media (DMEM, 4% Horse serum) was applied.

1.1.3 Plasmid transfection and generation of stable cell lines.

Primary myoblasts were cultured in 6 well dishes in the absence of antibiotics until they reached a confluency of 50-60%. Purified plasmid DNA was prepared by diluting 2 µg of DNA in 250 µL of 1X Opti-Mem I media (Invitrogen), in a separate eppidorf tube 10 µL of Lipofectamine 2000 (Invitrogen) was diluted in 250 µL of Opti-Mem I media and allowed to incubate at room temperature for 5 minutes. The DNA and Lipofectamine solutions were combined then gently mixed. This solution was

subsequently incubated at room temperature for 20 minutes to allow DNA-Lipofectamine complexed micelles to form. During this incubation cells were washed with 1X Opti-Mem I media (Invitrogen). Following the incubation the entire transfection solution was applied directly to the cells for 3 hours at 37ºC. After this 3 hour incubation 1 mL of antibiotic free growth media was applied and the cells allowed to grow overnight at 37ºC. The following day the growth media was replaced with fresh antibiotic free growth media.

48 hours post transfection antibiotic selection for the transfected myoblasts began, eukaryotic antibiotic selection was performed using G418 (Invitrogen) in growth media. G418 selection was achieved using a concentration of 400ug/mL. For the generation of stable pooled cultures, transfected cultures were cultured and passaged under selection as a whole.

1.2 Antibodies

The following primary antibodies were used in this experiment mouse (ms) anti-Myosin Heavy Chain (Developmental Hybridoma, Immunofluorescence (IF) 1:200, 1hr @ RT), ms anti-tubulin (Developmental Hybridoma, western blot (WB) 1:100, 1 hr@RT), and rabbit anti-HIS Tag (Cell Signal, WB 1:1000, overnight @ 4°C)

The following secondary antibodies were used for western blot: goat (gt) anti-rabbit HRP and gt anti-mouse HRP (BioRad, 1:5000, 1hr@RT).

The following secondary antibodies were used for immunofluorescence: gt anti-mouse Alexa Fluor 594. (Molecular Probes, 1:2500, 1hr@RT).

1.3 Immunofluorescent staining

Cells were cultured on collagen coated UV-irradiated 25 mm coverslips in 6 well petriplates. At the indicated time points the plates were removed to ice, culture media was removed by aspiration, and replaced with ice cold 1X PBS. The cells were further washed 2 more times with 1X PBS, then covered with 90% Methanol/10% 1X PBS for 10 minutes on ice. The fixative was removed and the cells were quickly washed 2 times with 1X PBS, followed by 2 further washes with 1X PBS each for a 2 minute duration. Fixed cells were incubated with blocking agent, 3% bovine serum albumin (BSA) in 1X PBS, overnight at 4ºC. Primary antibody solutions were made up in 3% BSA 1X PBS at the indicated concentrations and incubated for the described period of time. Following incubation with the primary antibody, the cells were washed 3 times with 1X PBS, then fluorescently labelled secondary antibody specific for the species of primary antibody was applied at the indicated concentrations for 1 hour under low light conditions. Secondary antibody was removed and cells were washed 3 times with 1X PBS. The DNA specific dye, DAPI, was used to counterstain the nuclei at a concentration of 1:10000 in 1X PBS for 10 minutes. The labelled cells were then washed a further 2 times with 1X PBS and then once with sdH_2O to remove excess salt. The coverslips were mounted onto glass microscope slides using a drop of Dako Fluorescent Mounting Medium (Dako). Cells were visualized on a Ziess Observer Inverted Microscope.

1.4 Protein isolation and analysis

1.4.1 Protein isolation and quantification

Protein was isolated from cultured cells at the indicated times and conditions. The culture media was removed and the cells were washed 2 times with ice cold 1X PBS on ice. The final PBS wash was removed and replaced with 500uL (for 10cm petriplates) PLC gamma lysis buffer supplemented with protease inhibitors. PLC gamma lysis buffer consisted of 0.05M HEPES (pH 7.5), 0.15M NaCl, 10% glycerol, 1% Triton X-100, 1mM EGTA, 1.5mM $MgCl_2$, 20mM NaF, 10mM Na pyrophosphate. Protease inhibitors: PMSF, Aprotinin, Pepstatin, and Leupeptin were added to 0.01µg/µL and NaV at 5mM. Plates were gently rocked on ice for 45 minutes then the lysate scraped and collected into an eppidorf tube. Lysate was cleared of debris by centrifugation at 14,000 rpm for 5 minutes at 4ºC. The supernatant was collected into a fresh tube and then stored at -80ºC until needed.

Protein concentration in the samples was determined by the Bradford assay. 1 µL of each sample was added to 799 µL dH_2O in disposable plastic curvettes, then 200 µL of Bio-Rad Protein Assay Dye reagent Concentrate (Bio-Rad) was added and the samples mixed by inversion. Sample absorbance at 595nm was measured using a spectrophotometer. Sample concentration was determined by comparison of the sample absorbance to the absorbance of a standard curve of protein concentrations generated using BSA (0, 1, 3, 5, 7, and 10 µg/mL BSA).

1.4.2 Western Blot Analysis of Protein Expression

Protein lysates were prepared for separation by SDS-PAGE (SDS-Polyacylamide Gel Electrophoresis) by boiling the samples at 100°C for 5 minutes following the addition of reducing 5X Lamelli Protein buffer (1:5 dilution). Samples were cooled on ice,

collected by touch centrifugation then loaded onto the prepared gel. The Benchmark Prestained Protein Ladder was run with each gel. The Hoefer Gel Electrophoresis Apparatus with 1X Running Buffer was used to electrophoresis the samples at 100V through the stacking gel, then 175V through the separating gel until the dye front had reached the end of the gel.

Following electrophoresis the separated protein was transferred from the gel to a PVDF membrane using a semi-dry transfer apparatus. The membrane was wetted with 100% Methanol then equilibrated with the gel in transfer buffer for 2 minutes. The membrane and gel were stacked between transfer buffer wetted Whattman filter papers, and transferred at 8V from 1hour and 45 minutes. Following the transfer the membrane was allowed to air dry allowing the protein to better adsorb onto the membrane before rewetting with 100% methanol.

The wet membrane was then rinsed with 1X TBST (Tris buffer saline with 0.1% Tween20) then blocked in 5% Powered Skim Milk or 3% BSA in 1X TBST for 1 hour at room temperature. The membrane was then probed with the primary antibody in blocking solution under the concentrations and conditions outlined in section 2.2. Following incubation unbound primary antibody was removed by three washes with 1X TBST. Bound primary antibody was subsequently detected by the appropriate horse radish peroxidise (HRP) conjugated secondary antibody in blocking solution for 1 hour at room temperature. Unbound antibody was again removed by washing the membrane three times with 1X TBST. The Amersham ECL kit (Amersham) was used to supply the chemiluminescent substrates to develop the blot, which was then visualized by exposure

to Kodiak LSM film. Analysis of western blots was performed using the AlphaEasyFC (Alpha Innotech) software.

1.5 Ribonucleic acid isolation and expression analysis.

1.5.1 RNA isolation from cultured cells.

Cells were plated onto 35mm petriplate and samples were taken under the indicated experimental conditions and time points. To prepare the cells for RNA isolation they were washed with 1X PBS, then under RNase free conditions 250 µL of TRIZOL reagent (Invitrogen) was added to the dish. Following a five minute incubation the lysated cells were scraped and collected into an RNase free eppidorf tube. Here the TRIZOL isolated samples were frozen at -80ºC until all samples were available for processing. Frozen samples were thawed on ice then 50 µL of chloroform (Fisher)was added to each, samples were vortexed and then allowed to incubate at room temperature for 3 minutes. Centrifugation at 10, 000xg for 10 minutes at 4ºC was used to separate the phases, the upper aqueous phase was isolated to a fresh tube. 125 µL of 100% isopropanol was used to precipitate the RNA for 20 minutes at room temperature with nutation. Following this incubation the RNA was pelleted by centrifugation at 10, 000xg for 15 minutes at 4ºC. The supernatant was removed and replaced by a 500 µL 70% Ethanol-DEPC wash, the samples were then re-centrifuged for 5 minutes at 7500xg at 4ºC. The wash was removed and the RNA pellet air dried. The dry RNA pellet was subsequently resuspended in 30 µl of nuclease free water and allowed to dissolve at 4ºC before being stored at -20ºC.

1.5.2 First strand cDNA synthesis

Isolated RNA was quantified by UV spectrophotometry. 1 µL of RNA was resuspended in 99 µL of RNase free water, then loaded into a quartz curvette, and absorbance measured at 260nm. Samples were measured in duplicate with the averaged concentration used to determine the amount of sample to use in the first strand synthesis reaction. A minimum of 500 ng of RNA in 10 µL of RNase free water was used for each reaction. Reagents for each reaction were added in the following order, 1 µL 0.5µg/µL Oligo (dT_{15}) primer (Invitrogen) and 1µL PCR Nucleotide Mix (dNTP) (10mM each dNTP, Roche) were added to the RNA samples, mixed and incubated for 5 minutes at 65ºC. Tubes were removed to ice then briefly touch centrifuged, 4 µL of 5X first strand synthesis buffer (Invitrogen), 2 µL 0.1 Dithiothreitol (DTT, Invitrogen), and 1 µL 40U/µL RNaseOUT (Invitrogen) was added to each tube. Following a brief 2 minute incubation at 42ºC, 1 µl 200U/µL Superscript II reverse transcriptase (Invitrogen) was added to each tube, mixed, and the first strand synthesis reaction was run at 42ºC for 50 minutes. The reaction was terminated by heat inactivation at 70ºC for 15 minutes, then RNA was removed by RNase H (2 units, Invitrogen) treatment for 30 minutes at 37ºC.

1.5.3 RT-PCR

For expression analysis from the generated cDNA samples, 0.5 µg of cDNA was used for PCR reactions depending on the starting concentration of cDNA available. The volume of a master mix was determined for the number of samples, and each reaction was run with a concentration of 1X PCR Reaction Buffer (Invitrogen), 0.25 mM PCR Nucleotide mix (dNTP, Roche), 2 mM Magnesium Chloride ($MgCl_2$, Invitrogen), 0.5 µM forward primer, 0.5 µM reverse primer, and 2.5 units Taq DNA polymerase Recombinant (Invitrogen). Pax7 primers: forward 5'-GTT TAT CCA GCC GAC TCT GG-3' and

reverse 5'-ATC GGC ACA GAA TCT TGG AG-3'. Foxo1 primers: forward 5'-TAT TGA GCG CTT GGA CTG TG-3' and reverse 5'- TGG ACT GCT CCT CAG TTC CT-3'. For the amplification of the Pax7-Foxo1 fusion transcript the Pax7 forward primer and the Foxo1 reverse primer were used for the PCR. GAPDH primers: forward 5'-TTG GGT TGT ACA TCC AAG CA-3' and reverse 5'-CAA GAA ACA GGG GAG CTG AG-3'. The PCR reaction was run in 200 µL Flat cap Thermowell tubes (Corning) using an Eppendorf PCR cycler. A typical cycler setting was 95ºC denaturation for 5 minutes, 30 cycles of 95ºC denaturation for 30 seconds, primer annealing for 30 seconds at 60ºC, and 45 seconds of extension at 72ºC, finished with 5 minutes of extension at 72ºC, then stored at 4ºC until the samples were to be analyzed. The PCR amplification were analyzed by separation on a 1% Agarose gel (1% w/v Agarose LE and 1µg/ml ethidium bromide in 100 µL 1X TAE buffer,). The samples were prepared for electrophoresis by the addition of 1:10 10X Orange G DNA loading dye to each sample. Samples were loaded into the agarose gel wells and then electrophoresed at 100 V until the dye front had migrated near the end of the gel. The gel was visualized and imaged using the Alpha Innotech Imager UV light box. For analysis of gel band intensity the AlphaEaseFC software (Alpha Innotech) suite was used.

1.5.4 Quantitative Real Time RT PCR

The quantitative measurement of gene expression was determined using quantitative RT PCR (qPCR). cDNA for qPCR was generated using Superscript III, following the protocol described for Superscript II in section 1.5.2, with the following modification first strand synthesis reaction was run at 50ºC for 50 minutes. 200 µg of cDNA was used per reaction, in QuantiFast SYBR Green PCR Master mix containing 5

μM forward and reverse primers, samples were run in triplicate. Samples were loaded into 100 μL tubes (Corbett Research), held in an ice cold metal tube rack, until they were ready to be loaded into the Qiagen RotoGene Q qPCR cycler. Gene expression analysis was measured using a 2 step cycle, this run began with a 5 minute hot start activation at 95ºC followed by 40 cycles of 10 second denaturation at 95ºC and a 30 second combined annealing/extension step at 60ºC. The critical threshold (CT) was set to include the exponential amplification curve of each sample. The delta CT was calculated by subtracting the CT of the gene of interest from the GAPDH control, delta CTs were then compared between the normal conditions and experimental conditions. Primers used for Pax7 forward 5'-GAC GAC GAG GAA GGA GAC AA-3' and reverse 5'-ACA TCT GAG CCC TCA TCC AG-3'. GAPDH primers: forward 5'-TTG GGT TGT ACA TCC AAG CA-3' and reverse 5'-CAA GAA ACA GGG GAG CTG AG-3'.

1.6 Statistical Analysis

Statistical significance was determined using Student's *t* test. A returned P-value of less than 0.05 was used to determine significance.

1.7 Chromatin Immunoprecipitation (ChIP) and Illumina Platform Sequencing

C2C12 cells were induced to differentiate as described for 12 hours, DNA-protein complexes were fixed with 1% formaldehyde for 30 minutes at room temperature with rocking. Following this incubation the reaction was quenched with the addition of glycine at a final concentration of 0.125M for 10 minutes at room temperature. Cells were scraped and collected by centrifugation. The cells were resuspended and washed in 5 mL of Buffer N (15mM Tris, 15mM NaCl, 60mM KCl, 250mM Sucrose, 5mM $MgCl_2$ and

1mM $CaCl_{2)}$. Cells were centrifuged again and resuspended in 1 mL of Buffer N. Nuclei isolation was achieved by the drop wise addition of 1 mL Buffer N+ 0.6% NP-40 while the cells were in a gentle vortex. Cells were incubated on ice for 10 minutes. Following this incubation the nuclei were collected by centrifugation and resuspended in 300 µL of 1% SDS Sonication Buffer (50mM HEPES (pH 7.9), 140 mM NaCl, 1 mM EDTA, 1% Triton X-100, 0.1% sodium deoxycholate, 1% SDS, and protease inhibitors). Chromatin was sheared by sonication using a Biorupter (Diagenode) to obtain a resolution of ~ 400 bp. 0% SDS Sonication buffer was added to the sheared chromatin to a final concentration of 0.1% SDS sonication buffer and debris was pelleted by centrifugation at 14,000 rpm for 15 minutes at 4C. Sonicated salmon sperm DNA (1µg/ml final) and OVA (1ug/ml final) were added to the chromatin containing supernatant. Subsequently, chromatin was precleared with 1/300 (v/v) Dynabeads-protein A for 1 hour at 4°C.

Normal rabbit IgG (mock) and rabbit anti-CAD antibodies (Santa Cruz) were coupled to Dynabeads with protein A for 2 hours at room temperature in IP100 buffer (). Preclearing beads were removed from the chromatin samples, and replaced with either the mock or CAD antibody bound Dynabeads. Samples were incubated overnight at 4°C with rotation. The next day samples were extensively washed and chromatin bound samples were eluted twice with elution buffer (50 mM Tris-HCl (pH 7.5) and 1% SDS) at 65°C for 5 minutes. NaCl and RNase H were added to a final volume of 0.2M and 10µg/ml respectively. DNA was subsequently purified by QIAquick PCR purification kit (QIAGEN).

10 ng of both CAD and mock ChIP samples were sent for sequencing on the Illumina sequencing platform at BC Cancer Agency Genome Sciences Centre,

Vancouver, BC, Canada. Here sample quality was assessed by Agilent Bioanalyzer, and genomic sequencing library and clusters were constructed. Two flow lanes were used on the Illumina Genome Analyzer, one for the CAD sample and the other for the mock sample. Sequencing data was returned as a text file. Returned sequences were mapped to the mm8 mouse genome assemble (NCBI36) using the Illumina ELAND Analysis Pipeline. Aligned CAD reads with up to two mismatches were provided to MACS together with control reads (Zhang et al., 2008). ChIP-Seq peaks were considered significant by MACS with a P-value less than $1X10^{-5}$. Peak regions were subsequently visualized as custom tracks on the UCLA genome browser.

1.8 ICAD cloning and site-directed mutagenesis.

The human ICAD cDNA encoding the long isoform of ICAD was obtain from Open Biosystems. Wild type human ICAD was cloned into the reading frame A, between the BamHI and NotI restriction site, of pcDNA3.1/HisC (Invitrogen) mammalian expression vector, PCR primers used included the BamHI (forward) and NotI (reverse) restriction sites (bold) , forward 5'-AT**GGATCC**GAGGTGACCGGGGACGCC-3' and reverse 5'-TA**GCGGCCGC**CTATGTGGGATCCTGTCTG-3'. Two step mega primer approach was used to introduce the D117E mutation. PCR using the forward primer from above and reverse primer 5'-CTGCCCCGCTCTCTGTTTCATC-3' generated the megaprimer that was purified and used with the reverse primer to generate the full length ICAD sequence containing the mutation by PCR. The D224E mutation was introduced as above however the reverse primer 5'-CTGATACCCGTCTCTACTGCATC-3'was used to generate the megaprimer. For the double D117/224E mutation, the D117E ICAD clone was used as a template for megaprimer generation using the D224E reverse primer. The

PCR products were inserted between the BamHI and NotI restriction site of pcDNA3.1/HisC as above. Constructs were verified by sequencing.

Appendix II

Table 1. MACS identified genomic regions enriched for CAD during C2C12 myoblast differentiation.

Chr	Location Start	End	Fold enrichment	FDR (%)	Overlap genes	Near genes
chr1	12629975	12630067	83.46	0		
chr14	103222648	103222698	146.68	11.11		
chr11	25000153	25000211	206.66	14.29		
chr5	114434107	114434180	236.46	27.27	Acacb:[5U] Acacb:[I1]	
chr9	62406581	62406689	139.1	29.03		
chr3	148180604	148180656	264.18	32.2		
chr6	69445927	69445967	264.18	32.2		
chr13	41000747	41000790	330.23	32.43		
chr9	122496766	122496825	286.2	32.43		
chr5	24812777	24813009	11.92	32.79	AY138582:Mll3[E17I17]	AK129377:AK164521:AY138582:Mll3[10DS]
chr10	21278083	21278136	155.79	33.33		1700020N01Rik:[10US]
chr1	33935554	33935593	94.58	34.55		
chr9	102630445	102630485	94.58	34.55		
chr13	39431345	39431386	89.02	34.85		
chr3	145628402	145628476	79.48	36.76		
chr2	120238067	120238103	222.55	37.1	AK089359:AK155019:NM_011743:SH3BP3:ZFP106:ZNF474[I3] AF060246:H3a:Sh3bp3:Sirm:Zfp106:Znf474[I20]	
chr6	131343236	131343279	111.28	37.14	Csda:[I4] Csda:[I5]	
chr7	80426520	80426560	92.73	37.68		
chr7	45491744	45491787	286.2	38.3	Izumo1:[I3]	Fut1:[10DS] Fut1:[10DS] AK011557:AK033276:BC072584:FLJ20401:NM_028544:RAIN:RASIP1[10US] Rasip1:[10US] Fgf21:[10DS]
chr8	101771653	101771712	40.91	39.13		
chr3	153061133	153061221	118.23	41.86		

chr1	138465595	138465633	204.01	42.11		
chrX	99467703	99467743	97.37	42.31		4930519F16Rik[10DS] 4930519F16Rik:BC107249[10DS]
chr14	22404465	22404536	86.55	42.67	BC065068:KCNMA1:KCa1.1:NM_010610:SLO[I27] Kcnma1:[I26] Kcnma:Kcnma1:NM_010610[I27]	
chr12	78180410	78180453	220.15	44.94	Fut8:[5U]	
chr5	109583417	109583456	220.15	44.94		
chr5	114897756	114897793	220.15	44.94	Trpv4:[5U] AF279672:NM_022017:Trp12:Trpv4:Vrl2:Vroac[I13] Trpv4:[I13]	
chr1	153863756	153863856	220.15	45.05		
chr15	103438510	103438562	153.01	45.65		
chr8	93335966	93336030	61.2	45.74		
chr1	8625646	8625682	92.73	46.26	AK038698:G1SYN:NM_027671:SNTG1:SYN4[5U] AK083241:NM_027671:Sntg1[I11] Sntg1:[I11]	
chr8	41089873	41089909	92.73	46.26	CD204:MSR1:NM_031195:SCARA1:Scvr[I2]	
chr17	55833771	55833810	92.73	46.26	AK131178:DPP9:NM_172624[I12] Dpp9:[I11]	
chr8	27292717	27292943	11.55	46.46	AK087934:AK146938:ASH2L:ASH2L1:ASH2L2:NM_011791[I6E7I7]	
chr15	93655284	93655346	89.02	46.53		
chr18	43101933	43101991	66.77	46.67	Ppp2r2b:[I8]	
chr5	24819660	24819873	11.92	47.06	AY138582:Mll3[I20]	AK129377:AK164521:AY138582:Mll3[10DS]
chr2	18190576	18190622	52.55	47.06	BC020078:LOC432823:NM_001013789[3U] Dnajc1:[I4]	

chr3	40194569	40194662	198.14	47.12		
chr11	87248068	87248112	176.12	47.22		
chr12	75779335	75779373	176.12	47.22		
chr15	66215754	66215794	176.12	47.22	Lrrc6:[I1]	
chr18	37759143	37759178	176.12	47.22	AF464180:CNR1:CRNR1:NM_007766:PCDHA4[I1]	AF332006:AY583456:Ornt2:Slc25a2[10US] Taf7:[10US]
chr2	43476150	43476191	176.12	47.22	AK040584:KYNU:NM_027552[I9] BC069848:Kynu:NM_027552[I10] Kynu:[I10]	
chr9	63929178	63929218	176.12	47.22	Lctl:[I9] Lctl:[I9]	Zwilch:[10US]
chrX	139220595	139220636	176.12	47.22		
chr5	70279917	70279953	185.46	47.42		
chr10	99149161	99149204	185.46	47.42		
chr4	96991933	96991979	185.46	47.42		
chr7	70957691	70957730	79.48	47.47		
chr14	58568423	58568468	111.28	47.58		
chr6	10136334	10136467	79.48	47.62		
chr10	71537143	71537176	198.14	47.71		
chr7	30931098	30931134	198.14	47.71		
chrX	9789924	9789964	198.14	47.71		
chr16	83899501	83899542	76.5	47.76		
chr3	125220447	125220483	76.5	47.76		
chr1	29625769	29625810	148.37	47.77		
chr11	28007203	28007240	148.37	47.77		
chr6	3594811	3594850	148.37	47.77		
chr19	15159994	15160045	166.91	47.9		
chr4	154607729	154607776	166.91	47.9		2610204G22Rik:[10DS] Atad3a:[10DS] AK153932:AK154077:AK165724:AK166099:AK172038:AK172350:ATAD3A:BC023301:BC0600

						36:FLJ10709:NM_179203[10DS] Vwa1:[10US] 4932416A11Rik:AK030019:AK077240:AY030094:BC020136:BC026919:FLJ22215:NM_147776:VWA-1:VWA1:WARP[10US]
chr8	69455635	69455674	166.91	47.9		
chr8	27284088	27284191	26.88	48.03	AK087934:AK146938:ASH2L:ASH2L1:ASH2L2:NM_011791[I2E3I3]	Star:[10DS] BC060970:NM_011485:STAR:STARD1[10DS]
chr15	21601229	21601272	39.74	48.09		
chr5	52943392	52943436	133.53	48.19	AK033654:AK049338:AK153792:D5Ertd135e:NM_172490[I3] D5Ertd135e:[I3]	
chr6	26065982	26066020	133.53	48.19		
chr6	36829604	36829640	133.53	48.19		
chr9	19325833	19325919	100.15	48.75		Olfr854:[10DS]
chr1	44895755	44895799	66.77	48.84		
chr9	46445493	46445530	125.19	48.91		
chr10	122495586	122495656	97.37	49.02		
chr8	27299306	27299388	21.77	49.06	AK087934:AK146938:ASH2L:ASH2L1:ASH2L2:NM_011791[E11]	
chr17	24990384	24990455	154.11	49.14	Ube2i:[I1]	BC037635:NM_011665:UBC9:UBE2I[10US]
chr6	125842521	125842667	38.52	49.57	AK044763:C12orf3:NM_153589:TMEM16B[I13] AK132944:NM_153589:Tmem16b[5U] Tmem16b:[I12]	
chr5	81575417	81575476	45.52	49.63		
chr1	16999305	16999344	129.82	49.77	Jph1:[I2]	
chr1	29266874	29266908	129.82	49.77		
chr1	63057123	63057163	129.82	49.77		
chr4	112275042	112275075	129.82	49.77		A030001H23Rik:NM_17

						7668[10DS] A030001H23Rik:[10DS]
chr15	37666181	37666218	129.82	49.77	Ncald:[5U]	
chr16	61653434	61653468	129.82	49.77		
chr18	56674511	56674556	129.82	49.77	AK145873:AK169195:ALDH7A1:ATQ1:NM_138600[I13] Aldh7a1:[I13]	
chr3	64552792	64552836	129.82	49.77		
chr4	18404452	18404490	129.82	49.77		
chr4	26200441	26200475	129.82	49.77		
chr4	79718197	79718237	129.82	49.77		
chr4	98317501	98317532	129.82	49.77		I0C0044D17Rik:[10DS] Ankrd38:[10DS]
chr5	51670416	51670450	129.82	49.77		
chr8	23512708	23512749	129.82	49.77	Atp7b:[I20]	
chr7	34548826	34548862	89.02	50		
chr12	72343506	72343543	89.02	50		
chr14	38186497	38186534	89.02	50	Nrg3:[I9]	
chr15	38514796	38514863	97.37	50		
chr16	33035625	33035661	102	50	Lmln:[I15]	
chr19	41606208	41606243	89.02	50	A630025C20Rik:[I1]	
chr2	16600855	16600901	185.46	50	Plxdc2:[I9]	
chrX	125103431	125103470	102	50	AK153986:Diap2:NM_017398[I1] AY312280:Diap2:Diaph2:NM_017398[I1] BC100759:Diap2:NM_017398[I1] Diap2:[I1]	
chr8	27298187	27298277	17.8	50.26	AK087934:AK146938:ASH2L:ASH2L1:ASH2L2:NM_011791[E10]	
chr8	27306121	27306285	21.2	50.31	AK087934:AK146938:ASH2L:ASH2L1:ASH2L2:NM_011791[I15E16]	
chr18	65553132	65553173	139.1	50.45		Malt1:[10US] AK045200:MALT1:MLT

						:NM_172833[10US] BC110487:Malt1:NM_172833[10US] AK041919:AK049821:AK085071:BC046536:Malt1:NM_172833[10US]
chr5	5697817	5697873	125.19	50.45	AK052981:AK162343:AK165644:AK166607:Steap2[5U]	
chr1	3326771	3326811	154.11	50.53	Xkr4:[I1]	
chr1	74653173	74653220	154.11	50.53	AK004977:BC002183:CP27:CTX:CYP27:CYP27A1:NM_024264[5U] Cyp27a1:[I1]	
chr10	122237998	122238033	154.11	50.53	AK029461:ARHCL1:FLJ13253:KIAA1157:NM_176919:PPM1H[I4] AK051434:AK134804:AK150309:NM_176919:Ppm1h[I4] Ppm1h:[I4]	
chr14	54456644	54456695	154.11	50.53	BC036313:[I31]	AK134548:CPNE6:NM_009947[10US] Cpne6:[10US]
chr16	69627853	69627894	154.11	50.53		
chr18	71356947	71356984	154.11	50.53		
chr4	26202724	26202760	154.11	50.53		
chr5	4441938	4441976	154.11	50.53		
chr6	132429462	132429507	154.11	50.53		
chr7	48546321	48546355	154.11	50.53	AK139009[3U]	
chrX	138072636	138072672	154.11	50.53	AW547186:[I5]	
chr1	16140265	16140317	100.15	50.62		
chr15	75431150	75431185	100.15	50.62		Gpihbp1:[10DS]
chr8	27300506	27300603	21.64	50.93	AK087934:AK146938:ASH2L:ASH2L1:ASH2L2:NM_011791[E12I12]	
chr11	4851913	4851947	111.28	51.12	ADTB1:AP1B1:BAM22:CLAPB2:NM_007454[5U]	
chr12	21724877	21724914	111.28	51.12		

chr7	125592554	125592602	111.28	51.12	AK052528:D430042O09 Rik[I3]	
chr8	124574374	124574414	111.28	51.12		
chrX	129363218	129363258	111.28	51.12		
chr11	97748534	97748578	139.1	51.25	2410003I07Rik:NM_028 199:PLXDC1:TEM3:TE M7[I4] Plxdc1:[I4]	
chr7	55378897	55378962	83.46	51.4		
chr2	143465101	143465136	97.37	51.69	AF483512:NEC2:NM_00 8792:Nec- 2:PC2:PCSK2:SPC2[I6] Pcsk2:[I6] Pcsk2:[I6]	
chr10	48224314	48224350	97.37	51.69		
chr3	98198269	98198302	97.37	51.69		
chr4	78895832	78895872	97.37	51.69		
chr6	111530180	111530214	97.37	51.69	Grm7:[I9]	
chr7	31790116	31790153	97.37	51.69		
chr7	102985903	102985938	97.37	51.69		
chr8	54766836	54766880	97.37	51.69		
chr11	103235742	103235831	104.32	51.97		Plekhm1:[10DS]
chr9	61086079	61086150	83.46	51.97		
chr1	49550451	49550487	83.46	52.02		
chr11	18125662	18125698	83.46	52.02		
chr4	10090046	10090082	83.46	52.02		
chr4	27161505	27161544	83.46	52.02		
chr17	4582769	4582883	44.51	52.12		
chr15	75313790	75313826	63.59	52.35		
chr7	45825484	45825520	63.59	52.35		BC013491:[10DS]
chr9	95480737	95480770	132.09	52.36	Pcolce2:[I3]	
chr10	27286817	27286852	132.09	52.36	AK030879:AK042011:L AMA2:LAMM:NM_008 481[I13]	
chr10	30265017	30265074	110.08	52.36	2410075D05Rik:NM_02 8604[I6]	

					2410075D05Rik:[I6]	
chr10	50818578	50818613	132.09	52.36		
chr11	36919388	36919421	132.09	52.36	Odz2:[5U]	
chr12	36927836	36927871	132.09	52.36	4930579E17Rik:NM_178629[I2] 4930579E17Rik:BC050993:NM_178629[I2] 4930579E17Rik:AK043122:NM_178629[I2] 4930579E17Rik:[I2]	
chr12	45360481	45360517	132.09	52.36	C130076O07Rik:[5U] AK122252:C130076O07Rik:NM_176930[5U] C130076O07Rik:[5U]	
chr13	54493602	54493636	132.09	52.36		
chr14	18689437	18689472	132.09	52.36	Gng2:[5U]	
chr14	51225874	51225912	132.09	52.36	Mettl3:[I10]	AK077601:Hsal2:KIAA0360:NM_015772:SALL2[10US] Sall2:[10US] 5730589K01Rik:NM_023434[10DS] 5730589K01Rik:AK088144:AK147023:AK147834:AK153278:AK173012:NM_023434[10DS]
chr14	80235744	80235781	132.09	52.36		
chr14	116171008	116171048	132.09	52.36	AK032866:GPC6:NM_011821[I2] AF105268:AK132531:Gpc6:NM_011821[I2] AK149312:Gpc6:NM_011821[I2]	
chr18	25557737	25557774	132.09	52.36		
chr2	3775143	3775186	132.09	52.36		
chr2	124288550	124288583	132.09	52.36		
chr2	145557869	145557907	132.09	52.36	Rin2:[I9] Rin2:[I9]	
chr4	10383191	10383231	132.09	52.36		
chr4	116691468	116691515	132.09	52.36		
chr4	139266066	139266099	132.09	52.36		

chr5	141853668	141853702	132.09	52.36	AK032883:AK035225:AY353236:BC060237:FLJ31425:NM_177879:SDK1[I2]	
chr6	107635579	107635613	132.09	52.36		
chr6	120560233	120560266	132.09	52.36		
chr7	48284184	48284218	132.09	52.36		
chr7	88697708	88697745	132.09	52.36		
chr7	126413671	126413703	132.09	52.36		Nupr1:[10US]
chr8	30085537	30085582	132.09	52.36		
chr9	86905991	86906027	132.09	52.36		
chr9	105468503	105468545	132.09	52.36		
chrX	8785152	8785191	132.09	52.36		
chrX	26070193	26070226	132.09	52.36		
chrX	59211586	59211622	132.09	52.36		
chrX	142502657	142502691	132.09	52.36		
chrY	695837	695879	132.09	52.36	Usp9y:[I24]	
chr18	32905352	32905389	55.64	52.63		
chr8	27285178	27285263	15.58	52.7	AK087934:AK146938:ASH2L:ASH2L1:ASH2L2:NM_011791[E4]	Star:[10DS] BC060970:NM_011485:STAR:STARD1[10DS]
chr3	70303260	70303341	111.28	52.86		
chr5	23273846	23273882	74.18	52.89	AK142271:AK145380:AK160849:AK173290:C330017I15Rik[5U]	
chr8	27282916	27283052	10.43	52.92	AK087934:AK146938:ASH2L:ASH2L1:ASH2L2:NM_011791[E13U]	Star:[10DS] BC060970:NM_011485:STAR:STARD1[10DS]
chr5	24810488	24810649	12.72	52.98	AY138582:Mll3[E16I16]	AK129377:AK164521:AY138582:Mll3[10DS] AK136029:AK161051:Mll3[10DS]
chr17	39455865	39456062	15.9	53.03		
chr8	80104392	80104485	132.09	53.12		
chr6	44166793	44166830	44.51	53.25		

chr2	111647444	111647485	71.53	53.3		
chr5	149558306	149558346	71.53	53.3		
chr9	53339503	53339537	71.53	53.3	AK053272:Npat[5U]	Acat1:[10US]
chr2	54911383	54911449	69.55	53.36	AK038387:GALNT13:GalNAc-T13:KIAA1918:NM_173030[I11] Galnt13:[I11]	
chr10	55347224	55347297	77.89	53.36		
chr16	80643119	80643209	97.37	53.6		
chr14	108925750	108925792	62.59	53.88		
chr5	24818503	24818619	14.31	54.12	AY138582:Mll3[E20I20]	AK129377:AK164521:AY138582:Mll3[10DS]
chr4	153752483	153752520	55.64	54.6		2810405K02Rik:[10DS]
chr1	144404016	144404057	111.28	54.77		
chr12	70423051	70423084	111.28	54.77		
chr14	106352939	106352971	111.28	54.77		
chr5	89062127	89062176	111.28	54.77		4931407G18Rik:[10DS]
chr10	85978367	85978403	111.28	54.77		
chr11	15232188	15232227	111.28	54.77		
chr12	68612014	68612052	111.28	54.77		
chr14	36400772	36400805	111.28	54.77		
chr14	55019133	55019169	111.28	54.77		AK144385:AY007569:M55617:Mcpt4:NM_010779[10DS]
chr14	106792726	106792762	111.28	54.77		
chr15	8343768	8343806	111.28	54.77	Nipbl:[5U] Nipbl:[5U] Nipbl:[5U]	
chr16	35376612	35376660	111.28	54.77	Pdia5:[I14]	
chr17	38117865	38117905	111.28	54.77		
chr18	5436778	5436818	111.28	54.77		
chr2	36432780	36432819	111.28	54.77		
chr3	117236270	117236306	111.28	54.77		

chr5	24686420	24686457	111.28	54.77		Galntl5:[10US]
chr6	102905082	102905122	111.28	54.77		
chr6	120039552	120039584	111.28	54.77		
chr7	12880474	12880506	111.28	54.77		
chr7	66117291	66117330	111.28	54.77		
chr7	123120099	123120135	111.28	54.77	Arhgap17:[I17] AK036468:AK036617:AK152266:Arhgap17:NM_144529[I18] AK149986:Arhgap17:NM_144529[I18] AK152301:Arhgap17:NM_144529[I19] Arhgap17:NM_144529[I19] Arhgap17:[I18]	
chr7	140601877	140601915	111.28	54.77		
chr8	23603715	23603777	92.73	54.77	AF093416:NEK3:NM_011848[I5] Nek3:[I5]	
chr9	25658398	25658459	92.73	54.77		
chrX	28562231	28562267	111.28	54.77		
chrX	75867167	75867205	111.28	54.77		2410003J06Rik:AK167347[10US]
chr15	84950050	84950092	107	56.38	Smc1l2:[I20]	4930579A10Rik:AK016311:Ribc2[10US]
chr17	19606787	19606823	107	56.38		
chr2	4069097	4069144	107	56.38		Frmd4a:[10US] Frmd4a:[10US] AK163887:FLJ10210:FRMD4:FRMD4A:KIAA1294:NM_172475:bA295P9.4[10US]
chr7	91179418	91179457	107	56.38		
chr8	20187139	20187174	107	56.38		
chr8	75262890	75262925	107	56.38		Eps15l1:[10US] AK152602:EPS15L1:NM_007944:eps15R[10US]
chrX	129251777	129251811	107	56.38		Srpx2:[10US] Srpx2:[10US] Tspan6:[10DS]

chrX	162397472	162397506	107	56.38		
chr4	148522275	148522311	107.69	57.19	AK040867:AK172222:NM_001029837:PIK3CD:p110D[5U] AK153304:NM_001029837:Pik3cd[5U] BC035203:CT010349:NM_001029837:Pik3cd[5U] Pik3cd:[5U]	AK171025:NM_001029837:Pik3cd[10DS]
chr17	46820578	46820644	110.08	57.24		
chr5	33050977	33051058	37.09	57.36		AK033483:AK162028:AK162737:AK167554:BC094594:NM_177298:PISD:dJ858B16.2[10US] Pisd:[10US]
chr9	76350780	76350900	55.64	57.48		
chr1	17454017	17454051	110.08	57.73		
chr1	44847954	44847987	110.08	57.73		
chr1	56721097	56721149	110.08	57.73		
chr1	98813651	98813696	110.08	57.73	Slco6b1:[I11] AK006249:AY461596:Slco6b1[I11]	
chr1	115170911	115170943	110.08	57.73		
chr1	116201411	116201446	110.08	57.73		
chr1	147706461	147706493	110.08	57.73		
chr11	9132936	9132978	110.08	57.73		AK036546[10DS]
chr11	19755630	19755678	110.08	57.73		
chr14	111740966	111741001	110.08	57.73		
chr10	21334541	21334574	110.08	57.73		
chr16	9665380	9665417	110.08	57.73	Grin2a:[I10]	
chr5	15000884	15000917	110.08	57.73	AK016672:Speer8-ps1[I1]	
chr7	61045710	61045742	110.08	57.73		
chr10	32097793	32097831	110.08	57.73	6330571D19Rik:FAM77B:NM_001013411:TCBA1[I6] Tcba1:[I3]	

chr10	34473750	34473786	110.08	57.73		
chr7	100804598	100804656	88.06	57.73		P2ry6:[10US]
chr8	126169589	126169651	66.05	57.73	AF178934:FA-H:FAA:FACA:FAH:FANCA:FANCH:NM_016925[I15] Fanca:[I15]	
chr11	28945054	28945090	110.08	57.73		
chr11	50060855	50060888	110.08	57.73		Sqstm1:[10DS] AK028898:NM_011018:PDB3:SQSTM1:p60:p62[10DS] Mgat4b:[10US]
chr11	78014254	78014287	110.08	57.73		Rab34:[10DS] AK129069:AK158846:KIAA0162:NM_009297:SPT6H:SUPT6H:U40375[10US] Supt6h:[10US]
chr11	89679856	89679906	110.08	57.73		
chr12	49762004	49762041	110.08	57.73		
chr12	52685429	52685462	110.08	57.73	AK169474:Hectd1[I3] AK077185:BC010205:Hectd1[5U]	
chr13	61466779	61466814	110.08	57.73		
chr14	43160506	43160542	110.08	57.73		
chr14	48452950	48452986	110.08	57.73		AB041538:C14orf36:FLJ37712:NM_029238:SLC35F4[10DS] Slc35f4:[10DS] AK046093:NM_029238:Slc35f4[10DS]
chr14	109284321	109284354	110.08	57.73		
chr15	35063533	35063566	110.08	57.73	BC037440:KRS1:MST2:NM_019635:STK3[I8] AY058922:Mst2:NM_019635:Stk3:U28726[I10]	
chr15	55503904	55503954	110.08	57.73	Sntb1:[I3]	
chr16	26969127	26969161	110.08	57.73		
chr16	71073659	71073695	110.08	57.73		
chr17	10527623	10527660	110.08	57.73	Pacrg:[I3]	

chr18	45181393	45181426	110.08	57.73		
chr19	52300779	52300840	88.06	57.73		
chr2	69437454	69437505	110.08	57.73		
chr2	97114105	97114138	110.08	57.73		
chr2	104217644	104217675	110.08	57.73		
chr3	14379741	14379772	110.08	57.73		
chr3	16822978	16823013	110.08	57.73		
chr3	119204942	119204976	110.08	57.73	Dpyd:[5U] Dpyd:[I18]	
chr3	145016873	145016906	110.08	57.73	AI586120:Clca5:NM_178697[I3] Clca5:[I4]	
chr3	151837118	151837151	110.08	57.73		
chr3	158566888	158566931	110.08	57.73		
chr3	159230929	159230963	110.08	57.73		
chr4	69359348	69359383	110.08	57.73		
chr4	78653023	78653056	110.08	57.73		
chr4	125996839	125996875	110.08	57.73	Eif2c4:[I1] Eif2c4:[I1]	
chr5	17123239	17123277	110.08	57.73	Sema3c:[I2]	
chr5	79115425	79115465	110.08	57.73		
chr5	140998596	140998633	110.08	57.73	6530401C20Rik:[I4]	
chr6	26887911	26887942	110.08	57.73		
chr6	66675191	66675226	110.08	57.73		
chr6	66748474	66748506	110.08	57.73		
chr6	68947486	68947519	110.08	57.73		
chr6	77943969	77944005	110.08	57.73		
chr6	119422311	119422343	110.08	57.73	AK049558:BC010775:M89799:NM_009525:WNT5B:Wnt-5b[5U] Wnt5b:[5U]	
chr7	43490222	43490256	110.08	57.73		4933405K07Rik:[10DS] 4933405K07Rik:AK015213:AK016669:NM_028913[10DS]

chr7	90294123	90294160	110.08	57.73		Sytl2:[10DS] AB057755:NM_031394: Sytl2:mKIAA1597[10DS] AB050742:AB057754:A B057760:AB057761:NM _031394:Sytl2:mKIAA15 97[10DS] Sytl2:[10DS] Sytl2:[10DS] Sytl2:[10DS] Sytl2:[10DS]
chr8	101588025	101588061	110.08	57.73		
chr8	129665306	129665338	110.08	57.73		
chr8	131670258	131670292	110.08	57.73		
chr9	24982483	24982533	110.08	57.73		
chr9	29418372	29418408	110.08	57.73	AK138263:Hnt:NM_172 290[I4] Hnt:[I7]	
chr9	35723931	35723965	110.08	57.73		
chr9	50031792	50031826	110.08	57.73		
chr9	67819217	67819256	110.08	57.73		
chr9	85055386	85055419	110.08	57.73		
chr9	90417748	90417781	110.08	57.73		
chrX	31539821	31539859	110.08	57.73		
chrX	40497010	40497046	110.08	57.73		
chrX	62736782	62736823	110.08	57.73		
chrX	65510759	65510794	110.08	57.73		
chrX	75400134	75400166	110.08	57.73		
chrX	117667441	117667478	110.08	57.73		
chrX	142165893	142165926	110.08	57.73		
chr16	70874963	70875028	107	57.89		
chr5	86590257	86590324	110.08	58.04		
chr11	25870699	25870736	77.89	58.05		
chr14	30282342	30282379	77.89	58.05		
chr17	52786935	52786975	77.89	58.05		

chr4	49444737	49444786	77.89	58.05		
chr5	121637739	121637774	77.89	58.05	AK150038:FLN29:NM_172275:TRAFD1[I6] Trafd1:[I6]	AK037367:AK129172:AU042671:BC051044:BC058664[10DS]
chr5	24815975	24816054	26.35	58.33	AY138582:Mll3[E19I19]	AK129377:AK164521:AY138582:Mll3[10DS]
chr10	66977177	66977217	79.48	58.38		AK133396[10DS]
chr12	81506778	81506822	79.48	58.38	AB045325:AK138883:AK173105:Galntl1[I9]	
chr1	124454345	124454385	119.22	58.42		
chr11	100233970	100234006	119.22	58.42	AK144185:FKBP10:FLJ22041:Fkbp-rs:Fkbp1-rs:Fkbp6:Fkbprp:NM_010221:hFKBP65[I1] Fkbp10:[I1]	1110036O03Rik:[10DS] Nt5c3l:[10US]
chr4	55413337	55413372	44.51	58.47		AK142280:HHR23B:NM_009011:RAD23B[10DS] Rad23b:[10DS]
chr7	6444115	6444190	69.55	58.48	Usp29:[5U]	
chr2	3881785	3881898	17.8	58.54		
chr14	50983141	50983243	66.05	58.58		
chr17	13344537	13344602	18.55	58.63		
chr15	27314555	27314589	92.73	58.65		
chr1	71965038	71965107	66.77	58.66		
chr11	47415415	47415503	92.73	58.7	AK047384:DAGD:LGMD2F:NM_011891:SGCD[5U]	
chr1	74470912	74470947	83.46	58.79	Usp37:[5U]	AK140231:NM_148937:Plcd4[10US] AK039149:NM_148937:PLCD4[10US] BC066156:NM_148937:Plcd4[10US] Plcd4:[10US] Rqcd1:[10DS]
chr10	65558141	65558179	83.46	58.79		
chr13	52309527	52309565	83.46	58.79		

chr14	104599383	104599416	83.46	58.79		
chr13	37514102	37514139	83.46	58.79		
chr13	90743259	90743293	83.46	58.79		
chr13	101239276	101239312	83.46	58.79		AK144778:AK152495:AK167832:NM_011420:Smn:Smn1:U63294:U77714:Y12835[10DS] AY821786:BCD541:NM_011420:SMA1:SMA2:SMA3:SMN:SMN1:SMNT[10DS] AY821787:NM_011420:SMN:Smn1[10DS] Birc1b:[10US] Birc1b:[10US]
chr17	5536635	5536676	83.46	58.79	AK080845:FLJ20984:NEW1CP:NM_146073:ZDHHC14[I1] AF542387:AK046719:AK080845:BC086758:NM_146073:Zdhhc14[5U] Zdhhc14:[I1]	
chr17	61838431	61838465	83.46	58.79		
chr2	169944965	169944999	83.46	58.79		
chr3	104556596	104556644	83.46	58.79		
chr3	106504271	106504303	83.46	58.79		
chr3	140455946	140455988	83.46	58.79		
chr4	52209153	52209194	83.46	58.79		
chr4	74981619	74981653	83.46	58.79		
chr7	84351172	84351214	83.46	58.79		
chr8	62409028	62409063	83.46	58.79		
chr9	82973074	82973112	83.46	58.79		
chr4	99098162	99098197	64.91	58.82		
chr6	64788692	64788734	64.91	58.82		
chr19	27563463	27563501	64.91	58.82		
chr6	74364177	74364212	64.91	58.82		
chr17	18805549	18805638	83.46	58.86		

chr5	62366831	62366870	55.64	58.89		
chr10	128593730	128593770	55.64	58.89		
chr13	108475888	108475934	55.64	58.89		
chr15	14029709	14029748	55.64	58.89		
chr2	54502789	54502827	55.64	58.89	AK038387:GALNT13:GalNAc-T13:KIAA1918:NM_173030[I3] Galnt13:[I3]	
chrY	1327949	1327992	55.64	58.89		
chr3	26509536	26509618	88.06	59.04	Nlgn1:[5U]	
chr14	106202721	106202766	45.52	59.04		
chr4	3010124	3010232	14.93	59.21		
chr8	27288237	27288440	5.45	59.21	AK087934:AK146938:ASH2L:ASH2L1:ASH2L2:NM_011791[I4E5I5]	Star:[10DS] BC060970:NM_011485:STAR:STARD1[10DS]
chr4	117284930	117285002	110.08	59.25		
chr11	97201636	97201704	47.69	59.27	Socs7:[I7]	
chr3	62784411	62784505	66.77	59.32		
chr11	117659254	117659350	92.73	59.37		Afmid:[10DS] Birc5:[10US] Birc5:[10US]
chr17	13345555	13345629	22.91	59.52		
chr17	57050922	57051008	110.08	59.52	AK155862:EMR1:NM_010130:TM7LN3[I2] Emr1:[I2]	
chr8	27305283	27305425	13.6	59.88	AK087934:AK146938:ASH2L:ASH2L1:ASH2L2:NM_011791[I13E14]	
chr2	157643719	157643752	87.85	60.06		Gm691:[10DS]
chr6	26069366	26069436	88.06	64.77		
chrX	80478898	80478969	66.05	64.84	Dmd:[I44]	
chr15	9676779	9676814	99.35	64.9	AK041992:C230086A09Rik[I7]	
chr18	51781445	51781477	99.35	64.9		
chr5	135780470	135780501	99.35	64.9	Hip1:[5U]	

chr14	95054166	95054202	66.77	65.02	Klhl1:[I4]	
chr18	4752159	4752195	66.77	65.02		
chr11	15908574	15908606	66.77	65.02		
chr18	55893207	55893246	66.77	65.02		
chr8	47114154	47114186	66.77	65.02		
chr12	81608305	81608336	66.77	65.02	0610009B14Rik[5U]	AK080462:AK090062:BC043112:Slc39a9[10DS]
chr18	38915504	38915543	66.77	65.02		
chr5	12635515	12635551	66.77	65.02		
chr5	86339811	86339853	66.77	65.02		
chr9	68713117	68713154	66.77	65.02	Rora:[I1]	AK142452[10DS]
chr1	179550155	179550232	88.06	65.25		
chr15	51418233	51418302	66.05	65.3		
chr10	82001399	82001437	34.24	65.31		
chr1	110773332	110773366	92.73	65.36		
chr10	115168381	115168412	92.73	65.36		
chr11	25204423	25204458	92.73	65.36		
chr1	150118165	150118222	74.18	65.36		
chr3	113751731	113751793	74.18	65.36		
chr4	53628722	53628753	92.73	65.36	Slc44a1:[I15]	
chr5	94202876	94202911	92.73	65.36	AK028475:D5Ertd606e:FLJ10849:NM_001009818:SEPT11[I1] AK171368:NM_001009818:Sept11[I1] BC062206:NM_001009818:Sept11[I1] Sept11:[I1]	
chr7	64373009	64373068	74.18	65.36		Apba2:[10US]
chr7	114670533	114670567	92.73	65.36		
chr12	17264941	17264976	92.73	65.36		
chr13	25450154	25450186	92.73	65.36		
chr13	27213563	27213597	92.73	65.36		Prlpj:[10DS]

chr13	80553334	80553367	92.73	65.36		
chr14	31683306	31683348	92.73	65.36		E130203B14Rik:[10US]
chr14	91847485	91847521	92.73	65.36		
chr15	65552119	65552155	92.73	65.36		
chr16	19088238	19088274	92.73	65.36		
chr16	27128357	27128391	92.73	65.36		
chr16	45669248	45669287	92.73	65.36	BC050915:BC060683:FLJ21791:LL5b:LL5beta:NM_153412:PHLDB2[I2] Phldb2:[I2]	Abhd10:[10DS] ABHD10:D230019K24Rik:FLJ11342:NM_172511[10DS]
chr16	69093529	69093561	92.73	65.36		
chr18	13348714	13348745	92.73	65.36		
chr18	65552849	65552888	92.73	65.36		Malt1:[10US] AK045200:MALT1:MLT:NM_172833[10US] BC110487:Malt1:NM_172833[10US] AK041919:AK049821:AK085071:BC046536:Malt1:NM_172833[10US]
chr19	51660774	51660805	92.73	65.36		
chr2	106869244	106869279	92.73	65.36		Fshb:[10DS]
chr3	11965134	11965173	92.73	65.36		
chr4	70805478	70805513	92.73	65.36		
chr4	86365689	86365727	92.73	65.36	2410116I05Rik:Asah3l:NM_139306[I3] 2410116I05Rik:Asah3l:NM_139306[I3] Asah3l:[I3]	
chr4	103760865	103760900	92.73	65.36	BC051993:Dab1[5U]	
chr4	134680866	134680896	92.73	65.36		AF237888:AK042201:AK043916:AK155270:BC059001:DSCR1L2[10US]
chr4	134759411	134759446	92.73	65.36	9130020G22Rik:AK082376:DJ462O23.2:NM_028995:NPAL3[I10] Npal3:[I10]	4930555I21Rik:[10US]
chr5	78100936	78100967	92.73	65.36	1700023E05Rik:[I1]	

chr6	63282842	63282876	92.73	65.36		
chr6	74363105	74363154	92.73	65.36		
chr6	80600799	80600833	92.73	65.36	AK032470:FLJ12568:LRRTM4:NM_178731[I1] BC037216:Lrrtm4:NM_178731[I2]	
chr6	125583646	125583693	92.73	65.36	Vwf:[I17]	
chr8	32706596	32706631	92.73	65.36	AK083041:FUT10:NM_001012517[I3] Fut10:[I4]	Fut10:[10DS]
chrX	36355993	36356027	92.73	65.36		
chrX	77004635	77004669	92.73	65.36	BC020078:LOC432823:NM_001013789[3U]	
chrX	101420439	101420473	92.73	65.36		
chrX	102243632	102243670	92.73	65.36	Atp7a:[5U] Atp7a:Mnk:NM_009726[5U]	
chrX	112344199	112344232	92.73	65.36		
chrX	115973951	115973987	92.73	65.36		
chrX	117700219	117700250	92.73	65.36		
chr4	72398362	72398426	74.18	65.49		
chr2	40780860	40780910	21.1	65.61	Lrp1b:[I48]	
chr18	75691315	75691351	48.68	66.39	Gm672:[I7]	
chr14	85175200	85175237	48.68	66.39		
chr3	50641479	50641516	48.68	66.39		
chr10	23170847	23170914	66.05	66.81		
chr1	106483313	106483354	47.69	66.82		
chr4	45533916	45533953	47.69	66.82		
chr14	89306177	89306218	47.69	66.82		
chr16	32039718	32039751	47.69	66.82		
chr16	39357190	39357225	47.69	66.82		
chr17	67739485	67739525	47.69	66.82		Arhgap28:[10US] Arhgap28:[10US] AU044757:Arhgap28:NM_172964[10US]

chr17	91852102	91852134	47.69	66.82		
chr9	16747394	16747434	47.69	66.82		
chr11	13417047	13417113	88.06	66.95		
chr11	61126414	61126449	55.64	67.08	4933429E10Rik:[I6]	
chr11	13171948	13171983	55.64	67.08		
chr2	52228158	52228212	55.64	67.08	Arl5a:[I2]	
chr13	58778061	58778096	55.64	67.08		
chr16	57163332	57163368	55.64	67.08		
chr16	84568950	84569006	46.37	67.08		
chr17	77301020	77301056	55.64	67.08		
chr2	121114458	121114494	55.64	67.08	Pdia3:[I2]	AK142380:CATSPER2: NM_153075[10DS] Catsper2:[10DS]
chr5	40014913	40014956	55.64	67.08	Hs3st1:[5U]	
chr5	83141002	83141041	55.64	67.08		
chr6	109069553	109069586	55.64	67.08		
chr9	41212257	41212294	55.64	67.08		
chr9	83742121	83742156	55.64	67.08		Bckdhb:[10US]
chr6	47190465	47190566	66.05	67.19	Cntnap2:[I21] Cntnap2:[5U]	
chr1	115868813	115868856	69.55	67.36		
chr1	124475619	124475662	69.55	67.36		
chr1	173303571	173303607	69.55	67.36		F11r:[10DS]
chr10	54306241	54306275	69.55	67.36		
chr11	30392728	30392764	69.55	67.36		
chr11	64498817	64498854	69.55	67.36		
chr11	32028153	32028193	69.55	67.36		
chr13	46719177	46719208	69.55	67.36	Nup153:[I14]	
chr13	98693134	98693171	69.55	67.36		
chr16	58746513	58746546	69.55	67.36		
chr18	84470233	84470274	69.55	67.36	AK132276:Zfp407[I2]	

chr7	109114282	109114315	69.55	67.36		
chr13	98291247	98291294	69.55	67.36	Hexb:[I11]	
chr15	14555659	14555696	69.55	67.36		
chr15	59957203	59957243	69.55	67.36		
chr17	31322761	31322793	69.55	67.36	Pknox1:[I4] Pknox1:[I4]	
chr19	30443728	30443765	69.55	67.36		
chr2	106147504	106147552	69.55	67.36		
chr2	125839333	125839383	69.55	67.36		Dtwd1:[10US]
chr3	23545118	23545155	69.55	67.36		
chr3	43953658	43953703	69.55	67.36		
chr3	106932486	106932520	69.55	67.36		
chr3	120192598	120192633	69.55	67.36		
chr5	80296112	80296147	69.55	67.36		
chr6	10147090	10147125	69.55	67.36		
chr6	40893326	40893359	69.55	67.36		1810009J06Rik:[10US]
chr6	126316732	126316766	69.55	67.36		
chr7	11732226	11732269	69.55	67.36		Zfp110:[10US] AJ242914:AK013583:AK040989:NM_022981:Zfp110[10US]
chr8	62633481	62633515	69.55	67.36		
chr8	112498084	112498118	69.55	67.36		Dhodh:[10DS] AK149350:DHODH:NM_020046[10DS]
chr9	11100731	11100764	69.55	67.36		
chr9	15919161	15919195	69.55	67.36		
chrX	63696204	63696246	69.55	67.36		
chrX	123262053	123262088	69.55	67.36		
chrX	128637217	128637253	69.55	67.36		
chr4	100757641	100757705	55.64	67.4	AK152128:JAK1:JAK1A:JAK1B:NM_146145[5U] Jak1:[5U]	

chr17	4582639	4582676	43.27	67.52		
chr17	25936835	25936871	43.27	67.52	AK039314:AK161551:BC049910:Rgs11[I4]	AI429612:[10US] Arhgdig:[10DS]
chr4	40623251	40623285	43.27	67.52		
chr2	3013147	3013238	44.03	67.58		
chr3	124825974	124826053	88.06	67.58		
chr4	56967611	56967702	88.06	67.58		Ctnnal1:[10DS]
chr10	41437528	41437561	86.93	67.64	2410017P07Rik:AF397908:AK006744:AK012710:NM_026643[5U] 2410017P07Rik:NM_026643[5U] 2410017P07Rik:[5U]	
chr1	155529208	155529243	86.93	67.64		Rnasel:[10DS] Rnasel:[10DS] AK054205:NM_011882:Rnasel[10DS]
chr1	37007777	37007835	65.46	67.66	A230074B11Rik:[I6]	
chr1	181319790	181319838	81.82	67.66	Smyd3:[I11]	
chr15	39148948	39148985	81.82	67.66	Rims2:[I4]	
chr2	135784087	135784121	81.82	67.66	Pak7:[I3]	
chr5	102513756	102513839	47.69	67.7		
chr13	43225387	43225438	38.95	67.81	Gfod1:[I1]	
chr12	24990818	24990863	38.95	67.81		
chr14	99230160	99230195	38.95	67.81		
chr6	19137053	19137090	38.95	67.81		
chr17	23660289	23660327	38.95	67.81		Sbp:[10US]
chrX	12611610	12611687	55.64	67.97	Nyx:[5U]	
chrX	97649335	97649416	52.16	67.97	Nono:[I11]	AF140691:CHORDC3:ITGB1BP2:NM_013712[10US]
chr5	23997151	23997231	88.06	68.01	Centg3:[5U] BC031173:Centg3:NM_139153[5U] Centg3:[I10]	AB078345:CENTG3:NM_139153[10DS]
chr18	40434177	40434287	16.49	68.03		

chr8	27296821	27296893	11.59	68.03	AK087934:AK146938:ASH2L:ASH2L1:ASH2L2:NM_011791[E9]	
chr1	75455208	75455291	55.64	68.08		
chr11	53742297	53742333	35.41	68.08		Slc22a5:[10DS]
chr15	22218362	22218448	88.06	68.3		
chr8	96967735	96967821	88.06	68.3	Bbs2:[I5]	
chr2	130102794	130102868	55.64	68.41		4933425O20Rik:[10DS] 1700020A23Rik:AK006141[10DS] A930025D01Rik:NM_178762[10US] A930025D01Rik:[10US] A930025D01Rik:AK032354:AK032762:NM_178762[10US]
chr11	101999214	101999281	46.37	68.51	2600001B17Rik:[I4]	G6pc3:[10US]
chr12	91970108	91970173	46.37	68.53	Gtf2a1:[I2]	
chr15	80681947	80682008	61.82	68.63	AK051922:D230019K20Rik:NM_144812:Tnrc6b[I1] Tnrc6b:[I4] Tnrc6b:[I1]	
chr2	63532536	63532571	77.28	68.63		
chr8	27301551	27301628	19.26	68.87	AK087934:AK146938:ASH2L:ASH2L1:ASH2L2:NM_011791[E13]	
chr5	135040030	135040119	88.06	68.99		Eln:[10DS]
chr15	14238604	14238694	74.18	69.21		
chr6	9118114	9118204	74.18	69.21	Nxph1:[I1]	
chr8	19856179	19856233	66.24	69.22		
chr13	86961659	86961698	66.24	69.22		
chr13	105230718	105230826	66.05	69.25	Sgtb:[5U]	AK138399:NM_029447:Nln[10DS] Nln:[10DS] Nln:[10DS]
chr3	13168358	13168451	55.64	69.42		
chr5	80498276	80498340	37.59	69.46		
chr13	100891086	100891190	22.26	69.5		

chr1	19424478	19424516	88.06	69.94	
chr1	24451220	24451252	88.06	69.94	Col19a1:[I40]
chr1	46020932	46020966	88.06	69.94	
chr1	54443345	54443376	88.06	69.94	
chr1	70749576	70749607	88.06	69.94	A830006F12Rik:NM_17 7164[I5] A830006F12Rik:[I3]
chr1	96636864	96636896	88.06	69.94	
chr1	102894544	102894578	88.06	69.94	
chr1	131623456	131623486	88.06	69.94	AK051714:D130067I03R ik:NM_172485[I10] D130067I03Rik:[I10]
chr1	147398967	147399014	88.06	69.94	
chr1	149286614	149286647	88.06	69.94	
chr1	150942729	150942760	88.06	69.94	
chr1	168389395	168389426	88.06	69.94	
chr10	15627598	15627633	88.06	69.94	
chr10	22217072	22217113	88.06	69.94	
chr10	28747868	28747920	88.06	69.94	
chr10	51560377	51560410	88.06	69.94	
chr10	62559421	62559453	88.06	69.94	
chr10	69590573	69590610	88.06	69.94	
chr10	72328350	72328381	88.06	69.94	
chr10	81261297	81261330	88.06	69.94	
chr10	111548689	111548724	88.06	69.94	
chr11	9824633	9824690	66.05	69.94	
chr11	13761294	13761330	88.06	69.94	
chr11	20352253	20352286	88.06	69.94	
chr11	28427340	28427377	88.06	69.94	AK173298:E030025D05 Rik:NM_181577[I2] BC066065:E030025D05 Rik:NM_181577[I2] E030025D05Rik:[I3]

chr11	29284780	29284833	88.06	69.94	A430106J12Rik:NM_176841:RP23-92B18.2:RP23-92B18.2-007[I2] A430106J12Rik:[I2]	
chr11	30617338	30617396	66.05	69.94		
chr11	46910512	46910557	88.06	69.94	AK047384:DAGD:LGMD2F:NM_011891:SGCD[I1] Sgcd:[I2]	
chr11	70453185	70453229	88.06	69.94		Gp1ba:[10US] Slc25a11:[10US]
chr12	12888852	12888900	88.06	69.94		
chr12	50654375	50654426	88.06	69.94		
chr12	63008656	63008693	88.06	69.94		
chr12	78121486	78121522	88.06	69.94		
chr12	90930050	90930087	88.06	69.94		
chr12	96397079	96397111	88.06	69.94		
chr1	85044769	85044816	88.06	69.94		
chr10	115395328	115395390	66.05	69.94		
chr11	22950349	22950380	88.06	69.94		
chr11	51658346	51658386	88.06	69.94	Phf15:[3U]	
chr12	7503198	7503260	66.05	69.94		
chr12	45467771	45467823	88.06	69.94	C130076O07Rik:[I30] AK122252:C130076O07Rik:NM_176930[I27] AJ543321:C130076O07Rik:NM_176930:Nrcam[I5] C130076O07Rik:[I30]	
chr13	5275842	5275876	88.06	69.94		
chr13	46738042	46738088	88.06	69.94	Nup153:[I21]	
chr13	63717155	63717207	88.06	69.94		
chr13	118754575	118754622	88.06	69.94	Hcn1:[I1]	
chr14	57500320	57500371	88.06	69.94		
chr13	48992162	48992192	88.06	69.94		
chr14	107592166	107592199	88.06	69.94		

chr14	119662302	119662362	66.05	69.94		
chr15	59785790	59785825	88.06	69.94		
chr16	88532337	88532400	44.03	69.94		2310002B14Rik:[10US]
chr18	22329806	22329839	88.06	69.94		
chr18	38059106	38059159	88.06	69.94		AF098295:AF125536:HDAC3:NM_010411:RPD3[10US]
chr3	18368650	18368683	88.06	69.94	Cyp7b1:[I5]	
chr3	73248208	73248240	88.06	69.94		
chr3	138395686	138395746	66.05	69.94		Metap1:[10US] Adh5:[10DS]
chr4	66095415	66095454	88.06	69.94		
chr4	142573761	142573806	88.06	69.94		AJ250246:AJ297944:AK158855:GP40:Gp38:NM_010329:Ots8:PA2.26:PDPN:T1A-2:aggrus[10DS]
chr5	30201968	30202020	88.06	69.94		
chr14	7673872	7673908	88.06	69.94		
chr5	104525524	104525572	88.06	69.94		
chr14	12647389	12647420	88.06	69.94		
chr14	16388977	16389017	88.06	69.94		
chr5	130484561	130484594	88.06	69.94	Rabgef1:[I3]	
chr6	143331470	143331504	88.06	69.94		
chr7	14941151	14941197	88.06	69.94		
chr7	49156795	49156828	88.06	69.94	5330421F07Rik:NM_175272[I1]	
chr8	71416370	71416426	66.05	69.94	4732435N03Rik:[5U]	
chr14	35091271	35091331	66.05	69.94		
chr14	37082846	37082877	88.06	69.94		
chr8	90609375	90609407	88.06	69.94	AY147407:Ebfaz:NM_033327:Zfp423[I3] AF188609:AK122365:AK133497:AY147407:BC059234:BC079586:NM_033327:Zfp423[I3]	

					Zfp423:[I3]	
chr14	44649408	44649451	88.06	69.94		
chr14	48202783	48202815	88.06	69.94		
chr8	110141201	110141262	66.05	69.94		
chr9	113733931	113733989	66.05	69.94	AJ276961:CLASP2:KIA A0627:NM_029633[I11] Clasp2:[5U] Clasp2:[I21]	
chrX	73463507	73463557	88.06	69.94		
chr14	82707929	82707960	88.06	69.94		
chr14	85426556	85426596	88.06	69.94		
chr14	109047726	109047762	88.06	69.94		
chr14	118589260	118589295	88.06	69.94	Hs6st3:[I1]	
chr14	123918088	123918125	88.06	69.94		
chr15	8930723	8930754	88.06	69.94	AK132406:C130037N17 Rik:NM_198024[I1] C130037N17Rik:[I1]	
chr15	14787011	14787052	88.06	69.94		
chr15	15212512	15212546	88.06	69.94		
chr15	22707014	22707077	66.05	69.94		
chr15	33593349	33593379	88.06	69.94		
chr15	33929171	33929201	88.06	69.94		
chr15	35530110	35530143	88.06	69.94	2310042E16Rik[5U]	
chr15	57401733	57401766	88.06	69.94		
chr15	86537166	86537206	88.06	69.94		
chr15	103087292	103087351	66.05	69.94		Nfe2:[10DS]
chr16	32021125	32021156	88.06	69.94	1500031L02Rik:[5U]	Pigx:[10DS]
chr16	48837776	48837807	88.06	69.94	LOC432823:[3U]	
chr16	72230079	72230110	88.06	69.94		
chr16	95887867	95887912	88.06	69.94		
chr17	27014768	27014807	88.06	69.94		
chr17	57065475	57065511	88.06	69.94	AK155862:EMR1:NM_0 10130:TM7LN3[I2]	

					Emr1:[I2]	
chr17	66619217	66619264	88.06	69.94	AK129005:AK164246:AK220171:NM_008984:Ptprm:X58287[5U] Ptprm:[I10]	
chr17	84471155	84471188	88.06	69.94	Plekhh2:[I6]	
chr18	3289963	3289998	88.06	69.94	AK015641:Crem:NM_013498[I1] AK016156:Crem:NM_013498[I2] AY738715:Crem:NM_013498[I2] AY738716:Crem:NM_013498[I2] AY738717:Crem:NM_013498[I2] AY738718:Crem:NM_013498[I3] AY738719:Crem:NM_013498[I4] AY738721:Crem:NM_013498[I3] Crem:[I3] Crem:[I3]	AK009841:AK010806:Crem:NM_013498[10US] AK161366:Crem:NM_013498[10US] AJ292222:CREM:NM_013498:S67786[10DS] AJ311667:CREM:NM_013498[10DS]
chr18	20005337	20005370	88.06	69.94		
chr18	20310906	20310937	88.06	69.94		
chr18	21683483	21683522	88.06	69.94		
chr18	31269540	31269573	88.06	69.94	Rit2:[I1] Rit2:[I1]	
chr18	45604439	45604475	88.06	69.94		
chr18	64180586	64180625	88.06	69.94		
chr2	15639870	15639907	88.06	69.94		
chr2	15905778	15905814	88.06	69.94		
chr2	40351254	40351288	88.06	69.94		
chr2	64030596	64030634	88.06	69.94		
chr2	81106868	81106904	88.06	69.94		
chr2	82211351	82211387	88.06	69.94		
chr2	106218729	106218760	88.06	69.94		
chr2	108223854	108223892	88.06	69.94		
chr2	119852711	119852743	88.06	69.94		Pla2g4e:[10US]

						Ehd4:[10DS]
chr2	123190654	123190687	88.06	69.94		
chr2	134440808	134440845	88.06	69.94		
chr2	142000030	142000068	88.06	69.94	2900006F19Rik:LOC433479:NM_028387[I14] LOC433479:[I9]	
chr2	151783868	151783903	88.06	69.94		
chr2	163919466	163919498	88.06	69.94		Wfdc15:[10DS] Svs2:[10US]
chr3	3098475	3098516	88.06	69.94		
chr3	5933294	5933332	88.06	69.94		
chr3	8951041	8951083	88.06	69.94	Tpd52:[I6] Tpd52:[I6] Tpd52:[I5]	Tpd52:[10DS] Tpd52:[10DS]
chr3	21141816	21141854	88.06	69.94		
chr3	22709624	22709661	88.06	69.94		
chr3	26690086	26690134	88.06	69.94		
chr3	27142410	27142443	88.06	69.94	Spata16:[I10]	
chr3	59656809	59656844	88.06	69.94		
chr3	74923752	74923785	88.06	69.94		
chr3	80427396	80427427	88.06	69.94		
chr3	93186230	93186260	88.06	69.94		
chr3	106514939	106514978	88.06	69.94		BC051070:[10US]
chr3	111476634	111476667	88.06	69.94		
chr3	112862386	112862419	88.06	69.94		
chr3	113636684	113636721	88.06	69.94		
chr3	118900765	118900797	88.06	69.94	Dpyd:[5U] Dpyd:[I10]	
chr3	144353439	144353473	88.06	69.94		
chr3	158817832	158817867	88.06	69.94		
chr4	4712922	4712955	88.06	69.94	Impad1:[I4]	AK052165[10US]
chr4	8593042	8593104	44.03	69.94		
chr4	9221671	9221729	66.05	69.94	4933402J24Rik:[I2]	

chr4	20381652	20381683	88.06	69.94	AK053823:E130310K16 Rik:NM_172987[I3] E130310K16Rik:[I2]	
chr4	22718916	22718949	88.06	69.94		
chr4	23531389	23531434	88.06	69.94		
chr4	30762109	30762140	88.06	69.94		
chr4	34330254	34330287	88.06	69.94		
chr4	37897225	37897257	88.06	69.94		
chr4	38532808	38532846	88.06	69.94		
chr4	67426964	67426998	88.06	69.94		
chr4	73181210	73181242	88.06	69.94		AK132691:FLJ31614:N M_001017427:OTTMUS P00000000335:RAB45:R ASEF:RP23-355N20.6-002[10US] Rasef:[10US]
chr4	90218559	90218591	88.06	69.94		
chr4	91903123	91903155	88.06	69.94		
chr4	115163324	115163358	88.06	69.94		
chr4	148291433	148291490	66.05	69.94		Rbp7:[10US]
chr4	150890902	150890935	88.06	69.94	4632412I24Rik:FLJ2332 3:NM_028727:NOL9[I6] 4632412I24Rik:AK1720 43:NM_028727:Nol9[I6] Nol9:[I6]	Tas1r1:[10DS] BC070448:GPR70:NM_0 31867:T1R1:TAS1R1:TR 1[10DS]
chr5	13111182	13111219	88.06	69.94		
chr5	13760623	13760677	88.06	69.94		
chr5	16827760	16827798	88.06	69.94		
chr5	25249475	25249505	88.06	69.94		
chr5	30026648	30026678	88.06	69.94		
chr5	45616806	45616840	88.06	69.94		
chr5	62562485	62562533	88.06	69.94		
chr5	64506195	64506235	88.06	69.94	AK122445:KIAA1108:N M_019636:TBC:TBC1:T BC1D1[I2] AK154591:NM_019636: Tbc1d1[I3]	

chr5	86011951	86011983	88.06	69.94		
chr5	107177356	107177390	88.06	69.94		
chr5	115283788	115283823	88.06	69.94	AK014709:NM_029012: Sppl3[5U] Sppl3:[I1]	
chr5	131804440	131804480	88.06	69.94	2700063G02Rik:AK012475:AK028848:AK035818:AK129144:AK135848:AK164158:Auts2:BC021509:BC058110:BC066072 [5U]	
chr5	133509624	133509661	88.06	69.94		
chr5	147321639	147321679	88.06	69.94		Lnx2:[10US]
chr6	7518666	7518698	88.06	69.94		Tac1:[10DS]
chr6	14077059	14077094	88.06	69.94		
chr6	19645788	19645824	88.06	69.94		
chr6	31682022	31682085	66.05	69.94		
chr6	46611109	46611148	88.06	69.94	Cntnap2:[I13]	
chr6	56944118	56944177	66.05	69.94		
chr6	67458124	67458154	88.06	69.94		Tacstd2:[10US]
chr6	68294449	68294483	88.06	69.94		
chr6	68774978	68775010	88.06	69.94		
chr6	70117842	70117875	88.06	69.94		
chr6	76252624	76252658	88.06	69.94		
chr6	78064668	78064707	88.06	69.94		
chr6	90964063	90964099	88.06	69.94		
chr6	120878273	120878324	88.06	69.94	Bid:[5U]	
chr6	124279795	124279831	88.06	69.94	CD163:M130:MM130:NM_053094[I6] Cd163:[I6]	
chr7	5550386	5550419	88.06	69.94		
chr7	33353635	33353668	88.06	69.94		
chr7	39579890	39579921	88.06	69.94		
chr7	48452979	48453013	88.06	69.94		AK139009[10US]

chr7	50997437	50997470	88.06	69.94		
chr7	51034437	51034472	88.06	69.94		
chr7	55946887	55946923	88.06	69.94	Herc2:[I4]	
chr7	58395268	58395305	88.06	69.94		
chr7	58901780	58901811	88.06	69.94		
chr7	62172760	62172799	88.06	69.94		
chr7	86773632	86773668	88.06	69.94		
chr7	88229243	88229276	88.06	69.94		
chr8	19727260	19727308	88.06	69.94		
chr8	32222387	32222417	88.06	69.94		
chr8	40961951	40961987	88.06	69.94		
chr8	41020618	41020661	88.06	69.94		
chr8	42557556	42557605	88.06	69.94	AY626783:BC089009:Mtus1[I11] Mtus1:[I12]	AY626782:BC043321:Mtus1[10DS] AK043214:Mtus1:NM_001005863[10DS]
chr8	50330436	50330484	88.06	69.94		
chr8	54767512	54767546	88.06	69.94		
chr8	58640320	58640352	88.06	69.94		
chr8	62441905	62441943	88.06	69.94		
chr8	62678625	62678656	88.06	69.94		
chr8	74074699	74074735	88.06	69.94		
chr8	76001575	76001608	88.06	69.94	Large:[I11]	
chr8	101727577	101727613	88.06	69.94		
chr9	6636042	6636089	88.06	69.94		
chr9	13004290	13004323	88.06	69.94		
chr9	26423027	26423060	88.06	69.94		
chr9	33965216	33965246	88.06	69.94		
chr9	103658655	103658715	66.05	69.94		
chr9	111152384	111152426	88.06	69.94		
chrX	22765890	22765929	88.06	69.94		

chrX	25074944	25074977	88.06	69.94	NM_009529:XMR[I3]
chrX	25814488	25814520	88.06	69.94	NM_009529:XMR[I7]
chrX	65447518	65447550	88.06	69.94	
chrX	71884336	71884370	88.06	69.94	
chrX	79806078	79806112	88.06	69.94	Dmd:[I7]
chrX	80992083	80992119	88.06	69.94	Dmd:[I55]
chrX	86444837	86444877	88.06	69.94	
chrX	108298332	108298366	88.06	69.94	
chrX	110527648	110527683	88.06	69.94	
chrX	111371546	111371595	88.06	69.94	
chrX	113564274	113564305	88.06	69.94	
chrX	117175997	117176033	88.06	69.94	
chrX	118896691	118896732	88.06	69.94	
chrX	122353956	122353989	88.06	69.94	
chrX	123854242	123854275	88.06	69.94	
chrX	126048552	126048584	88.06	69.94	
chrX	132812187	132812235	88.06	69.94	
chrX	137802239	137802272	88.06	69.94	
chrX	156663499	156663545	88.06	69.94	
chr8	27294308	27294414	14.36	69.95	AK087934:AK146938:ASH2L:ASH2L1:ASH2L2:NM_011791[I7E8I8]
chr3	8229570	8229635	15.9	70.02	
chr1	47691076	47691128	85.6	70.18	
chr14	98404447	98404484	85.6	70.18	
chr3	141577902	141577932	85.6	70.18	AK031655:AK142411:AK142974:NM_009472:Rcm:UNC5C:Unc5h3[I1] AK164239:NM_009472:Unc5c[I1] Unc5c:[I1]
chrX	153725543	153725597	85.6	70.18	

chr16	48645440	48645478	85.6	70.18	LOC432823:[3U]	Trat1:[10US] BC104350:HSPC062:NM_198297:TCRIM:TRAT1:TRIM[10US] AJ297969:AK030807:AK138735:NM_198297:Trat1[10US]
chr3	44912482	44912516	85.6	70.18		
chr3	125317797	125317827	85.6	70.18		
chr4	27969815	27969845	85.6	70.18		
chr6	125842729	125842791	21.4	70.18	AK044763:C12orf3:NM_153589:TMEM16B[I13] AK132944:NM_153589:Tmem16b[5U] Tmem16b:[I12]	
chr15	84089130	84089212	41.73	70.78	AF237770:CGI-56:NM_133167:PARVB[I1] Parvb:[I1]	
chr2	149985755	149985885	66.05	70.82		
chr8	27995784	27995858	66.05	70.85		
chrX	80341298	80341372	66.05	70.85	Dmd:[I44]	
chr16	49982521	49982585	66.05	70.86	LOC432823:[3U] B130050K08:[I3]	
chr5	52575240	52575304	66.05	70.86		
chr9	54322100	54322164	66.05	70.86		
chr4	22110961	22111025	66.05	70.86		
chr4	29193150	29193214	66.05	70.86		
chr7	93516354	93516418	66.05	70.86		
chr1	12945062	12945143	55.64	70.89	Slco5a1:[I5]	
chr11	3022239	3022319	41.73	71		4933439C20Rik:AK168892:AK169597:AK169755:NM_001004146[10US] AK133558:Sfi1[10US] 2310047I15Rik:AK133558:BC026390:Sfi1[10US] 2310047I15Rik:Sfi1[10US]
chrX	118948325	118948398	46.37	71.02		

chr1	110379883	110379914	55.64	71.06		
chr1	184466490	184466550	44.51	71.06	Capn8:[I19]	
chr10	36953178	36953225	55.64	71.06		
chr11	86520546	86520577	55.64	71.06	Cltc:[I7]	
chr12	116144717	116144753	55.64	71.06		
chr14	6466676	6466709	55.64	71.06		
chr14	94670687	94670718	55.64	71.06		
chr2	114821015	114821052	55.64	71.06		
chr3	90142974	90143006	55.64	71.06	4933434E20Rik:[I4]	4932431F02Rik:NM_028475:Ubap2l[10DS] 4932431F02Rik:NM_028475:Ubap2l[10DS] 4932431F02Rik:NM_028475:Ubap2l[10DS] Ubap2l:[10DS] Ubap2l:[10DS] 4932431F02Rik:AF276967:KIAA0144:NICE-4:NM_028475:UBAP2L[10DS] 1700094D03Rik:AK007060[10US] 4932431F02Rik:NM_028475:Ubap2l[10DS]
chr15	5933609	5933652	55.64	71.06		
chr8	20318266	20318325	44.51	71.06	LOC436177:[3U]	5330429B09Rik:A430108E01Rik:AK033345:AK083828:AK088897:NM_001033637[10DS]
chr8	30284501	30284535	55.64	71.06	Unc5d:[I14]	
chr9	39747221	39747256	55.64	71.06		Olfr980:[10US]
chrX	104004167	104004200	55.64	71.06	2610002M06Rik:[I6]	
chr15	17256877	17256911	55.64	71.06		
chr15	78969284	78969318	55.64	71.06	Polr2f:[I1]	1700088E04Rik:[10DS] 1700088E04Rik:NM_138581[10DS] 1700088E04Rik:BC068203:NM_138581[10DS] AK147274:D15Mit260:Kiaa1668:Mirab13[10DS] AK129419:D15Mit260:Kiaa1668:Mirab13[10DS]

						AK077217:AK129419:AK147587:D15Mit260[10DS]
chr16	48415360	48415391	55.64	71.06	Morc1:[I9]	
chr2	121214019	121214067	55.64	71.06	5830411K18Rik:Wdr76[I5] 5830411K18Rik:AK031592:Wdr76[I3]	
chr3	33960803	33960835	55.64	71.06		
chr3	82659584	82659627	55.64	71.06		
chr5	15150935	15150973	55.64	71.06	AK016672:Speer8-ps1[I1]	
chr5	108839818	108839859	55.64	71.06	Gak:[I17]	
chr6	24257644	24257684	55.64	71.06		
chr7	55335869	55335902	55.64	71.06		
chr7	61030229	61030264	55.64	71.06		
chr8	38037869	38037908	55.64	71.06	AK147539:Arhgap7:Dlc1:Stard12[3U] AK162413:Arhgap7:Dlc1:Stard12[3U]	
chr9	56614731	56614763	55.64	71.06		
chrX	17456860	17456893	55.64	71.06		
chrX	21982078	21982114	55.64	71.06		
chrX	53971488	53971525	55.64	71.06		
chrX	163265231	163265264	55.64	71.06	Frmpd4:[5U] Frmpd4:[5U]	
chr6	149201910	149202013	53.84	71.1		
chr12	15751358	15751415	34.77	72.26		
chr7	103328100	103328134	41.73	72.26		
chr8	74362102	74362139	41.73	72.26		
chr18	62438074	62438112	60.48	72.35		AK034506[10US]
chr17	26250009	26250104	53.84	72.43		
chr12	115418685	115418726	32.46	72.46		
chr16	28993071	28993144	41.73	72.55		

chr9	112316377	112316495	66.05	72.6		
chrX	111972236	111972275	57.96	73.25		
chr17	39455557	39455694	18.55	73.75		
chr1	89878041	89878074	46.37	88.87		Ugt1a10:[10US]
chr1	114881035	114881068	46.37	88.87		
chr12	59783622	59783660	46.37	88.87		
chr14	92981052	92981091	46.37	88.87		
chr2	164044770	164044804	46.37	88.87		AK010170:ALK1:ALP:BLPI:HUSI:HUSI-I:NM_011414:SLPI:U73004:U88093:U94341:WAP4:WFDC4[10US]
chr2	166586069	166586119	46.37	88.87		
chr8	19759638	19759688	46.37	88.87		
chr15	39216886	39216924	46.37	88.87	Rims2:[I5]	
chr15	43713642	43713675	46.37	88.87		
chr16	15422603	15422654	46.37	88.87		
chr18	9366271	9366306	46.37	88.87	5730405I09Rik:NM_026484[I7] 5730405I09Rik:[I7]	
chr2	39944551	39944584	46.37	88.87		
chr2	83996578	83996618	46.37	88.87		
chr2	151879106	151879140	46.37	88.87		
chr3	118308741	118308778	46.37	88.87		
chr4	12544518	12544550	46.37	88.87		
chr5	148633977	148634014	46.37	88.87		Slc7a1:[10US] C130038G02Rik:[10DS] AK019985:C130038G02Rik:NM_001033601[10DS] AK021162:C130038G02Rik:NM_001033601[10DS] AK002529:C130038G02Rik:NM_001033601[10DS]

chr6	139374296	139374337	46.37	88.87		
chr10	23170034	23170112	44.03	89.39		
chr3	102564910	102564988	66.05	89.39		
chrX	133535267	133535345	66.05	89.39	Il1rapl2:[I3]	
chr1	69765536	69765569	33.38	89.45	Spag16:[5U] Spag16:[I1]	
chr8	111462824	111462862	33.38	89.45		
chr5	24814740	24814803	16.21	89.52	AY138582:Mll3[I17E18]	AK129377:AK164521:AY138582:Mll3[10DS]
chr16	50542068	50542133	55.64	89.58		
chrX	105388692	105388757	37.09	89.58		
chr4	20766295	20766365	59.61	89.6	AK053823:E130310K16Rik:NM_172987[I5] E130310K16Rik:[I4]	
chr17	60174515	60174561	71.79	89.67	AK143547:L1Md-Tf29:LOC385718:NM_001014998[5U]	
chr11	53449358	53449433	44.03	89.93		AK053412:AK084748:AW124694[10DS] Kif3a:[10DS] AK147078:KIF3A:NM_008443:RP23-188H3.1-001[10DS] AK169425:Kif3a:NM_008443[10DS] Il4:[10US]
chr13	24767052	24767127	66.05	89.93	AF068780:AK131959:GMNN:Gem:NM_020567[I5]	
chr2	25129514	25129589	44.03	89.93	AK158175:GRIN1:NMDAR1:NM_008169[I15] BC039157:Grin1:NM_008169[I15] Grin1:[I16]	
chr3	96076835	96076910	66.05	89.93	Plekho1:[I2E3]	Vps45:[10US]
chr8	19697621	19697696	66.05	89.93		
chr16	51789673	51789737	55.64	90.18		
chr2	83416863	83416927	55.64	90.18		
chr2	128718574	128718638	37.09	90.18		Zc3h6:[10DS]
chr1	10095027	10095104	66.05	90.27		

chr10	8795453	8795530	66.05	90.27		
chr10	68349908	68349985	66.05	90.27		
chr15	11321725	11321802	66.05	90.27		Tars:[10US]
chr18	70794898	70794975	44.03	90.27		
chr3	20226674	20226751	44.03	90.27	AK049204:Hps3:NM_080634[I8] AK171997:Hps3:NM_080634[I16] Hps3:[I16]	AK037829:HPS3:NM_080634:SUTAL[10DS]
chr3	43209567	43209644	44.03	90.27		
chr6	90506257	90506334	66.05	90.27		
chr7	49547685	49547762	44.03	90.27		
chrX	125932143	125932220	44.03	90.27		
chr1	12886897	12886928	74.18	90.33	Slco5a1:[I2]	
chr1	48784813	48784872	55.64	90.33		
chr1	50607689	50607720	74.18	90.33		
chr1	100493554	100493591	74.18	90.33		
chr1	119713278	119713311	74.18	90.33		
chr1	157772957	157773014	55.64	90.33	AK149727:FLJ13142:LAP1B:NM_144791:TOR1AIP1[3U] AK152751:NM_144791:Tor1aip1[I1] Tor1aip1:[I1]	
chr1	158334852	158334894	74.18	90.33		
chr1	176883707	176883744	74.18	90.33		
chr10	16980553	16980608	55.64	90.33		
chr10	50254066	50254107	74.18	90.33		
chr10	54654115	54654153	74.18	90.33		
chr11	76548906	76548939	74.18	90.33	Gosr1:[I1]	
chr11	87205560	87205595	74.18	90.33	AK076551:NM_053269:RAD51C:RAD51L2[I3] Rad51c:[I3]	
chr12	31897402	31897434	74.18	90.33	AK013952:AK141833:BC032276:Lamb1-1:NM_008482[5U] Lamb1-1:[I23] Lamb1-	

					1:[I23]	
chr12	43642747	43642781	74.18	90.33		
chr12	48992966	48993002	74.18	90.33		
chr12	49504596	49504631	74.18	90.33		
chr13	3477964	3477996	74.18	90.33		
chr13	24733690	24733726	74.18	90.33	6330500D04Rik:AK007145:AK122269:BC059179:BC060202:NM_178658:RP23-461O24.1-003[I22]	
chr14	51078732	51078764	74.18	90.33	Rpgrip1:[I22] Rpgrip1:[I22]	Supt16h:[10US] AF323667:CDC68:FACT:FACTP140:FLJ10857:FLJ14010:NM_033618:SPT16/CDC68:SUPT16H[10US]
chr14	80850596	80850641	74.18	90.33		
chr14	83833628	83833664	74.18	90.33		
chr14	96091588	96091622	74.18	90.33		
chr15	15398283	15398315	74.18	90.33		
chr15	18263862	18263902	74.18	90.33		
chr1	72148241	72148285	74.18	90.33		Wdt2:[10DS]
chr10	74291995	74292028	74.18	90.33		
chr11	118049550	118049591	74.18	90.33	AB013464:AY126516:NM_011180:Pscd1[I12] Pscd1:[I12]	
chr15	77726503	77726554	74.18	90.33		
chr12	80586993	80587031	74.18	90.33	Rad51l1:[I8]	
chr13	77853203	77853235	74.18	90.33	2210408I21Rik:AK141602[I15]	
chr14	26768072	26768110	74.18	90.33	AY356531:Cast1:D14Ertd171e:Erc2:Kiaa0378:NM_177814[I5] AY356533:Cast1:D14Ertd171e:Erc2:Kiaa0378:NM_177814[I5] D14Ertd171e:[I6]	

chr16	40139887	40139920	74.18	90.33		
chr16	97236559	97236592	74.18	90.33	Dscam:[I32]	
chr19	10839877	10839939	55.64	90.33	A430093F15Rik:[5U]	
chr19	59106897	59106931	74.18	90.33	4930506M07Rik:AK220405:NM_175172[I15] 4930506M07Rik:[I13]	
chr16	41274054	41274093	74.18	90.33		
chr3	47631096	47631129	74.18	90.33		
chr4	31257412	31257448	74.18	90.33		
chr4	145397584	145397628	74.18	90.33		
chr5	51862348	51862381	74.18	90.33		
chr16	51875632	51875667	74.18	90.33		
chr5	122571262	122571295	74.18	90.33	Pptc7:[I2] Pptc7:[I2]	
chr16	62529829	62529861	74.18	90.33		
chr6	93836133	93836163	74.18	90.33	AK147358:Magi1:NM_001029850[I23] Magi1:[I20]	
chr7	125558072	125558128	55.64	90.33		
chr8	20314251	20314288	74.18	90.33	LOC436177:[3U]	5330429B09Rik:A430108E01Rik:AK033345:AK083828:AK088897:NM_001033637[10DS]
chr8	50261602	50261636	74.18	90.33		
chr16	92670289	92670325	74.18	90.33	AK137493:AML1:AMLCR1:CBFA2:NM_009821:PEBP2A2:RUNX1[I6]	
chr17	35383843	35383878	74.18	90.33		
chr17	53515105	53515140	74.18	90.33		
chr17	79011705	79011741	74.18	90.33		
chr18	21019359	21019391	74.18	90.33	D030074E01Rik:[I14]	
chr18	28021502	28021551	74.18	90.33		
chr18	31429393	31429432	74.18	90.33	Rit2:[I4] Rit2:[I4]	
chr19	40194941	40194972	74.18	90.33		

chr2	39543294	39543347	74.18	90.33		
chr2	59862944	59862989	74.18	90.33	5830435C13Rik:BAZ2B:NM_001001182[5U] Baz2b:[5U]	
chr2	76954491	76954522	74.18	90.33	2610301F02Rik:LOC545428:NM_001025576[I6] 2610301F02Rik:[I10]	
chr2	77813709	77813752	74.18	90.33		
chr2	93685859	93685892	74.18	90.33	AK135828:Gm1967:NM_001033452[5U]	
chr3	57789053	57789090	74.18	90.33		Gm410:[10DS]
chr3	102967226	102967259	74.18	90.33	Sycp1:[I3]	
chr3	159105686	159105717	74.18	90.33		
chr4	43094119	43094152	74.18	90.33	AK161056:NM_021468:UNC13:UNC13B:Unc13h2:hmunc13[I1]	
chr4	66205962	66205996	74.18	90.33		
chr5	7574534	7574568	74.18	90.33	AK143547:L1Md-Tf29:LOC385718:NM_001014998[5U]	
chr5	13222220	13222252	74.18	90.33		
chr5	42955806	42955838	74.18	90.33		
chr5	57707877	57707908	74.18	90.33		
chr5	104524388	104524418	74.18	90.33		
chr5	147236954	147236987	74.18	90.33		
chr6	44550026	44550061	74.18	90.33		
chr6	84681841	84681897	55.64	90.33	AK016259:AK220360:BC043037:Sec15l2[I2]	
chr6	101099765	101099799	74.18	90.33		
chr6	126423650	126423688	74.18	90.33		
chr7	15368501	15368552	74.18	90.33	Dhx34:[5U] Dhx34:[I10]	
chr7	62467962	62467997	74.18	90.33		
chr7	86548642	86548679	74.18	90.33		
chr8	99130652	99130686	74.18	90.33		

chr9	36127003	36127035	74.18	90.33		
chr9	54937711	54937764	74.18	90.33		Ube2q2:[10US] 3010021M21Rik:AK076148:AK083216:AK150776:DKFZp762C143:NM_180600:UBE2Q2[10US]
chr9	92553745	92553792	74.18	90.33		
chrX	4635179	4635211	74.18	90.33		AK132789:Mycs:NM_010850[10US]
chrX	58391520	58391557	74.18	90.33		
chrX	62314258	62314295	74.18	90.33		
chrX	78757177	78757240	37.09	90.33		
chrX	80273114	80273150	74.18	90.33	Dmd:[I43]	
chrX	100826150	100826180	74.18	90.33	Zdhhc15:[I10]	
chrX	131221198	131221245	74.18	90.33		
chrX	132891860	132891891	74.18	90.33		
chr14	13785321	13785397	66.05	90.42		
chr4	54423054	54423130	66.05	90.42		
chr7	113124615	113124691	66.05	90.42	Btbd10:[I6]	
chr7	143594284	143594360	66.05	90.42		Mrgpre:[10DS]
chr18	50098738	50098814	66.05	90.42		AK163339:GG2-1:MDC-3.13:NM_134131:SCC-S2:TNFAIP8[10US] AK050888:AK166520:BC056490:C630007L23Rik:Dmxl1:Dxml1[10DS]
chr10	90485422	90485491	59.61	90.63	AK220340:APAF1:BC083191:CED4:NM_009684 [I16] AF064071:Apaf1[I16]	
chr18	82355776	82355858	20.86	93.52		
chr10	116582056	116582098	79.48	93.6		
chr11	94528518	94528570	79.48	93.6		RP23-290B5.6:[10DS]
chr12	74317981	74318015	79.48	93.6		
chr12	99744407	99744443	79.48	93.6	Ches1:[I4]	3300002A11Rik[10US]

chr15	22571350	22571383	79.48	93.6		
chr16	96210667	96210700	79.48	93.6		
chr1	39810458	39810524	55.64	93.6		
chr5	104051307	104051361	79.48	93.6		
chr8	81386674	81386736	59.61	93.6		
chrX	53845802	53845836	79.48	93.6		AK138185:AK138370:GPR101[10US]
chr19	54826899	54826965	55.64	93.6		
chrX	64200702	64200741	79.48	93.6	BC020078:LOC432823:NM_001013789[3U]	
chr11	3603493	3603561	64.2	93.61		BC031794:BC051185:BC058602:NM_152818:Osbp2:RP23-309E11.7-002[10US] Osbp2:[10US] AK044598:KIAA1664:NM_152818:ORP-4:OSBP2:OSBPL1:RP23-309E11.7-002:RP23-309E11.7-003[10US]
chr11	60637572	60637642	44.03	93.63		Dhrs7b:[10US] Dhrs7b:[10US]
chr8	116191841	116191911	44.03	93.63		
chrX	35145607	35145677	44.03	93.63		
chr1	82192517	82192587	34.77	93.72		
chr14	25337040	25337106	44.03	93.82	AK141597:NM_032008:Slmap[5U] Slmap:[I22]	
chr18	8120907	8120973	66.05	93.82		
chr8	112536930	112536996	44.03	93.82		
chr15	63007067	63007174	27.82	93.83		
chr17	21188613	21188646	69.55	93.89		Zfp53:[10US]
chr12	9250966	9251032	64.2	93.89		
chr17	35528059	35528117	52.16	93.89	BC052059:Cat53:FB19:NM_175934:PNUTS:PPP1R10[5U] Ppp1r10:[5U]	AK002554:AK076033:AK076044:C6orf14:HSPC183:MRPS18-2:MRPS18B:NM_025878:PTD017[10DS] Mrps18b:[10DS]

						2610110G12Rik:NM_028476[10DS] 2610110G12Rik:NM_028476[10DS] 2610110G12Rik:NM_028476[10DS] 2610110G12Rik:AK014265:NM_028476[10DS] 2610110G12Rik:[10DS]
chr18	21515553	21515608	52.16	93.89		
chr4	80296763	80296795	69.55	93.89		Tyrp1:[10US]
chrX	78863739	78863816	64.2	93.89		
chr18	23119213	23119279	44.51	93.9	Nol4:[5U]	
chr4	12972634	12972718	55.64	93.93		
chr1	27688359	27688438	44.03	93.97		
chr15	24125320	24125399	66.05	93.97		
chr17	88089647	88089726	44.03	93.97		
chr10	16136370	16136449	66.05	93.97		
chrX	49242131	49242202	46.37	93.99	AK002286:AK088114:AK146626:BC004686:BC083145:HGPRT:HPRT:HPRT1:J00423[I1]	
chr16	85246299	85246367	66.05	94		
chr10	21832159	21832236	20.86	94.05		
chr3	37564354	37564389	23.43	94.09		
chr2	60203597	60203683	55.64	94.12		
chrX	55382539	55382654	37.09	94.12		
chr15	42648652	42648740	41.73	94.15		
chr16	78668891	78668960	44.03	94.15		
chr17	36307287	36307356	66.05	94.15		
chr5	9551925	9551994	66.05	94.15	Grm3:[I3]	
chr6	139402064	139402133	66.05	94.15		
chr10	24275307	24275367	61.82	94.18		Ctgf:[10US]
chr1	59112565	59112634	64.2	94.19	Als2:[I3]	AJ748820:DLG6:MPP4:NM_145143[10DS]

chr11	52140187	52140267	66.05	94.21		
chr12	41170915	41170995	44.03	94.21	AK030389:DOCK4:FLJ34238:KIAA0716:NM_172803[I8] Dock4:[I8]	
chr18	4494892	4494974	39.74	94.21		
chr1	42022457	42022537	44.03	94.21		
chr2	63793755	63793835	44.03	94.21	AF263913:AK143787:AK163474:AK164536:FIGN:NM_021716[5U] AF263913:AK143787:AK163474:Fign[I1]	
chr4	56030775	56030855	66.05	94.21		
chr4	98274312	98274392	66.05	94.21	Ankrd38:[I8]	
chr9	71854897	71854977	44.03	94.21	AK143246:NM_011544:Tcf12[I3] BC037097:NM_011544:Tcf12[5U] AK133958:NM_011544:Tcf12:X64840[5U] Tcf12:[I18]	
chr19	52300057	52300137	66.05	94.21		
chr3	65357433	65357513	66.05	94.21	AK015412:AKR6A3:KCNA1B:KCNAB1:Kvb1.3:NM_010597:hKvBeta3:hKvb3[I3] AK031362:Kcnab1:NM_010597[I2] AF033003:AK004666:AK015412:AK138467:AK153200:Kcnab1:NM_010597:X97281[5U] Kcnab1:[I2]	
chr4	118046163	118046214	37.09	94.28		6330530A05Rik:[10DS] 6330530A05Rik:AK160304:AK162829:AK162907:NM_172383[10DS] 1110020C03Rik:[10US]
chr8	19999135	19999175	37.09	94.28		
chr4	89669610	89669651	37.09	94.28		
chr4	91894761	91894797	37.09	94.28		
chr11	80179574	80179645	66.05	94.29	5730455P16Rik:AK078548:AK135352:AK153246	Rhbdl3:[10DS]

					:BC044897:RP23-252E4.2:RP23-252E4.2-001[3U]	
chr1	165020717	165020788	66.05	94.29		
chr11	22847689	22847760	44.03	94.29	AB076722:C2orf5:COMMD1:MGC27155:MURR1:NM_144514:RP23-242C19.3-001:U2/MU[I1] AK082909:AK133507:BC030052:BC038641:BC051210:Commd1:D85430:NM_144514[I1] Commd1:[I1]	
chr2	146904055	146904126	66.05	94.29		
chr4	128718336	128718407	44.03	94.29	Yars:[I11]	C77080:[10US] C77080:[10US] AK038020:C77080:NM_001033189[10US]
chr7	58641448	58641519	44.03	94.29	Atp10a:[I2]	
chr3	99007420	99007536	55.64	94.36	Hao3:[I3]	
chr3	56495423	56495490	66.05	94.57		
chr14	95194557	95194624	55.64	94.58	Klhl1:[I7]	
chr19	44660391	44660458	55.64	94.58		
chr9	121544703	121544770	55.64	94.58	Sec22l3:[5U]	
chr19	3958817	3958915	27.82	94.59		1700055N04Rik[10US] AK030488:AK155556:BC018388:NM_019449:UNC93B1:Unc93b[10DS] Unc93b1:[10DS]
chr5	81019855	81019926	44.51	94.8		
chr17	84804395	84804463	55.64	95.08		
chr2	27138611	27138679	55.64	95.08	BC053060:NM_009500:VAV2[I27] Vav2:[I24]	
chr3	68975385	68975453	55.64	95.08		Ift80:[10US]
chr12	16409477	16409558	44.03	95.34		
chr4	144333166	144333247	66.05	95.34		
chr8	38907903	38907984	44.03	95.34		

chr3	88550474	88550555	66.05	95.34		Sema4a:[10DS]
chr12	49779108	49779177	37.09	95.46		
chr17	69296345	69296414	55.64	95.46		Zfp161:[10DS]
chr14	89284304	89284386	66.05	95.62		
chr16	55617837	55617919	44.03	95.62		
chr1	100140749	100140831	66.05	95.62		
chr11	84744634	84744716	44.03	95.62		
chr18	32142912	32142994	44.03	95.62	Myo7b:[I35E36]	
chr8	115431367	115431449	66.05	95.62		
chr3	106779781	106779863	66.05	95.62		
chr6	43892320	43892402	66.05	95.62		
chr10	74620484	74620549	59.61	96.44		
chr1	89912604	89912676	66.05	96.53	HLUGP4:NM_201644:UGT1A9:Ugt1[I1] Ugt1a10:[I1] Ugt1a9:[I1]	
chr1	152018651	152018723	66.05	96.53		
chr10	66533089	66533161	66.05	96.53		
chr13	32249096	32249168	66.05	96.53	Gmds:[I10]	
chr4	149405750	149405822	66.05	96.53		
chr5	125431816	125431888	66.05	96.53	AF113002:NM_011424:Ncor2[5U]	
chr4	41376112	41376184	66.05	96.53	Ube2r2:[I3]	Ubap2:[10US]
chr11	57756721	57756804	66.05	96.73		
chr14	61605995	61606078	66.05	96.73		
chr16	37096120	37096203	44.03	96.73	Stxbp5l:[I4]	
chr1	154200811	154200894	66.05	96.73	Glt25d2:[I1]	
chr14	44540380	44540463	44.03	96.73	AK129425:DDHD1:DQ272482:KIAA1705:NM_001039106[I8] AK170271:Ddhd1:NM_001039106[I9] AK048690:AK155294:AK170271:DQ272481:Ddhd1:NM_001039106[I9]	

					Ddhd1:[I8] Ddhd1:[I9]	
chr14	103866994	103867077	66.05	96.73		
chr15	39938684	39938767	66.05	96.73		
chr9	9218702	9218785	66.05	96.73		
chr1	40743156	40743229	66.05	96.95		4931419K03Rik:[10DS]
chr14	62117711	62117784	44.03	96.95	Fdft1:[I6]	
chr2	147426618	147426691	66.05	96.95		
chr5	37923670	37923743	44.03	96.95	Stk32b:[I10]	
chr8	58380066	58380139	66.05	96.95		
chr15	62259953	62260048	23.84	96.98		
chr2	117953578	117953645	61.82	97.01		AK005924:FLJ35989:FSIP1:NM_027759[10DS] Fsip1:[10DS] A930104D05Rik:[10US]
chr13	38203577	38203642	52.16	97.03		5730453H04Rik:Dsp[10US] 6530403A03Rik:[10US]
chr19	55814912	55814970	50.58	97.03	AF107298:NM_009333:TCF-4:TCF4:TCF7L2[I3] AF363725:NM_009333:Tcf7l2[I3] AF363726:NM_009333:Tcf7l2[I4] AJ223070:NM_009333:Tcf4:Tcf7l2[I3] AK035059:NM_009333:Tcf7l2[I4] AK038720:NM_009333:Tcf7l2[I3] AK132465:NM_009333:Tcf7l2[I4] AY072035:NM_009333:Tcf7l2[I3] Tcf7l2:[I3]	
chr12	117996473	117996558	39.74	97.1	Rapgef5:[I3]	
chr12	88074956	88075057	41.73	97.12	Tmed8:[I5]	
chr8	96566468	96566558	55.64	97.13		
chr11	33342546	33342620	66.05	97.95	AK035897:NM_023146:RP23-323L8.4-002:Ranbp17[I16]	

					Ranbp17:[I15]	
chr11	112425577	112425651	66.05	97.95		
chr16	33423182	33423256	66.05	97.95		Zfp148:[10DS] AF316548:AK036835:AK146591:NM_011749:Zfp148[10DS] NM_011749:Zfp148[10DS]
chr2	131265841	131265915	44.03	97.95		
chr2	134811599	134811673	66.05	97.95	AK141164:KIAA0581:NM_019677:PLCB1:U85712[I3] Plcb1:[I3]	
chr4	150723849	150723923	44.03	97.95		
chr5	123454092	123454166	44.03	97.95		
chr6	9684172	9684246	66.05	97.95		
chr1	96963051	96963122	55.64	98.13		
chr2	165558523	165558594	55.64	98.13	AK008125:AK139219:AK155864:BC060508:NM_027230:Prkcbp1[5U] AK155864:NM_027230:Prkcbp1[I21] AB093284:NM_027230:Prkcbp1[I22] BC063267:NM_027230:Prkcbp1[I10] BC048186:Prkcbp1[I22] BC023300:Prkcbp1[I10]	AK132427:NM_027230:PRKCBP1:RACK7:ZMYND8[10DS]
chr12	37174786	37174870	44.03	98.21	4930579E17Rik:BC050993:NM_178629[I9]	
chr12	113017653	113017737	66.05	98.21		
chr8	129796681	129796763	33.38	98.21		
chrX	86173505	86173589	66.05	98.21		4930415L06Rik:[10US]
chrX	165345144	165345245	18.55	98.33	Mid1:[3U]	AF026565:FXY:MID1:NM_010797:OS:RNF59:TRIM18[10DS]
chr15	102561039	102561113	44.51	98.34		
chr14	109139727	109139759	65.46	99.52		
chr3	89522911	89522960	65.46	99.52	Pbxip1:[5U]	AK132759:AY486147:BC025531:Pygo2[10DS] Shc1:[10DS]

						AK155158:NM_011368:SHC:SHC1:ShcA[10DS]
chr3	137359006	137359051	65.46	99.52	AK145825[3U] AB034693:AK029348:Emcn:Muc14:NM_016885[I8] Emcn:[I7]	
chr7	126072635	126072673	65.46	99.52	Sbk1:[5U]	
chr13	96615883	96615968	66.05	99.84	AK144986:AK158462:AK160916:AX785009:BC025432:F2RL1:GPR11:Gpcr11:NM_007974:PAR2:Z48043[I1]	
chr1	82724605	82724690	44.03	99.84	AK029917:HRB:NM_010472:RAB:RIP[I1] Hrb:[I1]	
chr13	24368234	24368319	66.05	99.84	AB061276:AK166486:BC028474:CMAH:D21826:NM_007717[5U]	
chr14	122527294	122527379	66.05	99.84		
chr15	35534927	35535012	66.05	99.84	2310042E16Rik[5U]	
chr5	74418017	74418102	44.03	99.84		
chr5	15846272	15846357	66.05	99.84	Cacna2d1:[I21] Cacna2d1:[I22] Cacna2d1:[I21] Cacna2d1:[I21] Cacna2d1:[I21]	
chr5	47846725	47846810	66.05	99.84		
chr6	72758711	72758796	66.05	99.84		
chr1	20026726	20026763	37.09	100		
chr1	46378976	46379019	44.51	100		
chr1	50315053	50315094	27.82	100		
chr1	80543749	80543784	44.51	100	AK172588[I1]	
chr1	90688118	90688159	39.74	100		
chr1	96331900	96331985	55.64	100		
chr1	112394478	112394562	55.64	100		
chr1	113057293	113057330	55.64	100		

chr1	116932733	116932773	44.51	100		
chr1	127176447	127176483	37.09	100		
chr1	133366029	133366113	33.38	100	2700049P18Rik:[I3]	
chr1	149954817	149954866	55.64	100		
chr1	156307276	156307310	55.64	100	Cacna1e:[I40]	
chr1	164854046	164854086	39.74	100		4921528O07Rik[10US]
chr1	183238101	183238137	55.64	100	AK033911:CNIH3:FLJ38993:NM_028408[I1] Cnih3:[I1]	
chr1	184466398	184466480	33.38	100	Capn8:[I19]	
chr1	196928360	196928451	44.51	100		
chr10	34694255	34694286	37.09	100		
chr10	57616274	57616348	33.38	100		
chr10	72538841	72538877	44.51	100		
chr10	76853454	76853523	41.73	100	ADAR2:ADARB1:NM_001024837[5U] AF291049:AF403106:AF403107:AF403108:AF403109:AK139004:AK141777:AY162454:Adarb1:BC040200:NM_001024837[5U] Adarb1:[5U] Adarb1:[5U] Adarb1:[5U] Adarb1:[5U] Adarb1:[5U]	
chr10	91125461	91125496	55.64	100		
chr10	100606359	100606395	55.64	100		
chr10	103047957	103047993	37.09	100		
chr10	121911026	121911070	44.51	100		
chr10	128268027	128268057	37.09	100	1110005A23Rik:[I9]	
chr11	13846858	13846894	55.64	100		
chr11	14459573	14459660	44.03	100		
chr11	22697509	22697545	55.64	100		
chr11	40971430	40971463	55.64	100		

chr11	43290986	43291076	44.03	100	D11Ertd730e:[3U]	
chr11	47200826	47200861	55.64	100	AK047384:DAGD:LGMD2F:NM_011891:SGCD[5U] Sgcd:[5U]	
chr11	49186608	49186639	55.64	100		Olfr1390:[10DS]
chr11	49278848	49278878	44.51	100		
chr11	53297778	53297834	33.38	100		AK142660[10US] 1300007L22Rik:[10US] 1300007L22Rik:NM_027917[10US] 1300007L22Rik:NM_027917:RP23-188H3.7:RP23-188H3.7-002[10US]
chr11	53565385	53565415	44.51	100	Il5:[I2] Il5:[5U]	
chr11	59338069	59338147	37.09	100		AK155809:AK170582[10US]
chr11	70264469	70264513	37.09	100		1110030J09Rik:[10US] Cxcl16:[10US] AK159317:AK162889:AK170647:AK170889:Arrb2:BC016642[10DS] AK089542:ARR2:ARRB2:NM_145429[10DS]
chr11	83123791	83123877	55.64	100	Ap2b1:[5U] Ap2b1:[5U]	Pex12:[10DS]
chr11	95608996	95609028	55.64	100		
chr11	105868605	105868690	41.73	100	1700012F10Rik:AK154757:BC027095:HAN11:NM_027946:WDR68[5U] Wdr68:[I5]	
chr12	3884725	3884772	55.64	100	AF068625:AK090132:AK147263:AK147627:AK147642:AK147676:BC007466:Dnmt3a[I5]	AF068625:AF480164:AK090132:AK147263:AK147627:AK147642:AK147676:AK157792:BC007466:Dnmt3a[10US]
chr12	4424557	4424596	44.51	100	Ncoa1:[5U]	BC080866:F-SRC-1:NCOA1:NCoA-1:NM_010881:SRC1[10DS]
chr12	6660192	6660228	37.09	100		
chr12	7023839	7023878	44.51	100		

chr12	16179621	16179702	41.73	100		
chr12	28164586	28164618	44.51	100		
chr12	43107679	43107718	55.64	100		
chr12	54145225	54145314	37.09	100		
chr12	88771186	88771263	30.91	100	AK146348:LOC544881:NM_001033788[5U]	
chr12	95294744	95294829	41.73	100		
chr12	111749321	111749359	37.09	100	Cdc42bpb:[I8]	
chr13	26106596	26106635	39.74	100		
chr13	41667867	41667955	64.2	100		A030008J09:[10DS]
chr13	56161481	56161516	39.74	100		
chr13	71224298	71224340	44.51	100	ADAMTS16:Kiaa2029:NM_172053[I6]	
chr13	119705465	119705501	58.57	100		
chr13	120560411	120560446	44.51	100	Paip1:[I5]	
chr14	3837604	3837636	30.91	100	2610042L04Rik:LOC545007:NM_001029930[5U] 2610042L04Rik:LOC544988:NM_001024712[5U]	
chr14	19112025	19112080	33.38	100	Ecd:[I1]	BC049948:NM_026341:Nudt13[10DS] AK014204:BC037091:BC040807:DKFZp586P2219:NM_026341:NUDT13[10DS]
chr14	36472567	36472599	39.74	100		
chr14	50264032	50264112	34.77	100		
chr14	50977725	50977783	27.82	100		
chr14	60447451	60447531	27.82	100		
chr14	63846049	63846128	39.74	100	AK052729:F830020C16Rik:NM_177338[I7] AK161592[I1] AK140482:AK163036:BC002212:F830020C16Rik:NM_177338[5U] Hmbox1:[I7]	

chr14	75382025	75382115	55.64	100		
chr14	77520996	77521037	44.51	100		
chr14	94216599	94216631	55.64	100		
chr14	102159996	102160075	55.64	100	Phr1:[I68]	
chr14	117163752	117163839	44.03	100		
chr15	7980825	7980911	53.84	100	AK159714:AK160933:Wdr70[I10]	
chr15	12609233	12609316	55.64	100	AK159017:Pdzk3[5U]	
chr15	33096462	33096535	31.79	100	AK154361:NM_018755:Pgcp[5U] Pgcp:[5U]	
chr15	33102818	33102881	26.92	100	AK154361:NM_018755:Pgcp[5U] Pgcp:[5U]	
chr15	33263854	33263915	30.91	100	Pgcp:[I4]	
chr15	36482458	36482516	41.73	100	4631426E05Rik:NM_025712[I9] 4631426E05Rik:[I9]	
chr15	42230686	42230732	44.51	100		
chr15	45413568	45413601	37.09	100		
chr15	55953964	55953995	63.59	100		
chr15	64400458	64400538	52.16	100		
chr15	76708569	76708606	27.82	100	Zfp7:[I3]	Zfp251:[10DS]
chr15	100741178	100741208	44.51	100		
chr15	102507419	102507467	37.09	100		Atp5g2:[10DS]
chr16	9051756	9051826	27.82	100		
chr16	58039931	58039967	27.82	100		
chr16	64630359	64630393	55.64	100		
chr16	86810012	86810101	66.05	100		
chr17	6211945	6212067	31.79	100		
chr17	13343613	13343647	28.98	100		
chr17	13344667	13344701	21.64	100		
chr17	13827294	13827333	34.77	100		

chr17	18808503	18808536	44.51	100		
chr17	32257080	32257162	55.64	100		
chr17	52617479	52617511	55.64	100		
chr17	59593719	59593755	39.74	100	AK143547:L1Md-Tf29:LOC385718:NM_001014998[5U]	
chr17	69455589	69455622	44.51	100		
chr17	75570314	75570352	44.51	100		
chr17	83980585	83980649	27.82	100		
chr18	19382557	19382644	55.64	100		
chr18	24698512	24698553	30.91	100		
chr18	43039954	43039989	25.68	100	Ppp2r2b:[I8]	
chr18	63320550	63320587	55.64	100		
chr18	73844147	73844180	44.51	100		
chr19	7610316	7610347	55.64	100		5730596K20Rik:[10DS]
chr19	20526892	20526942	55.64	100		
chr19	61319074	61319120	39.74	100		
chr2	31047805	31047842	55.64	100		AI790205:[10DS]
chr2	37302604	37302677	37.09	100	AK031315:GAPCenA:NM_001033960:RABGAP1:Strbp:TBC1D11[I5] AK051644:NM_001033960:Rabgap1[5U] Rabgap1:[I5] Rabgap1:[I5]	Strbp:[10US]
chr2	81476410	81476498	66.05	100		
chr2	88867220	88867264	55.64	100		
chr2	98523399	98523432	55.64	100		
chr2	127175068	127175109	22.26	100	Kcnip3:[I7] Kcnip3:[I7] AF184624:AF274050:AF287733:AF300870:AK165711:BC026980:BC057329:Csen:DQ148499:NM_019789[I7] Kcnip3:[I7]	DQ148500[10DS]
chr2	127236646	127236722	33.38	100		Prom2:[10DS] Prom2:[10DS]

						BC039212:NM_138750:PROM2[10DS]
chr2	155282576	155282616	55.64	100	AK169276:GSS:NM_008180[5U] AK146486:AK149577:AK159630:AK169096:Gss:NM_008180:U35456[5U] Gss:[5U]	ACAS2:ACS:ACSA:ACSS2:AceCS:NM_019811:dJ1161H23.1[10DS]
chr2	155877147	155877182	37.09	100		AK146046:CAPER:CC1.3:HCC1:NM_133242:RBM39:RNPC2[10DS] Rnpc2:[10DS] Rnpc2:[10DS] AK135289:AK154989:BC092268:NM_133242:Rnpc2[10DS]
chr2	156103865	156103894	55.64	100		AK147272:Epb4.1l1:NM_001003815[10US] Epb4.1l1:[10US] Epb4.1l1:[10US] AK154704:Epb4.1l1:NM_001003815[10US] BC034751:Epb4.1l1:NM_001003815[10US]
chr2	166662580	166662634	37.09	100	AK151835:AK152744:NM_011490:STAU:STAU1[5U] AK145826:AK159602:NM_011490:Stau:Stau1[5U] AF395842:AK005002:AK139532:AK152269:AK159781:AK167637:BC082277:NM_011490:Stau:Stau1[5U] Stau1:[5U]	AY391773:NM_011490:Stau1[10DS]
chr2	174097691	174097731	44.51	100		Atp5e:[10US]
chr3	32118835	32118922	66.05	100	Kcnmb2:[5U]	
chr3	49529049	49529084	30.91	100		
chr3	60036334	60036415	41.73	100		AK140981:C130079G13Rik:NM_177661[10US]
chr1	17100424	17100511	44.03	100		
chr3	60973046	60973077	37.09	100		
chr3	68110103	68110187	55.64	100	D230050A05:[I1]	

chr1	40030105	40030188	37.09	100	AK132264:IL1R2:IL1RB:NM_010555:X59769[5U] Il1r2:[5U]	
chr3	73233413	73233500	66.05	100		
chr1	50959604	50959684	41.73	100	Tmeff2:[I4]	
chr1	58126507	58126565	41.73	100	Aox3:[I30]	
chr1	62883705	62883787	55.64	100		AK133321:BC010584:RP23-198I4.3:RP23-198I4.3-003[10US]
chr1	85134547	85134641	27.82	100	AK047983[I4] 5830484A20Rik:NM_175397[5U] LOC620078:[I4]	
chr1	87426270	87426307	34.77	100	5830484A20Rik:NM_175397[I10] 5830484A20Rik:AK077800:AY845948:Ipr1:NM_175397[I10] BC099598[3U] 5830484A20Rik:[I11]	LOC434484:[10US]
chr3	96671680	96671764	27.82	100	Polr3gl:[5U]	
chr1	90084572	90084639	27.82	100		6430706D22Rik:NM_198652[10US] 6430706D22Rik:[10US]
chr1	118393559	118393638	55.64	100		
chr1	119114252	119114340	66.05	100		
chr1	120724349	120724423	55.64	100		
chr3	123856282	123856354	37.09	100		
chr1	145999094	145999131	37.09	100		1R20:AK170957:BL34:IER1:IR20:NM_015811:RGS1[10US] Rgs1:[10US]
chr3	131247305	131247339	39.74	100	AK075609:AK132260:AK148486:AK167024:AK168877:AK169261:HADHSC:Hadh:Mschad:NM_008212:SCHAD[I7] Hadh:Hadhsc:Mschad:Schad[I7]	
chr1	148728647	148728680	34.77	100		

chr1	150136232	150136271	30.35	100		
chr1	166101420	166101497	27.82	100	Slc19a2:[3U] Slc19a2:[3U]	
chr3	141636677	141636752	55.64	100	AK031655:AK142411:AK142974:NM_009472:Rcm:UNC5C:Unc5h3[I2] AK164239:NM_009472:Unc5c[I1] Unc5c:[I2]	
chr3	148990038	148990170	11.92	100		
chr3	152906204	152906288	37.09	100	St6galnac5:[I3]	
chr3	153061283	153061315	34.77	100		
chr1	166430936	166430999	33.38	100		
chr1	171036814	171036893	37.09	100		
chr1	172535840	172535926	37.09	100		
chr1	192822706	192822794	44.03	100		
chr4	12500180	12500213	44.51	100		
chr4	12849635	12849670	55.64	100	C130086A10:[5U]	
chr4	20282720	20282784	20.23	100	AK053823:E130310K16Rik:NM_172987[I2]	
chr1	195681496	195681548	55.64	100		
chr10	21831929	21832023	18.55	100		
chr4	30007015	30007048	55.64	100		
chr10	44485777	44485867	26.49	100		
chr10	55051693	55051745	39.74	100		
chr10	57619338	57619407	20.86	100		
chr4	51572670	51572746	41.73	100		
chr4	52168582	52168621	44.51	100		
chr10	76508973	76509062	66.05	100	Col18a1:[E13I13]	
chr10	77121792	77121879	66.05	100		
chr10	79369148	79369238	66.05	100	Wdr18:[E5]	AK163465:NM_175450:WDR18[10DS] Grin3b:[10US]
chr10	80582237	80582289	37.09	100	Eef2:[E5]	4930442H23Rik[10US]

						Dapk3:[10US]
chr11	6171901	6171988	55.64	100	Tmed4:[I1]	Ddx56:[10DS]
chr4	68696863	68696898	55.64	100		
chr4	69220848	69220886	37.09	100		
chr11	11929139	11929229	41.73	100	Grb10:[5U]	BC016111:GRB10:NM_010345:RP23-119N24.1-002[10DS]
chr11	54791636	54791719	33.38	100	ABIN-1:KIAA0113:NAF1:NM_021327:TNIP1:VAN[5U] AJ242777:AJ242778:AK170841:NM_021327:Tnip1[5U] BC008665:NM_021327:Tnip1[5U] Tnip1:[5U]	
chr11	60095667	60095739	55.64	100	AK036788:NM_001039092:TOM1L2[I7] AK043095:NM_001039092:Tom1l2[I11] Tom1l2:[I12] Tom1l2:[I10] Tom1l2:[I13]	
chr11	87042005	87042041	55.64	100		Ppm1e:[10US] Trim37:[10DS]
chr4	120298228	120298262	55.64	100	AK156353:CBF-C:NFYC:NM_008692[5U] Nfyc:[5U]	
chr4	122418799	122418864	33.38	100		
chr11	91140386	91140429	44.51	100		
chr11	97378228	97378303	55.64	100	P140:[I19]	
chr11	99453893	99453930	37.09	100		1110033F04Rik:[10DS] Krtap4-7:[10US] 1110033F04Rik:NM_026807[10DS]
chr11	100235911	100235943	34.77	100	AK144185:FKBP10:FLJ22041:Fkbp-rs:Fkbp1-rs:Fkbp6:Fkbprp:NM_010221:hFKBP65[I1] Fkbp10:[I1]	Nt5c3l:[10US] 1110036O03Rik:[10DS] AK148222:C330027I04Rik:MGC20781:NM_026561:NT5C3L[10US] AK011707:AK148222:AK162770:C330027I04Rik:NM_026561:Nt5c3l[10U

						S]
chr11	106939750	106939837	37.09	100		
chr11	119920789	119920869	39.74	100	1810073N04Rik:AK159948:NM_024249[3U] 1810073N04Rik:NM_024249[3U] 1810073N04Rik:NM_024249[3U] 1810073N04Rik:[3U]	2410002I01Rik:NM_183137[10DS]
chr12	5189748	5189836	37.09	100	AK122572:Kbtbd9:Kiaa1921[5U]	
chr12	9350896	9350927	55.64	100		
chr12	44325958	44326048	37.09	100		
chr12	51821614	51821702	55.64	100		
chr4	154879064	154879106	27.82	100	Ttll10:[E1]	Tnfrsf18:[10DS] Tnfrsf18:[10DS] Tnfrsf18:[10DS] 4833412E22Rik:Ttll10:Ttll5[10US]
chr12	56513307	56513384	37.09	100		Garnl1:[10US] Garnl1:[10US]
chr12	92806051	92806119	27.82	100		
chr12	108019491	108019567	55.64	100		
chr5	14985981	14986061	41.73	100		AK016672:Speer8-ps1[10DS]
chr12	108459235	108459324	66.05	100		AB043551:BCL11B:CTIP-2:Ctip2:NM_021399:Rit1[10DS] AB043583:Bcl11b:NM_021399[10DS] Bcl11b:[10DS] AB043551:AB043553:AB043583:AK088588:AK169655:Bcl11b:NM_021399[10DS]
chr12	112992464	112992554	66.05	100		
chr5	22619893	22619979	44.03	100		
chr12	117550927	117551013	66.05	100	AK138655:IA-2beta:IAR PTPRP:ICAAR:KIAA0387:NM_011215:PTPRN2	AK144077[10DS]

					:phogrin[I12] Ptprn2:[I12]	
chr13	56710976	56711065	41.73	100		BC048233:Dwfc:JV5-1:MADH5:NM_008541:SMAD5[10US] Smad5:[10US]
chr13	58515235	58515314	41.73	100		
chr13	81957310	81957389	26.49	100	Mass1:[I38]	
chr13	96298897	96298994	37.09	100	AK036090:NM_172263:PDE8B[I16] AK043680:AK083166:NM_172263:Pde8b[I18] Pde8b:[5U] Pde8b:[I19]	
chr13	102798177	102798265	66.05	100	BC026146:M60651:NM_001024955:Pik3r1:U50413[I9]	Pik3r1:[10DS]
chr14	11017029	11017061	55.64	100	AK144283:NM_008981:PTPG:PTPRG:RPTPG[I13] Ptprg:[I26]	
chr5	28240887	28240924	44.51	100		
chr14	29935900	29935983	27.82	100	2610016F04Rik[I3] 2010107H07Rik[I1] 2610016F04Rik[I3]	
chr14	30459991	30460069	33.38	100	Phyh2:[E12I12]	
chr14	61773131	61773218	42.8	100		
chr14	64214680	64214714	55.64	100		Fbxo16:[10US] AK043554:FBX16:FBXO16:NM_015795[10US] Fzd3:[10DS]
chr5	50043029	50043083	55.64	100		
chr14	117466590	117466621	37.09	100	Abcc4:[I12]	
chr15	4029912	4030000	37.09	100	AK146342:NM_024188:OXCT:OXCT1:SCOT[I7] AB085609:AK011354:AK078086:AK146158:AK151662:AK151695:AK167681:BC003422:Oxct:Oxct1:Scot[I7]	
chr15	6304962	6305014	37.09	100	AK002850:DAB2:DOC-2:NM_001008702[5U]	

					Dab2:[5U]	
chr15	6315475	6315568	33.38	100	AK002850:DAB2:DOC-2:NM_001008702[5U] Dab2:[5U]	
chr15	7993901	7993975	33.38	100	AK159714:AK160933:Wdr70[I13]	
chr15	12334297	12334383	30.91	100		
chr15	12886534	12886612	37.09	100		AK003651:AK144147:AK148640:BC040801:BC050057:BC055696:BC057687:BC060265:DROSHA:Etohi2:HSA242976:NM_026799:RN3:RNASE3L:RNASEN[10DS] Rnasen:[10DS]
chr5	80512702	80512767	33.38	100		
chr15	20626886	20626972	66.05	100		
chr5	81482901	81482960	31.79	100		
chr5	86338928	86338985	41.73	100		
chr15	33033848	33033955	30.35	100	AK154361:NM_018755:Pgcp[5U] Pgcp:[5U]	
chr15	33232698	33232832	21.68	100	AK154361:NM_018755:Pgcp[I3] Pgcp:[I3]	
chr15	38531128	38531206	41.73	100		
chr15	40522286	40522319	44.51	100	BC059241:FOG2:NM_011766:ZFPM2:hFOG-2[I1] Zfpm2:[I1]	
chr15	54860569	54860606	39.04	100		AK051126:Taf2[10US]
chr5	112744587	112744675	16.36	100	AB206790[I15] AF220355:AI843918:AK083229:AK122401:BC056471:BC065129:BC094376:BC099839:Sez6l[5U] BC065129:Sez6l[I16]	
chr15	56539100	56539179	26.92	100		
chr15	62914527	62914606	32.1	100		
chr15	62977734	62977780	33.72	100		
chr15	63377815	63377867	34.24	100		

chr15	74913895	74914047	6.95	100		
chr5	126665303	126665338	55.64	100		
chr15	74914118	74914307	7.76	100		
chr15	76454787	76454873	39.74	100	Nfkbil2:[I1] Nfkbil2:[I1]	Vps28:[10DS] AK003572:NM_025842: VPS28[10DS]
chr5	137696585	137696644	33.38	100	Zan:[I77]	
chr5	140991474	140991508	39.74	100	6530401C20Rik:[5U]	
chr5	151882737	151882773	55.64	100		
chr15	76700086	76700160	55.64	100		Zfp251:[10DS] Zfp7:[10US]
chr15	85524022	85524110	66.05	100		
chr6	11415778	11415808	37.09	100		
chr6	16957033	16957064	55.64	100		
chr15	93738101	93738160	27.82	100		
chr6	29698308	29698395	10.12	100	Smo:[I1]	
chr6	29698786	29699023	13.91	100	Smo:[I1]	
chr6	30829644	30829726	49.09	100	Tsga13:[I1]	2-COP:COPG2:NM_017478[10DS] AK163668:Copg2:NM_017478[10DS] Copg2:[10DS] AK079599:Copg2:NM_017478[10DS]
chr6	30845494	30845556	41.73	100	Tsga13:[5U]	
chr6	32798051	32798085	44.51	100	AK006643:CHCHD3:FLJ20420:NM_025336[I1] Chchd3:[I3]	
chr16	15511967	15512055	66.05	100		Ube2v2:[10DS]
chr16	42313348	42313381	30.35	100		
chr16	50185454	50185544	44.03	100	AK029747:BBX:NM_027444[I10E11] BC066821:Bbx:NM_027444[I11E12] LOC432823:[3U] Bbx:[I11E12]	

chr16	82994723	82994790	41.73	100		
chr16	84034655	84034716	41.73	100		
chr16	94682889	94682976	27.82	100		
chr17	3035874	3035929	25.68	100	D030013I16Rik:[E6]	
chr17	30262175	30262265	27.82	100	AK087881:Btbd9:NM_172618[5U] Btbd9:[5U]	
chr17	30643749	30643785	39.74	100		AK138161[10US]
chr17	34891819	34891909	66.05	100		
chr17	35528737	35528823	27.82	100	BC052059:Cat53:FB19:NM_175934:PNUTS:PPP1R10[5U] Ppp1r10:[5U]	AK002554:AK076033:AK076044:C6orf14:HSPC183:MRPS18-2:MRPS18B:NM_025878:PTD017[10DS] Mrps18b:[10DS]
chr17	39451384	39451471	13.91	100		
chr6	94791533	94791566	55.64	100		
chr6	104655436	104655525	44.03	100	Cntn6:[I4]	
chr17	39456725	39456846	17.66	100		
chr6	116898222	116898254	55.64	100		
chr6	130989475	130989506	44.51	100		
chr6	133937727	133937816	66.05	100		
chr17	43467761	43467792	44.51	100	AB061524:DSCR1L1:NM_030598:ZAKI-4[I1] Dscr1l1:[I1] Dscr1l1:[I2]	
chr17	45014137	45014193	41.73	100		Gm323:[10DS] Nfkbie:[10US] AK088585:IKBE:NFKBIE:NM_008690[10US]
chr18	33472548	33472634	37.09	100		
chr18	48487253	48487292	37.09	100		
chr6	147801308	147801393	27.82	100		
chr18	52145201	52145265	31.79	100		
chr18	76001865	76001947	55.64	100	Zbtb7c:[5U]	
chr7	18844357	18844391	55.64	100		Apoc1:[10US] Apoc4:[10DS]

						Apoc2:[10DS]
chr7	20331813	20331853	44.51	100	AF324872:NM_030736:V1rd14[5U] BC020078:LOC432823:NM_001013789[3U]	
chr19	3528343	3528376	55.64	100	AK018652:C11orf23:D19Ertd703e:FLJ11058:NM_029456:SAP190:SAPLa:SAPS3[5U] AK088526:D19Ertd703e:NM_029456:Saps3[5U] Saps3:[5U]	
chr19	17180433	17180517	22.26	100	A230083H22Rik:AK054190:AK170001:BC095978[5U]	A230083H22Rik[10US]
chr19	32013183	32013271	44.03	100	AY566862:Acf:Asp[I11] AY566863[I11]	
chr19	32257626	32257660	44.51	100	AK076554:MGC17342:MOB:NM_144792:TMEM23[5U] Tmem23:[5U]	
chr7	55300791	55300866	41.73	100		
chr7	57011059	57011092	55.64	100	Gabrg3:[I7]	
chr19	38402378	38402468	44.03	100		
chr19	49160784	49160845	41.73	100		
chr19	57064253	57064331	55.64	100		AK220430:AU041783:Kiaa1914:NM_146102[10DS] AU041783:[10DS] AU041783:[10DS]
chr19	58166529	58166598	15.58	100	Atrnl1:[I28]	
chr19	61254399	61254465	27.82	100		
chr2	4002361	4002446	42.8	100		AK140403:AK162393[10US]
chr2	22591245	22591336	30.91	100		
chr2	25140331	25140418	44.03	100	AK158175:GRIN1:NMDAR1:NM_008169[I19] BC039157:Grin1:NM_008169[I18] Grin1:[I19]	
chr2	31236262	31236347	33.38	100		

chr2	44129349	44129385	37.09	100	Arhgap15:BC034881:NM_001025377[I12] Arhgap15:BC024887:BC034881[I12]	
chr2	49475485	49475569	59.61	100	Kif5c:[I1]	
chr2	75494588	75494664	33.38	100	Nfe2l2:[I4] NM_010902:Nfe2l2:Nrf-2:Nrf2[5U]	
chr2	79611167	79611251	41.73	100	AK051449:Inhibitor-1-like:NM_172420:PPP1R1C[3U] AK157871:NM_172420:Ppp1r1c[I4]	Ppp1r1c:[10DS]
chr2	89768649	89768730	61.82	100		
chr2	90985756	90985826	27.82	100	AF085745:AJ132601:AK143904:AK159250:AY195870:AY195871:BC012646:LXR-a:Lxra:NR1H3:RLD-1[I2E3]	BC003255:Madd:NM_145527[10DS] Madd:[10DS] Madd:[10DS] Madd:[10DS] Madd:[10DS] Madd:[10DS] AK036347:DENN:KIAA0358:MADD:NM_145527:RAB3GEP[10DS] AK122257:Madd:NM_145527[10DS] BC063386:Madd:NM_145527[10DS]
chr7	128127326	128127359	37.09	100		
chr2	91521485	91521572	44.03	100	AK045343:AK080671:AK147045:D230010M03Rik:NM_178724[E3]	AK041747:D230010M03Rik:NM_178724[10DS] D230010M03Rik:[10DS] AK148887:D030051N19Rik:NM_172669[10US] AK037516:D030051N19Rik:NM_172669[10US] AK083596:D030051N19Rik:NM_172669[10US] AK169280:BC032293:D030051N19Rik:NM_172669[10US] D030051N19Rik:[10US]
chr8	3886940	3886970	55.64	100		Cd209d:[10DS]
chr2	92565441	92565531	27.82	100		

chr2	116342460	116342495	34.77	100		
chr2	131048700	131048731	34.77	100		Rnf24:[10DS]
chr2	166290339	166290421	41.73	100	AK090301:BC057617:BC067047[5U]	
chr2	169549578	169549653	55.64	100	AK220569:Kiaa4248:NM_080455:Sdccag33l:Tsh2:Zfp218:Znf218[I1] Tshz2:[I1]	
chr3	17083745	17083796	44.51	100		
chr3	27809908	27809995	66.05	100	1600019O04Rik:DKFZp762K137:FAD104:FLJ23399:FNDC3B:NM_173182:PRO4979:YVTM2421[I6] 1600019O04Rik:AB098596:AK147346:AK220297:AY234860:DQ192037:Fndc3b:NM_173182[5U] Fndc3b:[I23]	
chr3	60460106	60460190	37.09	100		
chr3	84875461	84875496	39.74	100		
chr3	102392596	102392645	55.64	100		
chr3	123029762	123029851	37.09	100		Myoz2:[10DS]
chr3	129956020	129956053	37.09	100	9030408N13Rik:[5U] 9030408N13Rik:[I7]	
chr3	156552608	156552694	66.05	100	Negr1:[I1]	
chr4	5841011	5841098	27.82	100		
chr4	11130679	11130765	37.09	100	Ccne2:[3U] BC053727:Ccne2[3U] Ints8:[3U]	2810013E07Rik:AK049513:AK140829:AK169552:BC050192:BC057618:NM_178112[10US]
chr4	26418196	26418230	37.09	100	Manea:[3U]	
chr4	33525223	33525305	37.09	100		Acy1l2:[10DS]
chr4	53811987	53812071	55.64	100		Tal2:[10DS]
chr4	124640668	124640756	38.37	100		
chr4	144706953	144707001	30.91	100		
chr4	144846840	144846904	33.38	100		

chr4	145390909	145390964	27.82	100		
chr5	4022489	4022549	41.73	100	Akap9:[I21]	
chr5	9241116	9241150	55.64	100		
chr5	14984104	14984190	33.38	100	AK016672:Speer8-ps1[3U]	
chr5	16044416	16044494	27.82	100		
chr5	45237966	45238000	34.77	100		
chr5	71634766	71634845	55.64	100		
chr5	101138794	101138841	55.64	100	A230097K15Rik:[3U]	
chr5	115220591	115220624	55.64	100	Tcf1:[I8]	
chr5	124591653	124591690	44.51	100	2810006K23Rik:BC054073:NM_028310[5U] 2810006K23Rik:[5U]	
chr5	133995993	133996079	55.64	100		
chr6	5326884	5326970	44.03	100		Asb4:[10US]
chr6	48588351	48588438	44.03	100	Gimap8:[E5]	
chr6	50710522	50710611	66.05	100		
chr6	54135156	54135243	66.05	100	AK131641:Chn2:NM_023543[I3]	
chr6	74596285	74596355	22.26	100		
chr6	78604368	78604401	37.09	100		
chr8	41312597	41312635	44.51	100		
chr8	44131276	44131314	44.51	100		
chr6	87020740	87020818	37.09	100	AF334736:GFA:GFAT:GFAT1:GFPT:GFPT1:NM_013528[I4] Gfpt1:[I4]	
chr6	91754620	91754677	33.38	100		
chr6	112313663	112313749	44.03	100		
chr8	62571076	62571111	44.51	100		
chr6	134118936	134119026	37.09	100	AK035231:AK078773:AK154569:AK155150:AK157265:ETV6:NM_007961:TEL:Tel1:Y07915[I3] Etv6:[I2]	

chr6	137360919	137360953	44.51	100	AF135166:BC051976:BC063258:BC079649:GLEPP1:NM_011216:PTP-U2:PTPRO:PTPU2:PTPphi:U37465:U37466[I10] Ptpro:[5U] Ptpro:[I10]	
chr8	76515167	76515291	18.55	100		
chr6	144401882	144401927	25.68	100		
chr7	29628699	29628786	44.03	100		
chr7	65189573	65189660	66.05	100	Tjp1:[I5]	
chr8	96189851	96189912	33.38	100		Ces1:[10US]
chr7	75674297	75674327	55.64	100		
chr7	82647957	82648003	30.91	100	Eftud1:[I18]	
chr7	82648138	82648204	20.86	100	Eftud1:[I18]	
chr7	112199424	112199487	33.38	100	4921517J23Rik[I5]	
chr7	113712958	113713043	37.09	100	AK134774:KIAA0762:NM_145584:SPON1:f-spondin[I5] Spon1:[I5]	
chr7	121465419	121465449	55.64	100		
chr8	5404335	5404418	37.09	100		
chr8	7766797	7766831	37.09	100		
chr8	14331972	14332041	41.73	100	Dlgap2:[I3]	
chr8	122992099	122992171	27.82	100		Zdhhc7:[10DS] 6430548M08Rik:NM_172286[10US] 6430548M08Rik:AK172108:NM_172286[10US]
chr8	19759741	19759790	39.74	100		
chr8	19998305	19998348	48.38	100		
chr8	20088901	20088974	55.64	100		
chr8	129774999	129775089	55.64	100		
chr8	20295794	20295881	66.05	100	LOC436177:[3U]	
chr9	8484035	8484072	37.09	100		
chr8	20318396	20318456	33.38	100	LOC436177:[3U]	5330429B09Rik:A430108E01Rik:AK033345:AK083828:AK088897:NM_

						001033637[10DS]
chr9	13479629	13479666	39.74	100		
chr9	17190424	17190461	34.77	100		
chr9	21173476	21173562	64.2	100		AK005012:AK172231:DNM2:DYNII:NM_007871[10US] Dnm2:[10US] Dnm2:Dyn2:L31398[10US] AK011586:NM_021888:QTRT1:TGT:Tgut[10DS]
chr8	20343782	20343829	27.82	100	LOC436177:[3U]	
chr8	20348903	20348951	25.29	100	LOC436177:[3U]	
chr8	20393815	20393882	31.79	100	LOC436177:[3U]	
chr8	27283135	27283218	9.27	100	AK087934:AK146938:ASH2L:ASH2L1:ASH2L2:NM_011791[I1E2I2]	Star:[10DS] BC060970:NM_011485:STAR:STARD1[10DS]
chr8	27288686	27288861	5.88	100	AK087934:AK146938:ASH2L:ASH2L1:ASH2L2:NM_011791[E6I6]	Star:[10DS] BC060970:NM_011485:STAR:STARD1[10DS]
chr8	27305563	27305628	8.65	100	AK087934:AK146938:ASH2L:ASH2L1:ASH2L2:NM_011791[E15I15]	
chr8	39016706	39016741	55.64	100	AK048960:NM_145841:SGCZ[I3] AK048960:AK136779:BC104049:NM_145841:Sgcz[I3]	
chr9	73379929	73379962	55.64	100		
chr8	58708966	58709002	55.64	100		
chr8	65394993	65395027	61.82	100		
chr9	112180976	112181015	37.09	100		
chr8	89254453	89254539	33.38	100		
chr8	98462049	98462131	55.64	100		
chr8	108781741	108781806	27.82	100	AK146527:BC022641:NM_181594[I28E29] BC022641:[I28E29]	AK080711:G630049C14Rik:NM_175024[10US] G630049C14Rik:[10US] Pskh1:[10US]
chr9	119711835	119711870	44.51	100		

chr8	126626279	126626366	37.09	100		
chrX	4498946	4498980	44.51	100		
chrX	7815725	7815759	37.09	100	Ssxb9:[3U]	
chrX	7816163	7816193	37.09	100	Ssxb9:[3U]	
chr8	128747691	128747766	49.09	100	AK030215:AK087907:E330039K12Rik:NM_172917[5U] E330039K12Rik:[I7]	
chr9	8556133	8556166	37.09	100	AK133864:NM_013838:TRP6:TRPC6[I1] BC067391:BC068310:NM_013838:Trpc6[I1] Trpc6:[I1]	
chrX	22736800	22736844	37.09	100		
chrX	30566626	30566704	49.09	100		
chr9	45829898	45829932	55.64	100	AK129257:BC033915:BC080688:BC082313:NM_027498[5U] BC033915:[I1]	
chr9	49734599	49734687	37.09	100		
chrX	54689049	54689089	55.64	100		
chrX	55335852	55335938	37.09	100		
chr9	57992031	57992062	55.64	100		Islr2:[10US]
chr9	61623430	61623460	55.64	100		
chr9	116561089	116561179	44.03	100	AK030609:NM_178660:RBMS3[I7] AK033005:NM_178660:Rbms3[I7] AK041098:NM_178660:Rbms3[I6] AK046197:NM_178660:Rbms3[I7] AK051776:NM_178660:Rbms3[I3] AK052196:NM_178660:Rbms3[I8] Rbms3:[I7]	
chr9	118345609	118345699	34.77	100		Golga4:[10US]
chrX	93220768	93220804	55.64	100		
chrX	93717771	93717801	44.51	100		

chr9	123721814	123721849	27.82	100		
chrX	19826070	19826155	59.61	100	Ube1x:[I4E5]	
chrX	104416851	104416884	44.51	100		
chrX	104699193	104699231	39.74	100		
chrX	106353235	106353268	37.09	100		
chrX	112577751	112577785	55.64	100	Cpxcr1:[5U]	
chrX	117630496	117630533	55.64	100		
chrX	37040804	37040884	37.09	100		
chrX	66848620	66848658	55.64	100		
chrX	141938369	141938403	30.91	100		
chrX	127018848	127018934	66.05	100		
chrX	139068241	139068280	24.34	100	Capn6:[5U]	
chrX	146852020	146852088	33.38	100		AK134137:KIAA1111:NM_177201:PHF8:ZNF422[10US]
chrX	157566991	157567078	42.8	100		
chrX	150920322	150920370	55.64	100		AK135103[10DS]
chrX	165333423	165333526	12.94	100	AF026565:FXY:MID1:NM_010797:OS:RNF59:TRIM18[3U] AK160120:Mid1:NM_010797[3U] BC059027:Mid1:NM_010797[3U] Mid1:[3U]	AK136160:Mid1:NM_010797[10US]
chrX	165336031	165336066	19.35	100	AF026565:FXY:MID1:NM_010797:OS:RNF59:TRIM18[3U] Mid1:[3U]	AK160120:Mid1:NM_010797[10DS] BC059027:Mid1:NM_010797[10DS] AK136160:Mid1:NM_010797[10DS]
chrX	165410218	165410254	34.77	100		
chrY	2032540	2032571	37.09	100		

Appendix III

Cell Cycle 9:15, 2940-2945; August 1, 2010; © 2010 Landes Bioscience

Parole terms for a killer

Directing caspase3/CAD induced DNA strand breaks to coordinate changes in gene expression

Brian D. Larsen[1,2] and Lynn A. Megeney[1,2,*]

[1]Ottawa Hospital Research Institute; Sprott Centre for Stem Cell Research; Regenerative Medicine Program; Ottawa Hospital; Ottawa, ON Canada;

[2]Faculty of Medicine; Department of Cellular and Molecular Medicine; Centre for Neuromuscular Disease; University of Ottawa; Ottawa, ON Canada

In a series of discoveries over the preceding decade, a number of laboratories have unequivocally established that apoptotic proteins and pathways are well conserved cell fate determinants, which act independent of a cell death response. Within this context, the role for apoptotic proteins in the induction of cell differentiation has been widely documented. Despite these discoveries, little information has been forthcoming regarding a conserved mechanism by which apoptotic proteins achieve this non-death outcome. In the following discussion, we will explore the premise that the penultimate step in apoptosis, genome wide DNA damage/strand breaks act as a conserved genomic reprogramming event necessary for cell differentiation.[5] Moreover, we hypothesis that directed DNA damage, as mediated by known apoptotic proteins, may participate in numerous forms of regulated gene expression.

Key words: caspase-activated DNase, inhibitor of caspase-activated DNase, non-apoptotic caspase activity, genome reprogramming, epigenetics, gene regulation

Submitted: 04/30/10

Accepted: 05/11/10

Previously published online: www.landesbioscience.com/journals/cc/article/12335

DOI: 10.4161/cc.9.15.12335

*Correspondence to: Lynn A. Megeney; Email: lmegeney@ohri.ca

Introduction

DNA damage is largely assumed to be a detrimental event and is frequently associated with impaired cell survival. In addition, DNA damage is a common molecular trigger for the development of oncogenic mutations. For example DNA damage/strand breaks precede a recombination of two distinct genetic loci to produce a hybrid gene with growth altering properties. Given the dire outcomes associated with DNA damage, the cell has evolved a number of DNA repair pathways which recognize and redact genome damage that occurs from a variety of external insults.

Despite the propensity to consider DNA damage as a solely negative phenomenon, a growing body of evidence suggests that focal DNA damage is in fact required for normal cell function. Specifically, controlled or non-random DNA damage appears to be a conserved mechanism which propagates alterations in gene expression. The best studied example in this regard is the regulated DNA breakage that propels adaptive immunity. Here, the Rag1/2 nuclease complex induces controlled DNA breaks at specific loci that are paired with variable recombination events to create the unique genes that underwrite the diversity of antibody production.[1] Another well documented example of tolerable or beneficial DNA breakage occurs during the exchange of genetic material between homologous chromosomes in meiotic crossover. In this instance, DNA breaks are induced by the topoisomerase II-like protein Spo11, which propels an exchange between large intergenic regions.[2]

Additional studies suggest that directed DNA strand breaks may promote gene expression independent of follow-on recombination events. For example, work from the Rosenfeld Laboratory has shown that glucocorticoid induced gene expression is dependent on a topoisomerase IIbeta mediated DNA strand break. The strand breaks are directed to the promoter region of the glucocorticoid responsive gene, an alteration that prompts histone modifications which are favourable to initiating

gene transcription.[3,4] Undoubtedly, there is an inherent risk associated with such DNA damage yet these observations establish that limited DNA strand breaks can yield a notable beneficial outcome for a cell.[4]

Recently, work from our laboratory has transformed the paradigm described above and shown that genome wide DNA strand breaks act as a key regulatory step to promote muscle cell differentiation.[5] The DNA strand breaks are formed by a transient activation of caspase activated DNase or CAD, an observation that suggests apoptotic proteins and pathways act as conserved genomic reprogramming factors.

Caspase 3/CAD Signaling: The Executioners

The caspase family of cysteine proteases signal through proteolytic cleavage, altering the activity of an extensive repertoire of substrates. Caspase 3 is an integration point for a variety of canonical cell death pathways, acting to target cytosolic and nuclear factors which in turn accelerate cellular demise.[6] One key feature of this potent signal is the ability to activate the primary nuclease involved in disseminating extensive DNA strand breaks, termed caspase activated DNase or CAD.[7] DNA damage in the form of genomic fragmentation is a well characterized component of cell death or apoptosis. Although early stage DNA fragmentation is not an absolute requirement for all early stage forms of apoptotic cell death, these nuclear events are assumed to improve the efficiency of the process.[8] Indeed, the release of nucleotides and presentation of nucleosomes at the cell surface promote the removal of degenerate cells through attraction of phagocytic cells.[9,10]

The principle regulation of CAD comes by formation of a restrictive complex with its inhibitor, ICAD, an interaction that physically restrains inactive CAD monomers from dimerizing into the active form. Two isoforms of ICAD are observed, ICAD-long (L) and ICAD-short (S), with the ICAD-L isoform having the most defined role in regulating CAD. Association by N-terminal CIDE domains begins when the CAD protein is synthesized, here ICAD-L acts as a specific chaperone along with Hsp70 and Hsp40 to properly fold CAD.[11,12] Following translation the ICAD-L/CAD complex localizes to the nucleus, where it remains highly mobile; however, stable interactions with DNA have been noted suggesting that CAD can be activated not only in the free nuclear space but also in a DNA associated complex.[13-15]

To activate CAD, caspase 3 targets ICAD for proteolytic cleavage at 2 aspartic acids, D117 and D224. This caspase directed cleavage destabilizes the ICAD/CAD interaction and allows CAD dimerization. The CAD dimer aptly resembles an open scissor like structure, with the catalytic site of the dimer located in a crevice structure large enough to accommodate double stranded DNA.[16] The substrate DNA fully enters this structure and a double stranded DNA break is catalyzed. This protein conformation is believed to exclude nucleosome associated DNA, localizing the DNA break between nucleosomes. Under apoptotic conditions the extent of CAD activation is such that periodic DNA laddering is observed.[8]

Caspase 3/CAD Mediated DNA Strand Breaks: A Vital Genome Reprogramming Event

In addition to a well characterized role in apoptosis, caspase 3 activation is also a highly conserved step in the induction of cell differentiation. Transient caspase 3 activity has been shown to be essential for differentiation of most somatic cell types studied and for the maturation of both ES and germs cells.[17] The extent of caspase 3 activation appears to control the balance between differentiation and apoptosis, with lower versus higher levels of activity controlling each cell fate respectively.[18] Defining the caspase 3 substrates that convey the differentiation signal has been of considerable interest, yet limited information has been forthcoming. Studies have suggested that caspase cleavage activation of select kinases propels the differentiation program whereas other studies have shown that cleavage inactivation of transcription factors establishes a permissive environment for the process.[19-23] Although these specific caspase substrate interactions appear to be critical, these same catalytic events do not explain the ability of caspase 3 to induce the global genome reprogramming that typifies cell differentiation.

Recently, we have reported that caspase 3 activates CAD in healthy muscle cells and that this step is essential for completion of myogenic differentiation.[5] During early stages of differentiation, myoblast nuclei are subject to CAD dependent DNA strand breaks and inhibition of CAD activity (by limiting caspase 3 activation, repressing CAD expression or overexpressing a non cleavable version of the CAD inhibitor ICAD) leads to a near complete blockade in differentiation with a concurrent loss in the formation of strand breaks. The CAD mediated strand breaks are in part permissive, as the induction of the critical regulatory factor p21 is dependent on a caspase 3/CAD directed strand break within the p21 promoter.

Nevertheless, like many interesting discoveries, our recent work opens the door to many more questions than was answered in the initial study. Paramount among the unresolved mechanisms, once CAD is activated how is the DNase restrained sufficiently to induce strand breaks yet not destroy the genome? We hypothesize that two independent mechanisms may contribute to the restrained activation of CAD. First, we anticipate that it is the DNA associated pool of CAD that is activated during differentiation. CAD has been shown to be complexed with ICAD in a nuclear position, a localization that would permit ready activation once caspase 3 was activated.[13,14] In contrast, the excessive activation of caspase 3 during apoptosis would allow for targeting of both the DNA bound and unbound CAD/ICAD complexes, the later being free to inflict indiscriminate breaks throughout the genome. Consistent with this hypothesis we have noted that the p21 promoter is subject to consistently localized strand breaks during differentiation, while apoptotic muscle cells display widespread formation of strand breaks that are variable from experiment to experiment (see Fig. 4 in ref. 5). A confirmation of our hypothesis will require a definitive visualization of distinct ICAD/CAD pools and/or a mapping of the CAD targeted genome that is specific to each cell fate

outcome. Second, we hypothesize that caspase targeting of ICAD during differentiation is directed at the D117 cleavage site, whereas the greatly elevated caspase activity associated with apoptosis would result in cleavage at both D117 and D224. In this model of CAD activation, caspase cleavage at the D117 site would lead to a partial release of CAD while caspase targeting of both sites would remove any ICAD mediated inhibition with a higher resulting level of CAD activity. We have noted an ICAD cleavage event during differentiation that is consistent with a D117 only deletion, and a mutation in this site that renders ICAD caspase resistant leads to a reduction in myoblast differentiation (see Fig. 2 in ref. 5).

Our observations demonstrate that caspase 3 activation of CAD (through ICAD cleavage and release of active CAD) is the primary step in promoting DNA damage/strand breaks during myoblast differentiation. Nevertheless, caspase 3 is known to target a wide variety of substrates during apoptosis and cell differentiation.[18] Therefore, we hypothesize that caspase 3 targets multiple proteins to ensure efficient activity of the CAD nuclease. Apoptotic signalling pathways modify chromatin ultra-structure prior to DNA damage and nuclear dissolution. In this regard, post-translational modifications of histones assume prominent regulatory roles. As such it is reasonable to assume that similar events pre-empt or assist CAD to promote DNA damage during cell differentiation. Specifically, we assert that the ste20-like kinase MST1 participates in the formation of caspase mediated nicks/strand breaks in differentiating myoblasts by phosphorylating and modifying the activity of chromatin regulatory proteins. This supposition is based on the following observations. First, MST1 was initially characterized as a pro-apoptotic, caspase 3 sensitive kinase and more recently has been demonstrated to directly phosphorylate histone H2B (at serine 14) leading to chromatin compaction and apoptosis.[24-26] Secondly, our laboratory was the first to describe a non-apoptotic function for MST1, i.e., MST1 as a pro-differentiation kinase.[22] Subsequent to our observations, numerous groups reported a role for MST1 in limiting cell cycle progression in both mammalian and Drosophila systems (reviewed in Zeng and Hong 2008).[27] Our experiment was noteworthy in that an activated MST1 kinase (caspase 3 cleavage activated kinase domain) provided a partial rescue of differentiation in caspase 3 null myoblasts, yet prolonged expression of MST1 led to formation of picnotic nuclei and apoptosis.[22] Together, these observations suggest that MST1 may stimulate differentiation by modulating or by activating chromatin remodelling protein(s) to enhance CAD activity.

Caspase 3 can also target DNA binding proteins to modulate gene expression and several of these targets have the potential to modify CAD access to sensitive genomic elements. The matrix attachment protein, Special AT-rich binding protein 1 (SATB1), is a global organizer of chromatin that facilitates the interaction of DNA elements termed matrix attachment regions (MARs) to the nuclear matrix. SATB1 is a demonstrated cleavage target of caspase 3/6 under both apoptotic and non-apoptotic conditions.[28-30] Cleavage of SATB1 releases MARs from the nuclear matrix, leading to chromatin disruption.[31] A specific role for caspase cleavage of SATB1 during differentiation has not been demonstrated, yet it is reasonable to suggest that removal of SATB1 may in some instances expose genomic elements that are targeted by CAD to coordinate gene expression.

CAD activity during cell differentiation may also be moderated by additional chromatin modifications independent of caspase function. CAD/ICAD association to DNA can be potentiated by association with the C-terminal of histone H1, and this interaction can further stimulate the nuclease activity of CAD.[32] Specifically, CAD has been reported to dynamically associate with the histone H1 variants, namely H1.5 and H1.0 in both healthy and apoptotic cells.[33] Moreover, H1 variants can affect specific gene expression by cooperating with additional regulatory factors.[34] This preferential association to histone variants could partly influence where in the genome CAD inflicts DNA strand breaks. Of interest, coordination between the H1.5 variant and the transcription factor Msx1 has been demonstrated to occur at the promoters of repressed genes in proliferating myoblasts.[35] For example, expression of the cell cycle inhibitor p21 (which we have identified as a bona fide CAD target) is impeded by Msx1 prior to myoblast differentiation.[36] Based on our observations a reasonable conjecture is that CAD may be directed to relieve this repressed state and engage p21 expression by interacting with histone H1.5 and thereby displacing Msx1. How operative this mechanism is and how extensive across the genome it may be will require further investigation.

Curbing the Caspase3/CAD Signal

The transient activity of caspase and CAD in differentiating cells suggests the deployment of a mechanism(s) to moderate or terminate this signal prior to inducing extensive DNA damage. Several studies have examined the signal cascades that activate and modulate caspase 3 during non-death responses, yet a definitive control mechanism has not been elucidated.[37-39] Such inactivation could indirectly end CAD activity by discontinuing proteolysis of ICAD. Intact ICAD (both long and short isoforms) can disassemble the CAD dimer, moreover our observation that ICAD-L is only partial cleaved (with a large pool of intact ICAD-L remaining) suggests that this mechanism maybe operative to prevent extensive DNA fragmentation.[16]

Intriguingly, alternate methods that block the nuclease activity of CAD have been noted. Admittedly, these cellular responses have been implicated primarily in response to caspase activity in apoptotic settings or to restrain CAD activity when this nuclease is activated as a by product of another molecular mechanism. Nevertheless, it is reasonable to suggest that these same factors moderate CAD activity during cell differentiation. Polyribosylation of CAD by PARP-1 can further restrict CAD nuclease activity, and a transient increase in PARP-1 activity is reported in skeletal muscle differentiation concurrent with the observed DNA strand break formation reported in Larsen et al.[5,40,41] We have not examined a role for PARP-1 in CAD mediated DNA strand breaks and repair, yet PARP-1 has been demonstrated to play a role in regulating

gene expression that results from controlled DNA strand breaks in response to glucocorticoid stimulation. Nerve growth factor (NGF) may also provide a signal conduit to moderate CAD activity in both apoptotic and cell differentiation scenarios. For example, NGF protects neuronal cells from apoptosis through a number of mechanisms, two of these mechanisms involve inhibition of CAD. NGF stimulates nucleophosmin and Ebp1 to directly interact with CAD, diminishing its nuclease activity while not preventing caspase cleavage of ICAD itself.[42,43] Given that caspase 3 has been shown to mediate neuronal differentiation, a valid interpretation of the above experiment may be that NGF restrains CAD activity to act as a moderating influence on gene expression during neuron differentiation (as in skeletal muscle cells) while limiting a global escalation of CAD activity.[21]

CAD Induced DNA Strand Breaks as a General Component of Gene Expression

An intriguing question that arises from the study of Larsen et al. is whether CAD induced DNA strand breaks are simply a differentiation specific regulatory event or is CAD directed DNA damage a common mechanism for altering gene expression?

As noted above, the role of DNA strand breaks regulating changes in gene expression and genomic reprogramming has been characterized in a number of processes. However, in many instances the induction of the DNA breaks have been linked to proteins with weak or questionable nuclease activity. As such it is reasonable to assume that localized CAD activation may coordinate with the other DNA damage related proteins to promote break induced alterations in gene regulation. Glucocorticoid stimulated gene expression involves topoisomerase II dependent DNA strand breaks. These breaks are directed by the estrogen receptor (ER) and stimulate target gene expression through PARP-1 mediated exchange of histone H1 for HMGB1/2.[3,44] A cooperation between CAD and topoisomerase II in stimulating the formation of glucocorticoid stimulated breaks was not examined in this study, yet such a coordination could effectively direct and stimulate the induction of DNA strand breaks. Indeed, an interplay between CAD and topoisomerase II has been reported in the initial induction of DNA strand breaks during apoptosis, and the proteins co-localize in both healthy and apoptotic nuclei.[45] These observations combined with weak inherent nuclease activity of topoisomerase II suggest that CAD may provide the operative strand break capacity in such forms of gene regulation.

DNA demethylation has been postulated to involve the formation of DNA strand breaks as a means to excise the methylated base followed by a DNA repair step. In this regard several proteins have been implicated that can also contribute to the formation of regulated DNA strand breaks. The cytidine deaminase AID has been reported to act as a demethylation agent in primordial germ cells and in the nuclear reprogramming of somatic cells via induced pluripotency (iPS).[46,47] AID has been well studied for its role in antibody diversification where it is thought to stimulate a directed DNA strand break through deamination leading to activation of the base excision repair pathway.[48] AID has been shown to associate with methylated promoters of pluripotency genes in fibroblasts but not unmethylated promoters in undifferentiatied ES cells, and knockdown of AID gene expression impeded the demethylation of these promoters in heterokaryon fusions.[47] Interestingly global DNA demethylation is observed in skeletal muscle differentiation concurrent to the period of CAD induced DNA strand breaks.[49] Although we observed unaltered DNA methylation at the p21 promoter, these breaks may signal at other loci for the removal of the repressive mark, a step that may be dependent on a CAD like excision event. Alternatively, given the role of caspase/CAD in driving cell fate outcomes that are directly antagonistic to iPS (i.e., cell differentiation) achieving effective reprogramming may require a direct inhibition or limitation of caspase/CAD activity. As caspase mediated signal events are broadly conserved cell fate determinants, exploring the impact of a caspase/CAD signal nexus during nuclear reprogramming should be a priority.

Determining the genomic targets of caspase 3 activated CAD will assist in developing appreciation for the role these DNA strand breaks play in regulating gene expression (Fig. 1). Mapping these sites using rapidly developing next generation sequencing technology and determining protein interactions that direct CAD will begin to establish this understanding. Further examination of epigenetic changes that occur at these sites will provide insight into how the strand break is utilized to regulate gene expression not only in differentiation but potentially in other genomic reprogramming events.

Acknowledgements

We thank the members of the Megeney Lab for their ongoing contributions to this work. B.D.L. is supported by a Computational Regulomics Training Program Graduate Student Fellowship from the Ontario Ministry of Research and Innovation Ontario Research Fund. L.A.M. is the Mach Gaensslen Chair in Cardiac Research. This work was supported by grants from the Canadian Institutes of Health Research and the Muscular Dystrophy Association (L.A.M.).

References

1. Jung D, Alt FW. Unraveling V(D)J recombination; insights into gene regulation. Cell 2004; 116:299-311.
2. Li W, Ma H. Double-stranded DNA breaks and gene functions in recombination and meiosis. Cell Res 2006; 16:402-12.
3. Ju BG, Lunyak VV, Perissi V, Garcia-Bassets I, Rose DW, Glass CK, et al. A topoisomerase IIbeta-mediated dsDNA break required for regulated transcription. Science 2006; 312:1798-802.
4. Lin C, Yang L, Tanasa B, Hutt K, Ju BG, Ohgi K, et al. Nuclear receptor-induced chromosomal proximity and DNA breaks underlie specific translocations in cancer. Cell 2009; 139:1069-83.
5. Larsen BD, Rampalli S, Burns LE, Brunette S, Dilworth FJ, Megeney LA. Caspase 3/caspase-activated DNase promote cell differentiation by inducing DNA strand breaks. Proc Natl Acad Sci USA 2010; 107:4230-5.
6. Fischer U, Janicke RU, Schulze-Osthoff K. Many cuts to ruin: a comprehensive update of caspase substrates. Cell Death Differ 2003; 10:76-100.
7. Widlak P, Garrard WT. Roles of the major apoptotic nuclease-DNA fragmentation factor-in biology and disease. Cell Mol Life Sci 2009; 66:263-74.
8. Samejima K, Earnshaw WC. Trashing the genome: the role of nucleases during apoptosis. Nat Rev Mol Cell Biol 2005; 6:677-88.
9. Elliott MR, Chekeni FB, Trampont PC, Lazarowski ER, Kadl A, Walk SF, et al. Nucleotides released by apoptotic cells act as a find-me signal to promote phagocytic clearance. Nature 2009; 461:282-6.
10. Radic M, Marion T, Monestier M. Nucleosomes are exposed at the cell surface in apoptosis. J Immunol 2004; 172:6692-700.

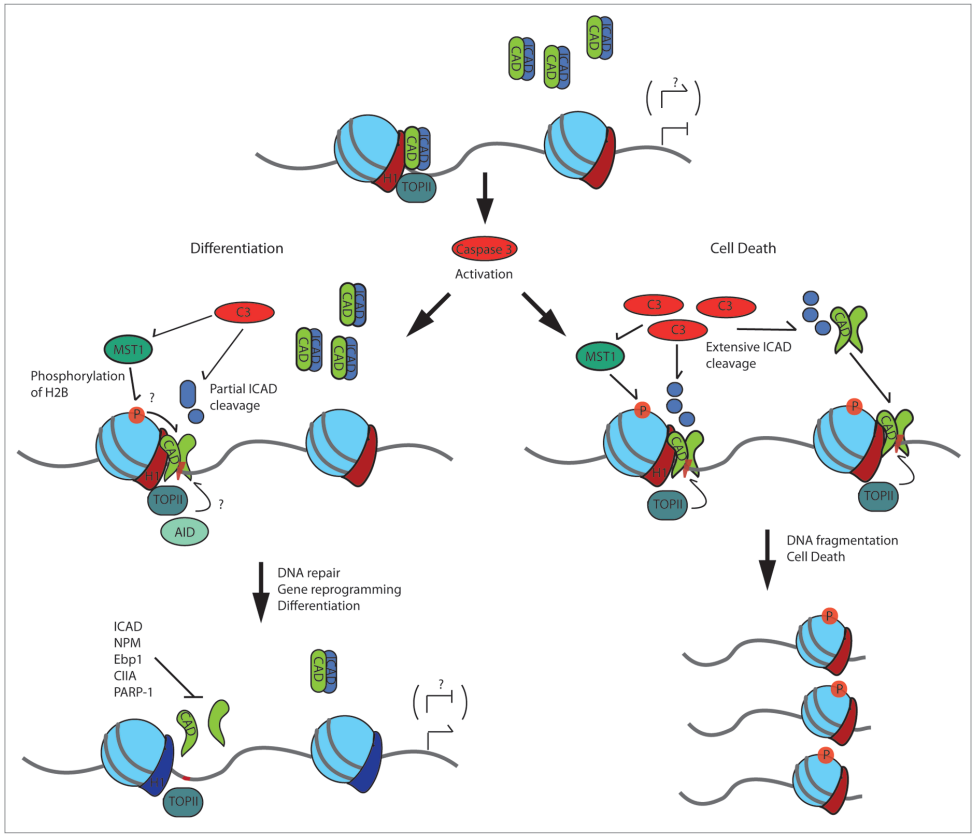

Figure 1. Caspase 3 activation balances the dissemination of CAD induced DNA strand breaks for gene reprogramming or fragmentation. This model depicts several factors that may regulate CAD induced DNA strand breaks in physiologic and apoptotic conditions.

11. McCarty JS, Toh SY, Li P. Study of DFF45 in its role of chaperone and inhibitor: Two independent inhibitory domains of DFF40 nuclease activity. Biochem Biophys Res Commun 1999; 264:176-80.
12. Sakahira H, Nagata S. Co-translational folding of caspase-activated DNase with Hsp70, Hsp40 and inhibitor of caspase-activated DNase. J Biol Chem 2002; 277:3364-70.
13. Lechardeur D, Xu M, Lukacs GL. Contrasting nuclear dynamics of the caspase-activated DNase (CAD) in dividing and apoptotic cells. J Cell Biol 2004; 167:851-62.
14. Korn C, Scholz SR, Gimadutdinow O, Lurz R, Pingoud A, Meiss G. Interaction of DNA fragmentation factor (DFF) with DNA reveals an unprecedented mechanism for nuclease inhibition and suggests that DFF can be activated in a DNA-bound state. J Biol Chem 2005; 280:6005-15.
15. Reh S, Korn C, Gimadutdinow O, Meiss G. Structural basis for stable DNA complex formation by the caspase-activated DNase. J Biol Chem 2005; 280:41707-15.
16. Woo EJ, Kim YG, Kim MS, Han WD, Shin S, Robinson H, et al. Structural mechanism for inactivation and activation of CAD/DFF40 in the apoptotic pathway. Mol Cell 2004; 14:531-9.
17. Abdul-Ghani M, Megeney LA. Rehabilitation of a contract killer: caspase-3 directs stem cell differentiation. Cell Stem Cell 2008; 2:515-6.
18. Fernando P, Megeney LA. Is caspase-dependent apoptosis only cell differentiation taken to the extreme? FASEB J 2007; 21:8-17.
19. Zeuner A, Eramo A, Testa U, Felli N, Pelosi E, Mariani G, et al. Control of erythroid cell production via caspase-mediated cleavage of transcription factor SCL/Tal-1. Cell Death Differ 2003; 10:905-13.
20. Fujita J, Crane AM, Souza MK, Dejosez M, Kyba M, Flavell RA, et al. Caspase activity mediates the differentiation of embryonic stem cells. Cell Stem Cell 2008; 2:595-601.
21. Fernando P, Brunette S, Megeney LA. Neural stem cell differentiation is dependent upon endogenous caspase 3 activity. FASEB J 2005; 19:1671-3.
22. Fernando P, Kelly JF, Balazsi K, Slack RS, Megeney LA. Caspase 3 activity is required for skeletal muscle differentiation. Proc Natl Acad Sci USA 2002; 99:11025-30.
23. Kanuka H, Kuranaga E, Takemoto K, Hiratou T, Okano H, Miura M. Drosophila caspase transduces Shaggy/GSK-3beta kinase activity in neural precursor development. EMBO J 2005; 24:3793-806.
24. Cheung WL, Ajiro K, Samejima K, Kloc M, Cheung P, Mizzen CA, et al. Apoptotic phosphorylation of histone H2B is mediated by mammalian sterile twenty kinase. Cell 2003; 113:507-17.
25. Ahn SH, Cheung WL, Hsu JY, Diaz RL, Smith MM, Allis CD. Sterile 20 kinase phosphorylates histone H2B at serine 10 during hydrogen peroxide-induced apoptosis in S. cerevisiae. Cell 2005; 120:25-36.
26. Graves JD, Gotoh Y, Draves KE, Ambrose D, Han DK, Wright M, et al. Caspase-mediated activation and induction of apoptosis by the mammalian Ste20-like kinase Mst1. EMBO J 1998; 17:2224-34.

27. Zeng Q, Hong W. The emerging role of the hippo pathway in cell contact inhibition, organ size control and cancer development in mammals. Cancer Cell 2008; 13:188-92.
28. Sun Y, Wang T, Su Y, Yin Y, Xu S, Ma C, et al. The behavior of SATB1, a MAR-binding protein, in response to apoptosis stimulation. Cell Biol Int 2006; 30:244-7.
29. Gotzmann J, Meissner M, Gerner C. The fate of the nuclear matrix-associated-region-binding protein SATB1 during apoptosis. Cell Death Differ 2000; 7:425-38.
30. Tan JA, Sun Y, Song J, Chen Y, Krontiris TG, Durrin LK. SUMO conjugation to the matrix attachment region-binding protein, special AT-rich sequence-binding protein-1 (SATB1), targets SATB1 to promyelocytic nuclear bodies where it undergoes caspase cleavage. J Biol Chem 2008; 283:18124-34.
31. Liu QY, Ribecco-Lutkiewicz M, Carson C, Testolin L, Bergeron D, Kohwi-Shigematsu T, et al. Mapping the initial DNA breaks in apoptotic Jurkat cells using ligation-mediated PCR. Cell Death Differ 2003; 10:278-89.
32. Widlak P, Kalinowska M, Parseghian MH, Lu X, Hansen JC, Garrard WT. The histone H1 C-terminal domain binds to the apoptotic nuclease, DNA fragmentation factor (DFF40/CAD) and stimulates DNA cleavage. Biochemistry 2005; 44:7871-8.
33. Ninios YP, Sekeri-Pataryas KE, Sourlingas TG. Histone H1 subtype preferences of DFF40 and possible nuclear localization of DFF40/45 in normal and trichostatin A-treated NB4 leukemic cells. Apoptosis 2010; 15:128-38.
34. Izzo A, Kamieniarz K, Schneider R. The histone H1 family: specific members, specific functions? Biol Chem 2008; 389:333-43.
35. Lee H, Habas R, Abate-Shen C. MSX1 cooperates with histone H1b for inhibition of transcription and myogenesis. Science 2004; 304:1675-8.
36. Odelberg SJ, Kollhoff A, Keating MT. Dedifferentiation of mammalian myotubes induced by msx1. Cell 2000; 103:1099-109.
37. Hunter AL, Zhang J, Chen SC, Si X, Wong B, Ekhterae D, et al. Apoptosis repressor with caspase recruitment domain (ARC) inhibits myogenic differentiation. FEBS Lett 2007; 581:879-84.
38. Murray TV, McMahon JM, Howley BA, Stanley A, Ritter T, Mohr A, et al. A non-apoptotic role for caspase-9 in muscle differentiation. J Cell Sci 2008; 121:3786-93.
39. Koto A, Kuranaga E, Miura M. Temporal regulation of Drosophila IAP1 determines caspase functions in sensory organ development. J Cell Biol 2009; 187:219-31.
40. West JD, Ji C, Marnett LJ. Modulation of DNA fragmentation factor 40 nuclease activity by poly(ADP-ribose) polymerase-1. J Biol Chem 2005; 280:15141-7.
41. Farzaneh F, Shall S, Johnstone AP. The dynamic nature of DNA-strand breaks present in differentiating muscle cells and quiescent lymphocytes. FEBS Lett 1985; 189:62-6.
42. Ahn JY, Liu X, Cheng D, Peng J, Chan PK, Wade PA, et al. Nucleophosmin/B23, a nuclear PI(3,4,5)P(3) receptor, mediates the antiapoptotic actions of NGF by inhibiting CAD. Mol Cell 2005; 18:435-45.
43. Ahn JY, Liu X, Liu Z, Pereira L, Cheng D, Peng J, et al. Nuclear Akt associates with PKC-phosphorylated Ebp1, preventing DNA fragmentation by inhibition of caspase-activated DNase. EMBO J 2006; 25:2083-95.
44. Ju BG, Rosenfeld MG. A breaking strategy for topoisomerase IIbeta/PARP-1-dependent regulated transcription. Cell Cycle 2006; 5:2557-60.
45. Durrieu F, Samejima K, Fortune JM, Kandels-Lewis S, Osheroff N, Earnshaw WC. DNA topoisomerase IIalpha interacts with CAD nuclease and is involved in chromatin condensation during apoptotic execution. Curr Biol 2000; 10:923-6.
46. Popp C, Dean W, Feng S, Cokus SJ, Andrews S, Pellegrini M, et al. Genome-wide erasure of DNA methylation in mouse primordial germ cells is affected by AID deficiency. Nature 2010; 463:1101-5.
47. Bhutani N, Brady JJ, Damian M, Sacco A, Corbel SY, Blau HM. Reprogramming towards pluripotency requires AID-dependent DNA demethylation. Nature 2010; 463:1042-7.
48. Petersen-Mahrt SK, Harris RS, Neuberger MS. AID mutates *E. coli* suggesting a DNA deamination mechanism for antibody diversification. Nature 2002; 418:99-103.
49. Jost JP, Oakeley EJ, Zhu B, Benjamin D, Thiry S, Siegmann M, et al. 5-Methylcytosine DNA glycosylase participates in the genome-wide loss of DNA methylation occurring during mouse myoblast differentiation. Nucleic Acids Res 2001; 29:4452-61.